VOLUME 105 PART B NUMBER 21 MAY 1958

The Proceedings

OF

THE INSTITUTION OF ELECTRICAL ENGINEERS

FOUNDED 1871 : INCORPORATED BY ROYAL CHARTER 1921

PART B

RADIO AND ELECTRONIC ENGINEERING
(INCLUDING COMMUNICATION ENGINEERING)

SAVOY PLACE · LONDON W.C.2

Price Ten Shillings and Sixpence

THE INSTITUTION OF ELECTRICAL ENGINEERS

FOUNDED 1871 INCORPORATED BY ROYAL CHARTER 1921

PATRON: HER MAJESTY THE QUEEN

COUNCIL 1957–1958

President

T. E. GOLDUP, C.B.E.

Past-Presidents

W. H. ECCLES, D.Sc., F.R.S.
THE RT. HON. THE EARL OF MOUNT EDGCUMBE, T.D.
J. M. DONALDSON, M.C.
PROFESSOR E. W. MARCHANT, D.Sc.
H. T. YOUNG.
SIR GEORGE LEE, O.B.E., M.C.
SIR ARTHUR P. M. FLEMING, C.B.E., D.Eng., LL.D.
J. R. BEARD, C.B.E., M.Sc.
SIR NOEL ASHBRIDGE, B.Sc.(Eng.).
COLONEL SIR A. STANLEY ANGWIN, K.C.M.G., K.B.E., D.S.O., M.C., T.D., D.Sc.(Eng.).
SIR HARRY RAILING, D.Eng.
P. DUNSHEATH, C.B.E., M.A., D.Sc. (Eng.).
SIR VINCENT Z. DE FERRANTI, M.C.
T. G. N. HALDANE, M.A.
PROFESSOR E. B. MOULLIN, M.A., Sc.D.
SIR ARCHIBALD J. GILL, B.Sc.(Eng.).
SIR JOHN HACKING.
COLONEL B. H. LEESON, C.B.E., T.D.
SIR HAROLD BISHOP, C.B.E., B.Sc.(Eng.)
SIR JOSIAH ECCLES, C.B.E., D.Sc.
SIR GEORGE H. NELSON, Bart.
SIR GORDON RADLEY, K.C.B., C.B.E., Ph.D.(Eng.).

Vice-Presidents

S. E. GOODALL, M.Sc.(Eng.). WILLIS JACKSON, D.Sc., D.Phil., Dr.Sc.Tech., F.R.S. G. S. C. LUCAS, O.B.E.
SIR HAMISH D. MACLAREN, K.B.E., C.B., D.F.C., LL.D., B.Sc. C. T. MELLING, C.B.E., M.Sc.Tech.

Honorary Treasurer

THE RT. HON. THE VISCOUNT FALMOUTH.

Ordinary Members of Council

PROFESSOR H. E. M. BARLOW, Ph.D., B.Sc.(Eng.).
J. A. BROUGHALL, B.Sc.(Eng.).
C. M. COCK.
SIR JOHN DEAN, B.Sc.
B. DONKIN, B.A.
J. S. FORREST, D.Sc., M.A.
PROFESSOR J. GREIG, M.Sc., Ph.D.
E. M. HICKIN.
J. B. HIGHAM, Ph.D., B.Sc.
D. MCDONALD, B.Sc.
F. C. MCLEAN, C.B.E., M.Sc.
B. L. METCALF, B.Sc.(Eng.).
J. R. MORTLOCK, B.Sc.(Eng.).
H. H. MULLENS, B.Sc.
A. H. MUMFORD, O.B.E., B.Sc.(Eng.).
R. H. PHILLIPS, T.D.
D. P. SAYERS, B.Sc.
C. E. STRONG, O.B.E., B.A., B.A.I.
H. WATSON-JONES, M.Eng.
D. B. WELBOURN, M.A.
H. WEST, M.Sc.

Chairmen and Past-Chairmen of Sections

Measurement and Control:
H. S. PETCH, B.Sc.(Eng.).
*D. TAYLOR, M.Sc., Ph.D.

Radio and Telecommunication:
J. S. MCPETRIE, Ph.D., D.Sc.
*R. C. G. WILLIAMS, Ph.D., B.Sc.(Eng.).

Supply:
PROFESSOR M. G. SAY, Ph.D., M.Sc., F.R.S.E.
*P. J. RYLE, B.Sc.(Eng.).

Utilization:
J. VAUGHAN HARRIES.
*H. J. GIBSON, B.Sc.

Chairmen and Past-Chairmen of Local Centres

East Midland Centre:
J. D. PIERCE.
*H. L. HASLEGRAVE, M.A., Ph.D., M.Sc. (Eng.).

Mersey and North Wales Centre:
T. MAKIN.
*P. D'E. STOWELL, B.Sc.(Eng.).

North Midland Centre:
A. J. COVENEY.
*W. K. FLEMING.

North-Eastern Centre:
T. W. WILCOX.
*J. CHRISTIE.

Southern Centre:
L. G. A. SIMS, D.Sc., Ph.D.
*H. ROBINSON, B.Sc.

North-Western Centre:
F. R. PERRY, M.Sc.Tech.
*T. E. DANIEL, M.Eng.

Northern Ireland Centre:
C. M. STOUPE, B.Sc.
*DOUGLAS S. PARRY.

Western Centre:
J. F. WRIGHT.
*PROFESSOR G. H. RAWCLIFFE, M.A., D.Sc.

Scottish Centre:
E. O. TAYLOR, B.Sc.
*PROFESSOR F. M. BRUCE, M.Sc., Ph.D.

South Midland Centre:
L. L. TOLLEY, B.Sc.(Eng.).
*C. J. O. GARRARD, M.Sc.

* Past Chairman

MEASUREMENT AND CONTROL SECTION COMMITTEE 1957–1958

Chairman

H. S. PETCH, B.Sc.(Eng.).

Vice-Chairmen

J. K. WEBB, M.Sc.(Eng.), B.Sc.Tech.; PROFESSOR A. TUSTIN, M.Sc.

Past-Chairmen

DENIS TAYLOR, M.Sc., Ph.D.; W. BAMFORD, B.Sc.

Ordinary Members of Committee

J. BELL, M.C.
E. W. CONNON, B.Sc.(Eng.), M.Eng.
D. EDMUNDSON, B.Sc.(Eng.).
W. S. ELLIOTT, M.A.
C. G GARTON.
PROFESSOR K. A. HAYES, B.Sc.(Eng.).
W. C. LISTER, B.Sc.
A. J. MADDOCK, D.Sc.
R. S. MEDLOCK, B.Sc.
G. A. W. SOWTER, Ph.D., B.Sc.(Eng.).
R. H. TIZARD, B.A.
M. V. WILKES, M.A., Ph.D., F.R.S.

And

The President (*ex officio*).
The Chairman of the Papers Committee.
PROFESSOR J. GREIG, M.Sc., Ph.D. (representing the Council).
W. GRAY (representing the North-Eastern Radio and Measurement Group).
E. ROSCOE, J.P. (representing the North-Western Measurement and Control Group).
P. R. HOWARD, Ph.D., B.Sc.(Eng.) (nominated by the National Physical Laboratory).
H. M. GALE, B.Sc.(Eng.) (representing the South Midland Radio and Measurement Group).

RADIO AND TELECOMMUNICATION SECTION COMMITTEE 1957–1958

Chairman

J. S. MCPETRIE, Ph.D., D.Sc.

Vice-Chairmen

G. MILLINGTON, M.A., B.Sc.
M. J. L. PULLING, C.B.E., M.A.

Past-Chairmen

R. C. G. WILLIAMS, Ph.D., B.Sc.(Eng.).
H. STANESBY.

Ordinary Members of Committee

A. J. BIGGS, Ph.D., B.Sc.
W. J. BRAY, M.Sc.(Eng.).
H. A. M. CLARK, B.Sc.(Eng.).
C. W. EARP, B.A.
V. J. FRANCIS, B.Sc.
R. J. HALSEY, C.M.G., B.Sc.(Eng.).
B. G. PRESSEY, M.Sc.(Eng.), Ph.D.
W. ROSS, M.A.
T. B. D. TERRONI, B.Sc.
D. R. TURNER, M.Eng.
F. WILLIAMS, B.Sc.
W. E. WILLSHAW, M.B.E., M.Sc.Tech.

And

The President (*ex officio*).
The Chairman of the Papers Committee.
PROF. H. E. M. BARLOW, Ph.D., B.Sc.(Eng.) (representing the Council).
E. H. COOKE-YARBOROUGH, M.A. (Co-opted Member).
A. E. TWYCROSS (representing the North-Eastern Radio and Measurement Group).
N. C. ROLFE, B.Sc.(Eng.) (representing the Cambridge Radio and Telecommunication Group).
J. MOIR (representing the South Midland Radio and Measurement Group).
G. J. SCOLES, B.Sc.(Eng.) (representing the North-Western Radio and Telecommunication Group).

The following nominees of Government Departments:
Admiralty: CAPTAIN R. L. CLODE, R.N.
Air Ministry: GROUP CAPTAIN A. FODEN, B.Sc.Tech., R.A.F.
War Office: BRIGADIER J. D. HAIGH, O.B.E., M.A.

Secretary

W. K. BRASHER, C.B.E., M.A., M.I.E.E.

Deputy Secretary

F. JERVIS SMITH, M.I.E.E.

Assistant Secretary

F. C. HARRIS.

Editor-in-Chief

G. E. WILLIAMS, B.Sc.(Eng.), M.I.E.E.

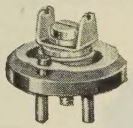

Preset Mk. 2 G type

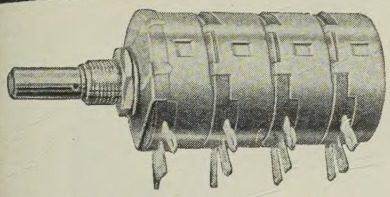

Type E four gang variation

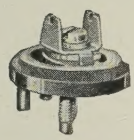

Preset Mk. 5 G type

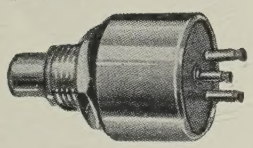

MH2 Miniature panel and Spindle Sealed

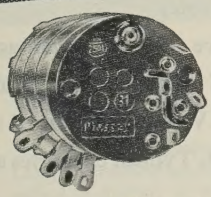

Type E gang with Switch

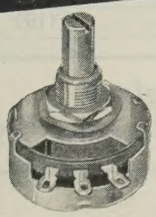

Type EN to RCS 1000

Plessey

potentiometers

for special applications

Moulded track potentiometers by Plessey possess a high standard of stability within a wide range of operational temperatures and can be stored for extended periods without deterioration. They can be manufactured to conform, within strictly specified limits, to a designed pattern of values at various positions on the track.

COMMERCIAL TYPES

These are available as single units, dual concentrics or special gangs and are available with or without double pole switch, also in preset form. The standard resistance values are linear 100 ohms to 5 MΩ, log 5KΩ to 2 MΩ. The maximum working voltage is 500 V.

Standard Type 'E'. 2 watts at 70°C for linear laws.

Standard with double pole switch Type 'ES'. 2 watts at 70°C for linear laws.

Dual Type 'ED'. 2 watts at 70°C for each section.

Dual with double pole switch Type 'EDS'. 2 watts at 70°C for each section.

Preset Type 'EP'. 1 watt for 70°C for linear laws.

GOVERNMENT AND INSTRUMENTATION TYPES

Available as normal and preset types. In general are in accordance with the appropriate Ministry Specifications.

Panel and Spindle Sealed Type 'EH2' 1 watt at 100°C for linear laws. (Type Approval Certificate 906/4 [1230].) Maximum working voltage 500V.

Instrumentation Type 'EN' 2 watts at 70°C for linear laws. (All materials to R.C.S.1000.) Maximum working voltage 500V.

Miniature, thumb operated, with switch, Type 'F' ¼ watt at 70°C for linear laws. Maximum working voltage 250V.

Sub-Miniature Preset Type 'G'. Marks 2 & 5. ¼ watt at 70°C for linear laws. (Type Approval Certificates 974/2 and 1075/1 [1373].) Maximum working voltage 250V.

Miniature Panel and Spindle Sealed Type 'MH2' ¼ watt at 70°C. (Type Approval Certificate 1032/1 [1373/1].) Maximum working voltage 250V. A fully sealed version of this potentiometer is also available.

Rating at 100°C is normally one half of that at 70°C.

SWINDON COMPONENTS DIVISION
THE PLESSEY COMPANY LIMITED
KEMBREY STREET · SWINDON · WILTS · Tel: 6211
Overseas Sales Organisation: Plessey International Limited
Ilford · Essex · England · Telephone: Ilford 3040

SCI

VAPOUR-COOLED VALVES

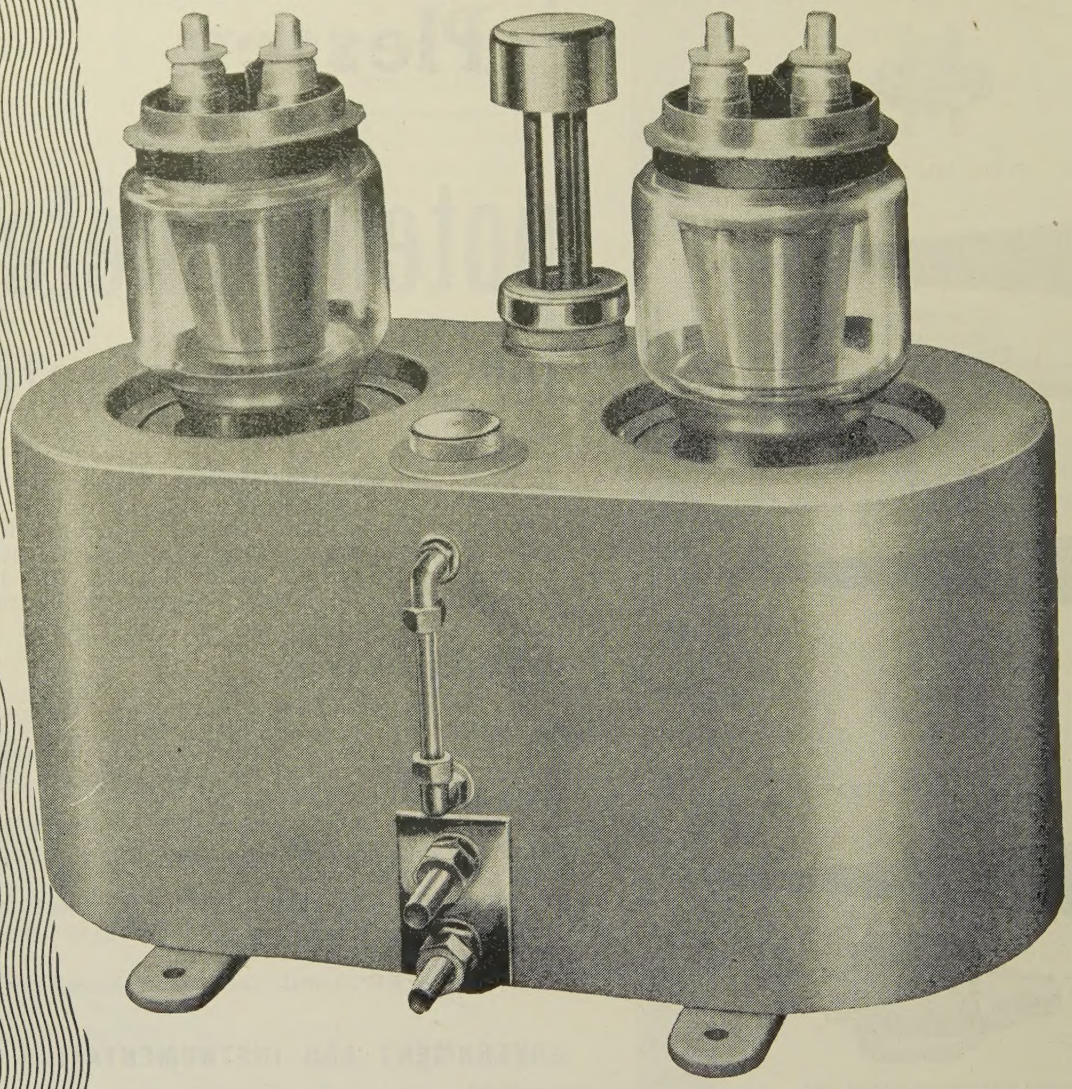

Conditions sometimes exist both in industry and in communications where neither forced air cooling nor water cooling of high power valves is entirely satisfactory. Air may be so dirt laden that the cleaning of filters and radiators calls for undue effort and cost and at the same time water may be expensive, scarce or otherwise unsuitable.

Under such conditions the E.E.V. vapour-cooled valves may give just the advantages needed: low water cost; built-in protection against failure of water supply; quiet operation; and greater overload capacity. Many types in the E.E.V. range of forced air and water-cooled valves are now available as vapour-cooled versions. Typical examples are

Forced air-cooled	Water-cooled	Vapour-cooled
BR1102	BW1102	BY1102
BR1121	BW1121	BY1121
BR189	BW189	BY189

'ENGLISH ELECTRIC'

ENGLISH ELECTRIC VALVE CO. LTD. *Chelmsford, England*
Telephone: Chelmsford 3491

AP101

The First of its Kind or The Familiar Product

Savage Transformers are continually pioneering techniques which later become standard practice. New industrial requirements often necessitate the scrapping of old ideas and the development of entirely new ones. Revolutionary or traditional, however, all instruments labelled "Massicore" have the same essential ingredient—conscientious craftsmanship. They are built to last a lifetime.

Equally important is the individual attention given to all enquiries and orders regardless of size; and we make a point of keeping our delivery promises.

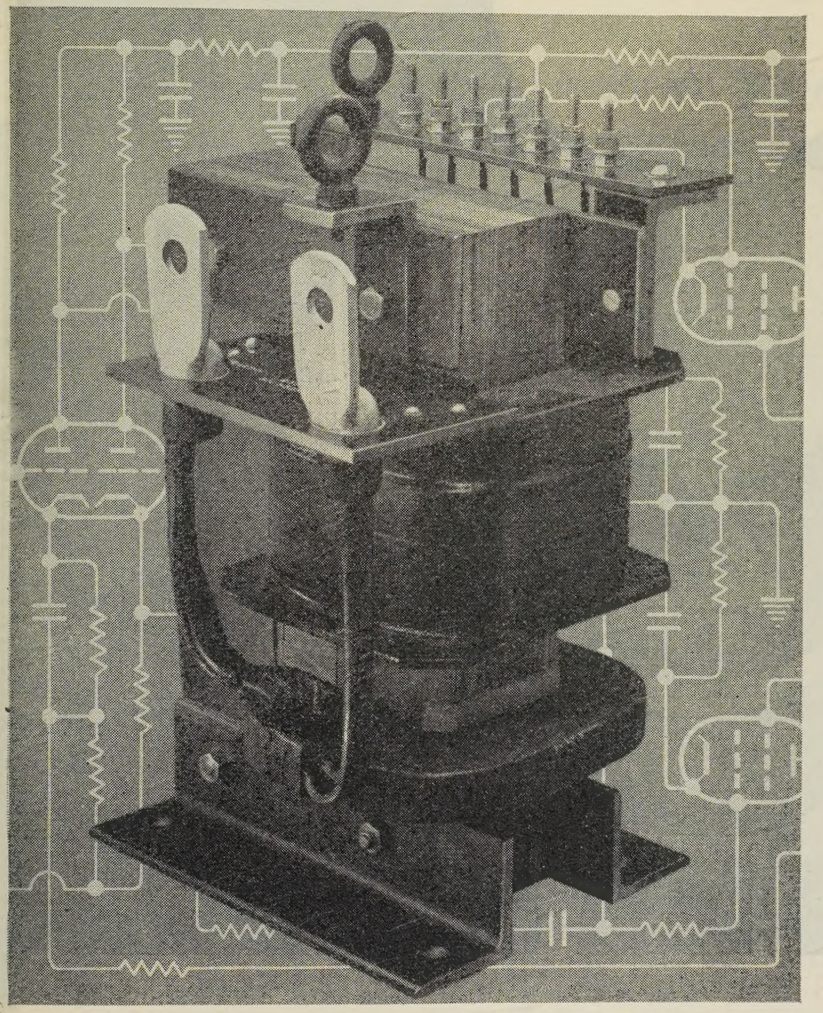

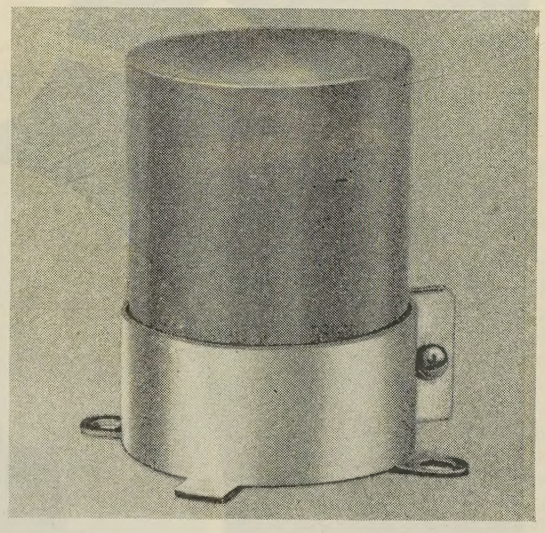

The unusual-looking instrument on the left is a special Massicore Current Limiting Transformer. The secondary gives 8.3v with load current of 230A. The maximum secondary current when short-circuited is 525A. And above, comparatively normal in appearance, is a mu-metal shielded Audio Transformer for 600 ohm line to amplifier grid. Primary balanced and electrostatically screened. Response ± 0.5 D.B. 30 c.p.s. to 15,000 c.p.s.

Your requirements may call for instruments very different from these examples. Please take advantage of our experience, knowledge and constructional skill in the production of all types of transformers.

Corner for Contented Customers

"According to an advertisement once run by Savage Transformers Ltd. your company received a letter from 'N.W.' in Chelston which started as follows: 'It is indeed refreshing to receive a letter in response to an enquiry such as I received from you yesterday and for which please accept my sincere thanks'.

If the response which 'N.W.' received was anything like the one you sent me on September 3rd, I can only say that he understates things beautifully. Personally, I would like to thank you very much for the extremely prompt and complete reply to my letter of August 20th."

J. C. H. WESTMOUNT. QUEBEC

MASSICORE SAVAGE

SAVAGE TRANSFORMERS LIMITED Devizes, Wiltshire Tel: Devizes 932

let us demonstrate any of these superb SOLARTRON oscilloscopes

write or 'phone now for appointment

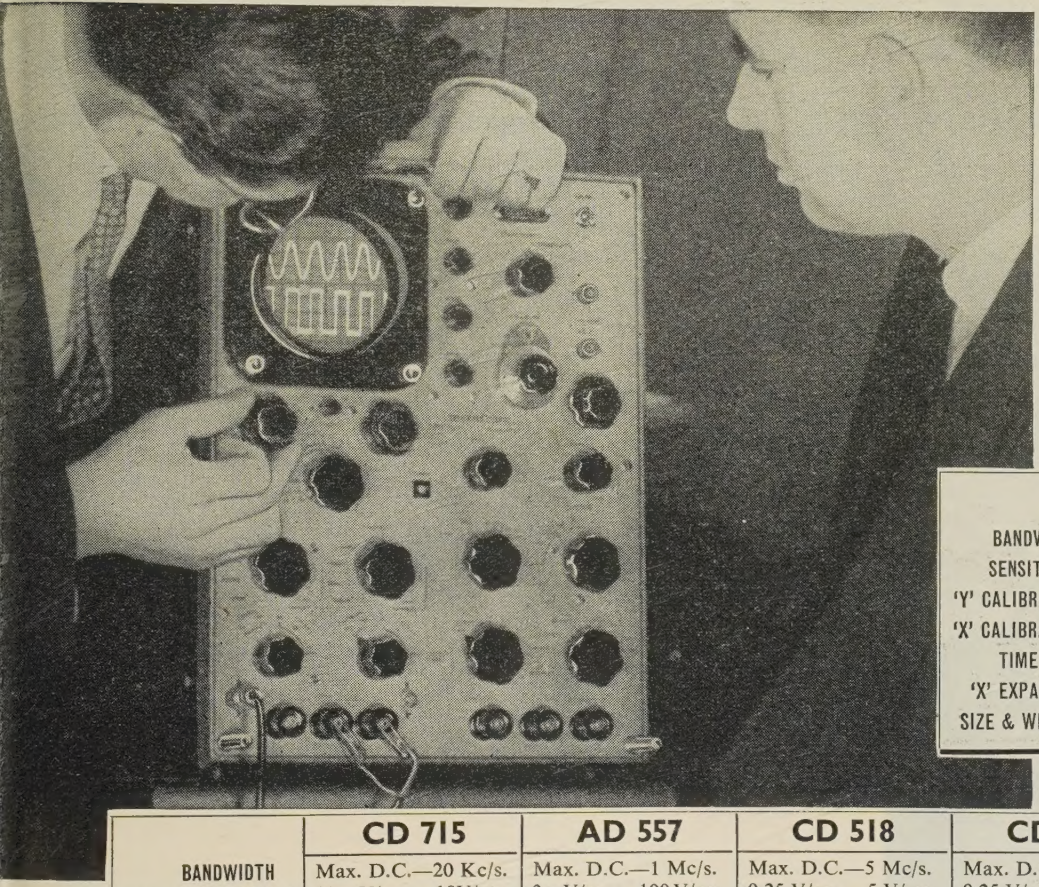

Have you seen the *new* Solartron Double-Beam Solarscope CD 711 being put through its paces?
Now, for the first time, you can choose a double-beam 'scope of Solartron quality, embodying all the latest design features and built to the finest standards of electronic and mechanical engineering.
Why not write or call us now for a demonstration of the Double-Beam Solarscope, or any of the eight other models listed below? Specialist instrument engineers are immediately available to assist you, whatever your problem or field of application.

	CD 711 DOUBLE BEAM
BANDWIDTH	Max. D.C.—7 Mc/s. at 100mV/cm.
SENSITIVITY	3mV/cm.—100 V/cm.
'Y' CALIBRATION	Cal. shift. Accuracy ±5%
'X' CALIBRATION	Cal. time scale. Accuracy ±5%
TIME BASE	Time scale 0.3μ Sec./cm.—3 Sec./cm.
'X' EXPANSION	Continuously variable ×10
SIZE & WEIGHT	16″ × 13″ × 27½″ deep. 110 lb.

	CD 715	AD 557	CD 518	CD 568	CD 513
BANDWIDTH	Max. D.C.—20 Kc/s.	Max. D.C.—1 Mc/s.	Max. D.C.—5 Mc/s.	Max. D.C.—5 Mc/s.	Max. D.C.—10 Mc/s.
SENSITIVITY	10 mV/cm.—10V/cm.	3 mV/cm.—100 V/cm.	0.25 V/cm.—5 V/cm.	0.25 V/cm.—5 V/cm.	1 mV/cm.—10 V/cm.
'Y' CALIBRATION	Special facilities	Cal. shift ±5%	Shift meter. Accuracy ±3%	Shift meter. Accuracy ±3%	Cal. sensitivity Accuracy ±10%
'X' CALIBRATION	Special facilities	Cal. time scale. Accuracy ±10%	'Cal Pips' and sine wave. Accuracy ±2%	Sine wave. Accuracy ±2%	Cal. time scale Accuracy ±10%
TIME BASE	Sweep time 10 Sec. to 0.1 Sec.	Time scale 1μ Sec./cm. —1 Sec./cm.	Sweep time 100m. Sec. —1μ Sec.	Sweep time 100m. Sec. —1μ Sec.	Time scale 0.1μ Sec./cm.—1 Sec./cm.
'X' EXPANSION	×1, ×0.5, ×0.2, ×0.1, ×0.05	Continuously variable × 10			×0.5, ×1, ×2, ×5
SIZE & WEIGHT	14″ × 10″ × 20″ deep. 47 lb.	16½″ × 10″ × 22″ deep. 70 lb.	12″ × 9″ × 18″ deep. 40 lb.	12″ × 9″ × 18″ deep. 40 lb.	16½″ × 10″ × 22″ deep. 70 lb.

	CD 523S	CD 814	CD 643
BANDWIDTH	Max. D.C.—10 Mc/s.	Constant 1c/s.–9Mc/s.	Constant D.C.—15 Mc/s.
SENSITIVITY	1 mV/cm.—10 V/cm.	30 mV/cm.—30 V/cm.	100 mV/cm.–60 V/cm.
CALIBRATION	Cal. sensitivity Accuracy ±10%	Comparison method Accuracy±5%	Cal. shift. Accuracy ±2%
CALIBRATION	Cal. time scale Accuracy ±10%	'Cal Pips' Accuracy ±5%	'Cal Pips'and brightup Accuracy ±2%
TIME BASE	Time scale 0.1μ Sec./cm.—1 Sec./cm.	Repetition Rate 6 c/s—185 Kc/s.	Time scale 0.1μ Sec/cm. —100m. Sec./cm.
EXPANSION	× 0.5, × 1, × 2, × 5	Continuously variable × 10	Continuously variable × 100
& WEIGHT	16½″ × 10″ × 23″ deep. 70 lb.	14½″ × 10½″ × 19½″ deep. 43 lb.	20″ × 14¾″ × 27¾″ deep. 140 lb.

PRICES Home & Export (F.O.B., packing extra)	
CD 711	£320
CD 715	£460
AD 557	£275
CD 518	£225
CD 568	£210
CD 513	£220
CD 523S	£265
CD 814	£115
CD 643	£490

SOLARTRON

THE SOLARTRON ELECTRONIC GROUP LIMITED

THAMES DITTON • SURREY • Telephone: EMBerbrook 5522 • Cables: Solartron, Thames Ditton

MARCONI

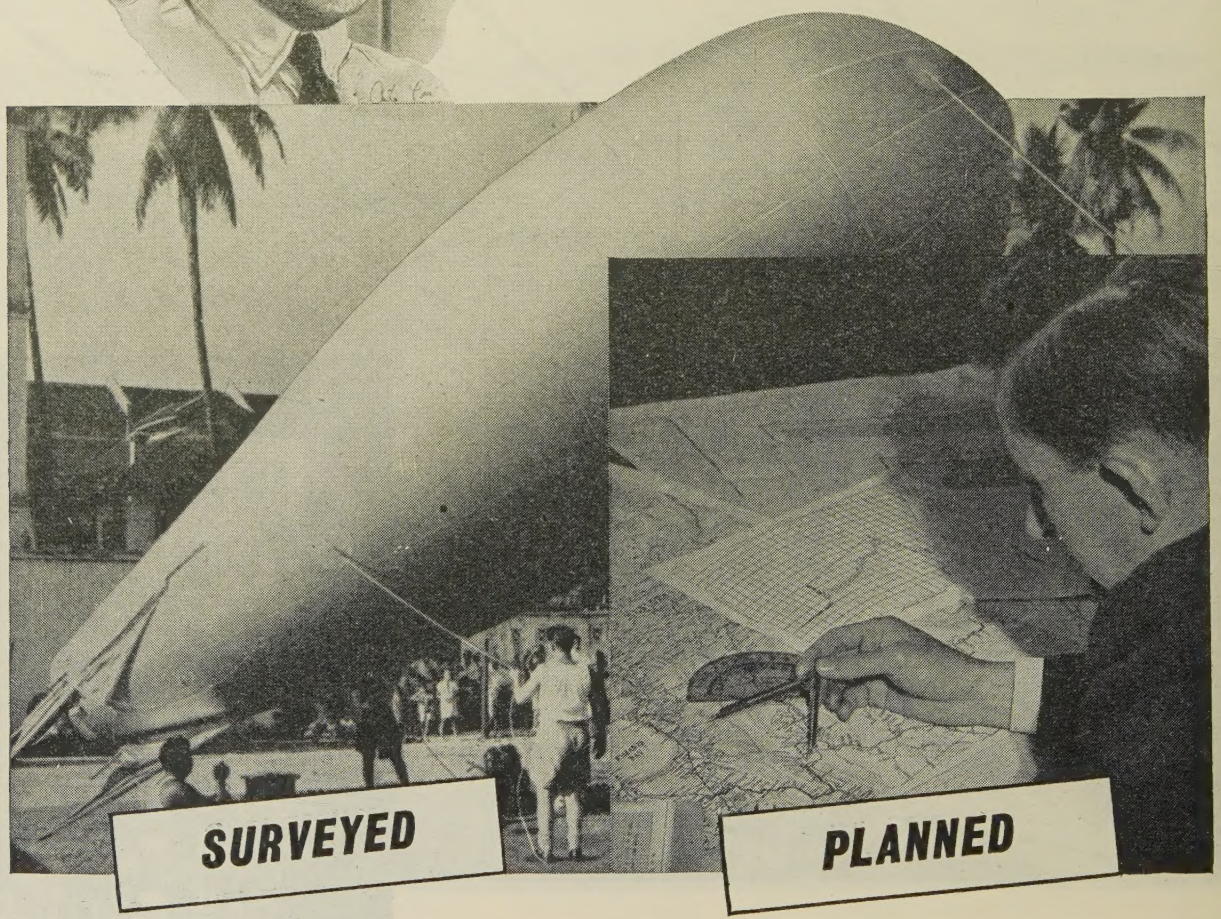

MULTI-CHANNEL SYSTEMS VHF radio telephony was welcomed in its early days as an economic means of providing communication over inhospitable or undeveloped terrain. Today, such is the flexibility and reliability of multichannel radio equipment, that radio links carrying up to 600 telephone channels or a colour television programme are recognised as being preferable to the use of line or cable systems in many instances on grounds of performance as well as installation cost.

THERE IS an intimate and complementary physiological partnership between the algoid and fungoid elements in lichens, and similar organisms, whereby each is entirely dependent upon the other, and each gives to the other that which it needs for its existence.

This partnership, known as symbiosis, achieved by one of the humblest forms of life, may not at first seem relevant to human relationships, or to the electronics industry, which it is our privilege to serve, but, on reflection, it is quite apparent that each of us is dependent in some way on the other, and that this partnership is an ideal towards which all of us must strive, and, indeed, is an ideal towards which even the nations are now striving, and must continue to strive if our civilization is not to follow the fate of those of the past.

Whilst we in Erie Resistor Limited cannot pretend that we have reached this ideal, or that we will ever reach it, we do try in our small way to "live together" with the customer in every phase of his day-to-day problems, and to give to the customer the full benefit of our knowledge and skill, built up over many years of specialised experience involving practically every sphere of electronics, besides the normal service which every customer has the right to expect from his supplier, and, in return, we receive from the customer, not only his confidence, his business, and his friendship, but also the answer to many of our own problems.

The fruits of living together can be seen in the wide range of our products, in their reliability, in their universal application, and above all, perhaps, in the introduction of the right product at the right time, properly tailored for the job for which it is intended.

ERIE ★ **RESISTOR LIMITED**

Carlisle Road, The Hyde, London, N.W.9, England. Tel: COL 8011

Factories: London and Gt. Yarmouth, England; Toronto, Canada; Erie, Pa., and Holly Springs, Miss., U.S.A.

in Sydney

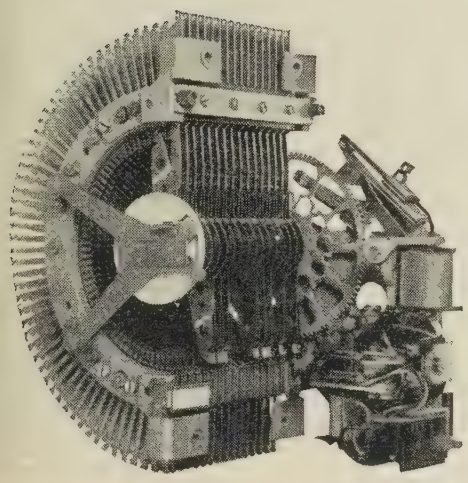

CORDLESS POSITIONS economise operator effort and stimulate efficiency. The metal and plastic positions are arranged in convenient small suites.

AUTOMATIC SWITCHING is carried out exclusively by our High Speed Motor Uniselector, the ideal trunk switching mechanism. It combines reliability and ease of maintenance with outstanding flexibility of application.

TRANSIT CALLS, also calls to the local area are routed without operator intervention. Code translation and automatic alternative routing facilities are available.

CALL QUEUEING equipment controls the distribution of incoming traffic to operators who may be assigned to meet fluctuations in route traffic.

CALL STORAGE facilities ensure maximum trunk occupancy. Demand service can be maintained despite route congestion.

KEYSENDERS are available to all operators and afford code translation and alternative routing facilities.

TRUNK LINES of many types are served—Voice Frequency signalling, D.C. dialling, Carrier signalling, etc.

TRANSMISSION performance is optimum due to the use of 4-wire switching and automatic pad-control.

SUPERVISION of traffic handling and of staff is centralised; the exchange can operate as a trunk switching unit of maximum efficiency.

SUBSCRIBER TRUNK DIALLING can readily be added to the system on a progressive basis.

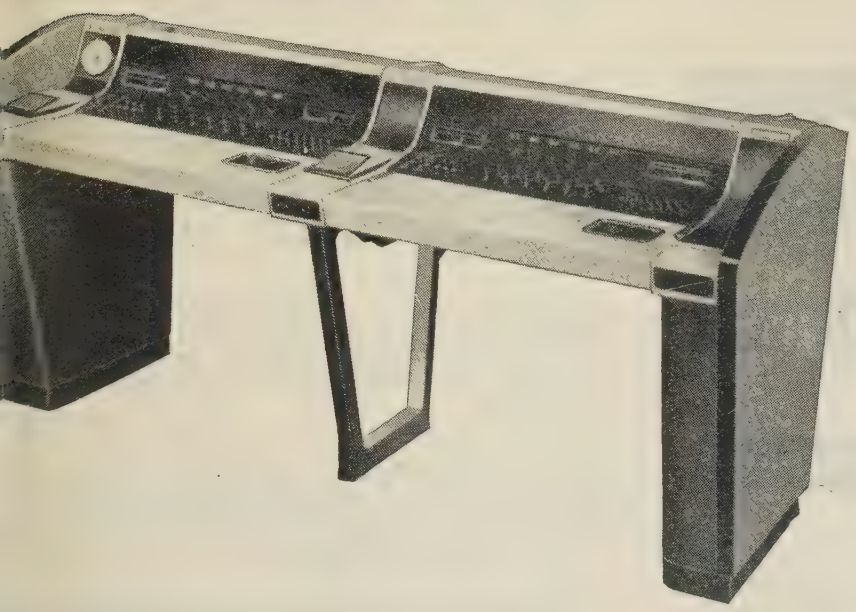

It is important to appreciate that the many features of our trunk switching system may be applied with equal effect to requirements much smaller than those described.

SIEMENS EDISON SWAN LIMITED

An A.E.I. Company

Public Telephone Division, Woolwich, London S.E.18.

Telephone: Woolwich 2020.

SIEMENS EDISWAN

a new valve for 470 Mc/s equipment

–unique double tetrode range extended

QQVO2-6

Here is a new six watt double tetrode for low cost 470Mc/s mobile equipment. This compact valve features a frame grid and the same unique twin construction as other Mullard double tetrodes — a construction which provides high efficiencies, high power gain and heater economy. Other features of the QQVO2-6 include built-in neutralising capacitors which enable circuitry to be simplified, and low inter-electrode capacitances which allow wide tuning ranges to be achieved and which contribute to high efficiency.
Write to the address below for full details of the QQVO2-6 and other Mullard double tetrodes.

BASE B9A

CATHODE ... ... Indirectly heated

HEATER (Centre tapped)

Series	...12.6V, 0.3A
Parallel	... 6.3V, 0.6A

CAPACITANCES

*ca–g′ (each section)	less than 0.16pF
cg′–all (each section)	6.4 pF
ca–all (each section)	1.6 pF
cout (two sections in push-pull)	0.95pF
cin (two sections in push-pull)	3.8 pF

* Internally neutralised for push-pull operation.

CHARACTERISTICS

(each section) measured at Ia = 25mA, Va = Vg″ = 150V

gm...	10.5mA/V
μg′–g″	31

TYPICAL OPERATING CONDITIONS

	Telegraphy or F.M.	*Telephony — A.M.*	
f	470	470	Mc/s
Va	180	180	V
Vg″	180	180	V
Ia	2 x 27.5	2 x 20	mA
pa	2 x 2.1	2 x 1.5	W
Pout	5.8	4.2	W
Pload	4.5	3.4	W

THE MULLARD DOUBLE TETRODE RANGE

. . . the most comprehensive and efficient in the world

	Typical F.M. Power Output
QQVO2–6	5.8 watts
QQVO3–10/6360 (CV2798)	11 watts
QQVO3–20A/6252 (CV2799)	25 watts
QQVO6–40A/5894 (CV2797)	56 watts

Mullard

COMMUNICATIONS AND INDUSTRIAL VALVE DEPARTMENT

MULLARD LIMITED · MULLARD HOUSE
TORRINGTON PLACE · W.C.1 · Tel: LANgham 6633

MVT343

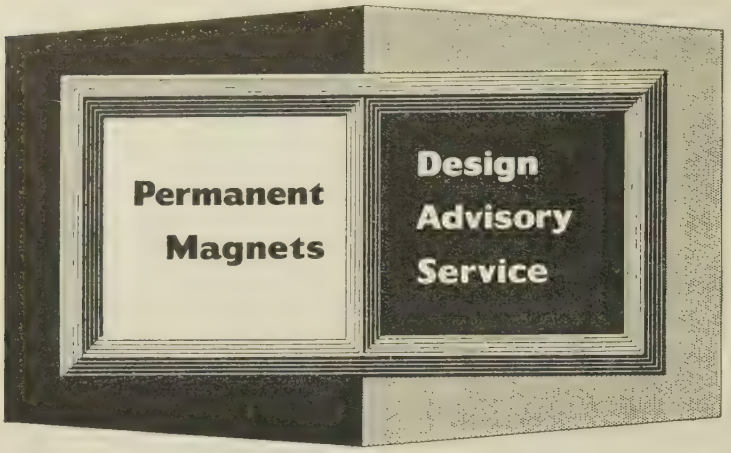

No. 2

Magnetic Circuits

Advertisements in this series deal with general design considerations. If you require more specific information on the use of permanent magnets, please send your enquiry to the address below, mentioning the Design Advisory Service.

The fundamental factors governing the design of a magnetic circuit are:—

(*a*) The magnetic field strength required in the air gap.

(*b*) The physical dimensions of the air gap.

(*c*) The leakage flux from the surface of the magnet (and pole pieces, if used).

If the dimensions of the gap and the flux required in it are known, the length of the magnet may be determined with the aid of either of the following simple formulae.

c.g.s. System

Length L_m of magnet in cm.

$$L_m = \frac{H_g \times L_g}{H_d} \times K_l$$

H_g is the field in the air gap in oersteds; L_g is the length of the air gap in cm; H_d is the design value of H from the magnet material characteristic.

M. K. S. System

Length L_m of magnet in metres

$$L_m = \frac{B_g \times L_g}{H_d} \times 4\pi \times 10^{-7} \times K_l$$

B_g is flux density in gap in webers/metre^2; L_g is length of gap in metres; H_d is in ampère-turns/metres.

K_l is a factor which may vary between 1.05 and 1.2. The lower value would apply if iron is of good magnetic quality operating well below saturation; also if joints in the magnetic circuit do not present appreciable reluctance.

The cross-sectional area of the magnet may be obtained by this formula.

Area A_m of magnet in sq. cm.

$$A_m = \frac{B_g \times A_g}{B_d} \times \text{Leakage Factor}$$

B_g is the flux density required in the air gap ($B_g = H_g$ in air); A_g = area of gap in sq. cm; B_d = design value of flux density of the magnetic material.

Leakage factors vary enormously with different applications and therefore, some experience or information is necessary in order to get a sufficiently close approximation for practical purposes. An example illustrating leakage is shown below.

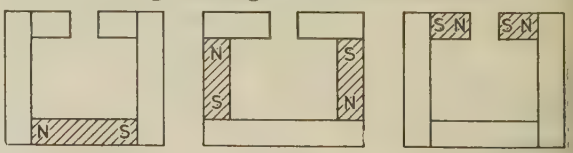

APPROX. EFFICIENCY

Using the M. K. S. System, the same formula still applies with B_g and B_d in webers/metre^2 and the area in square metres.

If you wish to receive reprints of this advertisement and others in this series write to the address below.

Mullard

'TICONAL' PERMANENT MAGNETS
'MAGNADUR' CERAMIC MAGNETS
FERROXCUBE MAGNETIC CORES

MULLARD LIMITED, COMPONENT DIVISION, MULLARD HOUSE, TORRINGTON PLACE, W.C.1 Tel. LANgham 6633
MC 262

FERRANTI

CERAMIC TO METAL SEALS

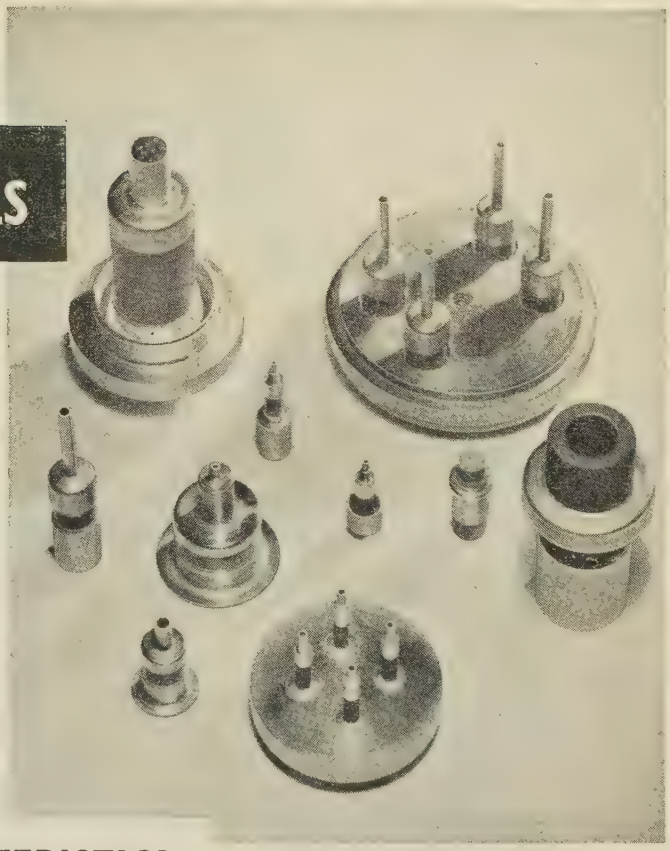

Ferranti Ceramic to Metal Seals have been developed to overcome the limits imposed upon valve performance by the use of conventional glass to metal seals. They perform so successfully that uses are apparent in other fields, particularly as terminals for vacuum and pressure vessels operated at elevated and sub-normal temperatures.

CHARACTERISTICS

Operating Temperature	intermittent 700°C maximum. continuous 300°C - 450°C dependent on atmosphere.
Operating Pressure	at least 100 atmospheres, depending on direction of compression.
Mechanical Strength	shearing force = 2,500 lbs per square inch of seal area.
Electrical Insulation	breakdown voltage in air is greater than 24 kV per inch of ceramic between seals.
Leakage Resistance (Typical)	10^{13} to 10^{15} ohms, at room temperature between two metal rings separated by 0·3″ of clean ceramic surface on a seal 0·440″ in diameter.
High Frequency Performance (Typical)	loss of 56 watts when 1 kW C.W. is passed through a seal incorporated in a ceramic-filled X-band circular wave-guide.

APPLICATIONS

The mechanical and electrical properties listed above suggest a wide variety of uses, a few of which are given below:-

Microwave and ordinary valve envelopes.
Semi-conductor envelopes.
Terminations for single and multicore cables.
Terminals and leads for vacuum and pressure vessels in atomic energy projects.
Thermocouple seals for furnaces.

FERRANTI

FERRANTI LTD · GEM MILL · CHADDERTON · OLDHAM · LANCS

London Office: KERN HOUSE, 36 KINGSWAY W.C.2.

FE 181

Prompt delivery of your RELAY needs...

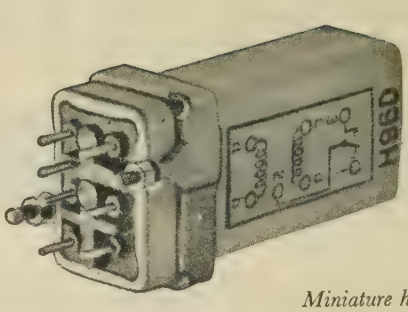

Miniature high speed sealed relay

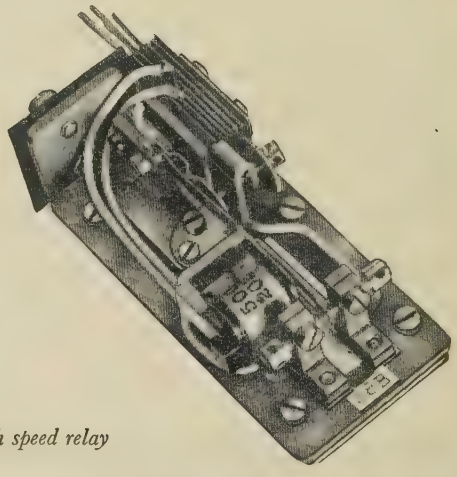

High speed relay

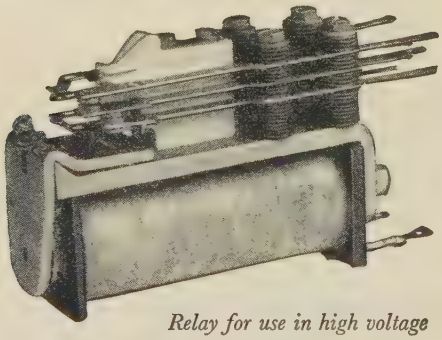

Relay for use in high voltage and high frequency circuits

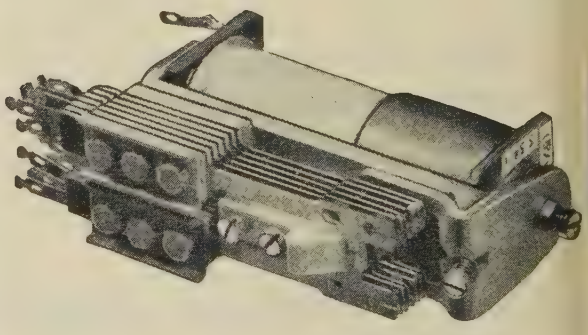

B.P.O. 3000 type relay

The versatility of the telephone type relay has led to its widespread use outside the telephone industry. Our Woolwich Works developed the original BPO 3000 type relay which has since won world renown. With unrivalled experience in the design of relays for a wide variety of special applications, our engineers can give individual attention to problems in this field. **Prototypes can be delivered almost immediately, with bulk supplies following in quick succession.** We would welcome your enquiries.

SIEMENS EDISWAN

SIEMENS EDISON SWAN LTD
An A.E.I. Company
Woolwich, London S.E.18
Telephone: Woolwich 2020 Extn. 621

TAB 506

MUTUAL & SELF INDUCTANCE BRIDGE

Designed for the accurate measurement of either mutual or self inductance and resistance in the range 0·001μH to 30mH and 100μΩ to 3000Ω respectively.

All measurements are made in the form of a four-terminal network and inductance and resistance of leads and clips are not included in the measurement.

Accuracy within ± 1% frequency 1592c/s (ω = 10 000)

Full technical information on this and other 'Cintel' Bridges is available on request.

CINEMA TELEVISION LTD

A COMPANY WITHIN THE RANK ORGANISATION LIMITED

WORSLEY BRIDGE ROAD · LONDON · S.E.26
HITHER GREEN 4600

SALES AND SERVICING AGENTS
Hawnt & Co. Ltd., 59 Moor St. Birmingham, 4
Atkins, Robertson & Whiteford Ltd., Industrial Estate, Thornliebank, Glasgow
McKellen Automation Ltd., 122 Seymour Grove, Old Trafford, Manchester 16

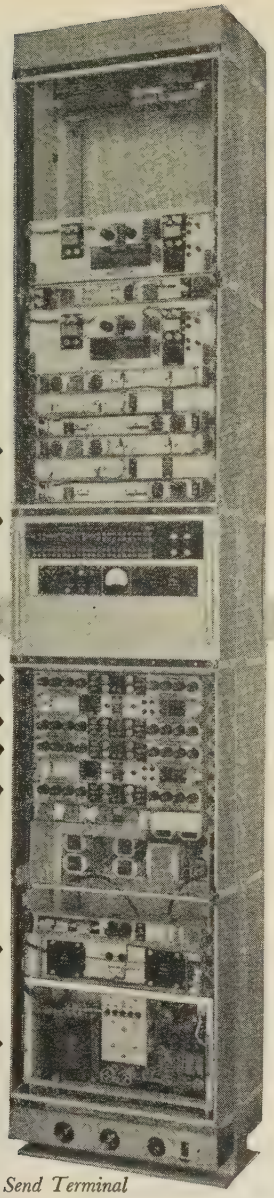

Send Terminal

HESE ILLUSTRATIONS ARE OF A TYPICAL
CHANNEL UNIDIRECTIONAL SYSTEM
Vide range audio input levels
utput 24 kc/s—34 kc/s
or 84 kc/s—94 kc/s

Programme Channel Equipment

CS12/CM

UNIDIRECTIONAL
OR BOTHWAY CIRCUITS
50 c/s—10 kc/s

The overall performance of three systems in tandem (6 terminals) is within the C.C.I.T.T. recommended limits for a 'normal' programme circuit.

Bays may be equipped for either unidirectional or bothway circuits, making the equipment suitable for both studio to transmitter circuits and national telephone network use.

Polyphase modulation is used and a small portable test set is supplied with the equipment for adjustment of the phase modulators.

A bothway channel is complete on one side of a standard 9ft. x 20½ in. rack with power supplies and control panel. The only wiring required to the main carrier system is for the carrier frequencies and input/output leads.

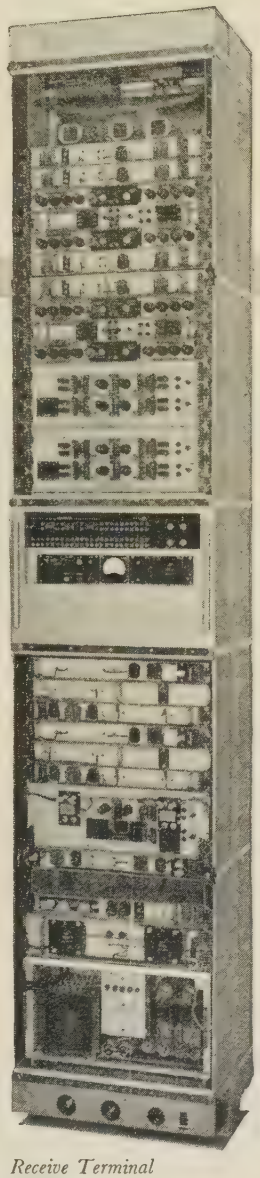

Receive Terminal

extending → **the frontiers of telecommunications**

SIEMENS EDISWAN

SIEMENS EDISON SWAN LTD *An A.E.I. Company*
Telecommunications Transmission Division, Woolwich, London SE18, England
Cables: Sieswan London

TAB 748

silence is...

only just sufficiently quiet, wherever the circuitry is critical. And Fox's potentiometers—Fox-pots—are designed to vary resistance, and not noise-level, within the circuits in which they are used.

They are constructed to do their job in absolute silence—electrical and mechanical—for many years of service, however exacting the local conditions. And every one is accurate within its specified tolerance.

Fox-pots are working all over the world—in purposeful silence. Whatever your requirement in a variable resistor, there is a Fox-pot to meet it. Have a word with our Technical Director.

FOX-POTS P·X·F FOX-POTS

P. X. FOX LTD., DEPT. 215,
HAWKSWORTH ROAD, HORSFORTH, YORKS.

NEWTON-DERBY

LIGHTWEIGHT ELECTRICAL EQUIPMENT

Our manufactures include:

- Aircraft Generators and Motors
- Automatic Voltage Regulators
- Rotary Transformers
- High Frequency Alternators
- H.T. D.C. Generators

The illustration shows a small high-speed fractional H.P. motor and miniature Rotary Transformers for "Walkie Talkie" and other RADIO applications.

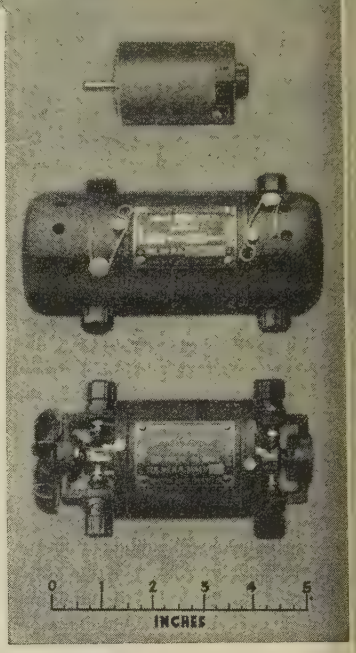

NEWTON BROTHERS (DERBY) LTD.

HEAD OFFICE & WORKS: ALFRETON ROAD, DERBY
TELEPHONE: DERBY 47676 (4 lines) TELEGRAMS: DYNAMO, DERBY
LONDON OFFICE: IMPERIAL BUILDINGS, 56 KINGSWAY W.C.2

ILLUSTRATED

$\frac{3}{16}$ **DETACHABLE BIT MODEL** (List No. 64.) (Factory bench line assembly, etc.)

PROTECTIVE SHIELD (List No. 68).

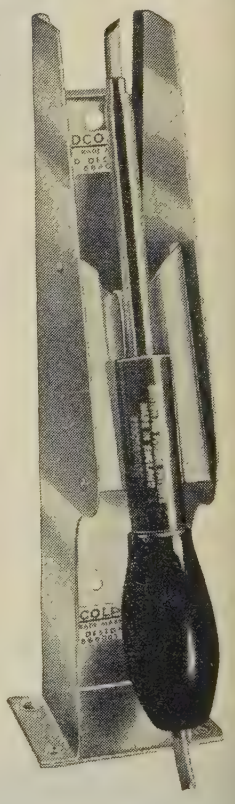

SOUND SOLDER JOINTING

Uniformity of shape, brightness of colour cofirnms permanent joints in any **SOUND UNIT.**

Sound Units are made with **SOUND JOINTS**

Sound Joints are only made by using

ADCOLA
(Regd. Trade Mark)
PATENTED

SOLDERING INSTRUMENTS and EQUIPMENT

Catalogues

Head Office, Sales and Service

ADCOLA PRODUCTS LTD.
GAUDEN ROAD
CLAPHAM HIGH STREET
LONDON, S.W.4

Telephones:
MACaulay 4272 & 3101

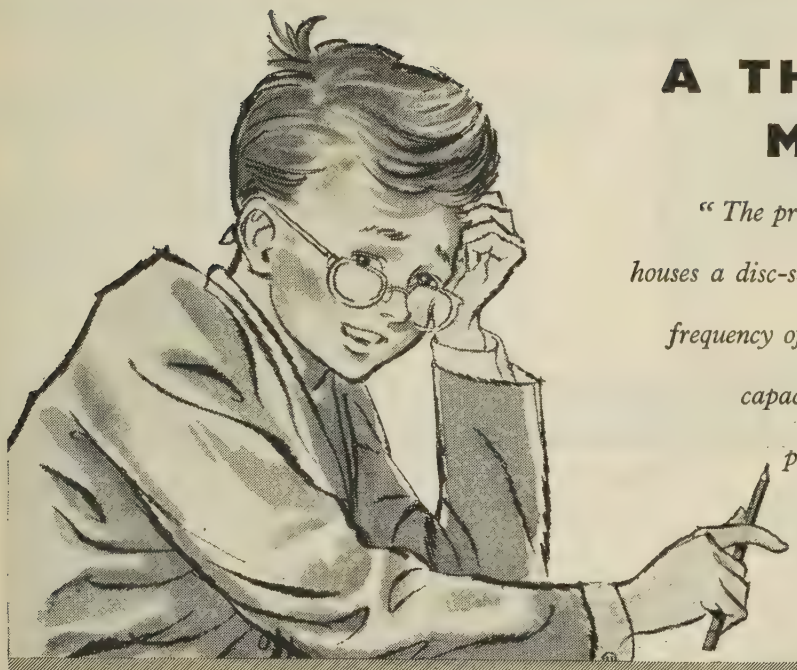

A THOUSAND MEGACYCLES!

" The probe unit used for a.c. measurements houses a disc-seal diode rectifier whose resonant frequency of 3,000 Mc/s, low inter-electrode capacitance and short transit time make possible a frequency range extending to no less than 1,000 Mc/s."

WHERE *does* our young friend get all his information about Marconi instruments? He certainly knows all about our new TF 1041A. He knows that, in addition to its unequalled performance in a.c. measurements, it measures balanced or unbalanced d.c. voltages and a wide range of resistance values. He knows that it has a large mirror-scale meter for fast, precise reading. He knows that there are three optional accessories for extending the a.c. and d.c. ranges and for making measurements on coaxial lines. In short, there's nothing about the TF 1041A that he *doesn't* know.

Infuriating, isn't he? Still, there's no reason why you shouldn't be just as well-informed. All the facts about this Marconi instrument are given in our leaflet K113. If you'd like a copy, you have only to ask. That's the way to get information about *any* Marconi instrument. Just ask.

THE *NEW* MARCONI
VACUUM TUBE VOLTMETER Type TF 1041A

A.C. Measurement: Range: 0·05 to 300 volts, or to 2 kV using multiplier. Frequency Response: ±0·2 dB from 50 c/s to 450 Mc/s, —1 dB at 20 c/s, +2 dB at 1000 Mc/s. Input Impedance: 5 MΩ at 1 kc/s with 1·5 μμF in shunt.

D.C. Measurement: Range: 0·02 to 1000 volts, or to 30 kV using multiplier. Input Resistance: 40 MΩ balanced.

Resistance Measurement: Range: 0·2 ohm to 500 MΩ.

MARCONI INSTRUMENTS

AM & FM SIGNAL GENERATORS · AUDIO & VIDEO OSCILLATORS · FREQUENCY METERS · VOLTMETERS POWER METERS · DISTORTION METERS · FIELD STRENGTH METERS · TRANSMISSION MONITORS DEVIATION METERS · OSCILLOSCOPES, SPECTRUM & RESPONSE ANALYSERS · Q METERS & BRIDGES

MARCONI INSTRUMENTS LTD · ST. ALBANS · HERTFORDSHIRE · TELEPHONE: ST. ALBANS 56161

London and the South: Marconi House, Strand, London, W.C.2. Tel: COVent Garden 1234

Midlands: Marconi House, 24 The Parade, Leamington Spa. Tel: 1408 *North:* 30 Albion Street, Kingston-upon-Hull. Tel: Hull Central 16347

WORLD-WIDE REPRESENTATION

TC 113

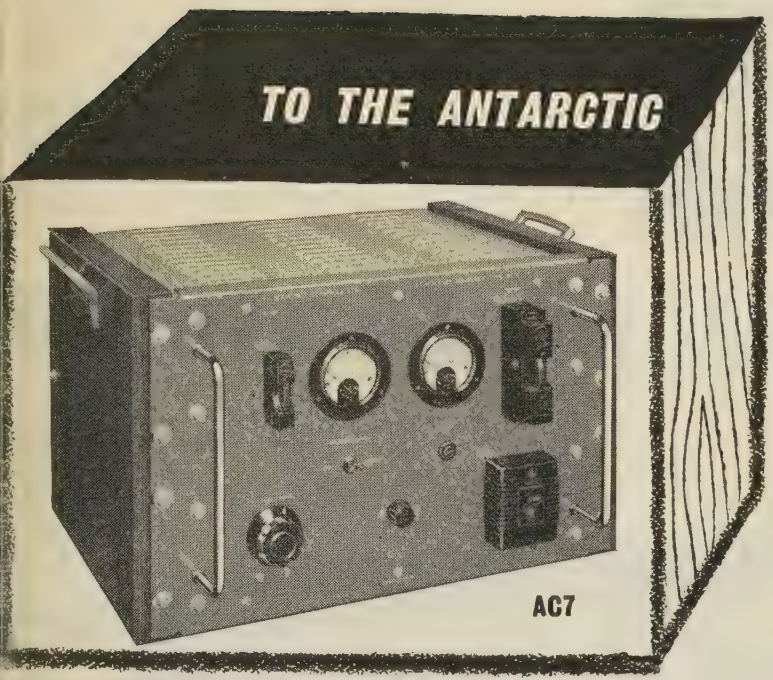

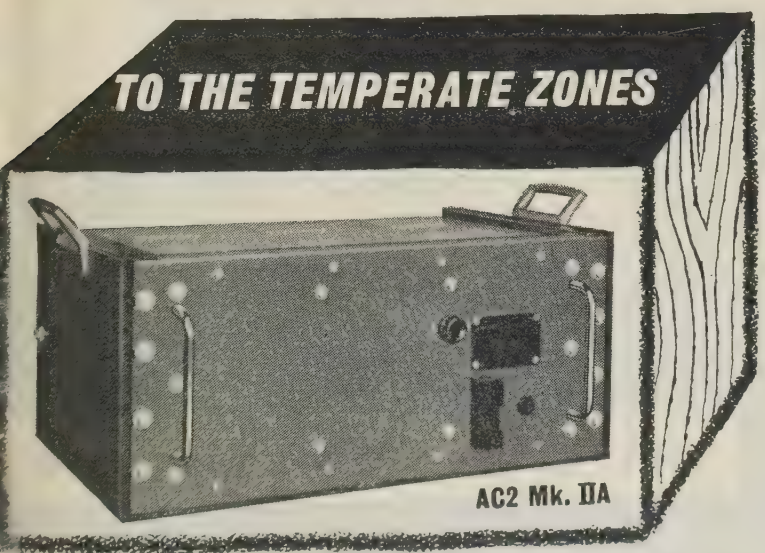

SERVOMEX

standard A.C. stabilisers give A.1 service in all climates for ONE price

SERVOMEX a.c. voltage stabilisers are in use in the I.G.Y. programme in the Antarctic and in tropical Nigeria. These are in every way identical with the instruments in common use in this country. By extremely conservative design and by using components selected from the current inter-service approved list wherever possible, a very high degree of reliability is achieved. They will all withstand shock accelerations up to 40 g. These instruments introduce no distortion in the waveform whatever, and are not upset by changes of frequency, power factor, temperature, etc.

AC2 Mk. IIB and IIA

- 0 to 9 amps
- Range minus 17.5% to plus 8.75%
- 15 volts per second

AC7

- 0 to 30 amps
- Range minus 20% to plus 10%
- 12 volts per second

Technical data sheets are available on request

Servomex Controls Limited, Crowborough Hill, Jarvis Brook, Sussex. Crowborough 1247

Redifon

— THE WORLD'S LEADIN

introduce the GR.40(

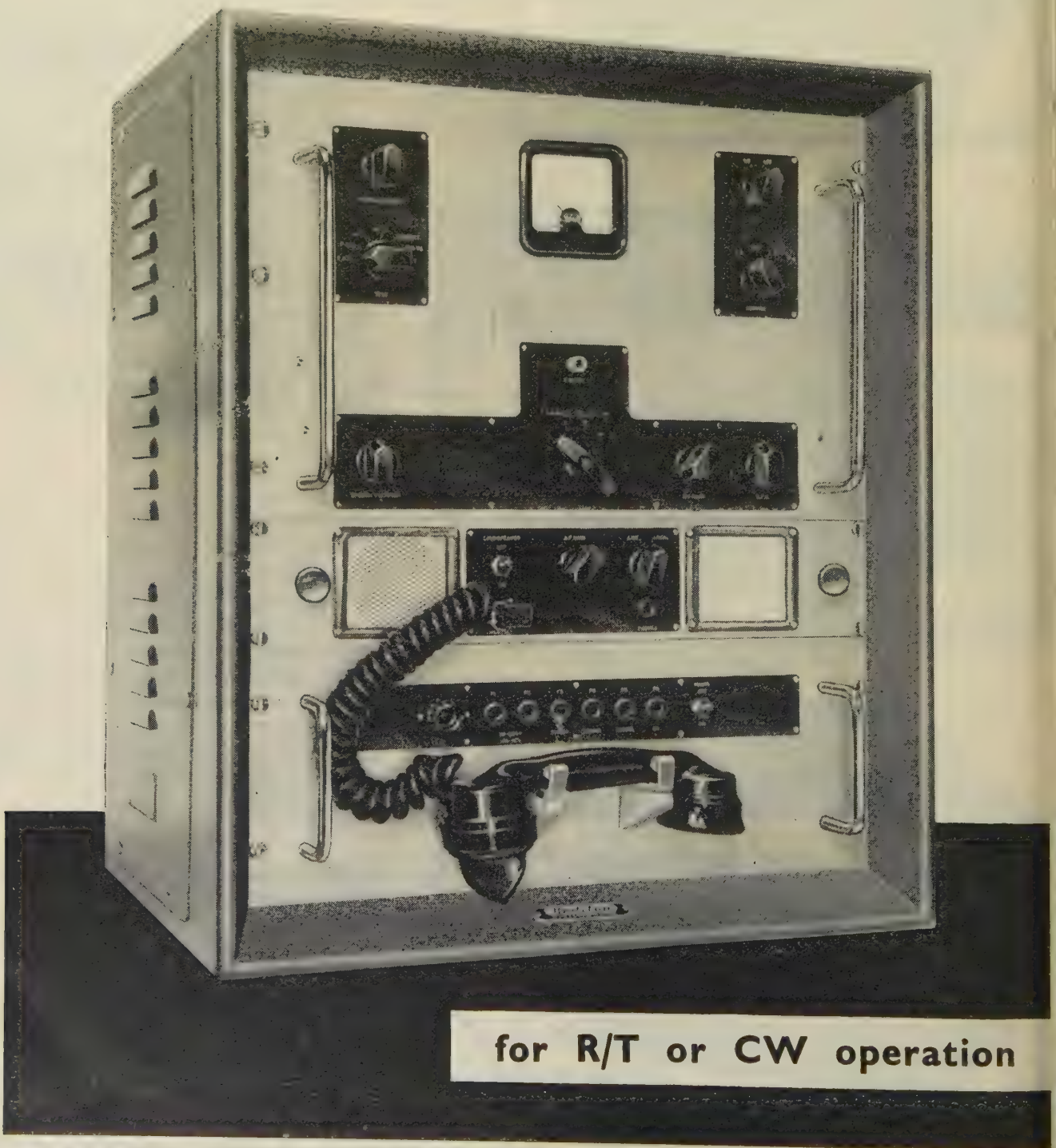

for R/T or CW operation

INDEX OF ADVERTISERS

THE PROCEEDINGS OF
THE INSTITUTION OF ELECTRICAL ENGINEERS

EDITED UNDER THE SUPERINTENDENCE OF W. K. BRASHER, C.B.E., M.A., M.I.E.E., SECRETARY

VOL. 105. PART B. No. 21 MAY 1958

681.374.32:681.142:621.382

The Institution of Electrical Engineers
Paper No. 2585 M
May 1958

A BASIC TRANSISTOR CIRCUIT FOR THE CONSTRUCTION OF DIGITAL-COMPUTING SYSTEMS

By P. L. CLOOT, M.Sc.(Eng.).

(*The paper was first received* 15*th October*, 1957, *and in revised form* 15*th January*, 1958.)

SUMMARY

There is a large field of application of digital-computing techniques where reliability and simplicity are far more important than speed. A basic circuit is described which uses one transistor, one capacitor and three resistors, from which a complete digital-computing system may be constructed economically. A system using this circuit is extremely simple to design, construct and maintain, and should prove very reliable, although it cannot achieve the speed of operation of systems using more complex circuits. The way in which well-known computer circuits are constructed from this basic circuit is described, and an account is given of a complete logical system, employing 184 such circuits, which was constructed to demonstrate their application.

LIST OF SYMBOLS

i_b = Current drawn from the base of a saturated transistor.
i_c = Current flowing from the collector of a saturated transistor.
V = Supply voltage relative to emitter potential.
R_A = Resistance between base and positive supply.
R_B = Resistance of the coupling network between transistors.
R_C = Collector load resistance.
C = Capacitance in parallel with R_B.
β_s = Collector-current/base-current ratio for a transistor just saturated with a collector current of 10 mA.
V_s = Potential difference between the collector and emitter of a saturated transistor.
i_k = Collector current flowing in a transistor in its 'off' state.
V_k = Voltage of the base above the emitter necessary to reduce i_k to a minimum.
n = Number of input terminals driven from one output terminal.
m = Number of input terminals of an 'and' gate.
p = Number of input terminals of an 'or' gate.

(1) INTRODUCTION

Much emphasis in the design of digital-computing circuits is currently placed on increasing their speed of operation, and for mathematical computation using large universal machines this increase in speed is still needed. However, in the next few years digital techniques will be applied to the solution of a large range of problems in which speed is of far less importance than reliability and simplicity. Such problems arise in the fields of data-handling and process control, where the speed at which information is to be handled is limited by some physical process and the amount of computation to be performed is small. Simple systems using frequencies sometimes as low as 50 c/s are required for data transmission and for automatic traffic control, while the control of manufacturing operations or the monitoring or processing of data referring to such operations may require digit rates of no more than a few kilocycles per second.

The special-purpose computers required for these operations must be as simple as possible to design and maintain, and their reliability is in some cases far more important than that of universal machines solving mathematical problems, since an error may well have immediate physical consequences. The present work gives an account of the design and application of a basic transistor circuit suitable for such special-purpose computers. Its simplicity makes it possible to formulate a set of design rules which take account of the variation in electrical characteristics of every component part of a computer. By observing these simple rules the logic of a system may be planned with confidence, and effort may be concentrated on the mechanical design, which is at least as important as the electrical design in any large system.

(2) CHOICE OF COMPONENTS

A digital computer requires elements capable of power amplification, information storage and logical decision. A source of power is also needed, and a means of defining time intervals is generally required. For a system to be reliable it must only use well-established components, and the choice of amplifiers lies between valves and transistors. There is little doubt that transistors will ultimately replace valves in all digital equipment, because of their smaller size and power consumption and greater reliability and efficiency as switches, and they are preferred to valves for this reason. The most important reason for the slow rate of introduction of transistors has been their

Written contributions on papers published without being read at meetings are invited for consideration with a view to publication.
Mr. Cloot is with Metropolitan-Vickers Electrical Co. Ltd.

low speed in comparison with valves, but this is no great disadvantage in the present application.

Information may be stored by using two amplifiers to form conventional bistable circuits, so that no different components are required for storage. In order to perform logical functions a component with a non-linear characteristic is required, and the choice for the present system lies between point-contact diodes, junction diodes and transistors. If point-contact diodes were used, their high forward voltage drop would necessitate the use of amplifiers after logical gating operations, and, although the forward voltage drop of junction diodes is much lower, some separate amplifiers would still be required. By using transistors as logical elements, gating and amplification could be carried out in the same component, and the total number of components thus reduced. The only possible objection to this procedure is that a transistor costs about twice as much as a diode; but the price of transistors has been falling steadily and will continue to fall for some time, and they have therefore been chosen as logical elements for the present system. The greater component cost is more than compensated for by the increased simplicity of the resulting circuits, so that the overall cost of a computing system using the present techniques would almost certainly be less than that of one using more conventional methods.

The power required is provided by means of two fixed-voltage supply lines, with resistors to define the currents drawn, and time intervals are established by the use of capacitors. In order to simplify the construction and maintenance of a system the number of different components used has been kept to a minimum, as also has the number of basic circuits. In fact only one basic circuit is used, comprising a transistor, a capacitor and three resistors.

(3) THE BASIC CIRCUIT

The ideal characteristics of a combined logical element and power amplifier are those of a switch, which in its 'off' state has no power supplied to its two input terminals and is open-circuited at its two output terminals, while in its 'on' state the output terminals are short-circuited by the application of a small amount of power to the input. By earthing the emitter of a transistor, a 3-terminal device with characteristics approaching this ideal may be obtained, and the basic circuit will always be treated as a switch having only two distinct steady states. The 'on' state of the transistor shown in Fig. 1 is defined by drawing

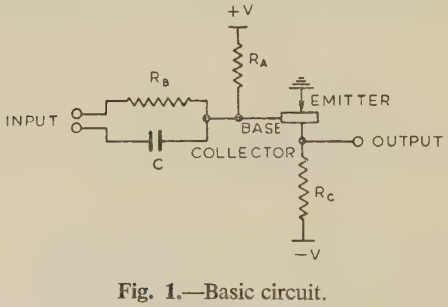

Fig. 1.—Basic circuit.

R_A = 120 kilohms. V = 12 volts.
R_B = 18 kilohms. C = 1 000 pF.
R_C = 1·2 kilohms.

sufficient base current, i_b, from its input terminal to saturate it, so that the emitter-collector impedance is very small and the current flowing in the collector circuit, i_c, is effectively determined by the collector load resistance, R_C, and the supply voltage, V. The 'off' state is such that the potential of the base is raised above that of the emitter by an amount, v_k, sufficient to reduce the collector current to a very small value, i_k. If th input to a similar circuit is connected to the output terminal, range of values of R_B can be chosen such that the second transi tor will be on when the first is off, and vice versa.

It will be shown from eqn. (1) that the number of transisto which may be held in saturation by coupling their inputs t the output of a transistor in its 'off' state is a maximum whe the coupling resistance is zero. Since the collector potential a saturated transistor can rise above its base potential, a syste with zero coupling resistance could be made to work reliably and has in fact been employed in several computers,[2, 3, 4] whic thus consist almost entirely of transistors and collector loa resistors. However, the exclusion of all reactive componen makes the performance of any timing or memory functions mo complicated, and more basic units are required to carry ou such operations than is the case in the present system. Th inclusion of the resistance R_B does reduce the number of circui which may be driven from one output, and reduces the speed a which the switches may be changed from one state to the othe but the addition of a capacitor C in parallel with R_B more tha compensates for this reduction in speed, and, in addition, b separating the inputs to R_B and C, the circuit may be used fo timing and memory functions.

(3.1) Choice of Component Values

In choosing the values for the components of the basic circui the transistor parameters which are significant are β_s, v_s, and v_k. Three restrictions are placed on the combination c basic circuits to form a logical system by these parameter The limit to the number of transistors, n, which may be saturate when connected to the output of a transistor in its 'off' state ma be shown to be given by

$$n \leqslant \beta_s\left(1 - \frac{R_C}{V} i_k\right) - \frac{R_B}{R_C} \quad . \quad . \quad . \quad . \quad (1$$

$R_c i_k / V$ is the ratio of the values of collector currents which flow in a transistor in its 'off' and 'on' states, and should ideally b zero. From eqn. (1) it may be seen that n is a maximum whe R_B is zero, tending to β_s as i_k tends to zero.

The methods of combining 3-terminal switches to form logica 'or' and 'and' gates are well known, and are illustrated in Figs. and 3 for a system in which a '0' is represented by earth potential

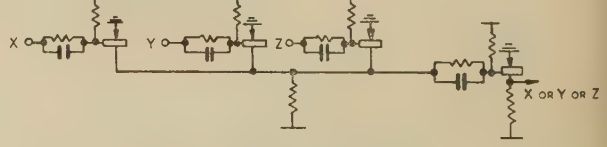

Fig. 2.—'Or' gate.

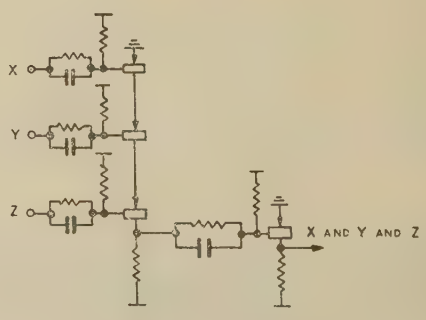

Fig. 3.—'And' gate.

nd a '1' by a negative potential. By considering an 'or' gate, here n transistors are driven from the common collector load f p input transistors connected in parallel, eqn. (1) gives

$$p \leqslant \frac{1}{i_k}\frac{V}{R_C}\left[1 - \frac{1}{\beta_s}\left(\frac{R_B}{R_C} + n\right)\right] \quad . \quad . \quad . \quad (2)$$

n an 'and' gate, the number of input transistors, m, which may e connected in cascade so that the base potential of the output ransistor is positive by an amount v_k when all the input transis- ors are on, may be shown to be limited to

$$m \leqslant \frac{VR_B - v_k(R_A + R_B)}{v_s R_A} \quad . \quad . \quad . \quad . \quad (3)$$

From the tests carried out on a batch of transistors (see ection 10.1), the limits assumed for the transistor parameters for emperatures up to 35° C are

$$\beta_s > 25;\ v_s < 0{\cdot}15 \text{ volt};$$
$$i_k < 37\,\mu\text{A};\ v_k < 0{\cdot}20 \text{ volt}.$$

t is evident from eqns. (1)–(3) that no single set of values for he circuit components will give maximum values for n, p and m, nd a compromise must therefore be made. Eqns. (1) and (2) equire R_B/R_C to be small and V/R_C large, while eqn. (3) requires oth V and R_B to be large, and R_A small. The manufacturers ecommend limits of 10 mA and 15 volts for i_c and V, and the alues chosen were: $V = 12$ volts; $R_C = 1{\cdot}2$ kilohms. he value of R_B should be small to satisfy eqns. (1) and (2), nd large to satisfy eqn. (3). In addition, it should be large or reasons given in the next paragraph, and the largest value hich would give useful limits for n and p was $R_B = 18$ kilohms. qn. (3) requires that R_A should be small, while neglecting it in qns. (1) and (2) is justifiable only if it is large compared with $_B$ and R_C. A value $R_A = 120$ kilohms is sufficiently small to ive a useful limit to m without affecting eqns. (1) and (2) gnificantly.

In order to switch a transistor on or off rapidly, the capacitance f the input network should be large, although the same switch- g speeds can be achieved with a smaller capacitance if R_B is ncreased. A small capacitance is desirable, since the connection f a capacitive load to the driving transistor affects the driving aveform considerably, especially during turn-off. The value f C which will give minimum switching time for a system of witches will depend on the number driven in parallel from each ollector. With $R_B = 18$ kilohms, a capacitance $C = 1\,000$ pF ves switching times for a single transistor of less than ·7 microsec (see Section 10.2), and less than 5 microsec if as any as nine are driven in parallel.

(3.2) Design Rules

By substituting in eqns. (1), (2) and (3) the component values st chosen and the limiting values of parameters obtained from he batch tests, the limits to the number of transistors which may e interconnected at temperatures up to 35° C are

$$\left.\begin{aligned} n &\leqslant 9 \\ p &\leqslant 10 \text{ (for } n \leqslant 9) \\ m &\leqslant 8 \text{ (for } n + m \leqslant 9) \end{aligned}\right\} \quad . \quad . \quad . \quad . \quad (4)$$

he restriction of m if more than one 'and' gate input is driven om one collector is necessary because each transistor in an n' gate carries the base currents of the transistors below it, addition to the normal collector current.

ules corresponding to any other temperature limit may be tb ined by substituting the appropriate value of i_k. For example, the maximum operating temperature recommended for the type GT3 transistor is 55° C ($i_k < 188\,\mu$A), and for any temperature up to this eqns. (1) and (3) show that the limits for n and m remain unchanged. From eqn. (2), the limit for p is given by

$$p \leqslant 2{\cdot}15(10 - n) \quad . \quad . \quad . \quad . \quad . \quad (5)$$

(3.3) Component Tolerances

The values of the transistor parameters used in deriving the design rules have been chosen to permit reliable operation of any type GT3 transistors likely to be encountered, and unless the characteristics of the transistors deteriorate, or circuits are operated too near their maximum speed, they should never cause a failure. Although no tests have been made of their long-term stability, the fact that the maximum continuous power dissipation in any transistor is only 1·5 mW should be advantageous. The peak dissipation in a transistor with a capacitive load during turn-on may rise to 150 mW, but the average over a period of 10 microsec would still not exceed 16 mW. All units have passed a simple switching test (see Section 10.2) and it should now be possible to dispense with individual tests altogether.

Considerable tolerance may be allowed in the value of C unless the circuits are required to operate too near their maximum speeds, while the resistances and supply voltages become critical only if the limiting cases defined by eqns. (1)–(3) are approached. The design rules may easily be modified to allow for any required tolerance by adjusting the circuit component values in these equations by the appropriate amount. For example, if ±10% tolerance is to be accommodated in V, R_A, R_B and R_C, with the worst possible accumulation of errors eqn. (4) becomes

$$\left.\begin{aligned} n &\leqslant 6 \\ p &\leqslant 7 \text{ } (n \leqslant 6) \\ m &\leqslant 8 \text{ } (n + m \leqslant 9) \end{aligned}\right\} \quad . \quad . \quad . \quad . \quad (6)$$

(4) COMPUTER CIRCUITS

Examples are now given of the way in which the basic circuit of Fig. 1 may be used to build any of the circuits required in a digital computer,* and since the same circuit is used throughout an abbreviated notation may conveniently be used. This is illustrated in Fig. 4 for circuits in which the capacitor and

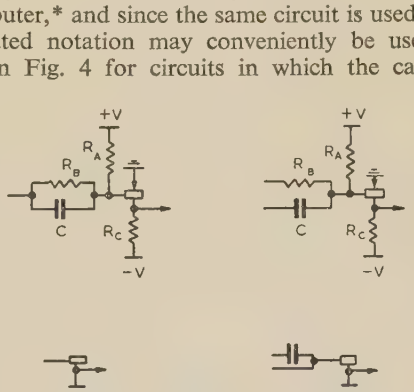

Fig. 4.—Abbreviated notation.

resistor are connected to the same or to different inputs. A line connected to a base represents R_B and C in parallel, unless the two input terminals are connected to different points, in which case the line represents R_B only, and a conventional capacitor symbol is used for C. The negative supply is represented by a horizontal bar, and a vertical line connected to it represents R_C if it is connected to a collector, and R_B if to a base. The current supply provided through R_A, which is connected to every transistor, is omitted from the abbreviated notation, as also are connec-

* Patents applied for.

tions between emitter and earth, which are to be understood wherever no other connection is made to the emitter.

The method of using transistors to construct gates has already been discussed, and it is only necessary to remember that the output from a gate is inverted unless the gate is followed by an output transistor, as shown in Figs. 2 and 3. It should be noted that when the emitters of several transistors are connected to one collector, only one of these transistors may be switched on at a time. By cross-coupling two basic circuits the familiar Eccles–Jordan bistable circuit may be obtained. The state of such a circuit may be changed either by the use of a third transistor for switching, or by applying a voltage step to one of the capacitor input terminals. If the switching transistor shares the collector load of one of the transistors to form an 'or' gate, that transistor may be switched on by turning on the switching transistor. If the switching transistor is connected in the emitter circuit of one of the transistors to form an 'and' gate, that transistor may be switched off by turning off the switching transistor. By disconnecting one of the capacitor input terminals from the opposite collector, a positive step may be applied to it to turn off one of the transistors if it was on, or a negative step to turn it on if it was off. For convenience in referring to circuits, the convention is adopted that a digit is represented by the voltage level of the right-hand collector, earth potential representing a '0', and a negative potential a '1'.

By returning the resistor input terminal of one of the transistors of a bistable circuit to the negative supply line, a monostable circuit may be obtained. With the component values chosen in Section 3.1 this circuit remains in its unstable state for about 41 microsec after being triggered.

(4.1) Scale-of-Two Circuit

A simple scale-of-two circuit may be constructed from three basic circuits, as shown in Fig. 5. In the absence of any change

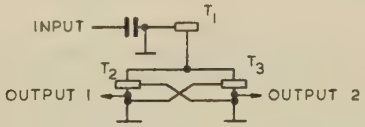

Fig. 5.—Scale-of-two circuit.

in the input, T_1 is saturated and T_2 and T_3 form a bistable circuit. A negative step at the input will have no effect on the state of the circuit, but a positive step will switch off T_1, so that the common emitters of T_2 and T_3 will fall towards the negative supply potential. If T_2 is initially on, the negative step occurring at its collector is transmitted through the cross-coupling capacitor to the base of T_3, so that when T_1 starts to conduct again the base of T_3 is at a lower potential than that of T_2, and T_3 is therefore switched on instead. This change will take place as long as the charge on the cross-coupling capacitor has not leaked away before T_1 is switched on again. With the same values for C and R_B in all three input networks this condition will always be met, since the capacitor in the bistable circuit is discharging from earth to $-V$, while that connected to the base of T_1 is discharging from $+V$ to $-V$, and T_1 is switched on as soon as the potential at its base has fallen to earth.

The maximum speed of operation of the circuit is limited by the speed at which T_2 or T_3 can be saturated when T_1 again supplies current, and is 50 kc/s using the components chosen.

(4.2) Pulse Separator

A circuit for producing serial timing waveforms P_0, P_1, P_2, etc., is shown in Fig. 6. All the bistable circuits except one

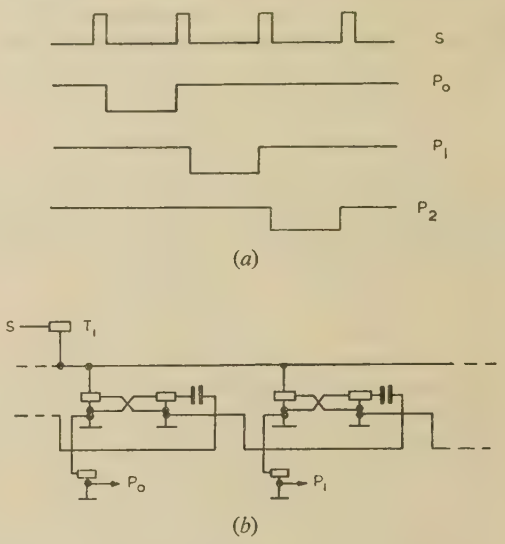

Fig. 6.—Pulse separator.
(*a*) Serial timing waveforms.
(*b*) Pulse-separator circuit.

represent '0's and the current for the one left-hand transistor which is on is supplied by T_1. When this supply is interrupted by waveform S switching off T_1 the right-hand collector of this circuit rises, switching off the right-hand transistor of the following circuit. If the waveform S has fallen again before the base of this transistor has fallen below earth potential, the next circuit will become stable in the '1' state. Pulses defined by an S-waveform of any frequency up to 50 kc/s can be separated by this circuit, and a suitable S-waveform may be obtained from the monostable circuit described above. If the outputs are obtained from additional transistors driven from the left-hand collectors of the bistable circuits as shown in Fig. 6(*b*), a number of transistors may be driven from each P pulse without affecting the maximum speed of the pulse separator.

(4.3) Shift Register

A circuit sometimes required is one capable of storing any configuration of binary digits, and shifting them one digit position on the application of a suitable pulse. Such a circuit, which requires six transistors per stage, is shown in Fig. 7.

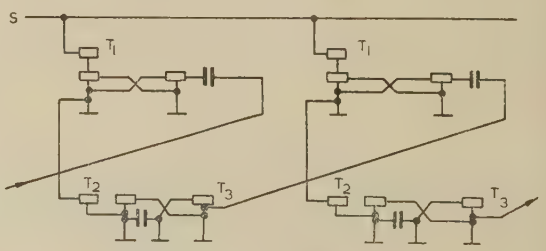

Fig. 7.—Shift register circuit.

The binary digits are stored in bistable circuits similar to those of the pulse separator, except that a separate switching transistor T_1 is required for each stage, as any number of left-hand transistors may be on simultaneously. The shifting waveform S switches all the bistable circuits to their '0' state, and any which were storing '1's trigger their associated monostable circuits through the transistor T_2. The pulse from the monostable circuit passes through a capacitor to the right-hand base of the following bistable circuit, and, provided that S has fallen before

the negative-going pulse from T_3 has ended, this bistable circuit is set to its '1' state. The shift register also operates at any frequency up to 50 kc/s.

(4.4) Static Register

The output from a shift register is obtained by inspecting one of the bistable circuits while the shift waveform is applied, so that each digit in turn is set up on that bistable circuit. It is sometimes necessary to use instead a static register, in which separate bistable circuits are set up to represent each digit of a number which may then be inspected at some later time, and which is retained until a resetting signal is applied to each circuit. Such a register, which requires five transistors per stage, is shown in Fig. 8. If a waveform representing a binary number is

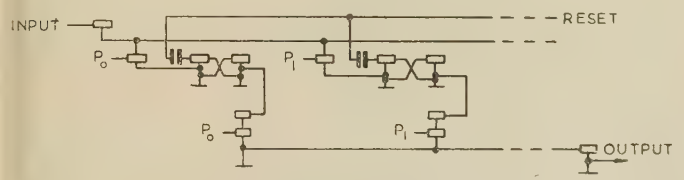

Fig. 8.—Static register circuit.

obtained by gating appropriate P pulses in an 'or' gate, and is then applied to the input terminal, the number will be stored on the bistable circuits, and may be inspected at any time at the output terminal. A positive step applied to the reset terminal will return all the circuits to their zero state.

(4.5) Binary Adder

'And' and 'or' gates may be combined, as shown in Fig. 9,

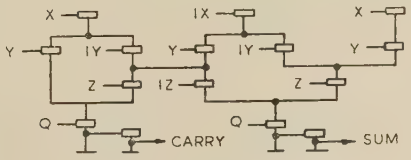

Fig. 9.—Adder circuit.

to form a binary adder which will produce sum and carry digits from three input numbers X, Y and Z and their inverses IX, IY and IZ. In practice it is necessary to sample the outputs to remove the usual unwanted signals which occur due to switching delays, so a sampling pulse Q is included. By feeding the carry output back to one of the inputs via a single-digit delay circuit, a serial adder may be obtained. This delay circuit may conveniently take the form of a single stage of a shift register.

(4.6) Phase-Modulation Circuit

The phase-modulation system of writing on to a magnetic drum requires a signal consisting of a square-wave which is in phase with the clock for every digit period containing a '0', and a square-wave in antiphase with the clock for a '1'. A circuit for producing such a signal is shown in Fig. 10(*a*), with corresponding waveforms in Fig. 10(*b*). If a serial number, X, in which '1's are represented by corresponding P pulses is applied to the input, a negative pulse occupying the half-digit period after a '1' has been completed is generated at A, since the positive step at the end of a '1' switches on T_1, which remains on until G rises. The waveform at B is I (G or X) which is equivalent to (IG and IX), where I represents the inverse of a waveform. The waveform at C is [I (G and DX) or I (IG and IX)], where DX represents X delayed by a digit period, and is the required

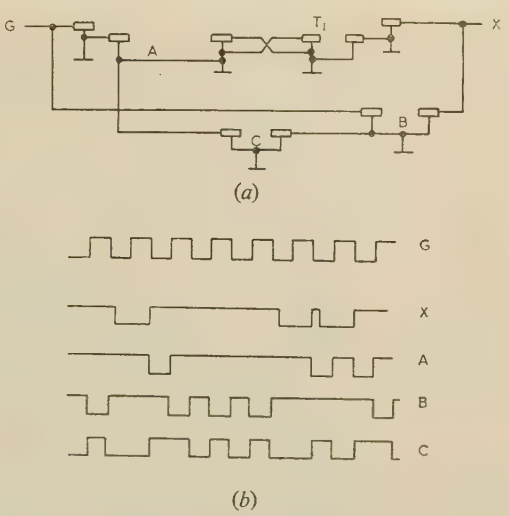

Fig. 10.—Phase-modulation.
(*a*) Circuit.
(*b*) Waveforms.

signal. The delay in the input is necessary since the beginning of a '1' occurs later than the falling edge of the G waveform by the width of the pulse S.

(5) EXPERIMENTAL LOGICAL SYSTEM

To demonstrate the operation of the circuits just described, a logical system has been constructed, comprising two input registers, an adder and an output register, operating serially on an 8-digit binary number. The system is constructed entirely from the basic circuit shown in Fig. 1, with the exception of the input and output equipment (key-switches and indicator lights) and the basic clock waveform which defines the digit periods.

A scale-of-eight circuit driven by the clock supplies a pulse to an 8-stage pulse separator every eighth digit period, and a set of serial timing waveforms (P_0–P_7) is produced. Two sets of key-switches and 'or' gates generate numbers X and Y in which '1's are represented by appropriate P pulses, and these may be set up in two shift registers when required by the operation of pushbuttons. The adder generates the sum of X and Y and sets it up in a static output register by which indicator lamps are operated. Three further pushbuttons are used to reset the registers.

Since one basic circuit only is used, the whole of this logical system may be contained in one type of plug-in unit. The optimum number of basic circuits to be contained in one unit depends on the system to be built, and as the present design was of an experimental nature this number was limited to two. A bench rack containing sockets for 12 such plug-in units was designed, all racks having power supplies and common signal lines provided by interconnecting plugs and sockets. Seven further sockets were provided on each rack for logical interconnections. The complete system requires eight such racks, with a ninth for the manual controls.

The frequency limit of individual circuits has already been given in Section 4, and the system operates at any clock frequency up to 20 kc/s with supply voltages of +12 and −12 volts. The system will operate correctly at 17 kc/s when the supply voltages have been reduced to +3 and −3 volts.

(6) HIGHER SPEEDS

As transistors with higher speeds are being developed, it is interesting to note the performance of samples of some of the

types available. The scale-of-two circuit described in Section 4.1 was redesigned for use with four different types of high-speed transistor, and the maximum scaling frequency with a single transistor load driven from each output is shown in Table 1.

Table 1

SCALE-OF-TWO CIRCUIT PERFORMANCE

Type	Frequency	C	R_B
	Mc/s	pF	kilohms
GT3	0·05	1 000	18
OC44	0·59	200	18
XA102	0·66	200	18
GT13	0·85	200	18
SB100	2·80	50	10

(6.1) High-Speed Circuits with Low-Speed Transistors

The limit to the speed of operation of several of the circuits described in Section 4 is set by the use of differentiating circuits, whose recovery time is necessarily slower than their initial switching time. By designing circuits so that all transistors are driven both on and off, considerably higher speeds may be achieved. As an example of this technique, a scale-of-two circuit with no differentiating couplings is shown in Fig. 11(*a*),

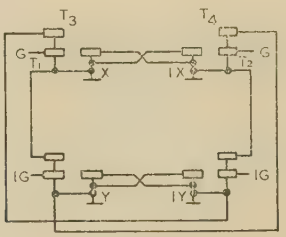

(*a*)

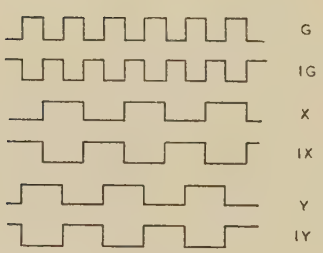

(*b*)

Fig. 11.—High-speed scale-of-two circuit.
(*a*) Circuit.
(*b*) Waveforms.

its waveforms being shown in Fig. 11(*b*). The waveform to be scaled (G) and its inverse (IG) are required to drive the circuit, and four output waveforms are available. The falling edge of G switches on either T_1 or T_2, depending on the state of the lower bistable circuit, which holds one of the transistors T_3 and T_4 on, and the other off. This changes the state of the upper bistable circuit, which is then used in an identical manner with IG to change the state of the lower one.

Such a circuit is clearly uneconomical of transistors, but provides a means of scaling at an input frequency of up to 250 kc/s using type GT3 transistors, as compared with 50 kc/s for the circuit described in Section 4.1.

The technique may be extended to other circuits, and, for example, a shift register capable of the same speed requires four driving waveforms and 10 transistors per stage, as compared with one driving waveform and six transistors per stage for the circuit described in Section 4.3.

(7) CONCLUSIONS

The idea of using standard building units for the construction of a logical system is far from new, but in many of the systems evolved the units themselves are complicated, with many different components and power supplies. With units of such complexity it is often necessary to have several different types to avoid the waste of components, and, while this may not be much of a disadvantage in some large systems, the use of one type of unit only would often be an advantage.

In some systems it is necessary to use complex circuit designs to obtain high speeds, and the present circuit does not attempt to compete in such cases; but it has advantages over existing systems in any field of application of computers where speed is not as important as reliability or ease of construction and maintenance.

The one basic circuit is designed to accept any components of the quality currently available, and rules have been given to enable any system to be designed. Consequently it should be possible to concentrate effort on mechanical design and layout, which are at least as important as the electrical design in making the system reliable. Maintenance and testing would certainly be facilitated by the use of one basic unit only, as also would any system design work.

A disadvantage of these techniques in the construction of a large system is that only a small number of transistors (with the present rules not more than nine) may be driven in parallel, but this is of no great consequence, since, for example, to drive 80 transistors from one point would require 89 basic circuits altogether, while the use of a special driving circuit with more powerful output would still require the 80 basic circuits. If it were considered worth while, the number driven, n, could be increased to about 20 by decreasing R_B, but this would cause a decrease in the maximum speed of operation of the system.

The slightly greater capital expense of the present system, as compared with one using diodes for logical functions, must be borne in mind, but can almost certainly be justified by its advantages.

(7.1) Current Developments

It is not suggested that the plug-in units described in Section 5 are of ideal form for a practical system, and for further work a larger unit with four transistors has been designed. Much of the work in constructing a logical system occurs in wiring the unit sockets on each rack, and the new unit has been designed to permit much of this wiring to be printed. As an example of this a 14-stage shift register is shown in Fig. 12. This circuit uses one printed socket-wiring card and 21 printed plug-in units each containing four basic circuits, and can itself be plugged directly into the main computer assembly.

(8) ACKNOWLEDGMENTS

The author thanks Dr. R. L. Grimsdale for reading the manuscript of the paper and making a number of helpful comments and suggestions, and Dr. Willis Jackson, Director of Research and Education, Metropolitan-Vickers Electrical Co. Ltd., for permission to publish.

(9) REFERENCES

(1) BETER, R. H., BRADLEY, W. E., BROWN, R. B., and RUBINOFF, M.: 'Directly Coupled Transistor Circuits', *Electronics*, 1955, **28**, No. 6, p. 132.

Fig. 12.—Fourteen-stage shift register.

(2) OLSEN, K. H.: 'Transistor Circuits in the Lincoln TX–2', *Proceedings of the Western Joint Computer Conference*, Los Angeles, February, 1957.

(3) GITHENS, J. A.: 'The Tradic Leprechaun Computer', *Proceedings of the Eastern Joint Computer Conference*, New York, December, 1956, pp. 29–33.

(4) MADDOX, J. L., O'TOOLE, J. B., and WONG, S. Y.: 'The Transac S–1 000 Computer', *ibid.*, pp. 13–16.

(10) APPENDICES

(10.1) Measurement of Transistor Steady-State Parameters

A circuit has been constructed to measure β_s, v_s, i_k and v_k under the conditions met in the circuits in which they are to be used. The test circuit has a 4-position switch to select the parameter to be measured, and its value is displayed on a meter. Results are given for tests on a batch of 176 type GT3 transistors, some of which have been in general laboratory use for 18 months, and the limits adopted were:

$$\beta_s > 25;\ v_s < 0{\cdot}15 \text{ volt};$$
$$i_k < 37\,\mu\text{A};\ v_k < 0{\cdot}20 \text{ volt}.$$

Three transistors had parameters outside these limits and were rejected.

The simplest method of checking that the current gain of a transistor, β_s, exceeds a certain minimum at a given value of collector current, i_c, is to set the base current to i_c/β_s, and verify that the collector current which flows does exceed i_c. In order to do this, the collector characteristics of a pilot batch of 50 transistors were plotted, and the ratio between collector and base currents at the point where each became saturated was taken as β_s. (It should be noted that β_s by this definition will always be a little lower than β, the small-signal current gain. From this test it was decided that the minimum value of current gain to be accepted was 25, at a collector current of 10 mA. The test set when switched to measure β_s connects a resistance of 30 kilohms between the base and the negative supply, and measures the collector current flowing. If the current exceeds 10 mA the gain is greater than 25 at that value. The results of the tests carried out are shown in Fig. 13. The

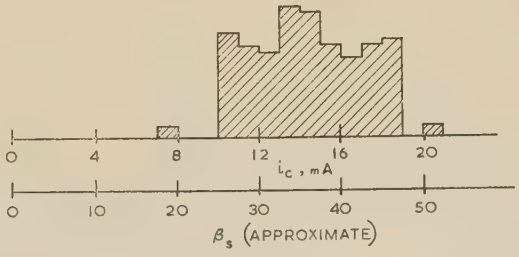

Fig. 13.—Batch test for β_s.

current scale in milliamperes may be multiplied by 2·5 to give β_s approximately, provided that it is remembered that β_s in fact falls a little as i_c is increased. Also a resistance of 600 ohms has been included in the collector lead to limit the power dissipated in the transistor, so i_c cannot increase beyond 20 mA for any value of β_s.

In order to measure v_s, the transistors are switched to their 'on' state using standard component values, and the voltage drop

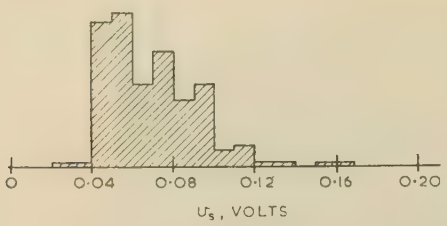

Fig. 14.—Batch test for v_s.

between emitter and collector is measured directly. The results of the tests are shown in Fig. 14.

Again using standard component values, the coupling network of the transistor to be tested is connected by resistances of 15 ohms to earth and 1·2 kilohms to the negative supply. The 15 ohms is used to represent the maximum emitter-to-collector resistance of a transistor in its 'on' state, and an ammeter in the collector lead measures i_k.

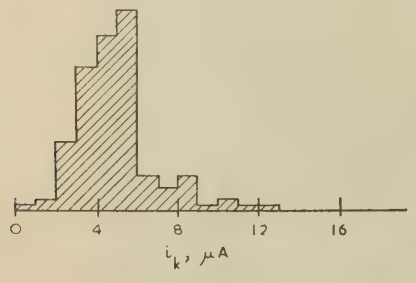

Fig. 15.—Batch test for i_k.

This test was carried out at a temperature of 25° C, and the results illustrated in Fig. 15 show that a design limit of 15 μA may be set for i_k at that temperature. To allow an adequate safety margin for the ambient temperatures likely to be encountered by any equipment in practice, a limit for i_k of 37 μA has been adopted. This corresponds to a temperature of 35° C, following the usual exponential law.

In order to measure v_k, the potential of the base of each transistor is raised by reducing R_A until i_k just reaches a minimum, and the potential of the base relative to the emitter is

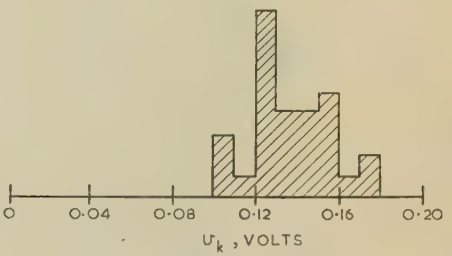

Fig. 16.—Batch test for v_k.

measured. The results obtained from this test are shown in Fig. 16.

(10.2) Transistor Switching Tests

Although it is not intended that these circuits should be operated at their maximum speed, it is necessary to apply at least a simple test to ensure that their frequency response is of an acceptable order. A test set was constructed (using type GT3 transistors) to supply a 100 kc/s square-wave, by which the transistor being tested was switched. The output waveform was inspected using an oscilloscope, and typical measured values of switching times were

Turn-on time = 1·2 microsec
Hole-stage time = 0·4 microsec
Turn-off time = 0·9 microsec

The maximum switching times for any of the 176 transistors tested were 1·7, 0·6 and 1·1 microsec, respectively.

621.382 : 621.317.79

The Institution of Electrical Engineers
Paper No. 2548 R
May 1958

AN INVESTIGATION OF THE CURRENT GAIN OF TRANSISTORS AT FREQUENCIES UP TO 105 Mc/s

By F. J. HYDE, M.Sc., Associate Member, and R. W. SMITH, B.Sc.

(*The paper was first received* 13*th August, and in revised form* 12*th December*, 1957.)

SUMMARY

Apparatus is described by means of which the short-circuit current gain is measured directly. Results of such measurements are presented for commercial alloy-junction and surface-barrier transistors; corrections are applied to yield the internal diffusion-current gain. The effects of stray capacitances on the measurements are discussed. The cut-off frequency of the internal current gain is compared with values derived indirectly from other measurements. For alloy-junction transistors the behaviour is closely in accord with existing one-dimensional diffusion theory, with some reservations, but for surface-barrier transistors the agreement is less close.

LIST OF PRINCIPAL SYMBOLS

A = Emitter area.
α, α_0 = Short-circuit external current gain, and its zero frequency value, between emitter and collector.
α_d, α_{d0} = Short-circuit internal diffusion-current gain, and its zero-frequency value, between emitter and collector.
α'_d, α'_{d0} = Equivalent-circuit current-gain parameter and its zero-frequency value.
C_E, C_C = Emitter and collector depletion-layer capacitances.
C'_C = Sum of collector diffusion capacitance and depletion-layer capacitance.
C_{EB}, C_{EC}, C_{BC} = External stray capacitances between emitter and base, emitter and collector, and base and collector respectively.
D_n, D_p = Diffusion constant for electrons and holes respectively.
e = Electronic charge.
$f_{\alpha d}$ = Cut-off frequency of the internal short-circuit diffusion-current gain between emitter and collector.
$f'_{\alpha d}$ = Cut-off frequency of the equivalent-circuit current-generator parameter.
$\hat{f}$ = Frequency at which the base input reactance, with the emitter and collector earthed, has its maximum value.
f_{max} = Maximum frequency at which a transistor can be made to oscillate.
G = Emitter input-hole-conductance of the 'internal' transistor at zero frequency.
I_E = Emitter current.
k = Boltzmann's constant.
$l_n \equiv (D_n\tau_n)^{1/2}$ = Diffusion length of electrons in p-type emitter.
$l_p \equiv (D_p\tau_p)^{1/2}$ = Diffusion length of holes in n-type base.
$\Lambda = e/kT$.
μ_p = Mobility of holes.
n_p = Equilibrium electron density in p-type emitter region for zero emitter voltage.
p_n = Equilibrium hole density in n-type base.
r_{b0} = Ohmic base resistance.
$r_d \simeq 1/G \simeq kT/eI_E$.
T = Absolute temperature.
τ_n = Bulk lifetime of electrons in p-type emitter.
τ_p = Bulk lifetime of holes in n-type base for low injection-level.
V_E = Applied emitter-to-base p.d.
V_C = Applied collector-to-base p.d.
w = Transistor base-width.

(1) INTRODUCTION

The relationships between the input and output currents and voltages of a 4-terminal network may be written in the general form

$$\left.\begin{aligned} i_1 &= y_{11}v_1 + y_{12}v_2 \\ i_2 &= y_{21}v_1 + y_{22}v_2 \end{aligned}\right\} \quad . \quad . \quad . \quad . \quad . \quad (1)$$

If the network is a one-dimensional transistor, i.e. one in which the emitter-base and collector-base interfaces are planar, and in which recombination of minority carriers on the surface of the base can be neglected, then the admittance, y^*, parameters of eqn. (1), pertinent to diffusive flow of minority carriers across the base, have been shown[1, 2] to be (for a p–n–p type of structure)

$$\left.\begin{aligned} y^*_{11} &= G\theta \coth \theta + Y_n \\ y^*_{12} &= -(G\theta/K) \operatorname{cosech} \theta \\ y^*_{21} &= -G\theta \operatorname{cosech} \theta \\ y^*_{22} &= (G\theta/K) \coth \theta \end{aligned}\right\} \quad . \quad . \quad . \quad . \quad (2)$$

where

$$G = \frac{Ae}{w}\mu_p p_n \varepsilon^{\Lambda V_E}$$

$$\theta = \frac{w}{l_p}(1 + j\omega\tau_p)^{1/2}$$

$$\frac{Y_n}{G} = \frac{D_n n_p w}{D_p p_n l_n}(1 + j\omega\tau_n)^{1/2}$$

$$\frac{1}{K} = \frac{1}{\Lambda l_p}\frac{\partial w}{\partial V_C}\operatorname{cosec}\frac{w}{l_p} + \varepsilon^{\Lambda(V_C - V_E)}$$

In addition to the diffusion (y^*) admittances, the emitter and collector depletion-layer capacitances, C_E and C_C, are required for the complete specification of the internal one-dimensional transistor (Fig. 1). Algebraically it is specified by admittance parameters $y_{11} = y^*_{11} + j\omega C_E$, $y_{12} = y^*_{12}$, $y_{21} = y^*_{21}$ and $y_{22} = y^*_{22} + j\omega C_C$.

Although practical transistors depart from the ideal one-dimensional model in a number of ways, there is considerable evidence to show that the one-dimensional equations, in which τ_p and D_p are given effective values which vary with injection level, represent reasonably well the a.c. performance of low- and intermediate-frequency alloy-junction transistors,[3–6] provided that account is also taken of the external base resistance,

Written contributions on papers published without being read at meetings are invited for consideration with a view to publication.
The paper is an official communication from the Radio Research Station, Department of Scientific and Industrial Research.

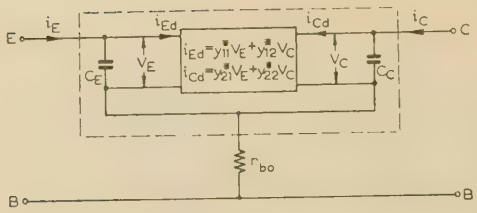

Fig. 1.—Schematic representation of a transistor.

The 'internal' transistor is within the broken line.

r_{b0}. In the remainder of the paper τ_p, D_p and l_p and any terms involving one or more of these parameters should be regarded as having values appropriate to the particular level of injection (emitter current) arising.

The first aim of the present investigation is to see to what extent such modified one-dimensional formulae apply to practical h.f. and v.h.f. alloy-junction and surface-barrier transistors, with particular reference to the frequency dependence of α_d. This parameter is the internal diffusion-current gain or amplification factor between the emitter and the collector and is defined by

$$\alpha_d = -y_{21}^*/y_{11}^* = \frac{1}{\cosh\theta + (Y_n \sinh\theta)/G\theta} \quad . \quad . \quad (3)$$

The form of the locus in the complex plane of α_d as the frequency is varied is shown in Fig. 2, for the special case of $Y_n \to 0$ and $w/l_p \to 0$, so that

$$\alpha_d = \frac{1}{\cosh x^{1/2} \cos x^{1/2} + j \sinh x^{1/2} \sin x^{1/2}}$$

where $x \equiv \omega w^2/2D_p$. For practical non-zero values of w/l_p and Y_n the theoretical locus will lie slightly inside this locus at low

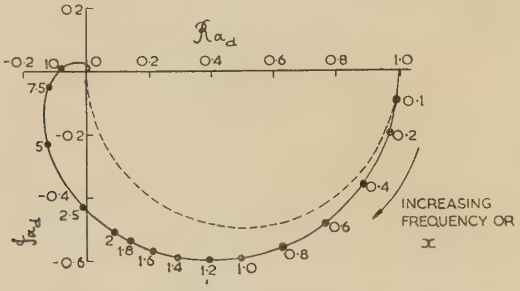

Fig. 2.—Theoretical frequency dependence of the locus of the internal diffusion current gain, α_d, for $w/l_p \to 0$, $Y_n \to 0$.

$x \equiv \omega w^2/2D_p$ is the parameter.

frequencies, but will coalesce with it at high frequencies. (It is assumed that $\omega\tau_n$ is always small compared with unity.) A comparison is made between this theoretical form and the experimentally determined loci of the internal diffusion current gain. These are derived from directly measured values of the external short-circuit current gain $\alpha = -i_C/i_E$ (see Fig. 1) in the frequency range 1–105 Mc/s. The cut-off frequencies, $f_{\alpha d}$,* of the experimental loci of α_d are compared with the theoretical values calculated from the relationship†

$$f_{\alpha d} = mD_p/2\pi w^2 \quad . \quad . \quad . \quad . \quad . \quad . \quad (4)$$

* i.e. that frequency at which $|\alpha_d|$ is reduced to $1/\sqrt{2}$ times its zero frequency value.
† This theoretical value is derived on the assumption that $Y_n \to 0$ and $j\omega C_E \ll y_{11}^*$.

due to Pritchard.[3] Here D_p/w^2 is derived from independent low-frequency measurements of the base-to-collector current gain,[5,6] while m is a coefficient whose value may be taken as 2·5 for most transistors.

The second aim of the work is to compare the values of $f_{\alpha d}$, determined by the two above methods, with the experimentally determined cut-off frequencies of the internal current generator used in the π–T equivalent circuit for the transistor, which was suggested by Angell.[7] Furthermore, it is shown that measurements of current transfer made at frequencies much greater than the useful operating frequencies of transistors may be interpreted in terms of transmission through the passive parameters C_C and r_{b0}.

(2) DETERMINATION OF CURRENT GAIN

(2.1) 'Short-Circuit' Current Gain, α

One method of measuring α is to compare, in amplitude and phase, the voltages developed across equal small resistances, R, in the emitter and collector circuits. Because an external resistance, albeit small, is included in the collector circuit, it is evident that the current gain measured is not rigorously the short-circuit current gain. The effect of R is taken into account, however, in the subsequent analysis. Measurements of this type have already been described by Coffey[8] at frequencies between 1 and 24 Mc/s, and essentially the same method is used here in the range 1–105 Mc/s.

(2.1.1) Measurement of α.

The schematic circuit is shown in Fig. 3. An r.f. signal generator with a balanced low-impedance (150 ohms) output is coupled into the emitter circuit through a wide-band transformer. A small current, i_E, is induced in the emitter circuit and a corresponding current, i_C, flows in the collector circuit. Voltages proportional to these currents, which are developed across the equal small resistances R, are fed via cathode-followers to an Admiralty pattern type FHB h.f. direction-finding receiver[9] for the frequency range 1–21 Mc/s, or intermediately via a twin-channel frequency-convertor unit for frequencies between 21 and 105 Mc/s. The r.f. voltages are amplified and converted to m.f. (450 kc/s) ones before being applied to the plates of a cathode-ray tube to give an elliptical trace. The two receiver channels are accurately matched in gain and phase, so that the attenuation and phase lag of i_C with respect to i_E may be obtained from the orientation and lengths of the ellipse axes.[10]

(2.1.2) Transistor Circuit.

Details of the transistor circuit are given in Fig. 4. It is apparent that any external capacitance, C_{EB}, between the emitter and the base will provide an alternative path to that into the transistor proper for current flowing out of the input transformer. Such by-pass current will contribute to the voltage drop V_{ER} but not to V_{CR} and so will lead to errors in determining α (V_{ER} and V_{CR} are the r.f. voltages developed across the emitter and collector circuit resistances, R, respectively). Some shunt capacitance between emitter and base leads is inherent in the transistor assembly and cannot be avoided. The input-transformer design should be such that any additional capacitance between the non-earthy end and earth is small.* The theory of the design of wide-band v.h.f. transformers[11] suggests that, for efficient coupling, flat-spiral strip windings with thin insulation should be used: capacitance to earth will be made small if narrow strip with as large a number of turns

* Capacitance to earth from the earthy end is not important. It appears virtually in parallel with the resistance R in the emitter circuit and, in consequence, its effect—which in any event is small—is nullified in the balancing operation described in Section 2.1.3.

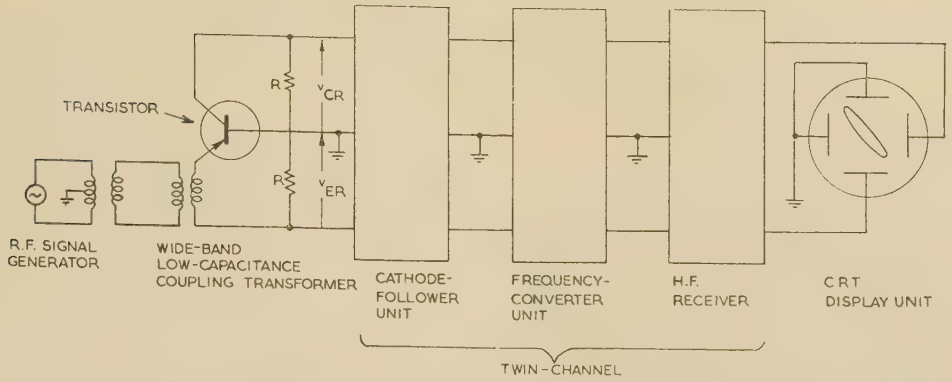

Fig. 3.—Measurement of transistor short-circuit current gain, α, over the range 1–105 Mc/s.

as possible is employed, together with thick insulating strip. The windings used were constructed of $\frac{1}{8}$ in × 4 mil copper strip with $\frac{3}{8}$ in × 5 mil polythene strip insulation, wound on a Ferroxcube type E former. The primary winding (nine turns) was wound first, with the secondary winding (eight turns) outside it, the non-earthy end of the latter being outermost. Coupling between the 150-ohm balanced output of the signal generator and the transistor circuit input impedance of about 100 ohms was adequate over the range 1–105 Mc/s. The capacitance to earth of the secondary winding, C, forming part of C_{EB}, was approximately 1 pF (see Section 2.1.4). The whole transformer was screened to minimize indirect coupling from it to the remainder of the circuit, and rigid output wires from the secondary winding were taken through a hole in this screen.

The following additional precautions were taken to obviate undesirable interaction between the various parts of the circuit:

(*a*) The emitter and collector circuits were separated by a metal screen.
(*b*) 470-ohm carbon resistors were inserted in the cathode-follower feeds, being connected directly to the non-earthy ends of the 51-ohm carbon resistors, R.
(*c*) The feed into the cathode-followers from these resistors was via screened connectors.
(*d*) All leads were kept short.

Despite all such precautions there appear residual stray capacitances (in part originating in the transistor) between emitter, base and collector: these may be designated as C_{EB}, C_{EC} and C_{CB}, where the suffices refer to the pair of electrodes with which the capacitance is associated. Their effect on the short-circuit current gain is considered in Sections 2.1.5 and 9.

The d.c. circuits were isolated from the r.f. circuits by r.f. chokes and blocking capacitors, the latter having a reactance small compared with R at the lowest frequency. The capacitances used were 0·1 μF up to 20 Mc/s and 0·0015 μF above 20 Mc/s.

(2.1.3) Setting-up Procedure.

The twin amplifying channels must be adjusted to have equal gain and phase characteristics at each measurement frequency. To achieve this the transistor is replaced by a short-circuit between the emitter and collector connectors. R.F. current is then induced in the circuit and, in the absence of stray capacitance in parallel with the collector resistance, equal voltages would be developed across the two resistors R. The adjustment of the receiver balance controls to give a straight line at 45° to the axes of deflection on the cathode-ray tube would then give the alignment sought. Because of the stray capacitance, however, such adjustment includes a built-in factor $(1 + j\omega CR)$ in the gain of the collector channel relative to the emitter channel. Provided that $\omega CR \ll 1$ in the working frequency range, this factor has

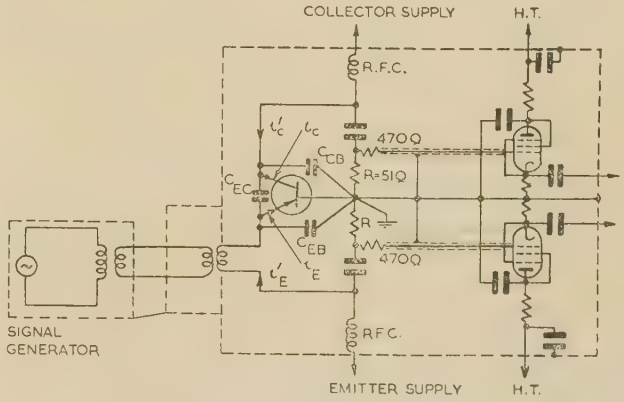

Fig. 4.—Transistor circuit for measurement of current gain.

negligible influence in subsequent transistor measurements. For $f = 10^8$ c/s, $R = 51$ ohms and $C = 1{\cdot}0$ pF, $\omega CR = 0{\cdot}032$, which is much less than unity, as required.

(2.1.4) Assessment of Performance.

Fig. 5(*b*) shows the semicircular transmission locus drawn through the experimental points (dots) for a network [Fig. 5(*a*)]

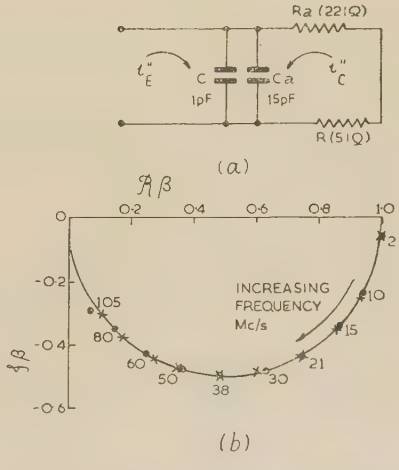

Fig. 5.—Transmission loci.
(*a*) *RC* network used.
(*b*) Loci of current transmission, β.
—●—●— Experimental.
—×—×— Theoretical.

consisting of a capacitance, C_a, of 15 pF in parallel with C and a resistance, R_a, of 221 ohms in series with the 'collector' resistance, R, of 51 ohms. The theoretical expression for current transmission, β, is

$$-i_C''/i_E'' = \frac{1}{1 + j\omega(C + C_a)(R + R_a)}$$

Because of the gain factor $1 + j\omega CR$ built in during balancing, the experimental points should be compared with theoretical points calculated from $(1 + j\omega CR)/[1 + j\omega(C + C_a)(R + R_a)]$. If $\omega CR \ll 1$, however, the numerator can be taken to be unity. Theoretical points calculated on the assumption that this was the case are shown as crosses in Fig. 5(*b*), a value for C of 1 pF being used in the denominator. The agreement between experimental and calculated values is good. As well as leading to an approximate value for C, these measurements also indicate satisfactory performance of the equipment over the whole frequency range.

The neglect of the inductances arising in the 'collector' loop in the above analysis is justified by the quality of the fit between experimental and theoretical points shown in Fig. 5(*b*).

(2.1.5) Effect of Stray Capacitances on the External Current Gain.

We wish to measure $\alpha = -i_C/i_E$, where i_E and $-i_C$ are the currents entering and leaving the emitter and collector electrodes respectively. In practice we measure $\alpha' = -i_C'/i_E'$, where i_E' and i_C' are the currents that flow in the equal resistances, R, in the emitter and collector circuits. The relationships between these currents are governed by the stray interelectrode capacitances referred to in Section 2.1.2 and Fig. 4. To take account of these capacitances analytically and so determine α from α' would be cumbersome, as may be seen from Section 9. The stray capacitances would seem to be about 1 pF,[12] but the difficulty of determining precise values precludes such an analytical correction in any event. The analysis carried out in Section 8 is useful, however, because it shows that, provided that $\omega C_{CB}R \ll 1$, the effect of C_{CB} can be ignored and the effects of both C_{EB} and C_{EC} are smaller, the smaller are the individual values of r_{b0} and C_C. Hence the smaller is $r_{b0}C_C$ the higher is the limiting frequency at which the effects of stray capacitance produce a marked disparity between α and α'. To define such a limiting frequency in the present work, an arbitrary criterion was adopted, namely that the addition of an extra capacitance of 1 pF to augment C_{EB} and one of 0·5 pF to augment C_{EC} did not produce more than a 5% change in either the modulus or phase angle of α'. (C_{BC} can be ignored.) Although measurements of α' are presented in some cases beyond such a limiting frequency, as an indication of the current gain actually arising under the conditions of the measurements, corrections to obtain α_d in accordance with eqn. (7) have not been applied to measurements made above this limiting frequency.

(2.2) Internal Diffusion Current Gain, α_d

Analysis of the circuit shown in Fig. 4 in terms of the transistor representation shown in Fig. 1 leads to the following expression for α:

$$\alpha = -\frac{\dfrac{y_{21}^* + y_{21}^* y_{12}^* r_{b0}}{(y_{11}^* + j\omega C_E)} - r_{b0}(y_{22}^* + j\omega C_C)}{1 + (R + r_{b0})(y_{22}^* + j\omega C_C) - \dfrac{y_{21}^* y_{22}^* (R + r_{b0})}{y_{11}^* + j\omega C_E}} \quad (5)$$

if stray capacitances are ignored. Now, in practice, terms including y_{12}^* may be omitted, while y_{22}^* can be ignored compared with $j\omega C_C$ (see Section 2.2.1). Furthermore, with direct emitter currents greater than a few hundred microamperes for low-power r.f. transistors, $\omega C_E \ll |y_{11}^*|$. Eqn. (5) may therefore be simplified to

$$\alpha = -\frac{\dfrac{y_{21}^*}{y_{11}^*} - j\omega C_C r_{b0}}{1 + j\omega C_C(r_{b0} + R)} \quad . \quad . \quad . \quad . \quad (6)$$

If α is written in rectangular co-ordinate form as $u - jv$, then by rearrangement of eqn. (6),

$$\alpha_d \equiv -\frac{y_{21}^*}{y_{11}^*} = u + v\omega C_C(r_{b0} + R) - j\{v + \omega C_C[r_{b0} - u(r_{b0} + R)]\} \quad (7)$$

It is therefore evident that both r_{b0} and C_C must first be measured if α_d is to be determined. Corrections to the real and imaginary parts of α to yield α_d will increase with increasing frequency.

(2.2.1) Measurement of r_{b0} and C_C.

A direct measurement of r_{b0} is made, while C_C is subsequently deduced from measurement of the product $r_{b0}C_C$. The method used for measuring r_{b0} has been described by Molozzi *et al.*,[13] and is based on high-frequency z-type neutralization of the transistor; Turner's[12] h-type neutralizing method was used to determine $C_C r_{b0}$. These measurements were made with low direct emitter current flowing, thereby ensuring that y_{22}^* was negligible compared with $j\omega C_C$ at the frequency at which the measurements were made (4 Mc/s) for all transistors [eqn. (2) shows that y_{22}^* has a low value under these conditions].

(2.3) Current Transfer at Frequencies above $f_{\alpha d}$

Measurements of current transfer at very high frequencies on transistors designed for l.f. or i.f. working are useful because they throw some light on the passive equivalent-circuit parameters used. Fig. 2 shows that at frequencies exceeding $10f_{\alpha d}$, say, $|\alpha_d|$ will become negligibly small because $y_{21}^* \to 0$. Under these circumstances the transistor tends to behave as a passive circuit element. Because y_{12}^* also tends to zero, while y_{22}^* becomes increasingly smaller than $j\omega C_C$, any current transfer from the emitter to the collector will be determined by the branches comprising r_{b0} in parallel with C_{EB} and C_C in series with R. At frequencies such that

$$\omega C_{EB} \ll \left|\frac{1}{r_{b0}} + \frac{j\omega C_C}{1 + j\omega C_C R}\right|$$

the current transfer is given by

$$-\frac{i_C}{i_E} = \frac{j\omega C_C r_{b0}}{1 + j\omega C_C(R + r_{b0})} \quad . \quad . \quad . \quad . \quad (8)$$

which tends to $r_{b0}/(r_{b0} + R)$ when $\omega C_C(r_{b0} + R) \gg 1$, i.e. the current-transfer locus, which is a semicircle in the first quadrant, will intercept the positive real axis at $r_{b0}/(r_{b0} + R)$. Furthermore, if the frequency, ω_0, at which the real and imaginary parts are equal is determined, $C_C = 1/\omega_0(r_{b0} + R)$. If appreciable current flows through C_{EB}, i.e. if the inequality preceding eqn. (8) is not satisfied, the current-transfer locus will depart from semicircularity at the highest frequencies. It will curve inwards, crossing the positive real axis at $C_C r_{b0}/[C_C(r_{b0} + R) + C_{EB}r_{b0}]$ before passing through the fourth quadrant back to the origin.

(3) DETERMINATION OF $f_{\alpha d}$

(3.1) From Experimental α_d Loci

If $f_{\alpha d}$ is greater than the maximum frequency at which trustworthy measurements of α_d can be made, an estimate of $f_{\alpha d}$ may nevertheless be obtained, provided that the locus of α_d is approximately of the ideal form shown in Fig. 2. The para-

meter $x \equiv \omega w^2/2D_p$ in this Figure becomes 1·2 at the cut-off frequency $f_{\alpha d} = \omega_{\alpha d}/2\pi$, so that, by comparing the frequency of some point on the experimental locus with the value of x at the corresponding point on the theoretical locus, an estimate of $f_{\alpha d}$ is obtained by simple proportion. A similar procedure may be carried out using experimental data for frequencies greater than 1 Mc/s when $f_{\alpha d}$ is less than this.

(3.2) Extrapolation from L.F. Data

L.F. bridge measurements of base-to-collector current gain[5] yield a value for D_p/w^2 which may be used directly in eqn. (4) to calculate $f_{\alpha d}$. This method is similar to the one above, in that an extrapolation is made in terms of one-dimensional theory, but in this case the extrapolation is of greater extent.

(3.3) From π–T Equivalent Circuit

The equivalent circuit shown in Fig. 6 was first proposed by Angell[7] with particular reference to the surface-barrier transistor,

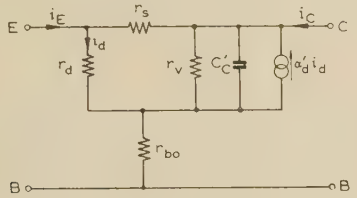

Fig. 6.—π-T equivalent circuit due to Angell.

although it has since been applied to alloy-junction transistors as well. The amplification factor α_d' of the internal current generator is usually assumed to have the following frequency dependence:

$$\alpha_d' = \frac{\alpha_{d0}'}{1 + jf/f_{\alpha d}'} \equiv \frac{\alpha_{d0}'}{1 + jy} \quad . \quad . \quad . \quad . \quad . \quad (9)$$

where $f_{\alpha d}'$ is a cut-off frequency* and α_{d0}' is the zero-frequency value of α_d'. (In practice the zero-frequency value of α, namely α_0, replaces α_{d0}' with negligible error: this is done because α_0 can be measured directly.) Pritchard[14] has shown that a closer approximation to the theoretical form of the amplification factor, α_d, of a transistor is given by

$$\alpha_d' \simeq \frac{\alpha_{d0}'}{1 + jy} \varepsilon^{-jy/5} \quad . \quad . \quad . \quad . \quad . \quad (10)$$

It is therefore more appropriate to use this frequency dependence for α_d' in the equivalent circuit.

Drouilhet[15] has suggested two experimental methods, based on the equivalent circuit shown in Fig. 6, in which the current amplification factor is defined as in eqn. (9), by means of which $f_{\alpha d}'$ may be determined. These are (*a*) measurement of the frequency, $\hat{f}$, at which the base input reactance of the transistor, with emitter and collector earthed, has a maximum value, and (*b*) measurement of the maximum frequency, f_{max}, at which the transistor will oscillate. He showed that the cut-off frequency of the internal current-amplification factor is related to $\hat{f}$ and f_{max} respectively as follows:

$$f_{\alpha d}' = \hat{f}/(1 - \alpha_0) \quad . \quad . \quad . \quad . \quad . \quad (11)$$

$$f_{\alpha d}' = f_{max}^2 8\pi r_{b0} C_C/\alpha_0 \quad . \quad . \quad . \quad . \quad (12)$$

It is more appropriate on theoretical grounds to use α_d' as defined by eqn. (10) for the current amplification factor. Instead of eqn. (11)* we then have

$$f_{\alpha d}' = \frac{\hat{f}(1 + \alpha_0/5)}{1 - \alpha_0} \quad . \quad . \quad . \quad . \quad . \quad (13)$$

This value will be some 20% higher than that deduced using eqn. (11). No correspondingly simple modified expression arises for $f_{\alpha d}'$ in terms of f_{max}, so that eqn. (12) will be used here, bearing in mind that it is based on only a coarse approximation to α_d.

In the present work, measurements of α_0 for use in eqns. (12) and (13) were made using a bridge of the type described by Boothroyd and Almond,[16] and were confirmed using the bridge described by Evans.[5]

* Different authors do not ascribe the same significance to the parameter $f_{\alpha d}'$. This point is discussed by Pritchard.[14]

* In deriving eqns. (11) and (13) the effect of the collector capacitance has been ignored; this point is discussed in Section 5.1.

Table 1

TRANSISTOR PARAMETERS

Transistor type	Fig. 7, curve	V_C	I_E	$r_{b0}C_C$	r_{b0}	C_C	α_0	Cut-off frequency			
								Direct measurement	$\frac{mD_p}{2\pi w^2}$	Equivalent circuit	
										Admittance measurement	Oscillation frequency
		volts	mA	picosec	ohms	pF		Mc/s	Mc/s	Mc/s	Mc/s
TS2	(*a*)	−4·5	1·0	12 200	420‡	29·0§	0·985	0·72†	0·76	0·72	—
EW59	(*b*)	−5·0	1·0	3 550	41‡	86·5§	0·980	1·5	1·8	1·5	—
CK760	(*c*)	−6·0	1·0	750	65‡	11·5§	0·960	4·7	4·3	5·0	—
V6/R8	(*d*)	−4·5	1·0	515	25	20·5	0·987	7·3	7·7	6·5	—
CK762	(*e*)	−6·0	1·0	1 100	70	15·5	0·975	23	22	16	—
L5134	(*f*)	−3·0	1·0	375	102	3·7	0·991	62	48	43	37
SB100	—	−3·0	1·0	940	325	2·9	0·967	95†	130	117	63
SB100	—	−3·0	1·0	1 270	455	2·8	0·976	100†	150	119	62
SB100	(*g*)	−3·0	1·0	940	325	2·9	0·957	95†	140	98	58
SBL5108	(*h*)	−3·0	1·0	585	215	2·7	0·975	—	190	150	70
SBL5108	—	−3·0	1·0	515	225	2·3	0·968	—	175	143	72

† Obtained by extrapolation.
‡ Bridge measurement: current-transfer measurements give 410, 57 and 70 ohms respectively.
§ Bridge measurements: current-transfer measurements give 30, 57 and 11·4 pF respectively.

(4) RESULTS

Measurements were made on the following types of germanium transistor:

Alloy-junction: TS2, EW59, CK760, V6/R8, CK762 and L5134.
Surface-barrier: SB100 and SBL5108.

The current-gain loci for one of each type, working under normal emitter and collector d.c. conditions for amplifying purposes, are presented in Figs. 7(*a*)–(*h*), the measured external current gains being shown as dots and the derived internal diffusion current gains, where applicable, as crosses. These latter values have been shown in the fourth quadrant only, because outside this the corrections to be made to the external current gains are a significant fraction of the measured value. A semicircle has been shown in the fourth quadrant in each case, which represents the frequency dependence of the approximate form of current gain defined by eqn. (9). Also, for the lower-frequency transistors, a semicircle has been constructed in the first quadrant passing through the origin and as nearly as possible through the experimental points. Such a locus is to be expected from eqn. (8) for passive transmission. Ancillary data concerning the transistors investigated, which included five of the surface-barrier type, are given in Table 1, together with cut-off frequencies as derived by the four methods discussed in Section 3. The maximum frequency of oscillation was measured only for those transistors for which the manufacturers specified such a frequency.

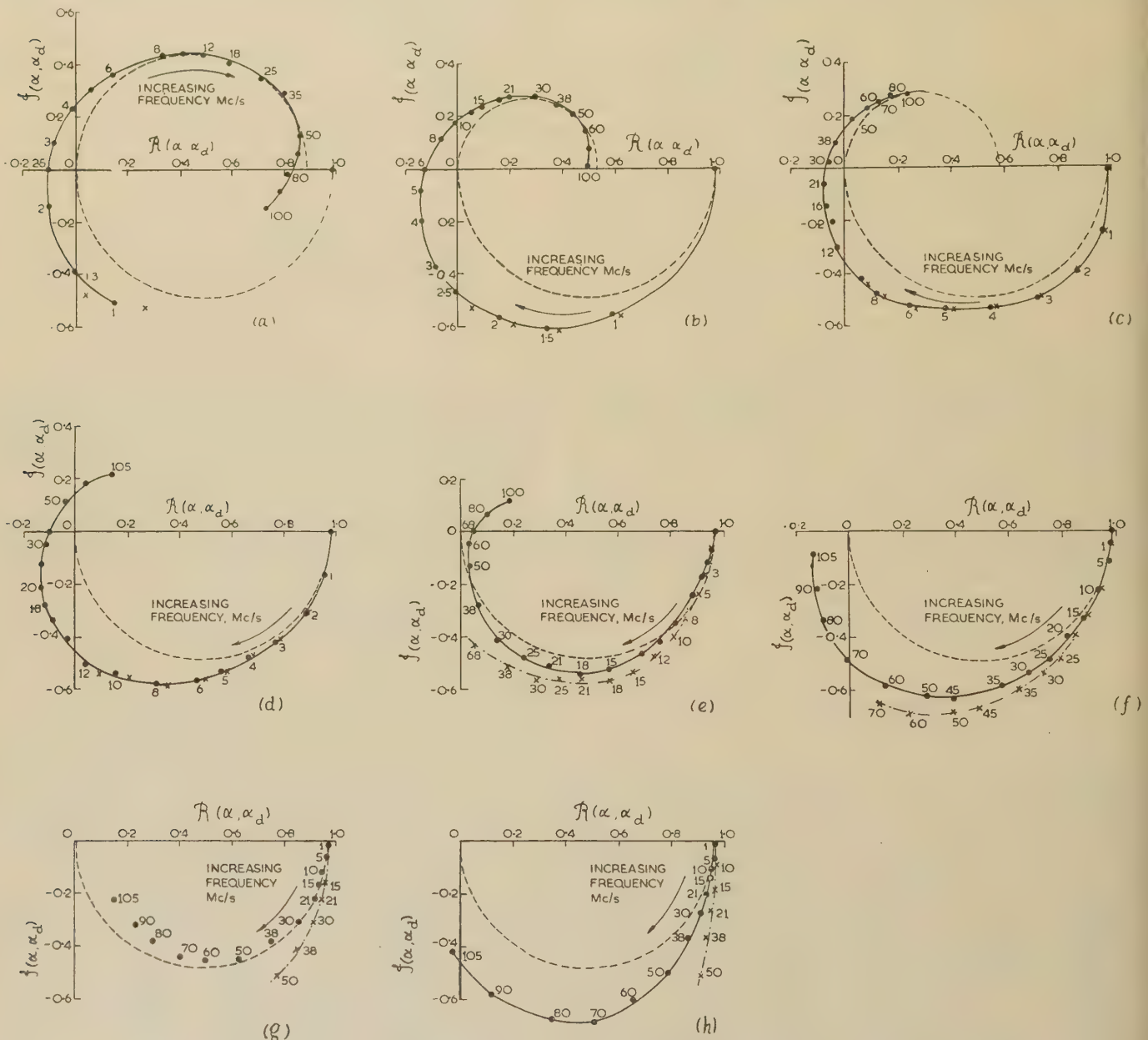

Fig. 7.—Frequency dependence of current gain of alloy-junction and surface-barrier transistors.

—●—●— α.
—×—×— α_d.

Parameters are given in Table 2.

(*a*) TS2. (*b*) EW59. (*c*) CK760. (*d*) V6/R8. (*e*) CK762. (*f*) L5134. (*g*) SB100. (*h*) SBL5108.

(5) DISCUSSION

(5.1) Alloy-Junction Transistors

The shapes of the loci of the internal current gain are seen to be in reasonably good agreement with the theoretical limiting form shown in Fig. 2. It will be noted, however, that for the type L5134 transistor, which is described by the manufacturers as a micro-alloy transistor (m.a.t.), the actual locus lies somewhat outside the limiting form. A locus of this type arises for the 'drift' transistor described by Kroemer[17]; it is therefore possible that a built-in drift field, which results when there is a decreasing concentration of donor atoms across the base from emitter to collector, may exist across all or part of the base of the type L5134 transistor.

There is good agreement between the directly measured values of $f_{\alpha d}$ and those calculated from the theoretical expression [eqn. (4)] in which effective values of D_p/w^2, determined from a.f. measurements,[5,6] were used—the type L5134 transistor excepted. The exception is to be expected, because it is impossible to explain the shape of the locus of the internal current gain of this transistor on the basis of a one-dimensional diffusion model.

For the lower-frequency transistors, values of $f'_{\alpha d}$ deduced from measurements of base input reactance also agree well with the directly measured values of $f_{\alpha d}$, thereby justifying the use of the close approximation to the internal diffusion current gain as given in eqn. (10). For the higher-frequency transistors there is a tendency for the base-input-reactance method to yield a low answer, because the effects of transistor capacitances have been ignored in deriving eqn. (13)—which is not always permissible. In addition to C'_C, which is the sum of collector depletion-layer and diffusion capacitances, two similar emitter capacitances should also be included in the equivalent circuit of Fig. 6 for completeness: they appear in parallel with r_d. When the effects of all these capacitances on the base-input reactance are considered, it is found that that of the emitter diffusion capacitance is negligible, but that of the emitter depletion-layer capacitance, augmented by that of C'_C, is not always negligible. It is then found, using eqn. (10), that $\hat{f}$ is approximately related to $f'_{\alpha d}$ by

$$f'_{\alpha d} = \frac{\hat{f}(1 + \alpha_0/5)}{1 - \alpha_0 - 2\pi\hat{f}Cr_d} \quad . \quad . \quad . \quad . \quad (14)$$

Here C represents the sum of the emitter depletion-layer capacitance and C'_C. It will be noted that if $2\pi\hat{f}Cr_d \ll 1 - \alpha_0$, the value of $f'_{\alpha d}$ derived from eqn. (14) will be greater than that derived using eqn. (13). Actual computation using eqn. (14) has not been employed, because of difficulty in determining the emitter depletion-layer capacitance with precision.

From v.h.f. measurements of passive current transmission the values of C_C and r_{b0} are in good agreement with those measured independently at 4 Mc/s for the type TS2 and CK760 transistors, although for the type EW59 transistor there is considerable discrepancy (see Table 1). For both the TS2 and the EW59 the current-gain loci depart from the semicircular as the positive real axis is approached at the highest frequencies. As was pointed out in Section 2.3, such behaviour is expected when appreciable current begins to flow through C_{EB}. In the TS2, where r_{b0} is high, the passive transmission is considerably affected by C_{EB}, so that the locus passes well inside the fourth quadrant at the highest frequency.

(5.2) Surface-Barrier Transistors

It has not been suggested in the literature that the one-dimensional equations (2) should be applied *in toto* to surface-barrier transistors. It is illuminating, however, to attempt to assess the performance of these transistors in terms of these theoretical equations, which *are* applicable to '*p–n* junction transistors'. Figs. 7(*g*) and 7(*h*) show that the locus of the internal current gain follows the ideal form (Fig. 2) for the SB100, whereas for the L5108, which is of similar construction, discrepant behaviour is observed at quite low frequencies. The loci of the current gains of all three SB100 transistors were closely similar to that shown in Fig. 7(*g*), while both SB L5108 transistors had the identical form shown in Fig. 7(*h*). The effects of stray capacitances have limited the data from which internal current gain may be derived to the frequency range below 50 Mc/s, which is lower than $f_{\alpha d}$ in each case. For the SB100 transistors, however, by comparing h.f. experimental points with the parameter x in Fig. 2 it has been possible to deduce values for $f_{\alpha d}$ by extrapolation. This is sensibly the same procedure as is adopted when, from l.f. measurements of base-to-collector current gain, $f_{\alpha d}$ is calculated from eqn. (4), because this equation specifies one point on the theoretical locus in Fig. 2. It will be noted that these extrapolations do not yield the same value for $f_{\alpha d}$; this seems to indicate that, for some surface-barrier transistors, although the locus of α_d may have the same shape as that in Fig. 2, the dispositions of the frequency points around it differ. There is, in fact, an expansion of the frequency scale towards higher frequencies, so that it is possible that, if direct measurements of $f_{\alpha d}$ could have been made, the values observed would have been lower than those inferred from the readings at 50 Mc/s. For the SBL5108 transistors it was impossible to determine $f_{\alpha d}$ by extrapolation, because the loci for α_d did not have the ideal form. As for the L5134 transistor, the actual loci lie outside the ideal limiting curve for diffusive transport of minority carriers across the base.

The values of $f'_{\alpha d}$ derived from the admittance measurements are seen to agree quite well with those for $f_{\alpha d}$ determined by extrapolation of the locus of α_d, the particular form of frequency-dependence of eqn. (10) being used. For all surface-barrier transistors the values of $f'_{\alpha d}$ determined from the maximum frequency of oscillation using eqn. (12) were considerably lower than the corresponding values using the admittance method.

It is to be expected that because of circuit losses the practical maximum frequency of oscillation will be less than the theoretical values calculated assuming no circuit losses. Accordingly, values of $f'_{\alpha d}$ calculated from eqn. (12) must inevitably be low. More serious perhaps, is that, in the vicinity of the maximum frequency of oscillation, which is of the order of $f'_{\alpha d}$, eqn. (11) can only be regarded as a crude approximation for $f'_{\alpha d}$ and eqn. (12) will correspondingly be in error.

(6) CONCLUSIONS

Apparatus has been described that may be used for measurement of current gain under near-short-circuit conditions in the frequency range 1–105 Mc/s. Measurements have been made on v.h.f. transistors using this apparatus, and the limiting effects of stray capacitances on such measurements have been emphasized. It has been shown that such stray capacitances would have less influence on measurements made on transistors that have smaller values of C_C and r_{b0} than those available at present. Measurements at frequencies far above the working range of i.f. and h.f. transistors have confirmed to some extent the values of the 'passive' elements of the transistor which are so important, namely C_C and r_{b0}.

By making corrections to the measured values of external current gain, the internal diffusion current gain, α_d, has been determined, and its cut-off frequency, $f_{\alpha d}$, has been compared

with values derived independently by other indirect methods. For alloy-junction transistors it may be concluded that α_d has quite closely the form expected on the basis of a modified one-dimensional diffusion theory involving effective values of D_p and τ_p. For surface-barrier transistors, however, although the equations of such theory may be used to specify performance, there is not the same measure of agreement. The cut-off frequency of the internal current gain of a surface-barrier transistor therefore remains in question, because we have been unable to measure it directly and values obtained by extrapolation depend on the particular method used.

(7) ACKNOWLEDGMENT

The work described above was carried out as part of the programme of the Radio Research Board. This paper is published by permission of the Director of Radio Research of the Department of Scientific and Industrial Research.

(8) REFERENCES

(1) EARLY, J. M.: 'Design Theory of Junction Transistors', *Bell System Technical Journal*, 1953, **32**, p. 1271.
(2) ZAWELS, J.: 'Physical Theory of New Circuit Representation for Junction Transistors', *Journal of Applied Physics*, 1954, **25**, p. 976.
(3) PRITCHARD, R. L.: 'Frequency-Variation of Junction Transistor Parameters', *Proceedings of the Institute of Radio Engineers*, 1954, **42**, p. 786.
(4) GIACOLETTO, L. J.: 'Study of *p–n–p* Alloy Junction Transistors from D.C. through Medium Frequencies', *RCA Review*, 1954, **15**, p. 506.
(5) EVANS, D. M.: 'Measurements on Alloy-Type Germanium Transistors and Their Relation to Theory', *Journal of Electronics*, 1956, **1**, p. 461.
(6) HYDE, F. J.: 'Some Measurements on Commercial Transistors and Their Relation to Theory', *Proceedings I.E.E.*, Paper No. 2438 R, January, 1958 (**105** B, p. 45).
(7) ANGELL, J. B.: 'Circuit Implications of Surface-Barrier Transistors', IRE-AIEE Conference on Transistor Circuits, February, 1954.
(8) COFFEY, W. N.: 'Measuring R.F. Parameters of Junction Transistors', *Electronics*, 1956, **29**, p. 152.
(9) DE WALDEN, S., ROCKE, A. F. L., BARRETT, J. O. G., and PITTS, W. J.: 'The Development of a High-Frequency Cathode-Ray Direction-Finder for Naval Use', *Journal I.E.E.*, 1947, Part IIIA, p. 823.
(10) ECKERSLEY, T. L., and MILLINGTON, G.: 'The Limiting Polarization of Medium Waves reflected from the Ionosphere', *Proceedings of the Physical Society*, 1939, **51**, p. 110.
(11) MAURICE, D., and MINNS, R. H.: 'Very Wide-Band Radio-Frequency Transformers', *Wireless Engineer*, 1947, **24**, p. 168.
(12) TURNER, R. J.: 'Surface-Barrier Transistor Measurements and Applications', *Tele-Tech*, 1954, **13**, p. 78.
(13) MOLOZZI, A. R., PAGE, D. F., and BOOTHROYD, A. R.: 'Measurement of High-Frequency Equivalent Circuit Parameters of Junction and Surface-Barrier Transistors', *Transactions of the Institute of Radio Engineers*, 1957, **ED-4**, p. 120.
(14) PRITCHARD, R. L.: 'Electro-Network Representation of Transistors—A Survey', *Transactions of the Institute of Radio Engineers*, 1956, **CT-3**, p. 1.
(15) DROUILHET, P. R.: 'Predictions based on the Maximum Oscillator Frequency of a Transistor', *ibid.*, 1955, **CT-2**, p. 178.
(16) BOOTHROYD, A. R., and ALMOND, J.: 'A Bridge for Measuring the A.C. Parameters of Junction Transistors', *Proceedings I.E.E.*, Paper No. 1681 M, September, 1954 (**101**, Part III, p. 314).
(17) KROEMER, H.: 'The Drift Transistor' from 'Transistors I' (R.C.A. Laboratories, 1956), p. 202.

(9) APPENDICES: EFFECTS OF STRAY CAPACITANCES ON THE EXTERNAL CURRENT GAIN

The three stray interelectrode capacitances involved and the currents which they influence are shown in Fig. 4. The purpose of the analysis is to show the first-order effects of these capacitances on current gain. Accordingly their effects are considered separately and independently.

(9.1) Collector-to-Base Capacitance, C_{CB}

This appears in parallel with the collector-circuit resistance R. Provided that $\omega C_{CB}R \ll 1$, by-passing of R by the collector terminal current will be negligible. At 100 Mc/s with $R =$ 51 ohms and $C_{CB} = 1$ pF, then, $\omega C_{CB}R = 0{\cdot}032$, which i much less than unity as is required. This capacitance has n influence on the currents in the emitter circuit.

(9.2) Emitter-to-Collector Capacitance, C_{EC}

This is likely to be the smallest of the three and will originate largely in the transistor itself. Any current, i_0, flowing through this capacitance will contribute to both v_{ER} and v_{CR}, so that in practice the ratio $-(i_C - i_0)/(i_E + i_0)$ will be measured instead of $-i_C/i_E$. It is desirable that $|i_0|/|i_C| \ll 1$. In analysis of the effect of C_{EC} on current gain the transistor representation in Fig. 1 is used. From eqn. (2) it may be seen that terms involving y_{12}^* and y_{22}^* may be ignored at high frequencies. Accordingly, y_{22} may be identified with $j\omega C_C$, so that the following expression arises for the ratio i_0/i_C:

$$\frac{i_0}{i_C} = \frac{j\omega C_{EC}\left[\left(\frac{y_{21}}{y_{11}} + \frac{j\omega C_C}{y_{11}}\right)(R + r_{b0}) + \left(\frac{1}{y_{11}} + r_{b0}\right)\right]}{\frac{y_{21}}{y_{11}}(1 + j\omega C_{EC}R) - \frac{\omega^2 C_{EC}C_C R}{y_{11}} - j\omega C_C r_{b0}} \quad (15)$$

If C_C is sufficiently small and I_E and hence y_{11} sufficiently large, $j\omega C_C/y_{11}$ and $\omega^2 C_{EC}C_C R/y_{11}$ may be neglected for our frequency range; y_{11} may also be approximated by y_{11}^* and hence $1/y_{11}$ may be neglected compared with r_{b0} at high frequencies. Finally, y_{21}/y_{11} may be identified with $-\alpha_d$, because $y_{21}^* \equiv y_{21}$. The following simplified form of eqn. (15) then results:

$$\frac{i_0}{I_C} \simeq \frac{j\omega C_{EC}[\alpha_d(r_{b0} + R) - r_{b0}]}{\alpha_d + j\omega C_C r_{b0}} \quad . \quad . \quad . \quad (16)$$

It is evident that, for the modulus of the numerator to be small compared with that of the denominator over a wide range of frequency, both R and r_{b0} should be small, while values of $\omega C_C r_{b0}$, which in practice turn out to be less than α_d for measurements of current gain in the fourth quadrant, should be as small as possible. Hence the effect of C_{EC} will be less at a given frequency, the smaller is the product $C_C r_{b0}$.

(9.3) Emitter-to-Base Capacitance, C_{EB}

This will be the largest of the three stray capacitances, because it includes the capacitance to earth of the input transformer ($\simeq 1$ pF). Its effect will be to increase the voltage drop v_{ER} by a factor $(1 + j\omega C_{EB}/Y_{in})$ above that due to the emitter terminal current i_E. Y_{in} here is the emitter-to-base terminal input admittance, exclusive of $j\omega C_{EB}$, and is given by

$$Y_{in} = y_{11}\left\{1 + \frac{r_{b0}[y_{21} + y_{11}(1 + j\omega C_C R)]}{1 + j\omega C_C(r_{b0} + R)}\right\}^{-1} \quad . \quad (17)$$

if terms involving y_{12}^* are ignored and $y_{22} \equiv j\omega C_C$. Making approximations similar to those in Section 8.2 we may write

$$j\omega C_{EB}/Y_{in} \simeq j\omega C_{EB} r_{b0} \frac{1 - \alpha_d + j\omega C_C R}{1 + j\omega C_C(r_{b0} + R)} \quad . \quad (18)$$

For the modulus of the numerator to be small compared with that of the denominator over a wide range of frequency, it is clear that both r_{b0} and $\omega C_C R$ should be small. The same desiderata arise, therefore, as in the preceding Section, if stray capacitances are to exercise a minimum effect: both r_{b0} and C_C should be as small as possible.

SUB-CENTRE CHAIRMEN'S ADDRESSES

The Institution of Electrical Engineers
Abstract No. 2496
Mar. 1958

NORTH LANCASHIRE SUB-CENTRE: CHAIRMAN'S ADDRESS

By H. G. COPE, Associate Member.

'SOME ASPECTS OF THE PRESTON TELEPHONE AREA'

(ABSTRACT *of Address delivered at* PRESTON, *9th October*, 1957.)

The Address covers a brief outline of the Area, with particular reference to some items of plant and equipment. The Area covers 524 square miles and contains 62 exchanges to which are connected just over 100 000 telephones. During recent years much has been done in the Area to increase the rate of supply of telephones and thereby to reduce the outstanding orders. One of the difficulties, because of limited capital development, has been the shortage of spare pairs in the local cable network.

External Plant Flexibility.—An interesting post-war development that has taken place with the object of making the local line plant more flexible has been the introduction of flexibility units, or cabinets and pillars.

The design and provision of the local cable network in an exchange area is based on a forecast of the telephone demand over a 20-year period. Whilst the forecast for the area as a whole can be made reasonably accurate, the forecast for any individual portion of it can be wide of the actual demand. Cabinets and pillars are now used, in the local cable network, to provide flexibility between the small 15-pair distribution-point cables, which are provided on the 20-year or long-term basis, and the larger branch and main cables closer to the exchange, which, for economic reasons, are provided on a short-term basis. The main cables from the exchange terminate on cabinets which, in turn, are connected by the smaller branch cables to pillars and the distribution-point cables. It is a simple operation at either cabinet or pillar to cross-connect any cable pair on the exchange side of the unit to any pair on the distribution side. The flexibility thus provided allows cable pairs to be distributed, without disturbing the cable layout, when it is necessary to cater for any serious deviation from the forecast. With a greater number of pairs on the distribution side of the pillars and cabinets the pairs on the exchange side can be made available over a very large area, and consequently the main and branch cables can be used to a high percentage of efficiency. Some 45% of the total pairs connected to the exchanges in the Area now terminate at flexibility points.

All-Polythene-Insulated Cable.—Increasing use is being made of polythene insulated and sheathed cables for distribution, i.e. from the pillars onwards. It is made in a range of sizes from one to 50 pairs; its cost is comparable with the same size of lead-sheath cable; it is free from the corrosion troubles that affect lead-sheathed cable and it can, in many cases, be laid direct in the ground, thus saving duct costs. In a recent local exchange development scheme, out of a total of 35 miles of cable, 24 miles are of polythene and 16 miles of this are laid direct in the ground.

Ernie.—The most topical item of internal equipment maintained by the Area staff is Ernie or, to give it its full title, the 'Electronic Random Number Indicator Equipment',* which has operated each month since June, 1957, to generate the prize-winning Premium Savings Bond numbers. The bonds are issued in 23 denominations each with a number range up to 100 million. At present the numbering range has been limited to 30 million numbers in each denomination, i.e. 690 million in all, from which the winning numbers are selected in entirely random fashion. Electronic equipment is used to generate the 9 character-bond numbers which are printed on teleprinters.

Noise generators, with a mean pulse output of 11 000 pulses/sec, are used to drive electronic counters having a scale appropriate to the character to be subsequently printed. The counters are arranged in pairs, one pair per bond character. Every 160 millisec the pulses are suppressed and the nine pairs of counters stop, each indicating the digit position it has reached. Each pair of counters passes this information into a combiner circuit, in which the two digits are electrically subtracted, and the nine digits so obtained from the counters are transferred to a store to form the bond number. The object of the combining process is to ensure that, if any non-random element is present in either of the noise generators contributing to a particular digit, the output from the combiner will still be random.

Before the numbers are released from the store for printing they are checked for redundancy. Varying quantities of bonds have been sold in each denomination, and there are inevitably many gaps due to unsold bonds in the issued number series. The function of the redundancy equipment is to restrict the printing of the numbers on the teleprinters to approximately the same as the purchases in each denomination. It is, however, impracticable to reject every unsold bond number at the redundancy check stage, and therefore some ineligible numbers will be printed on the teleprinters. These are eliminated manually in the course of the subsequent checking processes. For the first draw in June the issue of each of the 23 denominations was restricted to 30 million numbers of the total of 690 million, all but 118 million were rejected by the redundancy equipment; and, of these, some 48 million were valid for the first draw. Each month, after each draw, the redundancy equipment is adjusted for the relevant range of numbers eligible for the next draw. The equipment is then subjected to various checks before the next draw takes place.

The equipment takes about 2·5 sec to print one bond number followed by a draw serial number. In all, the message consists of 18 characters, i.e. the bond and draw serial numbers, figure and letter shift signals, etc. During this period some 15 bond numbers can be generated and checked for redundancy; but the first valid bond number to be generated is stored and further generation ceases, pending the completion of the printing of the preceding bond number.

Acknowledgment.—The author is indebted to the Post Office Engineering Department Research Branch, who designed and built Ernie, for certain information used in this Address and especially for the loan of a working model.

* HAYWARD, R. K., and BUBB, E. L.: 'Ernie', *Post Office Electrical Engineers' Journal*, 1957, 50, p. 1.

Mr. Cope is in the Post Office Engineering Department.

The Institution of Electrical Engineer
Abstract No. 259
Mar. 195

SOUTH-WESTERN SUB-CENTRE: CHAIRMAN'S ADDRESS

By C. H. FOULKES, Member.

'REVIEW OF TWENTY YEARS OF VALVE DEVELOPMENT'

(ABSTRACT *of Address delivered at* TORQUAY, 17*th October*, 1957.)

The story of valve development in the past twenty years has been largely that of a struggle to achieve satisfactory operation at higher and higher frequencies. By the mid-1930's the diode, triode, tetrode and pentode had become quite firmly established as receiving valves, and transmitting triodes were in use giving output powers of some 200 kW or more. Valves were available to meet most of the demands of electronic engineers up to the stage where the signal frequencies involved became too high for one reason or another. Generally speaking, large transmitting valves were satisfactory up to 50 Mc/s and receiving valves up to about 300 Mc/s.

As signal frequencies become higher, two main difficulties are encountered. Electrons themselves have finite inertia, and the time required for them to travel from the cathode to the anode of a valve can become an appreciable fraction of a cycle. This 'transit time effect' can be minimized by using close electrode spacings and high voltages. The second difficulty is that earlier valves had quite large electrodes and comparatively long electrode leads, producing high internal capacitance and inductance. Since these form part of the tuned circuit, operation at high frequencies demands that they must be minimized. An example of the valve engineer's efforts to achieve these desirable features in the case of the receiving valve is given by the development of the Acorn valve in the mid-1930's. This proved to be very difficult to manufacture in quantity, and was eventually superseded by later developments.

The advent of the Second World War demanded vast quantities of receiving valves suitable for operation at very high frequencies, and so the standard miniature valve, familiar in modern domestic radio and television receivers, came into being. In these valves, the electrode assemblies are mounted directly on to the valve pins, so that the circuit-elements can be mounted close to the electrodes for high-frequency operation. Useful amplification can now be obtained up to 1 000 Mc/s.

The continued development of radar during the war called for valves to operate at even higher frequencies, and an entirely different mode of operation had to be sought. The principle of velocity modulation of an electron beam, first attempted by Oscar A. Heil and subsequently developed by W. C. Hahn and G. F. Metcalf and the brothers R. H. and S. F. Varian, resulted in the coaxial-line valves and the klystron. This was followed by the invention, by R. Kompfner, of the travelling-wave tube, and even more recently the backward-wave oscillator has been discovered. Klystrons and travelling-wave tubes have been brought to the stage of development where signals can be amplified several hundredfold at frequencies up to 5 000 Mc/s. The travelling-wave tube can also be used as an oscillator whose frequency can be made to vary with the applied voltages, no other tuning being necessary.

In this same frequency range, klystrons and magnetrons can be used as pulsed oscillators giving peak output powers of several megawatts. Valves of this type now being developed can oscillate at frequencies of 70 000 Mc/s, i.e. a wavelength of 4 mm, which appears to be the limit for valves working on the principle of velocity modulation.

The circuits associated with these devices are very differen from the coils and condensers of the early days. In general microwave circuits consist of rectangular conducting pipes alon which radio-frequency energy is conducted in the form of waves Such pipes are called waveguides, and the whole circuit assembl is commonly referred to as 'plumbing'.

It would not be true, however, to say that all the developmen in this period has been directed towards higher and highe frequencies. Many other changes have taken place at th same time.

The process of miniaturization did not stop with the introduc tion of miniature valves, for there are certain applications, such as in missiles and very small portable light-weight equipments where great emphasis is placed upon space-saving. Sub-miniature valves $\frac{3}{8}$ in in diameter and about 1 in long perform very satisfactorily in these applications.

In the field of conventional high-power transmitting valves, th advances made have been less concerned with transit time, a this can be reduced by increasing the electrode voltages suffi ciently, causing the electrons to accelerate much more quickly than is possible in receiving valves. The limitation here i rather the large circulating currents flowing through the self capacitances of the valve elements at the very high frequencies concerned. In order to overcome this, coaxial structures were developed consequent upon the invention of special metal-to-glass sealing alloys. These special alloys were introduced into valve manufacture in the late 1930's and their use has now almost completely ousted copper, which was used until then.

Another major change in large transmitting tube design came about during the war years, when pure tungsten filaments were replaced by filaments of thoriated tungsten, i.e. tungsten with 1% or 2% of thoria added, which enhances the electron emission from the filament. These very efficient emitters lead to a considerable saving in cathode heating power. Furthermore, the consequently cooler electrode assemblies are less likely to emit electrons on their own account. Medium-to-high-frequency valves are now being made which are air-blast cooled and will dissipate 50 kW of power on the anode. The tendency nowadays is to move away from high-power low-frequency transmitters to the region of 10 kW transmitters at very much higher frequencies.

The submerged-repeater valve, with its oxide-coated cathode has now been developed to the stage where it can confidently be expected to give a life in excess of 20 years. This has made possible such major projects as the transatlantic telephone cable, which was recently laid down.

Gas-filled valves have been developed in a variety of forms since the war. They are being used as sensitive relays in switching circuits, as counter tubes in computers and as operational elements in automatic telephone exchanges.

Considerable progress has also been made in many other fields of vacuum physics, resulting in such valves as light amplifiers, information storage tubes and special cathode-ray tubes for display purposes, to mention but a few.

Mr. Foulkes is with Standard Telephones and Cables, Ltd.

621.374.32 : 621.385.12

The Institution of Electrical Engineer
Paper No. 2440 M
Nov. 1957

DEKATRONS AND ELECTRO-MECHANICAL REGISTERS OPERATED BY TRANSISTORS

By G. B. B. CHAPLIN, M.Sc., Ph.D., Graduate, and R. WILLIAMSON.

The paper was first received 4th June, and in revised form 2nd September, 1957. It was published in November, 1957, and was read before a joint meeting of the MEASUREMENT AND CONTROL SECTION *and the* RADIO AND TELECOMMUNICATION SECTION *3rd December, 1957.)*

SUMMARY

In nucleonic work a common requirement is the counting of pulses ccurring at relatively long intervals of 250 microsec or more. Cold-athode decade tubes (e.g. Dekatrons) and electro-mechanical registers ave proved their value in this field, but their performance and eliability depend to a large extent on the means employed to drive iem. The use of transistors for this purpose should result in efficient nd reliable circuits.

In the circuits described the Dekatron is driven by a transistor locking oscillator which, when triggered, produces a pulse of defined mplitude and width, followed by a similar pulse of opposite polarity. . secondary winding on the blocking-oscillator transformer applies ese pulses, in the correct phase and amplitude, to the Dekatron guide ectrodes. When decades are cascaded, the negative edge of the tput cathode waveform, instead of the normal positive edge, is used r triggering the next stage. This system reduces the delay between put and output pulses to a few microseconds, which is the triggering me of the blocking oscillator, and so reduces the error when the ekatrons are used for counting standard time intervals.

For operating a mechanical register two transistors are cross-oupled in a monostable circuit. The register is in the collector circuit f one transistor, which conducts for 0·1sec when triggered. Since nly a small fraction of the supply voltage appears across the ansistor when it is conducting, registers requiring several watts can e operated by low-power transistors.

The transistor circuits produce accurate waveforms for operating e Dekatrons and registers, enabling the minimum resolving times to e realized.

(1) INTRODUCTION

Cold-cathode decade tubes (e.g. Dekatrons) and electro-echanical registers are well established in low-speed counting pplications, and have the advantage that they automatically dicate the count in decimal form. However, the reliability of ese two devices depends to a large extent on the circuits driving em, particularly if the scalers are operated at their theoretical aximum speed. Although correct driving waveforms can be btained from thermionic valves,[1,2] the power consumption lative to that of the counting device itself is excessive. On the ther hand, driving circuits using cold-cathode valves can be uite economical,[3] but, since their waveforms only approximate those ideally required, the counting rate must be reduced for liable results.

The transistor promises to combine the economy of the cold-athode valve with a reliability even greater than that of the ermionic valve, and the paper describes transistor circuits itable for driving Dekatrons and mechanical registers.

(2) DEKATRON DRIVE CIRCUITS

The two driving waveforms specified for a typical Dekatron[4] e shown in Fig. 1(*a*). A negative pulse of 100 volts amplitude it a minimum duration of 80 microsec is applied to guide 1, nd followed by a similar pulse applied to guide 2. The upper level of these pulses should be about 30 volts positive with respect to the cathodes of the Dekatron, and the leading edge of the second pulse should be coincident with or slightly overlap the trailing edge of the first. A third interval of 80 microsec must elapse before another such pair of pulses can be applied, resulting in a minimum resolving time of 240 microsec.

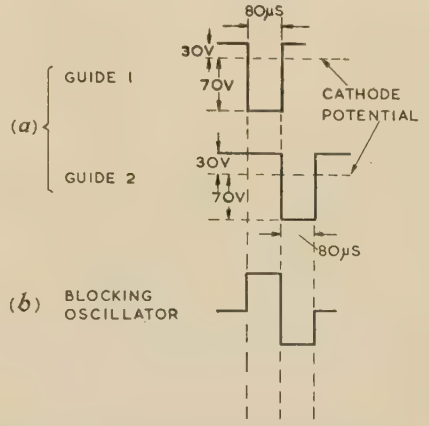

Fig. 1.—Guide and blocking-oscillator pulses.
(*a*) Specified guide pulses of Dekatron.
(*b*) Blocking oscillator pulse.

The amplitude of these guide pulses is greater than the voltage rating of a transistor, but this difficulty can be overcome by using a transformer to connect the transistor to the guides. This transformer can be made to serve a dual purpose by using it in conjunction with the transistor to form a monostable blocking oscillator, since the shape of the resulting guide waveform is then independent of the input waveform.

The waveform produced by a blocking oscillator consists of a voltage pulse of one polarity followed by a voltage overshoot of the opposite polarity. If both the pulse and the overshoot can be made substantially square and of the same amplitude and width, as shown in Fig. 1(*b*), then the waveforms of Fig. 1(*a*) could be derived from two antiphase secondary windings on the blocking-oscillator transformer by gating out the unwanted positive pulses. However, the use of two large secondary windings would unduly increase the size and self-capacitance of the transformer, and it is shown in Section 2.2 that it is possible to derive the waveforms of Fig. 1(*a*) from one secondary winding only.

(2.1) The Blocking Oscillator

A blocking-oscillator trigger circuit relies on a transformer to obtain the necessary positive feedback, and in the simplest case the transformer inductance can be used for defining the duration of the output pulse, as illustrated in Fig. 2.

The circuit is of the common-base type, except that a diode D_1, in conjunction with a base bias current I_b, causes the base to be a few tenths of a volt positive to earth. This ensures that

Mr. Chaplin and Mr. Williamson are at the U.K.A.E.A. Atomic Energy Research Establishment.

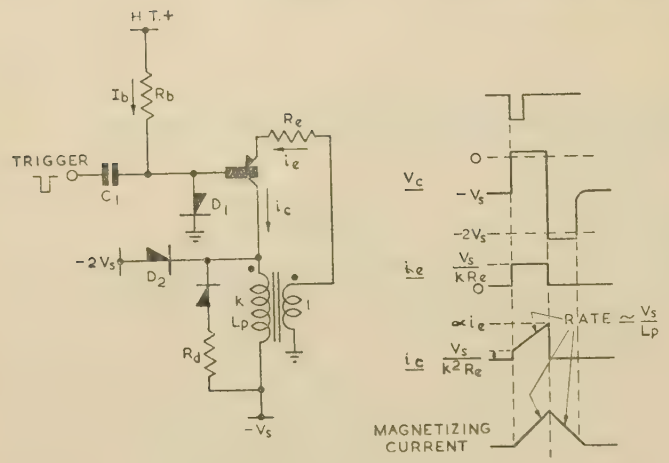

Fig. 2.—Blocking oscillator.

no emitter current flows in the stable 'off' state, and also allows a negative trigger pulse to be applied to the base. The trigger pulse initiates emitter current i_{e1}, of which a fraction αi_{e1} flows out of the collector into the transformer primary winding. The resulting transformer secondary current is $k\alpha i_{e1}$, where k is the turns ratio, and for regeneration it is essential that $k\alpha$ is greater than unity. Regeneration ceases when the collector potential bottoms, the voltage across the transformer primary (of inductance L_p) being approximately V_s, and the emitter current being therefore $i_{e2} = V_s/(kR_e)$. Since there is now a voltage V_s across the primary, the magnetizing current increases substantially linearly, at a rate V_s/L_p, until the total collector current reaches αi_{e2}. A further increase in magnetizing current causes V_c to fall, and the resulting cumulative action cuts off the emitter current. Owing to the transformer inductance, the collector voltage now overshoots negatively until held by D_2 at $-2V_s$. The magnetizing current thus decreases at the same rate at which it previously increased and approaches zero after a time approximately equal to the duration of the positive-going half-cycle. The collector voltage then returns to its rest potential $-V_s$ with a time-constant determined by the transformer constants and the damping resistance, R_d. Since the negative pulse has the same amplitude, and hence the same duration, as the positive pulse, it is sufficient to define the duration of the latter for the total duration to be determined.

The duration of the positive pulse is determined by the time taken for the collector current to increase from the initial step, $V_s/(k^2R_e)$, to the limiting value $\alpha i_{e2} = \alpha V_s/(kR_e)$, the rate of increase being V_s/L_p. The duration is therefore

$$\frac{L_p}{kR_e}(\alpha - 1/k)$$

and for accurate timing these quantities must be adequately reproducible. α, k, and R_e can all be controlled within a few per cent, but the reproducibility of L_p will depend on the transformer core material. However, very consistent results have been obtained with ferrite E-cores, a batch of a few dozen cores tested being within 2% of the mean.

The positive pulse duration is independent of supply voltage, and so too is the ratio of the positive pulse duration to the negative pulse duration, provided that V_s and $2V_s$ suffer the same fractional change, which will of course normally be the case.

(2.2) Connections to the Dekatron Guides

The method of deriving the waveforms of Fig. 1(*a*) from the blocking-oscillator secondary winding, L_s, is shown in Fig. 3.

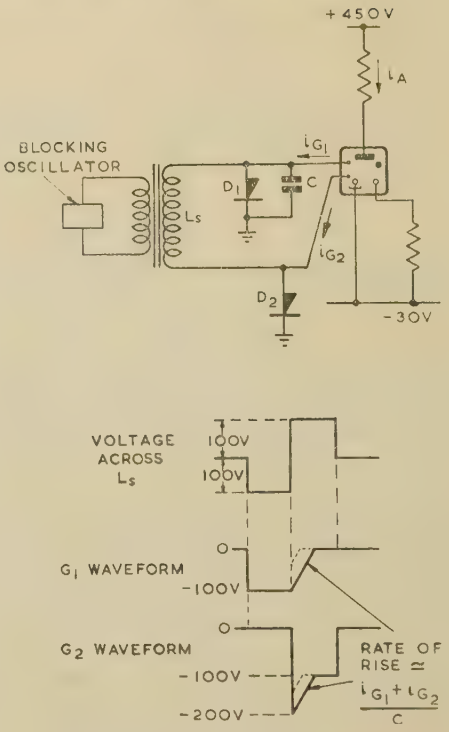

Fig. 3.—Guide connections.

The secondary winding is normally held at earth potential by th positive residual guide currents, i_{G1} and i_{G2}, flowing in D and D_2. When the transistor is triggered, the D_1 anode falls t −100 volts, charging C negatively and also causing i_{G1} to increas to about 0·4 mA, which is the anode current. The current i_G and the transient currents required to charge both C and stra capacitances are supplied by D_2, which prevents guide 2 risin above earth potential. When the voltage across the secondar winding reverses, the D_1 anode potential is temporarily prevente from rising by the condenser C, and so the D_2 anode fall initially to −200 volts and captures the 0·4 milliamp anod current via guide 2. This current, together with any transien current due to stray capacitance is supplied by C, which dis charges positively at a fairly constant rate until D_1 conducts During this time the voltage across the winding remains constan at 100 volts, so that the negative voltage on the D_2 anode decrease to −100 volts, remaining at this potential until the voltage acros the winding collapses, whereupon the D_2 anode potential return to zero.

In practice, stray capacitance on the G_2 side of the secondar winding forms a potential divider with C, reducing the amplitud of the negative spike on the G_2 waveform. The broken line indicate the effect on the waveforms. The value of C is chose to produce a spike of a few tens of volts, which is sufficient t ensure the rapid and reliable transfer of the glow from G_1 to G_2

(2.3) A Complete Decade Unit

A complete decade unit, comprising the blocking oscillator o Fig. 2 and the guide connection of Fig. 3, is shown in Fig. 4 The high peak current required to charge the guide condense C_2, to −100 volts when the circuit is triggered would drastically reduce the rate of regeneration, and so instead of returning on plate of C_2 to earth, as in Fig. 2, it is returned to the base of th transistor. The condenser now exerts positive feedback, an enhances both the rise-time and triggering sensitivity of th circuit.

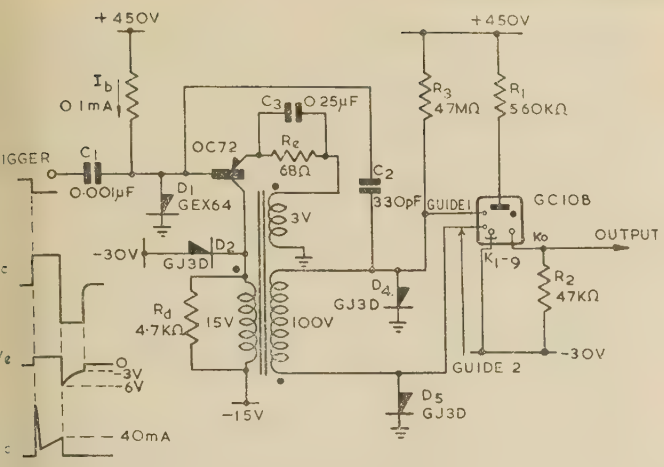

Fig. 4.—Complete decade unit.

The connection of C_2 to the base instead of earth has no trimental effect on the shape of the guide waveforms, because c base voltage is constrained by the emitter and D_1 to within volt of earth potential.

The purpose of C_3, which shunts the emitter resistor, R_e, is provide the extra emitter current during the rise of the pulse, d also to cause the emitter to cut off more rapidly at the end the pulse.

The diode which was in series with the damping resistor R_d s been removed, since the effect of the latter on the triggering nsitivity of the circuit is negligible.

(2.4) Choice of Circuit Values

The maximum allowable collector voltage of the transistor nd is −30 volts, and V_s is therefore made equal to −15 volts. ne transformer ratio k is made as large as possible, so that the emitter current when reflected back to the transformer primary imposes a relatively small load.

The maximum value of k is limited by the need for sufficient voltage on the emitter winding of the transformer to make i_e independent of any small changes of V_e due to change of emitter-to-base potential and the forward conducting potential of D_1. Since 3 volts is ample for this purpose, k is made equal to 5.

The value to which the collector current builds up depends on the choice of R_e. Part of the collector current will be used for the positive feedback and for driving a load connected to the circuit, and the rest will be available as magnetizing current, which will subsequently supply the load during the negative half-cycle. Accordingly, the magnetizing current should be large compared with the load current, so that small variations in the latter do not appreciably affect the pulse duration. The load consists of the guide currents, which have a maximum value equal to the 0·4 mA anode current of the Dekatron, together with an approximately equal load due to the damping resistor. Referred to the primary winding the load becomes $7 \times 0{\cdot}4 + 3 = 5{\cdot}8$ mA, and a peak primary current of about 40 mA is adequate. Accordingly, R_e is chosen to be $3/40 \times 10^{-3} \simeq 68$ ohms.

The design of the transformer is given in Section 7.

(2.5) Triggering Sensitivity

To trigger the circuit of Fig. 4 a negative-going step of current is applied to the base. This trigger pulse must be able to remove the bias current, I_b, and in addition extract sufficient current from the base to make the loop gain greater than unity. If the guide winding and the guide condenser C_2 are removed, triggering will occur when the emitter voltage has risen to approximately 0·3 volt, requiring a collector voltage change of 1·5 volts. Provided that the rise-time of the trigger pulse is sufficiently short, the collector load will be dominated by R_d and the base trigger current need be only $1{\cdot}5/(\alpha' 4{\cdot}7 \times 10^3) \simeq 15 \times 10^{-6}$ amp if $\alpha' = 20$.

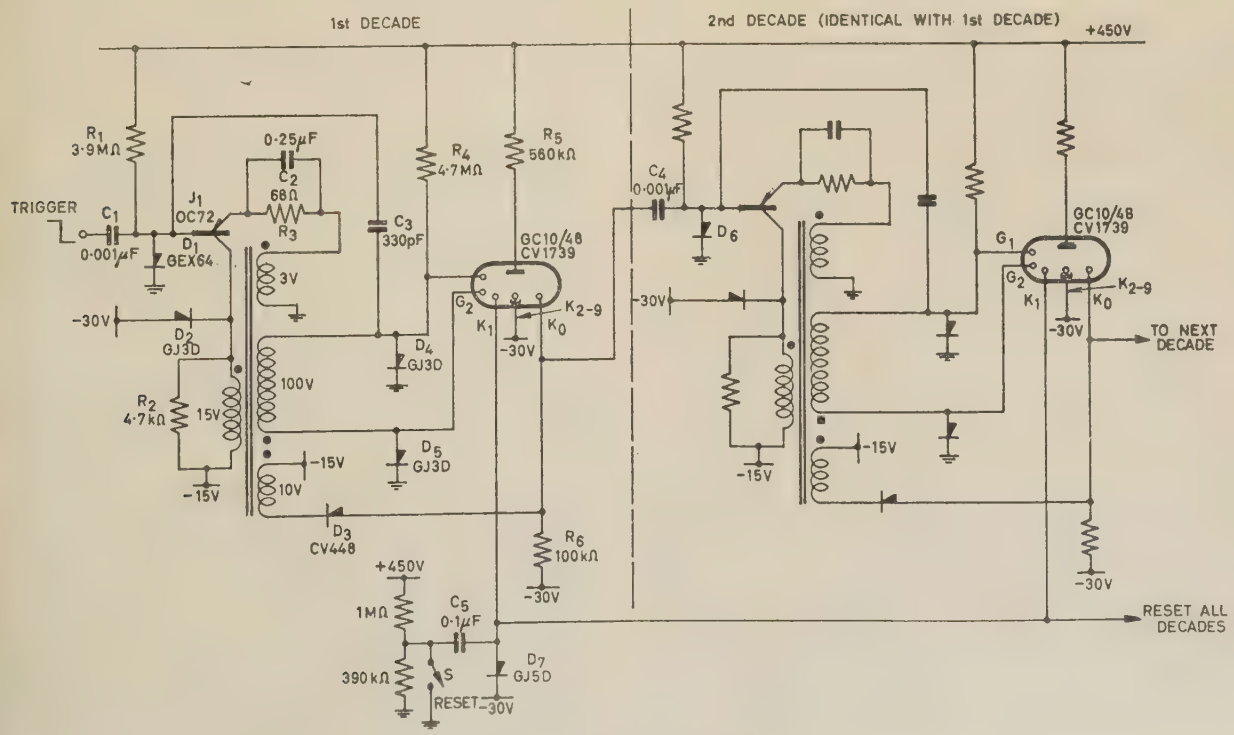

Fig. 5.—Interstage coupling.

When the guide winding is added the sensitivity is greatly reduced, because of the shunt loading effect of the winding self-capacitance and by hole storage in D_4. This latter effect is caused by the 100 μA residual guide current and the 100 μA current in R_3 both flowing into D_4 and D_5. The further addition of the guide condenser C_2 introduces extra positive feedback and partially restores the sensitivity, but an accurate analysis of the resultant triggering sensitivity is difficult. In practice, a total trigger current of 350 μA has been found adequate.

The cathode current of the Dekatron is typically 400 μA, but if a tolerance of $\pm 20\%$ is allowed the lower value will not be sufficient to trigger the next stage. It is possible, however, to increase the available trigger current considerably, and at the same time reduce the rise-time, by using an extra winding in the transformer. Fig. 5 shows the system applied to two complete decades.

The extra winding is the lower winding on either transformer and is connected to the output cathode K_0 via a diode D_3. The glow discharge must rest on K_0 for at least 80 microsec, and during this time the cathode current divides itself between the cathode load, R_6, and the coupling condenser, C_4. Since the right-hand plate of C_4 is prevented from rising by D_6, the charge in the condenser is changed. When the first stage is triggered the glow leaves K_0, and, at the same time, a sharp negative pulse is applied to K_0 by the extra winding via D_3. This causes C_4 to discharge rapidly into the base of J_2, resulting in a greatly increased trigger current.

(2.6) Cascading Dekatrons

The usual practice when cascading Dekatrons is to use the positive edge of the K_0 waveform for triggering the next stage, instead of the negative edge as described above. Thus the trigger pulse occurs when the 'glow' arrives at K_0, instead of when leaving it. The Dekatrons are then normally reset so that the glow rests on their output cathodes, K_0, corresponding to time T_0 in Fig. 6. After 10 trigger pulses a positive edge again

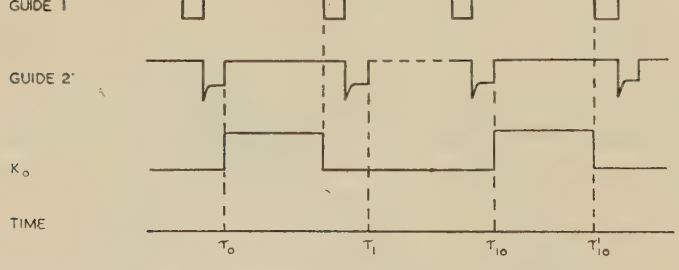

Fig. 6.—Interstage triggering sequence.

occurs on K_0, at time T_{10}, and is used to trigger the next stage. If, instead, the negative edge of the K_0 waveform is to be used for triggering, the Dekatron must be reset to K_1, corresponding to time T_1, so that a negative edge does not occur until 10 input pulses have been applied at time T_{10}'. Since K_1 is now the zero position, the tube must be reorientated to make K_1 read '0' on the escutcheon. The process of resetting to K_1 can be accomplished by resetting to K_0 and injecting a single input pulse.

The choice of trigger pulses derived from the negative edge of the output cathode waveform of the preceding Dekatron, instead of the more usual positive edge, was primarily made to facilitate the triggering of the blocking oscillator, but in fact it also confers an important advantage if the Dekatrons are being used f timing purposes. For example, it is sometimes required to sc down from a source of regular input pulses, derived perhaps fr a crystal oscillator, and produce output pulses of a substantia lower frequency but having the same timing accuracy. If th is some delay between an output pulse and the input pulse t produces it, then the time standard of the output pulses is shift with respect to that of the input pulses, and if the delay is varia the accuracy of the output pulse frequency will be impaired.

The waveforms of Fig. 6 show that there is a delay appro mately equal to two guide pulse widths between the first trig pulse and the positive edge of the K_0 waveform (T_0) which the corresponding output pulse. This delay is about 160 micros and may vary by several tens of microseconds with compone changes.

On the other hand, the delay between the second input pu and the first negative edge of the K_0 waveform is relatively sma being the triggering time of the transistor if the triggering windi of Section 2.5 is used. This is only 1 or 2 microsec for an audi frequency transistor, resulting in much greater accuracy timing applications.

(2.7) Resetting the Dekatrons

The normal method of resetting a Dekatron is to allow bo guides and K_{1-9} electrodes to rise to some positive voltage, a so force the glow on to K_0. The guides and K_{1-9} electrod are then returned to their normal potentials and the glow remai on K_0. If the Dekatron is orientated as described above, a sing pulse must then be injected into the drive circuit to transfer t glow to K_1. However, this system involves two separa operations and requires a 2-pole switch in which the contac are mechanically biased so that one operates before the other.

To avoid this difficulty it is preferable to use a type of Dekatr in which two adjacent cathodes are taken out to separate pi on the base. One of these cathodes is then used as the outp cathode, K_0, and the other as the reset cathode K_1, the latt corresponding to zero on the escutcheon. Resetting is no accomplished by taking the reset cathode from its norm potential of -30 volts to a negative potential of about 150 vol to allow it to capture the glow, which it retains on returnir again to -30 volts.

Referring to Fig. 5, closure of the reset switch S applies negative edge of just over 100 volts amplitude to the left-han plate of C_5 and hence to all the reset cathodes K_1. The tot glow current now flows into C_5, and restores the right-han plate to earth potential, causing the diode to conduct agai Releasing the switch then restores the charge on C_5 to its initi value but does not affect the potential of the reset cathodes.

(2.8) Performance

The resolution of the complete decade is limited solely by t Dekatron, since the blocking oscillator has recovered well befo the glow has been completely transferred from G_2 to the followin cathode.

To ascertain the effect of variation of supply voltage on t performance of the circuit, a decade unit was operated from t mains, using germanium rectifiers for the -15- and -30-vo supplies and selenium rectifiers for the +450 volt supply.

Changing the mains voltage from 190 volts to 300 vol resulted in a change of only 5% in the pulse width and hen the resolving time of the circuit. The main result of alteratio of mains voltage is that the amplitudes of both the guide wav forms and the Dekatron-anode supply voltage change in pr portion, and the extreme limits of mains voltage over which t circuit functioned correctly were 190–300 volts. In practic

wever, mains voltage rarely varies more than ±10%, so it ems unnecessary to stabilize the supplies to the circuit.

Under certain conditions the net current drawn from the 15-volt supply can reverse in sign, and so a standing current ould be contrived by connecting a few kilohms between the 15-volt supply and earth potential.

(3) MECHANICAL REGISTER DRIVE CIRCUIT

If the pulses to be counted are separated by intervals of 0·2 sec more, the use of an electro-mechanical register becomes ssible. The register consists of an electromagnet which, when ergized, actuates a ratchet causing the counter to advance by ie digit. Since the register usually contains four digits it con- tutes a useful high-capacity low-speed counting device.

A typical register requires an actuating pulse lasting for 1 sec, having an amplitude of 24 volts and capable of supply- g a current of 50 mA. The pulse width should be fairly curately controlled if the minimum resolving time is to be alized, and it is convenient for the driving circuit to be capable being triggered from a Dekatron output cathode. A suitable iving circuit is shown in Fig. 7.

Although a blocking-oscillator circuit could produce the ssired pulse, the long duration would require a transformer ving a relatively large inductance. For the same reason it has ot been possible to use the windings of a standard register as the ocking-oscillator transformer, since they have not sufficient ductance. Instead, a monostable cross-coupled circuit is used, e register being connected in the collector circuit of one nsistor (J_1 of Fig. 7) which is made to conduct for a time fined by the discharge of the condenser C_1. The other nsistor, J_2, provides the required phase reversal and extra rrent gain round the positive-feedback loop.

The register coil comprises an inductance L in series with the inding resistance R_1 and is damped by R_5 in series with D_1. he J_1 collector is cross-coupled to the J_2 base by the condenser , and the J_2 collector cross-coupled via D_2 to the J_1 base.

During the quiescent state, J_2 conducts and the collector otential is near earth, since $i_{R3} > i_{R2}/\alpha'$, where i_{R3} and i_{R2} are e base and collector currents, respectively, of J_2. The cathode D_2 is thus near earth potential, and the base of J_1 is positive th respect to the emitter owing to the voltage dropped across 2 by $(i_{R6} - i_{c0})$, where i_{R6} is the bias current and i_{c0} is the se leakage current of J_1. J_1 is therefore cut off and the register rrent is substantially zero.

A negative pulse applied to the J_1 base triggers the circuit, nd the J_1 collector potential rises, cutting off the J_2 base via C_1. he current which was flowing from the J_2 collector, i_{R2}, now ows from the J_1 base via D_2, and J_1 is held hard 'on' since $_2 > i_{R1}/\alpha'$. The current flowing in the register now rises with time-constant of L/R, until limited by R_1 at about 50 mA, hich is maintained for a time determined by C_1. The rise of e J_1 collector potential causes the J_2 base potential to rise from ear earth to $24R_3/(R_3 + R_4)$ volts ($\simeq +22$ volts), and the ration of the pulse on the register is determined by the time ken for the J_2 base to fall below earth potential as C_1 is dis- arged by i_{R3}. When this happens J_2 conducts again and J_1 cut off, which was the original state. The effect of the base a age current of J_2 on the timing is negligible, since it is always a l compared with i_{R3}. Since the register is inductive the J_1 lector potential overshoots negatively below −24 volts when is cut off, but a suitable choice of damping resistance, R_5, re ents the collector-to-base potential from exceeding −30 volts, h h is the maximum rated voltage of the transistor.

During the overshoot of the J_1 collector potential, D_1 conducts, if this diode is of the germanium junction type the cathode l be negative with respect to the base by about 0·5 volt.

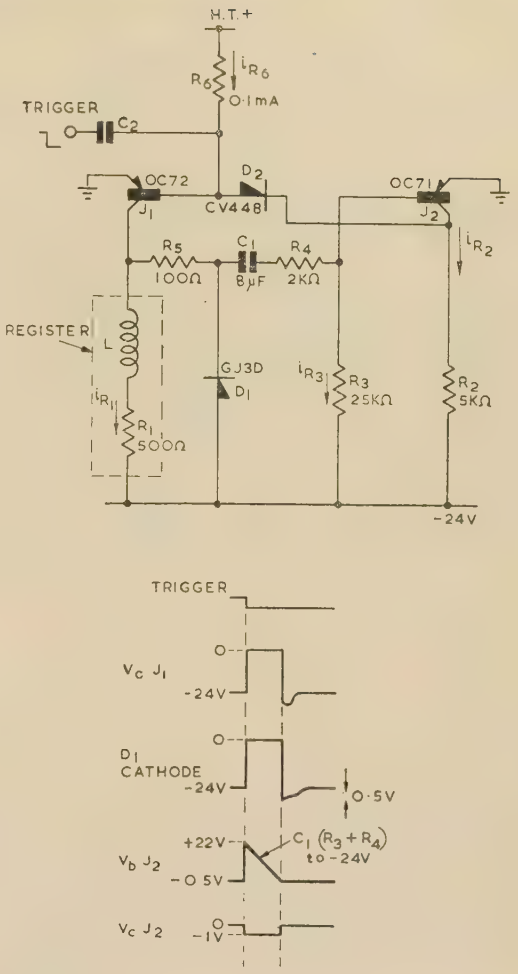

Fig. 7.—Monostable trigger circuit for electro-mechanical register.

When the overshoot finishes the D_1 cathode rises to its anode potential and hence applies a 0·5-volt positive step to C_1. If this step is sufficient to switch off J_2 the circuit will oscillate. However, R_4 ensures that this 0·5-volt step reduces the current extracted from the J_2 base by only $0{\cdot}5/R_4 = 0{\cdot}25$ mA from the initial value of 1 mA, and the circuit thus remains stable.

The efficiency of the transistor is such that, although the register dissipates 1·2 watts during the pulse, J_1 dissipates only about 20 mW. Since the pulse repetition frequency is low and the switching time of the circuit is short, transient dissipation can be ignored, and a low-power transistor (100 mW) is capable of driving registers dissipating several times the power of the one described, provided that the voltage rating of the transistor is slightly greater than the voltage required by the register.

(4) CONCLUSIONS

In operating Dekatrons and electro-mechanical registers, the transistor combines the waveform-shaping properties of the thermionic valve with the power economy of the cold-cathode valve. Experience with a 5-decade mains-powered Dekatron scaler supports the expectation of high reliability. Dekatrons in which the glow failed to switch from a particular cathode when used in a standard cold-cathode-operated unit functioned correctly when used in the transistor-operated unit.

The reduction of the delay between input and output pulses in the Dekatron scaler, resulting from the use of negative pulses

for interstage triggering, considerably increases the usefulness of the unit.

(5) ACKNOWLEDGMENTS

The authors are grateful to Messrs. E. H. Cooke-Yarborough and K. Kandiah for many helpful comments.

(6) REFERENCES

(1) CHURCHILL, J. L. W.: 'New Trigger Circuits for use with Cold-Cathode Counting Tubes', *Journal of the British Institution of Radio Engineers*, 1952, **12**, No. 9, p. 497.
(2) KANDIAH, K.: 'A Scaling Unit employing Multi-Electrode Cold-Cathode Tubes', *Proceedings I.E.E.*, Paper No. 1529 M, July, 1953 (**101**, Part II, p. 227).
(3) FLORIDA, C. D., and WILLIAMSON, R.: 'An All-Cold-Cathode Scaling Unit', A.E.R.E., Harwell, Report No. EL/R1257.
(4) BACON, R. C., and POLLARD, J. R.: 'The Dekatron, a New Cold-Cathode Counting Tube', *Electronic Engineering*, 1950, **22**, p. 173.
(5) STEPHENSON, W. L.: 'Junction Transistor Blocking Oscillators', Mullard Report No. 220, August, 1955.

(7) APPENDIX: BLOCKING-OSCILLATOR TRANSFORM DETAILS

The primary inductance of the transformer must be su that with 15 volts impressed across it the magnetizing curr increases from zero to $40 - 5{\cdot}6 = 34{\cdot}4$ mA in 80 micros where 5·6 mA is the total steady-load current. The prim inductance is therefore

$$\frac{15 \times 80 \times 10^{-6}}{34{\cdot}4 \times 10^{-3}} \text{ henry} \simeq 35 \text{ millihenrys}$$

and the winding details are as follows, in the order in which th are wound.

Ferrite E-core type FX1239/A4.

Guide winding: 980 turns, 40 s.w.g.
Emitter winding: 28 turns, 30 s.w.g.
Interstage winding: 92 turns, 30 s.w.g.
Collector winding: 140 turns, 30 s.w.g.

It is preferable to interleave the windings to reduce se capacitance.

[The discussion on the above paper will be found on page 266.]

621.375.3

The Institution of Electrical Engineers
Paper No. 2353 M
Apr. 1957

SOME ASPECTS OF HALF-WAVE MAGNETIC AMPLIFIERS

By G. M. ETTINGER, B.Sc.(Eng.), M.Sc.(Eng.), Graduate.

The paper was first received 21st October, 1955, in revised form 7th November, 1956, and in final form 8th February, 1957. It was published in April, 1957, and was read before the MERSEY AND NORTH WALES CENTRE *28th November, and before a joint meeting of the* MEASUREMENT AND CONTROL SECTION *and the* RADIO AND TELECOMMUNICATION SECTION *3rd December, 1957.)*

SUMMARY

The paper deals with the properties of half-wave magnetic amplifiers ving finite control-circuit resistance or rectifier reverse conductance. e analysis is based on the concept of 'reset factor', which is related the magnetic-amplifier Q-factor during the reverse half-cycle of citation voltage.

It is shown that maximum power gain of a half-wave magnetic plifier is a function merely of the ratio of unsaturated load-winding ctance to load resistance. In most practical cases maximum gain btained with a very small number of control turns, so that nearly the winding space can be used for the load winding. Curves are sented which may be used to determine optimum turns ratio and ximum gain for various combinations of control-circuit resistance d rectifier leakage.

Experimental results for magnetic amplifiers using different core terials are presented. These results agree well with theory. Finally, effect of various bias circuits on half-wave magnetic-amplifier rformance is examined.

LIST OF PRINCIPAL SYMBOLS

θ = Phase angle of load circuit during conducting period.
Φ = Magnetic flux.
ω = Angular frequency of excitation.
A_{max} = Power gain, maximum power gain.
B_m = Saturation flux density.
V_{max} = Peak alternating voltage applied to load circuit.
F = Reset factor = $1 - \exp[-(\pi - \theta)/Q]$.
G = Relative current gain = FN_c/N_l.
k = Turns ratio = N_c/N_l.
N_c, N_l = Control turns, load turns.
p = $\pi R_c/\omega L$.
Q = Control-circuit Q-factor = $k^2\omega L/R_c$.
Q_l = Load-circuit Q-factor = $\omega L/R_l$.
R_c, R_l = Control-circuit resistance, load-circuit resistance.
R_c' = Parallel connection of R_c and R_d, referred to control circuit.
R_d = Rectifier reverse resistance.
S, S_0 = Current gain, current gain for $k = 1$.
u = $R_d/\omega L$.
X_{opt} = $(p/k^2)_{opt}$, the value of p/k^2 for which current gain, with a particular rectifier-leakage coefficient u, is a maximum.
Y_{opt} = A factor (dependent on rectifier leakage) determining maximum current gain.

(1) INTRODUCTION

(1.1) Half-Wave Magnetic-Amplifier Circuits

The half-wave bridge circuit is fast replacing other types of gnetic amplifiers in servo applications. Its advantages include t response, low sensitivity to line voltage changes and the ce of d.c. or reversible-phase a.c. output. Input signals may ther direct current or alternating current at a frequency l to the excitation frequency of the magnetic amplifier.

e performance of half-wave bridge-connected magnetic amplifiers (illustrated in Fig. 1, and studied in detail by Lufcy, Schmid and Barnhart[18]), as indeed that of all magnetic amplifiers, depends on control-circuit impedance.[1-5] Previous work has generally assumed very high[1] or infinitely low[2, 3]

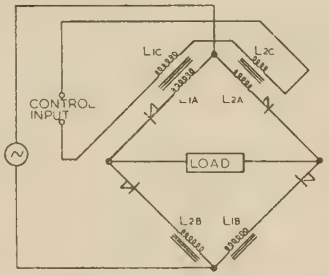

Fig. 1.—Half-wave bridge-connected magnetic amplifier.
There are two cores having windings L_{1A}, L_{1B}, L_{1C} and L_{2A}, L_{2B}, L_{2C} respectively.

control-circuit resistance, and the need for a rigorous theory allowing for finite control-circuit resistance (partly-suppressed even harmonics) has been emphasized.[3] Magnetic amplifiers are usually required to give power gain; the assumptions of infinitely low or extremely large control-circuit resistance are unrealistic. With finite magnetomotive-force gain in the magnetic amplifier, the former assumption implies infinite and the latter assumption zero power gain.

An analysis for half-wave magnetic amplifiers is presented which allows for control-circuit resistance. It is established that rectifier reverse conductance has effects qualitatively similar to those of control-circuit resistance.

(1.2) Time-Constants of Magnetic Amplifiers

Magnetic amplifiers, when fed from available power lines, e.g. 50 c/s or 400 c/s, can be made fast enough for most servo applications. This is especially so if their time-constants are reduced to the minimum for any sampled servo mechanism, i.e. one half-cycle of the excitation frequency.

Time-constants of magnetic amplifiers described before Ramey's paper[2] were relatively large. Faster response could be obtained by connecting series resistance in the control circuit. Alternatively, higher excitation frequencies could be provided; this, however, placed a limit to maximum power outputs, since locally generated or converted high-frequency alternating current is, of course, much more expensive than power at standard line frequency. Circuits having greater gain-bandwidth product have already been described,[6, 7] but these required vacuum tubes so that the advantages of magnetic-amplifier reliability were lost.

The response time of cascaded half-wave magnetic amplifiers has been discussed by Woodson, Schmid and Thrower,[1] who suggest an approximate figure for the time-constant of $(n + 1)/2$ cycles of the excitation frequency, where n is the number of stages. A multistage magnetic-amplifier circuit of much faster response has been described by Hill and Fingerett,[8] who quote a response time of one half-cycle for three stages.

Mr. Ettinger is with Marconi Instruments Ltd.

In 1951 Ramey showed that the response time of half-wave magnetic amplifiers is constant and not greater than one cycle of the excitation frequency. Expressed qualitatively, control current is set up in a Ramey circuit during the forward half-cycle while the magnetic core material is substantially saturated. During this period the incremental permeability is low (and equal to unity in an ideal core material). In a full-wave self-excited magnetic amplifier, on the other hand, some unsaturated iron is always linked by at least one control winding. Hence the time-constant is longer.

(1.3) Power Gain

The difference between half-wave and full-wave magnetic amplifiers is illustrated by the two basic circuits of Fig. 2. The respective time-constants* are, very approximately, π/ω and L/R for a single stage, where ω is the angular frequency of excitation and L and R are the unsaturated inductance and the resistance of the control circuit.

The ratio of the gain-bandwidth products of the two amplifiers of Fig. 2 is not as great as the inverse ratio of their time-constants.

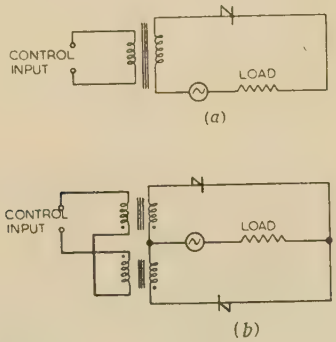

Fig. 2.—Magnetic amplifier circuits.
(*a*) Half-wave. (*b*) Full-wave.

Current gain of the full-wave magnetic amplifier can be readily computed from simple expressions concerned with core geometry, core material properties and number of turns. Gain of the fast half-wave magnetic amplifier, however, is greatly affected by currents induced in the control circuit. Hence, current gain of a half-wave magnetic amplifier with finite control-circuit resistance is equal to current gain of a full-wave magnetic amplifier multiplied by a factor which is always less than unity. It is an object of the paper to determine the magnitude of this factor, here termed the 'reset factor'.

Reset factor is also affected by reverse conductance of the self-excitation rectifiers, and it is a further object of the paper to show the relation between reset factor, control-circuit resistance, effective rectifier reverse resistance and the usual magnetic-amplifier parameters.

ANALYSIS OF HALF-WAVE MAGNETIC AMPLIFIERS

(2.1) Power Gain with Infinite Control-Circuit Resistance

The characteristics of full-wave and half-wave magnetic amplifiers with self-excitation (direct feedback) become similar under conditions of infinite control-circuit resistance (current forcing). Therefore, the various expressions which have been developed in the literature for full-wave magnetic amplifiers can be employed for half-wave circuits if allowance is made for t reset factor already mentioned.

Consider the basic half-wave circuit of Fig. 5(*a*), which indica the quantities to be used in the succeeding analysis. For infin control-circuit resistance and perfect rectifier characteristi the load current will rise from substantially zero to V_{max}/π for a change of control current* approximately equal to $2I_s$, the basis of equal turns in load and control windings. Tl result has been quoted by Maine[5] and others.

We may therefore express the average sensitivity, S_0, of t magnetic amplifier as

$$S_0 = \frac{\Delta I_l}{\Delta I_c} = \frac{V_{max}}{\pi R_l 2I_s} \quad . \quad . \quad . \quad . \quad . \quad (1$$

and, for a turns ratio k,

$$S = k\frac{1}{2\pi}\frac{V_{max}}{R_l I_s} \quad . \quad . \quad . \quad . \quad . \quad (1$$

When the control current is zero, the rectangular-hysteres loop core material [Fig. 3(*a*)] is returned to the point A at t

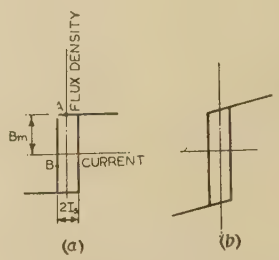

Fig. 3.—Hysteresis loops of core material.
a) Idealized. (*b*) Practical.

end of the conducting half-cycle. In the absence of rectifi leakage or equivalent effects, the core remains in this conditic until, nearly one half-cycle later, current again flows throug the rectifier.

The core is already at positive saturation, so that no voltag time product is required to build up flux; conduction throug the load commences immediately. Clearly, then, the load curre takes the form of half-sinusoids and has a mean val $V_{max}/\pi R_l$.

With direct control current the core material reaches a co dition such as that represented by point B of Fig. 3(*a*). T reach saturation during the conducting half-cycle a voltage-tir area proportional to the flux difference, $B_m - B_B$, has to b supplied. Hence the core conducts later, load current flov during a smaller fraction of each cycle, and average load curre is reduced.

The process by which the remanent flux in the core is reduce from B_m (or B_r, the remanence, in materials not having rec angular hysteresis loops) is termed 'reset'. It has been discusse for example, by Walker and Wilson.[9] This process is mo important; it forms the basis of magnetic-amplifier operatio Reset may be achieved by passing steady current through control winding in a direction to demagnetize the core, or b applying a pulse[10] of arbitrary shape during some part of th non-conducting half-cycle.†

Referring again to Fig. 5(*a*), an expression for sensitivity

* Where time-constants are mainly due to control-circuit inductance, as in full-wave magnetic amplifiers, the conventional definition of time-constant as time taken for current to rise to 63% of final value may be used (subject to non-linearity for large changes). With half-wave magnetic amplifiers, however, effective time delay depends also on the instant during the cycle when the control signal is applied.

* Many modern magnetic amplifiers are wound on core materials having near rectangular hysteresis loops, as in Figs. 3(*a*) and 3(*b*). Therefore I_s, the current need to saturate the core material, may be replaced by I_{HC}, the current corresponding the coercive force.

† Pulses applied during the forward or conducting half-cycle have almost no effe Hence, attention must be paid to correct phasing when half-wave magnetic amplifie are cascaded. Two identical magnetic amplifiers fed from the same supply transform cannot be cascaded unless their rectifiers are connected in opposite directions. Th ensures that the amplifiers conduct during alternate half-cycles.

ntrol flux (rather than to control current) may be developed follows:

$$I_l \text{ (average)} = \frac{V_{max}}{2\pi R_l} \int_{\psi_1}^{\pi} \sin \omega t \, d(\omega t)$$

here the angle ψ_1 is represented in Fig. 4, and is termed the

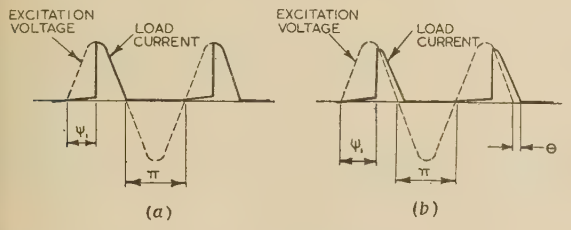

Fig. 4.—Load-current waveforms in half-wave magnetic amplifiers.
(*a*) Resistive load circuit.
(*b*) Inductive load circuit.

iring angle'.[11] For $\psi_1 = 0$, the load current reaches its maxi-um of $V_{max}/\pi R_l$. The firing angle is given by

$$V_{max} \int_0^{\psi_1} \sin \omega t \, d(\omega t) = N(\Phi_m - \Phi_B) = N\Delta\Phi \quad . \quad (2)$$

reset is not inhibited, then, from the definition of inductance, e flux change due to a current change ΔI is given by

$$\Delta\Phi = \Delta IL/N \quad . \quad . \quad . \quad . \quad . \quad . \quad (3)$$

The expressions so far are straightforward and imply merely rfect rectifiers (infinite reverse resistance) whence load current t the end of the conducting or forward half-cycle is zero and mains zero until the beginning of the conducting period. If is condition holds, the control flux is determined from the c. hysteresis loop of the core material (subject to transients lated to the rate of flux penetration, as discussed by Shu Hsien now[12]). In the case of a.c. control, the control flux is affected r the shape of minor or incremental hysteresis loops.

(2.2) Effect of Control-Circuit Resistance

Consider a square-hysteresis-loop magnetic core carrying two ual windings [Fig. 5(*a*)]. The right-hand (load) winding is

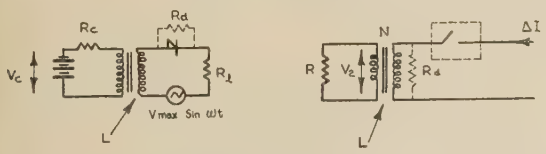

Fig. 5.—Basic circuits.
(*a*) Two-winding core.
(*b*) Equivalent circuit during reverse half-cycle.

nnected in series with a rectifier and a source of alternating ltage. The left-hand (control) winding is connected to a eady voltage source V_c in series with a resistance R_c.

When zero load current is reached at the end of the conducting riod, the rectifier presents a high resistance. It might be mpared with a switch which produces a negative-going step nction of current in the load circuit. The demagnetizing or se process can be attributed to the fall of magnetomotive force om NI_s to $N(I_s - I_c)$, where NI_s represents the m.m.f. corre-onding to magnetic saturation and I_c is the control current. n equivalent circuit may be drawn for the 2-winding reactor, in Fig. 5(*b*). This circuit will be applicable from the time when e maginary 'switch' opens to the time when the rectifier begins nduct again.

In the ideal case of infinite control-circuit resistance, the change of flux level in the circuit of Figs. 5(*a*) and 5(*b*) is simply obtained from eqn. (3) as $\Delta\Phi = \Delta IL/N = (I_s - I_c)L/N$. In a practical case the control-circuit resistance cannot be infinite, so that the voltage V_2 induced in the circuit of Fig. 5 is reduced. Thus the flux change $\Delta\Phi$ and the reset become smaller.

The mean current in the control circuit is, of course, constant; it is determined by Ohm's law and is independent of current in the load circuit. If an induced positive current, for example, is superposed on the steady control current during the reverse half-cycle, then negative current must be superposed during the following half-cycle.

In the present analysis, the effects on reset of currents induced during the reverse half-cycle only are considered; these induced currents depend, of course, on control-circuit resistance and on turns ratio. Transients in the control circuit may, however, be ignored during the conducting or forward half-cycle, where increase of core flux is mainly controlled by the supply voltage applied through the relatively low rectifier forward and load resistances.

The voltage induced in the perfectly coupled circuit of Figs. 5(*a*) and 5(*b*) in response to ΔI, a step change of current from I_s to I_c, will thus be given by

$$V_2(t) = \Delta IR\varepsilon^{-t/\tau} \quad . \quad . \quad . \quad . \quad . \quad . \quad (4)$$

where τ, the time-constant, equals L/R.

Therefore $V_2(t) = \Delta IR\varepsilon^{-tR/L}$

and $$\Phi(t) = \frac{1}{N}\int V_2(t)dt = \Delta I\frac{L}{N}(1 - \varepsilon^{-tR/L}) \quad . \quad . \quad (5)$$

which gives the time variation of flux in response to the fall of current from saturation.

In the simple case of a purely resistive load circuit, reset can continue for a time equal to one half-cycle, as shown in Fig. 4(*a*). If the frequency of excitation is ω radians per second, the maximum time available for reset is π/ω, or one half-cycle. Substituting π/ω for t in eqn. (5) we have

$$\Delta\Phi = \Delta I\frac{L}{N}[1 - \varepsilon^{-R\pi/(\omega L)}] = \Delta I\frac{L}{N}(1 - \varepsilon^{-\pi/Q}) \quad . \quad (6)$$

where ωL is the reactance and Q the effective Q-factor of the magnetic amplifier during the non-conducting half-cycle.

If $Q = 0$ (infinitely large control-circuit resistance or infinitely small control-circuit reactance), then reset given by eqn. (3) takes place. For finite Q, the reset is given by eqn. (6). The ratio of these two flux changes defines the reset factor, F, as

$$F = 1 - \varepsilon^{-\pi R_c/(\omega L)} = 1 - \varepsilon^{-\pi/Q} \quad . \quad . \quad . \quad (7a)$$

For a given number of turns, half-wave magnetic-amplifier gain is substantially proportional to the reset factor. Fig. 6(*a*) shows F plotted against control-circuit Q-factor for various load-circuit phase angles (see next Section).

(2.3) Effect of Load-Circuit Phase Angle

If the current in the load circuit lags behind the excitation voltage, as shown in Fig. 4(*b*), less time is available for reset. This is unimportant in the case of infinite control-circuit resistance, where reset may be completed within a small fraction of a cycle. However, it is seen from eqn. (5) that the amount of reset with finite control-circuit resistance depends on the time available before the rectifier begins to conduct again under the influence of the positive half-cycle of the supply voltage. The reset time is therefore $(\pi - \theta)/\omega$ instead of π/ω, where θ is the phase angle of the load circuit.

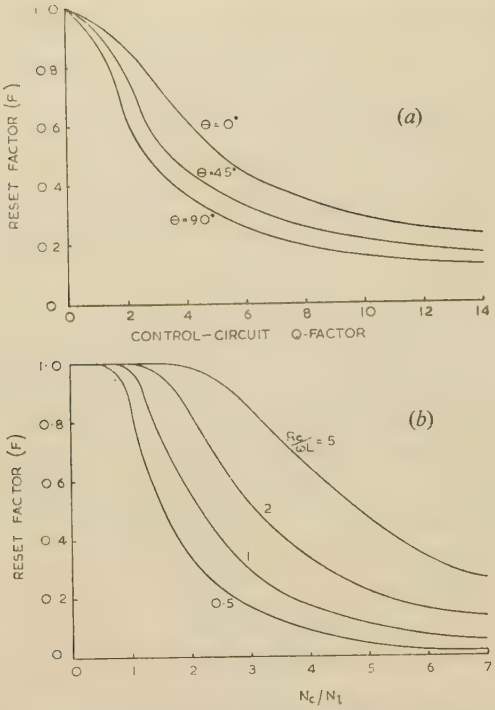

Fig. 6.—Variation of reset factor with magnetic-amplifier parameters.
(*a*) Effect of control-circuit Q-factor on reset factor (computed) for various load-circuit phase angles.
(*b*) Effect of turns ratio on reset factor (computed) for various control-circuit resistances.

Hence, by substitution in eqn. (7*a*),

$$F = 1 - \varepsilon^{-(\pi-\theta)/Q} \quad . \quad . \quad . \quad . \quad . \quad (7b)$$

Eqn. (7*b*) shows that increased phase lag causes reduced reset factor and hence reduced sensitivity.*

In modern magnetic materials, which may have rectangularity coefficients[14] as high as 0·98, the permeability is much greater than unity even when m.m.f.'s equivalent to several times the coercive force are supplied. An approximation to the hysteresis loop, consisting of finite-slope portions for the 'saturated' region and a 2-valued unsaturated region, as described by Finzi and Pittman[15] and shown in Fig. 3(*b*), is more appropriate. Here the saturated load circuit is inductive even with a purely resistive load, and phase angle must be considered in evaluating the reset factor. The effect of phase angle on reset factor is shown in Fig. 6(*a*).

(2.4) Effect of Number of Control Turns

Equal turns in load and control winding were assumed in the previous Section. In practical magnetic amplifiers the turns ratio will not, of course, be unity. Hence eqn. (7*b*) may be expressed for the case of perfect rectifiers as

$$F = 1 - \exp\left[\frac{-(\pi-\theta)}{k^2\omega L}R_c\right] \quad . \quad . \quad . \quad (7c)$$

The turns ratio k must be taken into account in order to obtain the reactance referred to the control circuit and hence the correct reset factor.

In this Section, the effect of control turns with constant control-circuit resistance is considered. Once the load circuit has been designed, load-circuit inductance L, but not control-circuit inductance, is fixed. Therefore, the various expressions for re factor are developed in terms of control-circuit resistance a load-circuit inductance. In Fig. 6(*b*) the reset factor is plott against turns ratio for various control-circuit resistances.

(2.5) Effect of Rectifier Leakage

(2.5.1) Negative Bias.

Rectifier reverse current flowing during the negative half-cy of supply voltage produces negative bias, and therefore increas reset action. This is useful because the effect is one of consta bias which shifts the operating point of the magnetic amplif downwards along its characteristic. In this way, standing curre is reduced and high gain can be obtained by working over t steepest portion of the characteristic.

(2.5.2) Reduction of Reset Factor.

Reverse conductance of the self-excited rectifier also increas the effective Q-factor of the magnetic amplifier during the re period, and therefore causes a reduction of reset factor. Qua tatively it may be said that, in addition to permitting the flo of bias current, rectifier reverse conductance permits continuati of load current flow during the supposedly non-conducting ha cycle. Hence reset is reduced.

It is convenient to substitute Q_{eff} for Q in eqn. (7*b*), where Q is the effective Q-factor of a circuit containing a reactance ωL a a parallel connection of the reflected control-circuit resistance and the rectifier reverse resistance R_d. It is given by

$$Q_{eff} = \omega L \frac{R_d + R_c/k^2}{R_c R_d/k^2}$$

and the reset factor becomes

$$F = 1 - \exp\left[\frac{-(\pi-\theta)}{\omega L}\,\frac{R_c R_d/k^2}{R_d + R_c/k^2}\right] \quad . \quad . \quad (7$$

It is clear from this equation that no useful purpose is serve by increasing R_c much above the reflected rectifier rever resistance. Correspondingly, a half-wave magnetic amplifi with infinite control-circuit resistance will still have a reset fact less than unity if the rectifiers are not perfect. The effect rectifier leakage on magnetic-amplifier performance is furth considered in Sections 3.3 and 8.

(3) DESIGN OF MAGNETIC AMPLIFIERS FOR MAXIMU GAIN

(3.1) Optimum Turns Ratio

In the previous Section the reset factor was defined as th ratio of current gain of a magnetic amplifier with finite contro circuit resistance (and with finite rectifier reverse resistance) t the current gain of a magnetic amplifier having the same cor number of turns and load impedance, but infinite control-circu resistance and perfect rectifiers. Therefore, if we define th maximum possible current amplification of a magnetic amplifie from eqn. (1), as kS_0, i.e. $(N_c/N_l)S_0$, then S, the current amplifica tion of a magnetic amplifier with finite control-circuit resistanc is given by

$$S = (N_c/N_l)FS_0$$

or

$$S/S_0 = (N_c/N_l)F = G \quad . \quad . \quad . \quad . \quad (8$$

where

$$G = \frac{N_c}{N_l}\left\{1 - \exp\left[\frac{-(\pi-\theta)R_c}{\omega L(N_c/N_l)^2}\right]\right\}$$

$$= (N_c/N_l)(1 - \varepsilon^{-p/N_l^2}) \quad . \quad . \quad . \quad . \quad . \quad . \quad (9$$

where

$$p = R_c(\pi-\theta)N_l^2/(\omega L)$$

* With loads of very long time-constants, load-shunting or 'commutating' rectifiers are sometimes employed.[13] These increase the magnetic-amplifier time-constant and are not considered here, where one-cycle-response magnetic amplifiers only are dealt with.

To find N_c which will give maximum G for a given control-circuit resistance, differentiation of eqn. (9) with respect to N_c yields

$$\frac{dG}{dN_c} = \frac{1}{N_l}\left[1 - \varepsilon^{-p/N_c^2}\left(1 + \frac{2p}{N_c^2}\right)\right]$$

and $$dG/dN_c = 0$$

when $$\varepsilon^{-p/N_c^2}(1 + 2p/N_c^2) = 1$$

or $$p/N_c^2 = 1{\cdot}257$$

Substituting $p/N_c^2 = 1{\cdot}257$ in the equation for p, the following expression is found for the turns ratio which will give maximum relative current gain G in a given magnetic amplifier:

$$N_c^2\Big]_{max\,G} = \frac{(\pi - \theta)N_l^2 R_c}{1{\cdot}257\omega L} \quad . \quad . \quad . \quad . \quad (10a)$$

In the case of purely resistive load circuit ($\theta = 0$),

$$\left(\frac{N_c}{N_l}\right)^2\Big]_{max\,G} = 2{\cdot}5\frac{R_c}{\omega L}$$

or $$\frac{N_c}{N_l}\Big]_{max\,G} = 1{\cdot}58\sqrt{\frac{R_c}{\omega L}} \quad . \quad . \quad . \quad . \quad (10b)$$

For the optimum condition represented by eqn. (10*b*), the value of G_{max} [the maximum value of the relative current gain $(N_c/N_l)F$] is obtained by substituting $p/N_c^2 = 1{\cdot}257$ in eqn. (9) as:

$$G_{max} = 1{\cdot}13\sqrt{\frac{R_c}{\omega L}} \quad . \quad . \quad . \quad . \quad . \quad (11)$$

(3.2) Maximum Current Gain

The quantity of interest in a magnetic amplifier is not a normalized factor such as F or G, but the overall gain. This may be found by combining eqns. (8) and (11) with eqn. (1) to obtain

$$S_{max} = \left(\frac{\Delta I_l}{\Delta I_c}\right)_{max} = 1{\cdot}13\sqrt{\left(\frac{R_c}{\omega L}\right)}\frac{V_{max}}{2\pi R_l I_s} \quad . \quad (11a)$$

V_{max}/I_s is of course the reactance ωL of the load winding, where the magnetization curve is represented by three straight lines.[15] Hence, eqn. (11*a*) can be expressed as

$$S_{max} = \frac{1{\cdot}13}{2\pi}\sqrt{\left(\frac{R_c}{\omega L}\right)}\frac{\omega L}{R_l} = 0{\cdot}18\sqrt{\left(\frac{R_c}{\omega L}\right)}Q_l \quad (11b)$$

(3.3) Maximum Power Gain

Power gain A is given by $I_l^2 R_l/(I_c^2 R_c)$ or $S^2 R_l/R_c$ where S is the current gain defined in Section 2.1. From eqn. (11*b*) and the definition of A, power gain reaches a maximum value given by

$$A_{max} = 0{\cdot}18^2\frac{R_c}{\omega L}\frac{\omega^2 L^2}{R_l^2}\frac{R_l}{R_c} = 0{\cdot}032\frac{\omega L}{R_l} = 0{\cdot}032Q_l \quad (12a)$$

Eqns. (11) and (12) assume that the effect of control-circuit resistance on reset is much greater than the effect of rectifier shunt conductance. Where rectifier leakage is appreciable,* R_c in eqns. (11) and in the numerator of eqn. (12) must be replaced by R_c', which represents the parallel connection of R_c (control-circuit resistance) and the rectifier leakage referred to the control circuit.

Thus $$S_{max} = 0{\cdot}18\sqrt{\left(\frac{R_c'}{\omega L}\right)}Q_l \quad . \quad . \quad . \quad . \quad (11c)$$

and $$A_{max} = 0{\cdot}032\frac{R_c'}{R_c}Q_l \quad . \quad . \quad . \quad . \quad . \quad (12b)$$

Computed effect of control-circuit resistance on current gain and power gain, with turns ratio as a parameter, is shown in Figs. 7(*a*) and 7(*b*). The broken curves of Fig. 7(*b*) show the variation of full-wave magnetic-amplifier power gain, computed under the assumption of constant gain-bandwidth product.

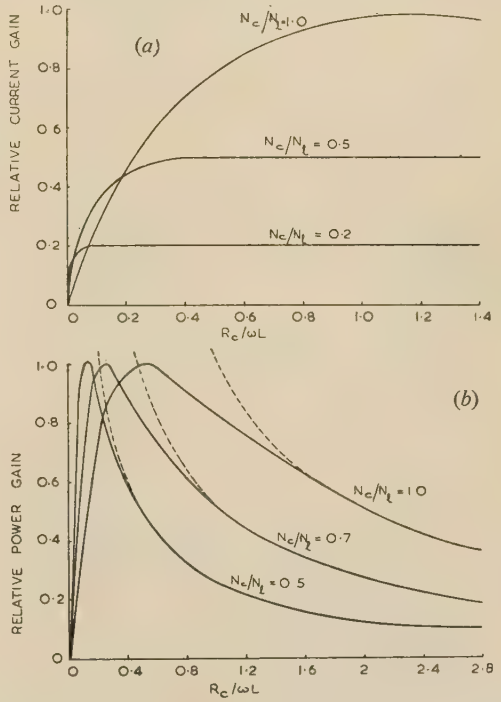

Fig. 7.—Variation of gain with magnetic-amplifier parameters.

(*a*) Effect of control-circuit resistance on current gain (computed) for various turns ratios.
(*b*) Effect of control-circuit resistance on power gain (computed) for various turns ratios.

(4) EXPERIMENTAL RESULTS

(4.1) Details of Measurements

The theoretical expressions for reset factor F, normalized gain G, current gain S, and power gain A were compared with experimental results for two magnetic amplifiers wound on H.C.R. laminations and on a tape-wound toroid, respectively, and for magnetic amplifiers wound on Mumetal and on Permalloy F (a hydrogen-annealed Permalloy, similar to Supermalloy).

Details of the four magnetic amplifiers are given in Table 1. Selenium rectifiers, operated at about 10 volts r.m.s. per disc, were employed in three of the magnetic amplifiers; rectifier reverse resistance was obtained approximately by oscilloscopic measurements. For the tape-wound toroidal H.C.R. magnetic-amplifier germanium junction diodes, having very small reverse conductance, were used.

* For very accurate computation the reset factor given by eqn. (7*d*) must be maximized, rather than that given by eqn. (7*c*). This is considered in Section 8, where it is shown that if R_d, the diode shunting resistance, is greater than $2\omega L$, then eqn. (10*b*) gives turns ratios within 10% of optimum.

(4.2) Effect of Control-Circuit Resistance: Constant Turns Ratio

Fig. 8 shows the test circuit for the laminated H.C.R. magnetic amplifier. The control characteristics of this amplifier are shown in Fig. 9 for two load-circuit phase angles (two different load resistances were employed in a circuit otherwise unchanged to obtain different phase angles). The relative current gain for constant control turns was found by taking the mean slope of the control characteristics over a control-current range of 2 mA. The slopes are plotted in Fig. 10. It is seen that current gain increases with increasing control-circuit resistance. The theoretical curves of Fig. 10 were plotted from eqn. (7*d*), taking a value of 130 kilohms for rectifier reverse resistance. Maximum

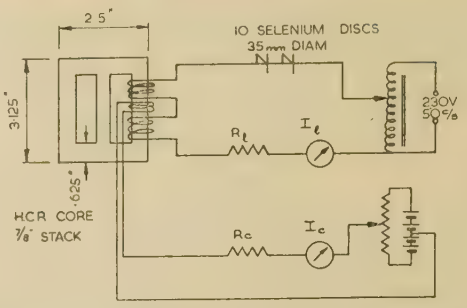

Fig. 8.—Test circuit for H.C.R. magnetic amplifier.

Table 1

DETAILS OF MAGNETIC AMPLIFIERS TESTED

Material	Construction	Length of magnetic circuit	Cross-sectional area	Load winding		Computed current gain (mean)*	Experimental current gain (maximum)*
				Turns	Reactance 50 c/s		
		in	in²		kilohms		
H.C.R. (0·004 in)	Laminations	8	0·52	5 700	200	2	2·14
H.C.R. (0·004 in)	Toroid	15·7	1·00	1 600	50	4·5	5·3
Mumetal (0·007 in)	Laminations	3·75	0·14	3 650	165	5·8	8
Permalloy F (0·003 in)	Toroid	6·3	0·25	1 200	19	35	27

* Current gain computed and measured for infinite control-circuit resistance (F = 1).

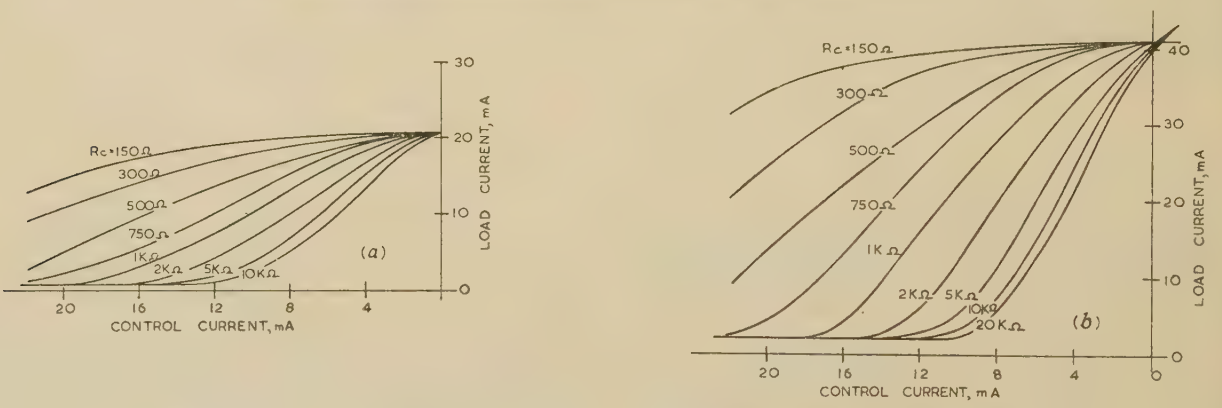

Fig. 9.—Effect of control-circuit resistance on H.C.R. magnetic-amplifier characteristics.
(*a*) Load-circuit phase angle = 25°.
(*b*) Load-circuit phase angle = 45°.

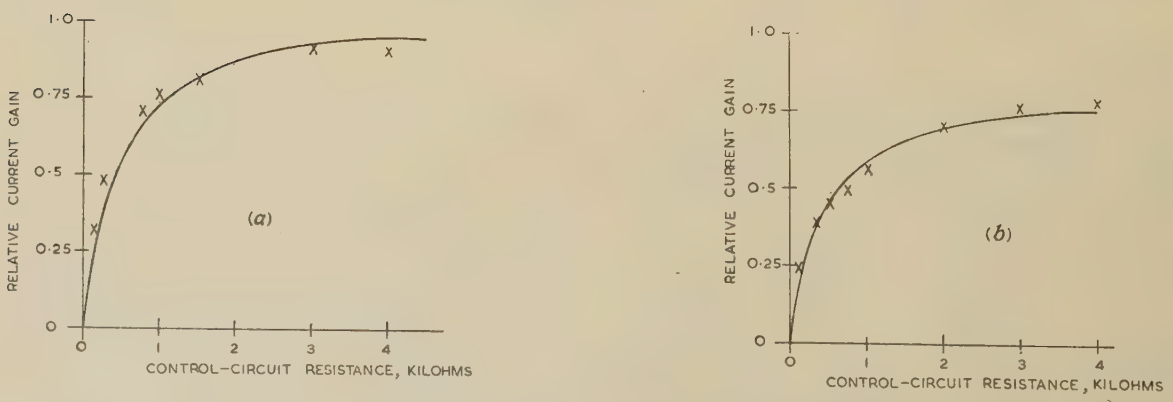

Fig. 10.—Effect of control-circuit resistance on H.C.R. magnetic-amplifier current gain.
(*a*) Load-circuit phase angle = 25°.
(*b*) Load-circuit phase angle = 45°.
——— Computed for rectifier reverse resistance = 130 kilohms.
× × × Experimental.

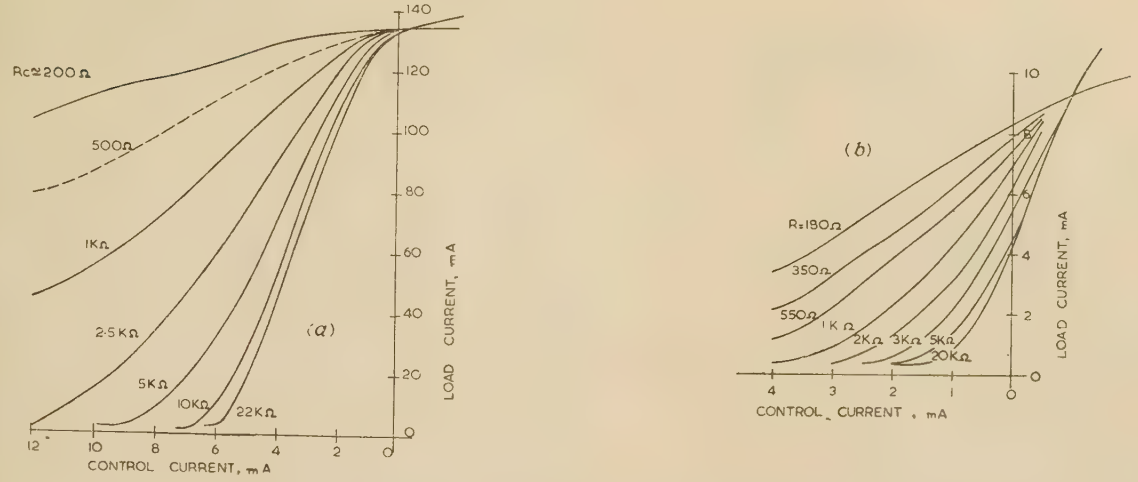

Fig. 11.—Effect of control-circuit resistance on magnetic-amplifier characteristics.
(*a*) Permalloy F. $N_l = 1200$; $N_c = 500$; $R_l = 72$ ohms.
(*b*) Mumetal. $N_l = 3650$; $N_c = 450$; load-circuit phase angle = 60°.

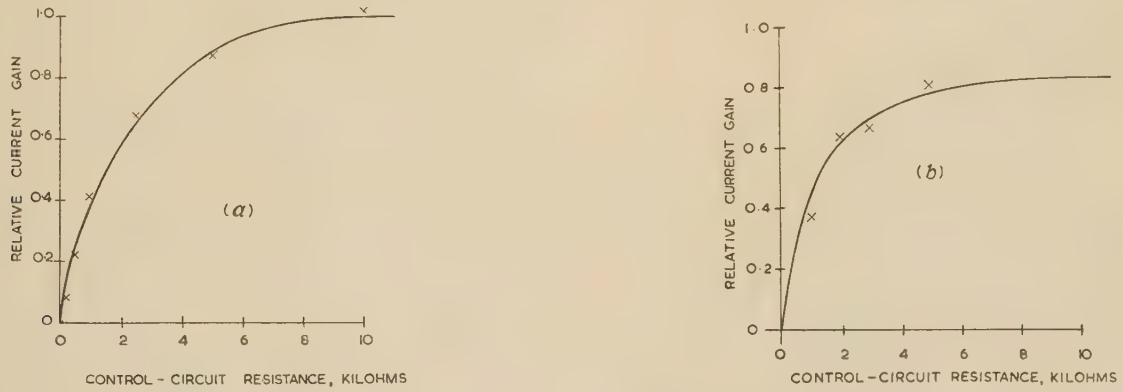

Fig. 12.—Effect of control-circuit resistance on magnetic-amplifier current gain.
——— Computed.
× × × Experimental.
(*a*) Permalloy F.
(*b*) Mumetal.

urrent gain of this amplifier was found to be 2·14 (see Table 1), omputed maximum gain was 2·0.

Similar measurements were made on the Permalloy F magnetic mplifier whose details are given in Table 1. Control charac-eristics are shown in Fig. 11(*a*) and experimental and computed ensitivities are compared in Fig. 12(*a*). The agreement is seen o be good.

Figs. 11(*b*) and 12(*b*) show the control characteristics and ensitivities, respectively, as functions of the control-circuit esistance for a Mumetal magnetic amplifier. The agreement etween experimental and computed values is fair. The com-uted characteristic is shown asymptotic to a relative current ain of 0·85. The difference between this figure and unity epresents the effect of finite rectifier reverse conductance, which as 200 kilohms in this case, or 3 kilohms referred to the control ircuit.

(4.3) Effect of Turns Ratio: Constant Control-Circuit Resistance

Measurements were made on magnetic amplifiers of two core materials, keeping constant the control-circuit resistance and varying the control turns.*

* Preliminary experiments had indicated that total control-circuit resistance would be to be many times higher than the resistance of the control windings themselves. Control-winding resistance was, in fact, small enough to be neglected compared with external control-circuit resistance.

Figs. 13(*a*) and 13(*b*) show control characteristics of the magnetic amplifier on H.C.R. laminations, already referred to, for two values of control-circuit resistance. The slopes of the characteristics are plotted in Figs. 14(*a*) and 14(*b*), which also show computed curves of relative gain as a function of the number of control turns. The computed curves were obtained from eqn. (7*c*).

Agreement between experimental and computed values is good. In particular, the experimental number of control turns (approximately 400) needed for maximum current gain is close to the computed figure of 355.

The results of similar measurements on a Mumetal magnetic amplifier are shown in Fig. 15. The importance of selecting the correct number of control turns for a magnetic amplifier, once the control-circuit resistance is fixed, is shown clearly by the curves of Figs. 14(*a*) and 15(*b*).

(4.4) Maximum Power Gain

From the current-gain curve of Fig. 12(*b*), the variation of power gain with control-circuit resistance (Fig. 16) was obtained for a Mumetal magnetic amplifier. It is seen that power gain falls to less than 90% of its maximum if control-circuit resistance departs from its optimum value by more than about ±50%.

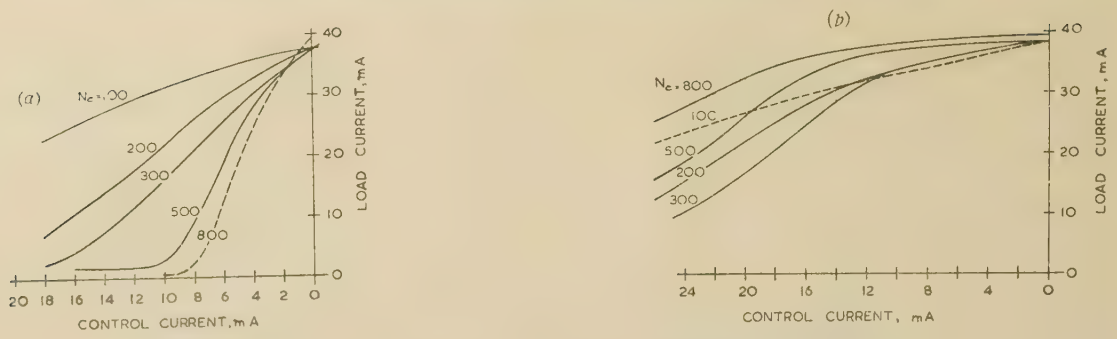

Fig. 13.—Effect of turns ratio on H.C.R. magnetic-amplifier characteristics.
(*a*) Control-circuit resistance = 5 000 ohms. (*b*) Control-circuit resistance = 250 ohms.

Fig. 14.—Effect of turns ratio on H.C.R. magnetic-amplifier current gain.
(*a*) Control-circuit resistance = 5 000 ohms. (*b*) Control-circuit resistance = 250 ohms.

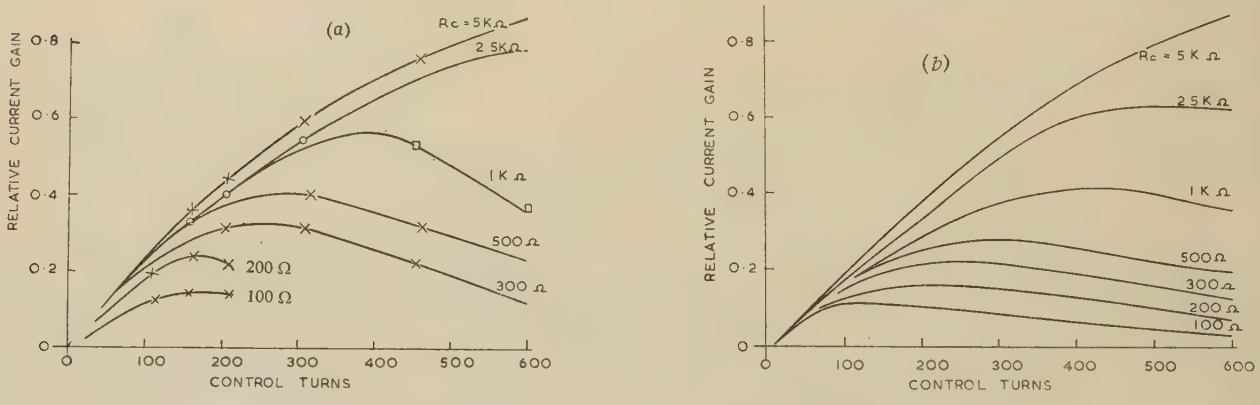

Fig. 15.—Effect of turns ratio on Mumetal magnetic-amplifier current-gain.
(*a*) Experimental. (*b*) Computed.

(5) MAGNETIC-AMPLIFIER BIAS

(5.1) Bias Circuits

(5.1.1) Effect of Bias.

Bias must often be provided to produce characteristics which can be combined for symmetrical or balanced working.* This is important since, as seen from Figs. 9, 11(*a*) and (13), the slope of the transfer characteristics for zero control current is very much less than the maximum slope.

(5.1.2) D.C. Bias.

D.C. bias is used where a fixed m.m.f. can be superposed on the variable control m.m.f., either by bias current flowing

* This applies especially to magnetic servo amplifiers which must, of course, have bi-directional output. For certain other applications, unidirectional output may be sufficient, so that an origin of characteristics corresponding to the zero-control ordinates of Fig. 12(*a*) would be acceptable.

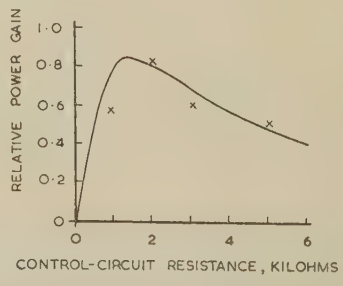

Fig. 16.—Effect of control-circuit resistance on Mumetal magnetic-amplifier power gain.
N_l = 3 650 turns; N_c = 450 turns; rectifier reverse resistance = 200 kilohms.
——— Computed from Fig. 12(*b*).
× × × Experimental values.

through the control or signal windings or by using separate bias windings. If all other parameters of a magnetic amplifier can be kept constant, d.c. bias merely shifts the characteristics parallel to the axis of ordinates. This form of bias has little effect on the sensitivity of magnetic amplifiers to line voltage changes.

5.1.3) **A.C. Bias.**

It has been shown, by Geyger[17] for example, that bias for magnetic amplifiers can be provided by passing alternating current through separate bias windings. It is merely necessary to ensure that phase shift between bias supply voltage and magnetic amplifier excitation voltage is not excessive. Part of the positive cycle of bias current is ineffective because the magnetic material is substantially saturated during this period. The negative half-cycle of bias, however, adds to or subtracts from the voltage-time area represented by the control signal. Therefore, a shift of the control characteristics is obtained.

Geyger found also that a.c. bias, when derived from the same power source as the excitation signal, reduces the dependence of magnetic amplifier output on line voltage. An increase of line voltage, in the absence of bias, will of course, tend to increase the load current. However, an increase of a.c. bias, if connected in a sense to reduce the load current [see Fig. 18(*b*)] causes partial cancellation of this line-voltage dependent increase. Geyger[16, 17] showed improvements of the order of 5 : 1 in line-voltage effects by this method.

A.C. bias, then, can serve two functions: shift of operating point to a desired position, and reduction of line voltage dependence. Lufcy, Schmid and Barnhardt[18] also discuss a.c. bias, but suggest that it is preferable to employ rectified bias, as discussed in Section 5.1.5.

5.1.4) **Part-Winding A.C. Bias.**

It is shown in Section 2.2 that any resistance shunting the magnetic-amplifier windings reduces reset factor and gives lower sensitivity to control currents. It was also shown that F, the reset factor, depends on Q, as shown in eqn. (7*a*). To produce a bias of NI ampere-turns from a supply line of V volts, there is obtained an equivalent Q-factor, due merely to the a.c. bias resistance, given by Table 2.

Table 2

EFFECT OF A.C. BIAS TURNS ON RESET FACTOR

N_b (bias turns)	I_b (relative bias current)	R_b (relative resistance to establish I_b)	Q (relative Q-factor)	F (reset factor) $1-\varepsilon^{-\pi/Q}$	P_b (relative power dissipated in R_b)
100	1	1	10	0·27	1
50	2	0·5	5	0·47	2
20	5	0·2	2	0·79	5
10	10	0·1	1	0·96	10

Therefore, when a.c. bias is employed in a half-wave magnetic amplifier, the smallest possible number of bias turns should be used, subject to power dissipation in the bias resistance. From Table 2, it is seen that, if possible, the Q-factor of the bias winding should not appreciably exceed unity if a reset factor close to unity is desired. If it is impracticable to provide an additional bias winding, then a.c. bias may be passed through a part only of the existing load windings, as shown in Fig. 17(*a*). This, of course, requires an additional tapping on the winding. However, in a bridge arrangement a tap is in effect provided part-way along the winding. This may be utilized for a.c. bias as shown in Fig. 17(*c*).

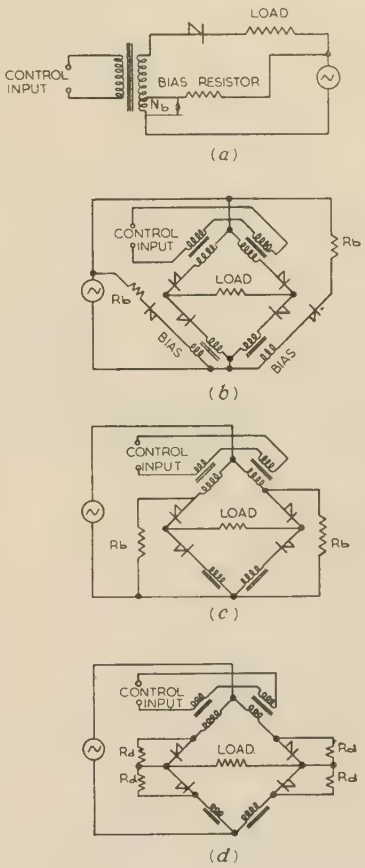

Fig. 17.—Bias circuits for magnetic amplifiers.
(*a*) Part-winding a.c. bias.
(*b*) Bias with blocking rectifiers.
(*c*) Half-winding a.c. bias.
(*d*) Diode shunt bias.

(5.1.5) **Rectified Bias.**

The circuit of Lufcy, Schmid and Barnhardt[18] is shown in Fig. 17(*b*). The half-cycle of bias current which is almost ineffective is removed by rectifiers. Lufcy *et al.* suggest that circulating currents are reduced in this way, so that higher gain may be obtained.

(5.1.6) **Bias through Rectifier Shunts.**

Bias through rectifier shunts is illustrated in Fig. 17(*d*). Magnetic-amplifier sensitivity is reduced owing to shunting of the load windings during reset. For certain simple magnetic amplifiers, where extremely high gain is not required, this form of bias is very convenient. It has one other use: where rectifiers have poor reverse characteristics it is sometimes desirable to employ additional shunt resistances as shown in Fig. 17(*d*), in order to reduce gain and to make magnetic amplifier performance less dependent on variation of rectifier properties. Shunted rectifiers may be used in conductance-controlled magnetic amplifiers (see Section 5.3).

(5.2) Experiments with Various Bias Circuits

Tests were made on an H.C.R. laminated core with a.c. bias and with diode-shunt bias; further tests on a Permalloy F core were made with part-winding a.c. bias.

Bias by means of rectifier shunts is illustrated in Fig. 18(*a*). Sensitivity falls with decreasing shunt resistance, just as with decreasing control-circuit resistance (Fig. 9). The effect of a.c.

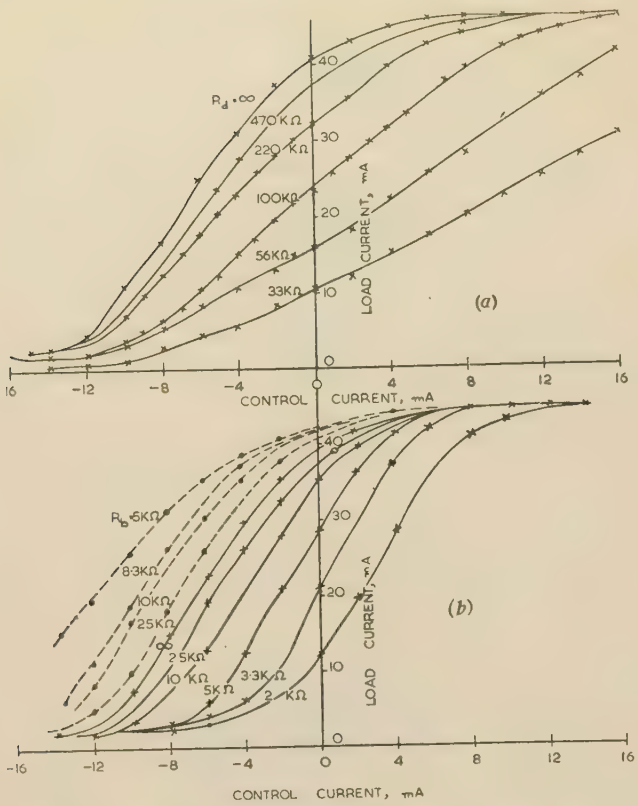

Fig. 18.—Effect of bias on H.C.R. magnetic-amplifier control characteristics.

n_1 = 5700 turns; n_c = 500 turns; control-circuit resistance = 3000 ohms.
(*a*) Diode shunt bias.
(*b*) A.C. bias through separate 100-turn winding.
● ● ● Bias opposing excitation (positive bias).
× × × Bias in phase with excitation (negative bias).

bias is shown in Fig. 18(*b*). It is seen that the magnetic-amplifier characteristics remain almost parallel.

Fig. 18(*a*) shows, therefore, the amount of bias which can be applied to a particular magnetic amplifier through rectifier shunts without appreciable reduction of sensitivity. More important, it shows the form of bias which may be obtained from using imperfect rectifiers.

Line voltage dependence of an H.C.R. magnetic amplifier as a function of a.c. bias was investigated. It was found that negative (resetting) a.c. bias reduced sensitivity to line voltage changes by more than 50%.

(5.3) Conductance-controlled Magnetic Amplifiers

Referring again to Fig. 18(*a*), it is seen that the output of a self-excited magnetic amplifier, for zero control current, is a function of rectifier shunt resistance. It was realized, therefore, that control windings might be dispensed with altogether by employing variation of rectifier-shunt resistance to control magnetic-amplifier output.

Bi-directional output was required; hence a conductance-controlled bridge circuit was employed, as shown in Fig. 19. Its characteristics are plotted in Fig. 20; these are reasonably linear. Reversible output power of the order of 25 mW was controlled by a change of resistance of 30 kilohms; maximum power dissipated in the controlling resistance was about 1 mW.

The conductance-controlled magnetic-amplifier circuit might be employed in certain position-control systems where servo-amplifier inputs are, basically, in the form of shaft rotations

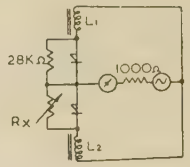

Fig. 19.—Conductance-controlled magnetic amplifier.

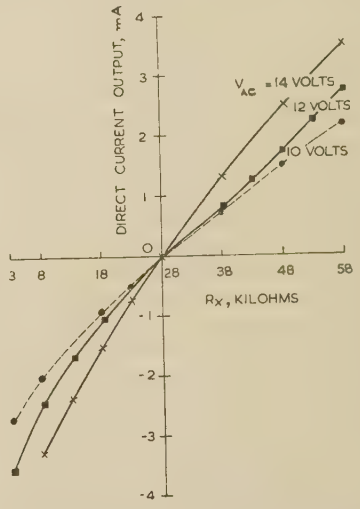

Fig. 20.—Control characteristics of conductance-controlled magnetic amplifier for various excitation voltages.

(or differences of shaft rotations) rather than in the form of electrical quantities, or in strain-gauge amplifiers.

(6) CONCLUSIONS

A theory of half-wave magnetic amplifiers is presented which takes account of the effect on reset of control-circuit resistance or rectifier leakage resistance and of imperfect core properties. A reset factor is defined, relating current gain of a half-wave magnetic amplifier which is subject to the above effects to current gain of a similar half-wave magnetic amplifier with infinite control-circuit resistance, no rectifier leakage and rectangular hysteresis loop. The theory is supported by measurements on magnetic amplifiers of various core materials.

Simple expressions are developed for current gain and power gain of half-wave magnetic amplifiers and conditions for maximum gain are determined. It is shown that these simple expressions hold where rectifier reverse resistance is greater than twice the load circuit reactance. Correction factors are computed and plotted which may be used where rectifier leakage is appreciable.

Means for providing bias in half-wave magnetic amplifiers, especially in half-wave bridge circuits, are reviewed, and a technique termed 'part-winding' bias is recommended. Finally, a conductance-controlled magnetic amplifier is described.

(7) BIBLIOGRAPHY

(1) Woodson, H. H., Thrower, C. V., and Schmid, A. E.: 'Compensation of Magnetic-Amplifier Servo System', *Proceedings of the National Electronics Conference*, 1952, **8**, p. 159.

(2) Ramey, R. A.: 'On the Mechanics of Magnetic Amplifier Operation', *Transactions of the American I.E.E.*, 1951, **70**, Part II, p. 1214.

(3) STORM, H. F.: 'Magnetic Amplifiers' (New York: John Wiley and Sons; London: Chapman and Hall, 1955), Chapter 19, p. 309.
(4) MELVILLE, W. S.: 'Magnetic Amplifiers and Saturable Reactors' (George Newnes, 1954), p. 51.
(5) MAINE, A. E.: 'High-Speed Magnetic Amplifiers', *Electronic Engineering*, 1954, **26**, p. 180.
(6) ETTINGER, G. M.: 'Negative Inductance Cuts Magnetic Amplifier Lag', *Electronics*, 1954, **27**, p. 162.
(7) ETTINGER, G. M.: 'Magnetic Amplifiers' (New York: John Wiley and Sons; London: Methuen and Co., 1953).
(8) HILL, F., and FINGERETT, J. A.: 'Fast-Response Magnetic Servo Amplifier', *Electronics*, 1954, **27**, p. 170.
(9) WALKER, J. R., and WILSON, D. G.: 'Study of Fundamentals and Characteristics of Magnetic Amplifiers for Flight Control Systems', U.S.A.F. Technical Report 5881, Wright Air Development Center, 1951.
(10) FINZI, L. A., and MATHIAS, R. A.: 'Magnetic Amplifier performs Analytic Operations', *Electrical Engineering*, 1953, **72**, p. 1097.
(11) CARLETON, J. T., and HORTON, W. F.: 'The Figure of Merit of Magnetic Amplifiers', *Transactions of the American I.E.E.*, 1952, **2**, Part I, p. 239.
(12) CHOW, SHU-HSIEN: 'On Non-Linear Diffusion Equations Applied to Magnetization of Saturable Reactors', *Journal of Applied Physics*, 1954, **25**, p. 377.
(13) REYNER, J. H.: 'The Magnetic Amplifier' (Rockliff Publishing Corporation, London, 1953), 2nd ed., p. 105.
(14) HORSTMAN, C. C.: 'Core Materials for Small Transformers', *Tele-Tech*, 1952, **11**, pp. 40–2, 90.
(15) FINZI, L. A., and PITTMAN, G. F.: 'Comparison of Methods of Analysis of Magnetic Amplifiers', *Proceedings of the National Electronics Conference*, 1952, **8**, p. 144.
(16) GEYGER, W. A.: 'A New Type of Magnetic Servo-Amplifier', *Transactions of the American I.E.E.*, 1952, **2**, Part I, p. 272.
(17) GEYGER, W. A.: 'Magnetic-Amplifier Circuits' (McGraw-Hill, 1954).
(18) LUFCY, C. W., SCHMID, A. E., and BARNHART, P. W.: 'An Improved Magnetic Servo-Amplifier', *Transactions of the American I.E.E.*, 1952, **2**, Part I, p. 281.

(8) APPENDIX

(8.1) Sensitivity of Half-Wave Magnetic Amplifiers with Rectifier Leakage

(8.1.1) Conditions for Maximum Sensitivity.

From eqns. (1*b*) and (7), the current gain of a half-wave magnetic amplifier with turns ratio $k = N_c/N_l$ is given by eqn. (13*a*), where the circuit parameters are as follows.

Load-circuit reactance and resistance, ωL and R_l; control-circuit and diode reverse resistance, R_c and R_d; and width of hysteresis loop $2I_s$ (referred to load circuit). Amplitude of excitation voltage is V_{max}.

$$\gamma = \frac{\Delta I_l}{\Delta I_c} = \frac{V_{max}}{2\pi R_l I_s} kF$$

$$= \frac{1}{2\pi}\frac{\omega L}{R_l} k\left\{1 - \exp\left[\frac{-R_d \pi R_c/k^2}{\omega L(R_c/k^2 + R_d)}\right]\right\} \quad . \quad (13a)$$

Now let $R_d = u\omega L$ and $\frac{\pi R_c}{\omega L} = p$.

Then

$$S = \frac{1}{2\pi} Q_l k\left(1 - \exp\left\{-\frac{p}{k^2[p/(\pi u k^2) + 1]}\right\}\right). \quad (13b)$$

Differentiating eqn. (13*b*) with respect to the turns ratio k, in order to maximize S, we obtain

$$\frac{dS}{dk} = \frac{1}{2\pi} Q_l$$

$$\times \left(1 - \left\{1 + \frac{2p}{k^2[p/(\pi u k^2) + 1]^2}\right\} \exp\left\{-\frac{p}{k^2[p/(\pi u k^2) + 1]}\right\}\right)$$

and dS/dk becomes zero when

$$\exp\left\{\frac{p}{k^2[p/(\pi u k^2) + 1]}\right\} = 1 + \frac{2p}{k^2[p/(\pi u k^2) + 1]^2} \quad . \quad (14)$$

To obtain the optimum p/k^2 for any rectifier leakage coefficient, it is merely necessary to substitute the proper value of u in eqn. (14). The solution of eqn. (14) is plotted in Fig. 21(*a*),

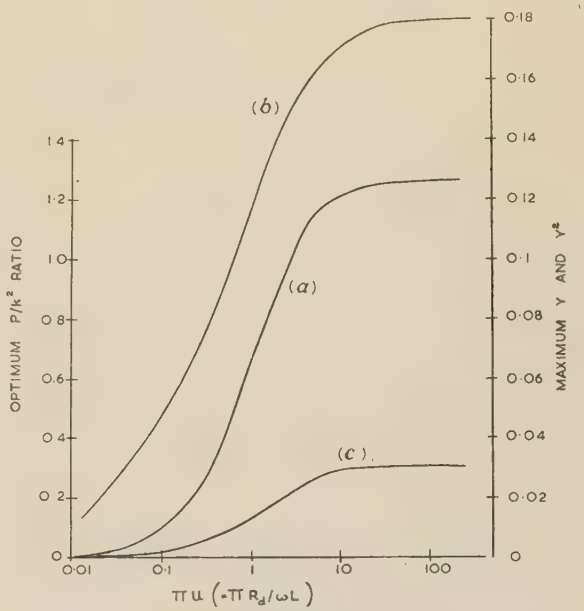

Fig. 21.—Factors for magnetic amplifiers with rectifier leakage.
(*a*) Optimum p/k^2.
(*b*) Maximum current-gain factor (Y).
(*c*) Maximum power-gain factor (Y^2).

which gives the optimum p/k^2 or $\pi R_c/k^2\omega L$ as a function of πu or $\pi R_d/\omega L$. It is seen that the optimum p/k^2 ratio is within 10% of 1·257, the value for $u = \infty$ (no diode reverse conductance) if $u > 2$. Thus, provided that R_d is greater than about $2\omega L$, eqn. (10*b*) may be used to determine optimum control-circuit resistance.

(8.1.2) Maximum Sensitivity.

Maximum sensitivity may be found from eqn. (13*a*), and can be rewritten as $(1/2\pi)Q_l k_{opt} F_{opt}$. Let the optimum value of p/k^2, which is plotted in Fig. 21(*a*), be termed X_{opt}. Then, by rearrangement of the terms of eqn. (13*b*), maximum sensitivity is given by

$$S_{max} = \frac{1}{2\pi} Q_l \sqrt{\left(\frac{R_c}{\omega L}\right)} (X_{opt})^{-1/2} \left\{1 - \exp\left[\frac{-X_{opt}}{1 + X_{opt}/(\pi u)}\right]\right\}$$

$$= Q_l \sqrt{\left(\frac{R_c}{\omega L}\right)} Y_{opt} \quad . \quad . \quad . \quad . \quad . \quad . \quad . \quad . \quad . \quad (15)$$

The function Y_{opt} is plotted against πu $[= \pi R_d/(\omega L)]$ in Fig. 21(*b*). For infinite u (where $X_{opt} = 1{\cdot}257$), S_{max} becomes $0{\cdot}18Q_l\sqrt{[R_c/(\omega L)]}$. This, of course, is the same value as that given by eqn. (11*b*).

(8.1.3) Maximum Power Gain with Rectifier Leakage.

Maximum power gain is given by

$$A_{max} = S_{max}^2 R_l/R_c$$

or, by reasoning similar to that leading to eqn. (12*a*),

$$A_{max} = Q_l^2 \frac{R_c}{\omega L} \frac{R_l}{R_c} Y_{opt}^2 = Q_l Y_{opt}^2 \quad . \quad . \quad (16)$$

The quantity Y_{opt}^2 is plotted in Fig. 21(*c*). It is seen that optimum power gain is within 10% of the gain with perfect rectifiers if the leakage factor u or $R_d/\omega L$ is greater than about 2. Furthermore, the shape of the Y_{opt}^2 curve [Fig. 21(*c*)] is similar to that of the $(p/k^2)_{opt}$ curve [Fig. 21(*a*)] over a wide range of values for u.

[The discussion on the above paper will be found on page 266.]

621.375.4.024

The Institution of Electrical Engineers
Paper No. 2382 M
July 1957

SOME TRANSISTOR INPUT STAGES FOR HIGH-GAIN D.C. AMPLIFIERS

By G. B. B. CHAPLIN, M.Sc., Ph.D., and A. R. OWENS, M.Sc., Graduates.

(*The paper was first received 22nd September*, 1956, *in revised form 7th January and 29th January*, 1957, *and in final form 12th March*, 1957. *It was published in July*, 1957, *and was read before a joint meeting of the* MEASUREMENT AND CONTROL SECTION *and the* RADIO AND TELECOMMUNICATION SECTION *3rd December*, 1957, *the* SOUTH-EAST SCOTLAND SUB-CENTRE *20th January, the* SOUTH-WEST SCOTLAND SUB-CENTRE *21st January, the* NORTH-EASTERN RADIO AND MEASUREMENT GROUP *17th March, and the* TEES-SIDE SUB-CENTRE *2nd April*, 1958.)

SUMMARY

The sensitivity of a d.c. amplifier using transistors is mainly limited by the variation with temperature of the inter-electrode potentials and currents of the transistors, the variation between any two temperatures being termed the thermal drift.

A typical low-frequency germanium transistor connected as a directly-coupled common-emitter amplifier may introduce current and voltage drifts, referred to the input, of 50 μA and 100 mV, respectively, when the temperature changes from 20 to 50° C. By using two such transistors in a balanced circuit, in which the drifts oppose, the net drifts are reduced to about 1 μA and 2 mV, respectively, if several inter-dependent component values are adjusted at different temperatures. By selecting transistors, and using greater care in balancing the amplifier, the drift can be reduced by one or two orders of magnitude, but such a procedure is usually unacceptable.

The same transistor connected as a simple modulator introduces a fundamental current drift of only 3 μA, but it still has a voltage drift of 100 mV. It is thus most suitable for use with devices having a high source impedance such as an ionization chamber for measuring radiation intensity. The current error can be reduced by a factor of 10 to 0·3 μA if two such transistors are used in a balanced modulator which requires only one adjustment at a single temperature.

The use of the transistor in a common-emitter chopping circuit results in a current drift of 50 μA and a voltage drift of only 2 mV, while reversing the functions of emitter and collector reduces these drifts to 3 μA and 100 μV, respectively. The latter voltage drift is considerably less than that of most thermionic-valve amplifiers, but the current drift is still large by thermionic-valve standards, and limits the use of the chopper to low-impedance sources.

A modification to this chopper eliminates the leakage current, but leaves the voltage drift unchanged at 100 μV. This voltage drift, acting on the transistor impedance, produces a current drift of only 3×10^{-8} amp, which makes this chopper suitable for use with high-impedance sources.

The chopper drift figures are obtained without recourse to selection or balancing of transistors, and are low enough to enable the transistor to contribute its many other advantages to such applications as sensitive null detectors and analogue computers.

The current drift can be reduced still further by using higher-frequency transistors, which, in general, have lower leakage currents. For example, the surface-barrier SB100 transistor ($f_{c\alpha} \simeq 50$ Mc/s) introduces a maximum current drift of only 3×10^{-9} amp.

The silicon junction transistor, promising even lower leakage currents, should enable direct currents of less than 10^{-11} amp to be measured.

LIST OF SYMBOLS

I = Defined direct current.
$\hat{I}$ = Alternating current
i = Instantaneous current.
v = Instantaneous voltage.
$\hat{V}$ = Alternating voltage.
V_{eb}, etc. = Voltage between emitter and base, etc.
i_{c0} = Collector reverse leakage current.
i_{e0} = Emitter reverse leakage current.
i_{csim} = Simultaneous collector leakage current.
i_{esim} = Simultaneous emitter leakage current.
Δi_{c0}, etc. = Change of i_{c0}, etc., from 20 to 50° C.
V_E = Chopper error voltage.
ΔV_E = Change in value of V_E from 20 to 50° C.
r_0 = Open-circuit resistance of chopper.
r_s = Closed-circuit resistance of chopper.
Z = Amplifier transfer impedance (gain in volts per ampere).
R_{in} = Amplifier input resistance.
R_s = Source resistance.
α = Current gain (common base).
α' = Current gain (common emitter).

Dr. Chaplin and Mr. Owens are at the U.K.A.E.A. Atomic Energy Research Establishment.

(1) INTRODUCTION

The sensitivity of a d.c. amplifier or measuring system is determined by the amount of noise which is present, since input signals of smaller amplitude than the noise cannot be distinguished. This noise may be manifested as a random variation about the operating point of the amplifier, or as a gradual drift of the operating point. In the case of transistors, the latter effect predominates, and is almost entirely due to change in temperature.

A convenient definition of drift is the magnitude of input current, or voltage, required to restore the output voltage of the amplifier to its original state, following a change in temperature. This definition is independent of the gain of the amplifier.

Although each stage of an amplifier will contribute to the drift, the effect at the output will depend on the intervening amplification. Thus, for reasonably large stage gains, little accuracy is lost if all the drift is assumed to originate in the input stage.

Several methods have been suggested for reducing the drift in junction-transistor d.c. amplifiers,[1,2,3,4] some of which use balanced circuits, and others chopper systems in which the transistor itself is the chopper.

This paper investigates several types of input stage and provides suggestions for some new techniques to reduce the drift still further.

(2) DIRECT-COUPLED AMPLIFIER STAGE

If it is assumed that all the drift originates in the input stage, the latter must have adequate voltage and current gain. Of the three possible connections for a single transistor amplifier, common base, common collector, and common emitter, only the last gives both voltage and current gain, and so only this connection will be considered.

(2.1) Drift in a Common-Emitter Amplifier Stage

Fig. 1 shows a simple common-emitter stage. A direct current, i_b, is extracted from the base by the negative input voltage through the source resistance R_s. The resulting collector current consists of $\alpha' i_b$, due to the base biasing current, and $\alpha' i_{c0} + i_{c0}$, due to the collector leakage current i_{c0}.

An increase in temperature will tend to cause an increase in collector current. The compensating current which must be applied to the base to keep the collector current constant is

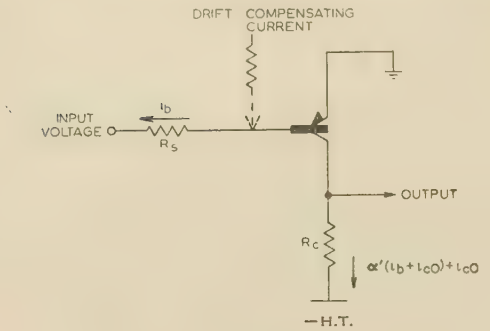

Fig. 1.—Directly coupled input stage.

equal to the drift of the amplifier, and consists mainly of two parts, corresponding to two main changes in the transistor characteristics as follows:

(*a*) *An increase in* i_{c0}.—If an increase Δi_{c0} occurs in the value of i_{c0}, the base current must be reduced by an amount $\Delta i_{c0}/\alpha$ to keep the collector current constant.

(*b*) *A decrease in the emitter-base voltage,* v_{eb}.—A decrease of Δv_{eb} in the value of v_{eb} causes an extra current $\Delta v_{eb}/R_s$ to flow in R_s, and a similar current must be supplied to the base to oppose this effect.

The total compensating current is therefore

$$\frac{\Delta i_{c0}}{\alpha}+\frac{\Delta v_{eb}}{R_s}$$

By definition this is the magnitude of the drift. The relative importance of the two sources of drift depends on R_s. For a typical type OC71 transistor $\Delta i_{c0}=50\,\mu$A over the range 20–50° C, and $\Delta v_{eb}\simeq 100$ mV. Thus if $R_s=2$ kilohms the two components of drift are approximately equal.

(2.2) Drift Compensation by Balancing

The drift compensating current required by the circuit of Fig. 1 could be supplied automatically by a circuit element having a resistance varying appropriately with temperature. For accurate compensation throughout the required temperature range, the compensating element would have to follow closely a particular resistance/temperature law, and to possess a similar thermal time-constant to the transistor. Thermistors and semi-conductor diodes have been used for this purpose, but perhaps the most obvious choice is another similar transistor. The use of a transistor for the purpose allows the changes in i_{c0} and v_{eb} to be compensated separately, and also provides the correct thermal time-constant.

A suitable balanced circuit in which J_2 is the compensating transistor is shown in Fig. 2. The emitter supply current, I_e, divides between the two emitters in the ratio $i_1 : i_2$, depending on the respective emitter-base voltages. The two collector currents consist of the emitter currents multiplied by the current gains, plus the collector–base leakage currents.

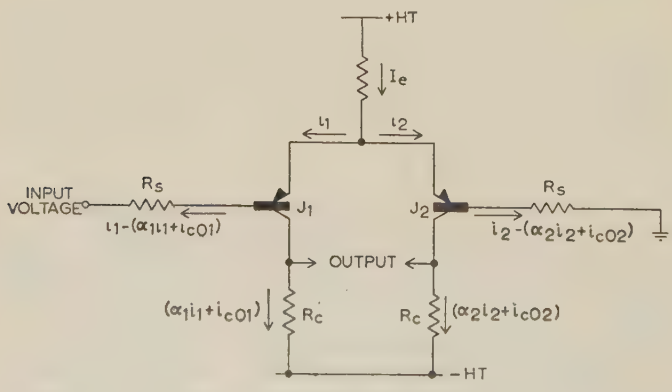

Fig. 2.—Balanced input stage.

If the transistors are identical and the input voltage is zero, an increase in temperature will cause identical increases in collector current and hence in collector voltage. Thus, if the output is taken as the differential collector voltage of the two transistors it will be zero, and there will be no drift. On the other hand, a change in input voltage applied to J_1 will unbalance the pair and produce a differential collector output voltage.

The extent to which the changes in v_{eb} are balanced can be deduced from Figs. 3 and 4. Fig. 3 is a plot of v_{eb} against i_e

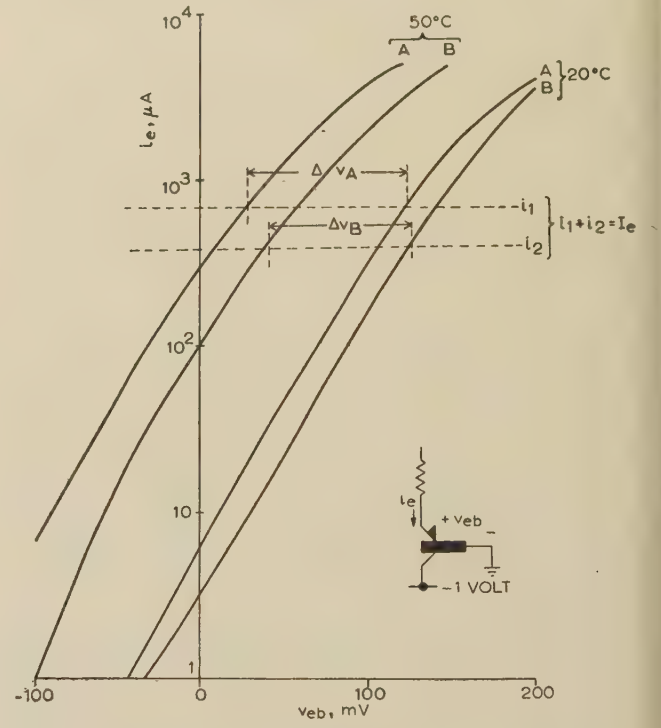

Fig. 3.—Emitter characteristics for two type OC71 transistors A and B.

for two type OC71 transistors, A and B, on a logarithmic current scale. The right-hand pair of curves were plotted at 20° C and the left-hand pair at 50° C. The emitter supply current, I_e of Fig. 2, is shown dividing between the two transistors in the ratio of $i_1 : i_2$, where $i_1+i_2=I_e$. An increase in temperature causes both curves to move to the left, and, unless the changes in v_{eb}, Δv_A and Δv_B at the two currents shown are equal, accurate balancing will not be obtained. Fig. 4 shows Δv_A and Δv_B between 20 and 50° C plotted against emitter current on a logarithmic scale for the same two transistors. The voltage difference between the two varies only slightly with emitter current, and is about 10 mV at currents below 1 mA, which is equivalent to a current drift in Fig. 2 of 10 mV/R_s. The two transistors were the opposite extremes of a batch of ten, and so the figure of 10 mV represents the maximum unbalance that is likely to occur.

The circuit also compensates for changes of i_{c0}, since identical changes would produce no differential output. The changes of $\Delta i_{c0}R_c$ which occur in each collector potential, however, are undesirable, since they may move the operating point into a non-linear region. By applying negative feedback, as shown in

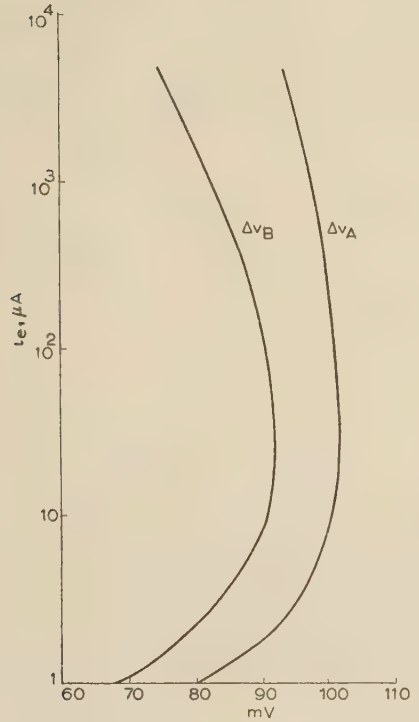

Fig. 4.—Curve showing change in emitter characteristics in the range 20–50° C for the transistors used in Fig. 3.

the higher temperature. These controls are interdependent, and so it is necessary to go through several temperature cycles when adjusting the amplifier. Two or three temperature cycles are sufficient to reduce the input drift to 1 or 2 mV over the temperature range 20–50° C, but a greater reduction is possible if the process is repeated.

An alternative balanced amplifier, in which the emitters of J_1 and J_2 are earthed and the mean of their collector potentials is fed back to their bases, is described in Reference 3.

(2.3) Possible Elimination of i_{c0}

A more fundamental way of preventing the drift caused by the change of i_{c0} would be to eliminate i_{c0}, and this can be achieved by reducing to zero the collector-base voltage which causes it.

That this is feasible is shown by the collector characteristic for a common-base transistor plotted in Fig. 6. The full lines are plotted at 20° C and the broken lines at 50° C. The collector current for a fixed emitter current is the sum of two currents, i_{c0} and αi_e. The leakage current i_{c0} is substantially constant if the collector is more than 0·05 volt negative to the base, but falls to zero when v_{cb} is reduced to zero, leaving a collector current of αi_e. The broken lines (for 50° C) show that the increase in collector current, due to the rise in temperature, is caused almost entirely by an increase in i_{c0}. Thus, by arranging for the transistor to operate with a collector-base voltage of almost zero, corresponding to the cross-over points of the dotted and solid curves, the drift due to i_{c0} may be eliminated. Fig. 6 shows that a deviation of as little as ± 10 mV from $v_{cb} \simeq 0$ results in i_{c0} contributing appreciably to the collector current, and so it is

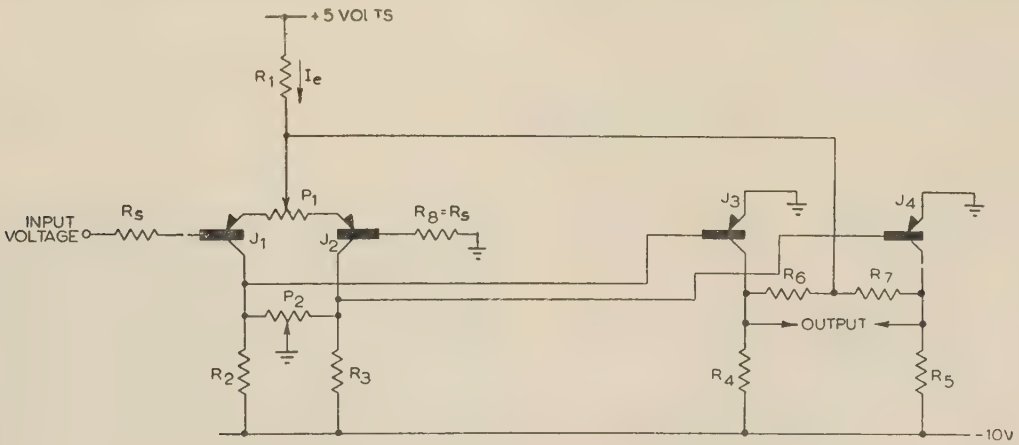

Fig. 5.—Balanced input stage with stabilizing feedback.

Fig. 5, the amplifier operating point can be stabilized in the linear region. The differential output from J_1 and J_2 is amplified in a pair of common-emitter stages J_3 and J_4. The mean of the collector voltages of J_3 and J_4, obtained at the junction of R_6 and R_7, is maintained substantially constant by feeding it back to control the common-emitter supply current of J_1 and J_2. The feedback, however, does not operate for differential amplification produced by an input signal. This system provides adequate compensation against changes in both temperature and h.t. voltage, even when a single-ended output is taken from the collector of either J_3 or J_4.

To make the compensation worth while it is essential to use matched transistors and to adjust two or more component values. In Fig. 5, P_1 controls the division of emitter current between J_1 and J_2 and is adjusted for zero differential output voltage at one lower temperature, while P_2 controls the relative voltage gains of J_1 and J_2 and is adjusted for zero differential output at necessary to stabilize the collector voltage to within narrow limits if full advantage is to be taken of the method.

It can be seen from Fig. 6 that the collector slope resistance decreases rapidly as v_{cb} is reduced towards zero, and that this effect is magnified when the temperature is increased. With low-frequency germanium transistors the slope resistance becomes so low at the higher temperatures that the stage gain is reduced to a value which precludes their use in this manner. The collector slope impedance, however, is a function of i_{c0}. With the advent of transistors having lower values of i_{c0}, and hence higher collector impedances, it should be possible to operate directly-coupled amplifiers in this region of zero i_{c0}.

(3) MODULATED AMPLIFIERS

It is possible to equal or reduce the drifts obtained with the balanced amplifier, without having to adjust component values, by using a modulated amplifier.

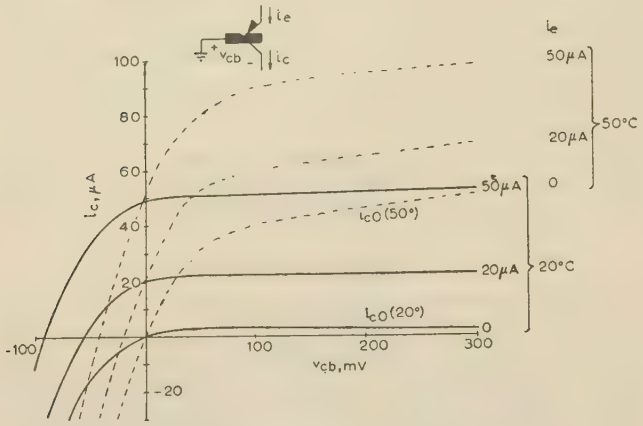

Fig. 6.—Collector characteristics of common-base transistor (type OC71).
—— 20° C.
---- 50° C.

In this type of amplifier the d.c. signal is converted into an a.c. signal in a suitable modulator. The a.c. signal is then amplified in an a.c. amplifier and rectified to provide an amplified d.c. output.

(3.1) Current Modulator

If the source of direct current to be amplified has a high resistance, such as an ionization chamber, a modulator having a relatively large voltage drift can be tolerated, provided that the current drift is sufficiently small. The current from an ionization chamber is unidirectional, and so a modulator which responds to current of only one polarity is adequate.

A simple modulator which meets these requirements is shown in Fig. 7. It consists of a transistor having the base earthed and

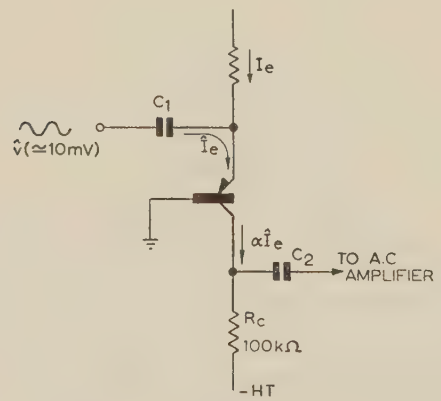

Fig. 7.—Simple current modulator.

with a collector load R_c. A direct input current, I_e, is fed into the emitter. If a small alternating voltage $\hat{V}$, of a few millivolts amplitude, is applied to the emitter through a capacitor C_1, the alternating component of the emitter current, $\hat{I}_e$, is equal to $\hat{V}/r_e$ [if $r_e \gg r_b/(1-\alpha)$]. The emitter resistance, r_e, is inversely proportional to $(I_e + i_{esim})$, where i_{esim} is the simultaneous emitter leakage current measured when both collector and emitter are simultaneously negative with respect to the base. Thus if $I_e \gg i_{esim}$ and $\hat{V}$ is held constant, $\hat{I}_e$ is directly proportional to I_e. The resulting alternating component of collector voltage is $\alpha\hat{I}_eR_c$, which may then be amplified by an a.c. amplifier and demodulated by a rectifying system.

When the input current, I_e, is zero, i_{esim} can no longer be neglected, and there remains a residual alternating output voltage at the collector directly proportional to i_{esim}. The magnitude and temperature dependence of i_{esim} in relation to the other transistor leakage currents is shown in Fig. 8. All these currents

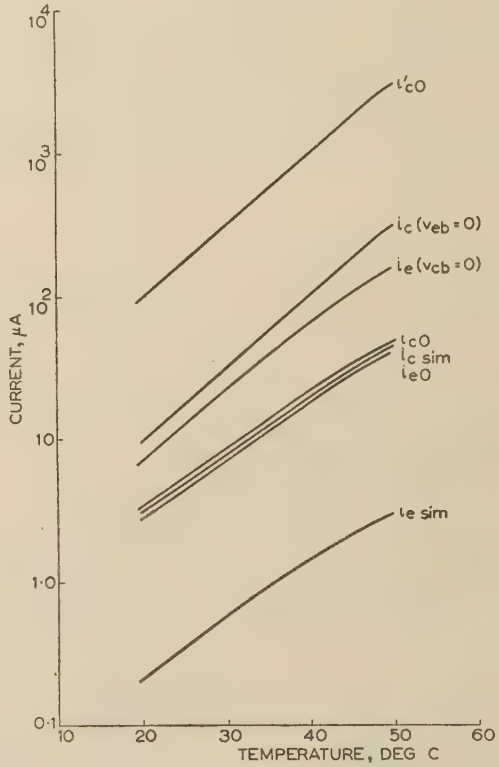

Fig. 8.—Temperature dependence of transistor type OC71 leakage currents.

increase by a factor of approximately two for every 7° C rise in temperature. Now i_{esim} is the smallest of these currents, being approximately equal to $i_{c0}/15$ (see Section 8) for many types of transistors, and so the drift of i_{esim} through a given range of temperature is only 1/15th that of i_{c0}. Typically, between 20° and 50° C, i_{esim} increases from 0·2 to 3 μA for a type OC71 transistor, resulting in a drift of only 2·8 μA for the modulator of Fig. 7. This is to be compared with almost 50 μA for the direct-coupled amplifier of Fig. 1.

With a higher-frequency transistor, such as the type OC45 ($f_{c\alpha} \simeq 5$ Mc/s), i_{c0} is smaller by approximately a factor of ten, but the ratio $i_{c0} : i_{esim}$ is only five, resulting in a drift of i_{esim} of just under 1 μA. The corresponding figure for the surface-barrier SB100 ($f_{c\alpha} \simeq 50$ Mc/s) is about 0·4 μA.

By balancing the residual error signal against a similar temperature-dependent signal from another transistor a further reduction in drift is possible. The circuit arrangement is shown in Fig. 9, in which J_1 is the modulator and J_2 provides the cancelling signal. The alternating carrier voltage is applied to the base of J_2, which is arranged to have no direct emitter current, so that the alternating current at the collector of J_2 is a function of i_{esim} only. Because the carrier is applied to the base of J_2, instead of to the emitter, the output at the collector of J_2 is in anti-phase to the output at the collector of J_1, and cancellation takes place in the common-collector load. The relative magnitudes of the carrier voltages applied to J_1 and J_2 are governed by P_1, which is adjusted for zero output voltage when I_e is zero. A

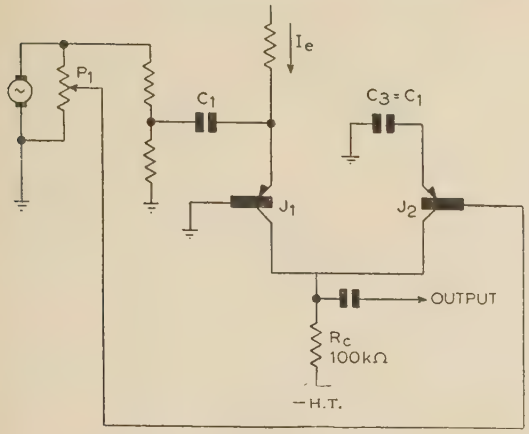

Fig. 9.—Balanced current modulator.

reduction in drift of between 10 and 100 times is typical using this type of cancellation.

There are two important advantages of the transistor modulator of Fig. 7 over a simple diode modulator. Such a diode modulator would be obtained by disconnecting the collector in Fig. 7 and connecting the base to R_c instead of to earth. The modulator is now the emitter-base diode, which has a leakage current of i_{e0} (Fig. 8). This leakage current is approximately 10 times greater than $i_{e\,sim}$, and so the drift is increased by a factor of 10, reducing the sensitivity of the modulator by the same factor. The second disadvantage is the presence of emitter-base capacitance, which shunts the modulator, allowing part of the modulating voltage to appear directly at the output. The emitter–base capacitance of a type OC71 transistor is about 250 pF when $I_e = 0$, and produces a residual output signal of approximately the same magnitude, for a modulating frequency of 100 kc/s, as that due to i_{e0}. At higher frequencies this residual error is proportionately greater. When a transistor is used for the modulator, most of this capacitive current flows into the base and so to earth, and only a small fraction of it reaches the collector. The base thus acts as an earthed screen.

It is of interest to note that the alternating output current in this type of modulator is a function of both I_e and $\hat{V}$, so that the circuit could form the basis of a simple analogue multiplier.

(3.2) Chopper Amplifier

If both the current and voltage drift are required to be small, and both polarities of output voltage are required, the modulator and demodulator may consist of switches, known as choppers, operated synchronously. A basic system is shown in Fig. 10.

Switches S_1 and S_2 are periodically opened and closed synchronously. When they are closed, the capacitors C_1 and C_2 are allowed sufficient time for their charges to reach equilibrium, after which the switches are opened. If there is no d.c. input signal, opening the switches will have no effect on the a.c. amplifier output voltage. However, if a d.c. input signal, V_1, is present at the d.c. input terminal, a step of current, $V_1/(R_s + R_{in})$ will be applied to the a.c. amplifier when S_1 is opened, producing an output voltage $ZV_1/(R_s + R_{in})$ at the point B, where Z is the amplifier transfer impedance. Whilst closed, S_2 clamps the right-hand plate of C_2 to earth potential, so that the opening of S_2 allows the voltage at B to change from earth potential by a voltage $ZV_1/(R_s + R_{in})$. This step of voltage is then smoothed by R_2 and C_3 to produce a direct output voltage, which is an amplified version of the d.c. input signal.

If the switches are operated sufficiently rapidly the drift which occurs when they are open will be negligible.

Mechanical vibrators, magnetic modulators, etc., may be used for the synchronous switches, but only the use of the transistor for this function will be discussed. Furthermore, it is only necessary to consider the operation of S_1, since any drift originating in S_2 is reduced by a factor of the gain of the a.c. amplifier when referred to the input.

(4) THE TRANSISTOR AS A SWITCH

The collector–emitter impedance of a transistor depends on the relative magnitudes of the base and collector currents, as can be seen from the collector characteristic of a common-emitter transistor shown in Fig. 11. If the base current, i_b, is large compared with I_c/α', as at A, the collector impedance is only about 20 ohms. On the other hand, if the base voltage is positive with respect to the emitter, as at B, then $i_b \simeq -i_{c0}$ and the collector impedance is increased to 1 megohm or more. This large ratio of collector impedances enables the transistor to be used as a switch.

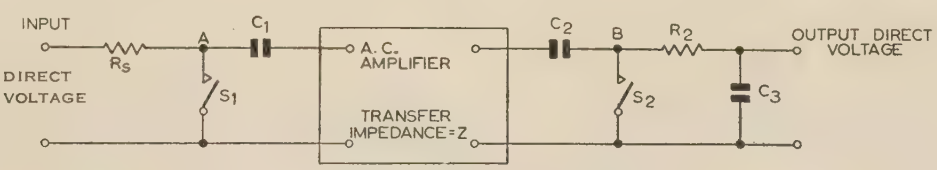

Fig. 10.—Basic chopper amplifier.

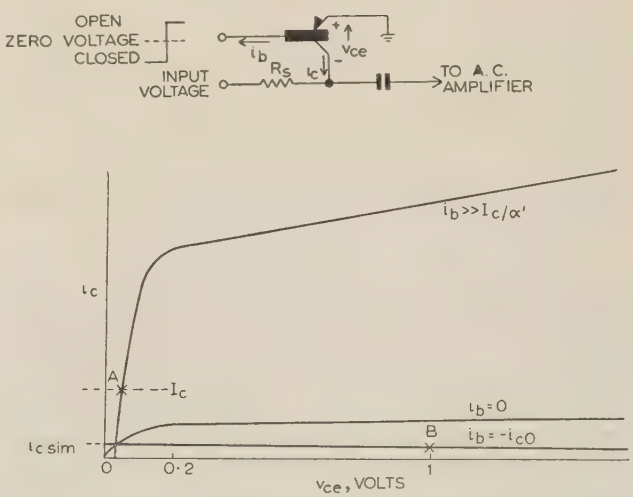

Fig. 11.—Transistor switching characteristics.

(4.1) Errors in a Transistor Chopper

Ideally a switch should have zero impedance and no internal voltage when closed, and infinite impedance and no leakage

current when open. Although a transistor switch is defective in these respects, the resulting errors can be reduced sufficiently to allow the function of S_1 in Fig. 10 to be performed by a transistor chopper.

The current interrupted by S_1 is normally only a few microamperes if the a.c. amplifier gain is to be large, and in analysing the performance of the chopper it is legitimate to assume that the input current is almost zero. The closed condition of the chopper represented by point A in Fig. 11 can thus be moved down the curve to the zero-current axis. An enlargement of this part of the characteristic is given in Fig. 12(*a*), which shows a

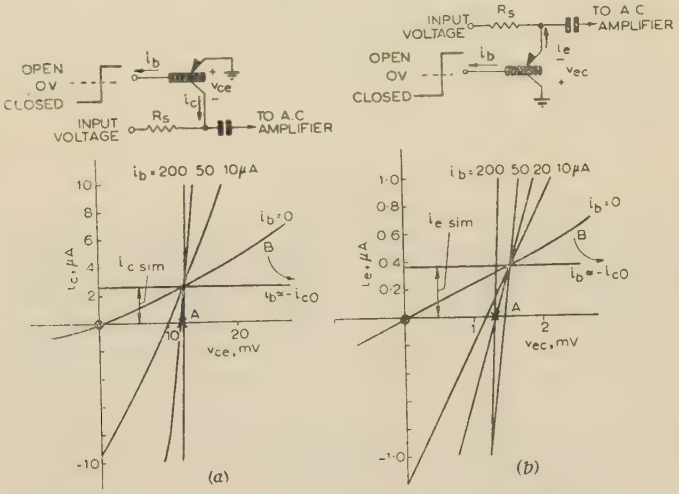

Fig. 12.—Enlarged characteristics near origin for type OC71 transistor.
(*a*) Transistor normally connected.
(*b*) Transistor reversed.

voltage error, V_E, of about 12 mV at the new point A when the switch is closed, and a current error, i_{csim}, which is slightly less than i_{c0}, when the switch is open. These errors would be fed into the a.c. amplifier as unwanted input signals, and although they could be 'backed off', their variation with temperature would give rise to a considerable drift. Between 20 and 50° C, the current drift would be typically 50 μA and the voltage drift 2 mV.

By reversing the emitter and collector connections[1,2,3,4] a substantial improvement in performance is obtained, as shown by the output characteristic of the reversed transistor [Fig. 12(*b*)]. The voltage error, V_E, is now only 1 mV and the current error is reduced to i_{esim}. Since the drift of the voltage error is approximately proportional to its magnitude, reversal of the transistor reduces the voltage drift by a factor of approximately 20 to 100 μV.

The voltage error, V_E, for the reversed-transistor switch is plotted against temperature in Fig. 13 for various values of i_b and with zero emitter current. The drift of V_E with temperature can be of either sign, depending on the base current, and it is possible to choose an optimum value of base current for a particular transistor which gives a voltage drift of only a few microvolts between 20 and 50° C. The optimum value of i_b varies between transistors of the same type, but tests on batches of 24 transistors showed that there is an average value for any one type of transistor which results in a maximum voltage drift of 100 μV. For example, transistor types OC71 and V10/50 have an optimum base current of about 1 mA, whereas types OC72 and SB100 require 6 mA and 100 μA, respectively, for least drift.

Although drifts of up to 100 μV were recorded in the tests, the majority of transistors had drifts of less than 50 μV when

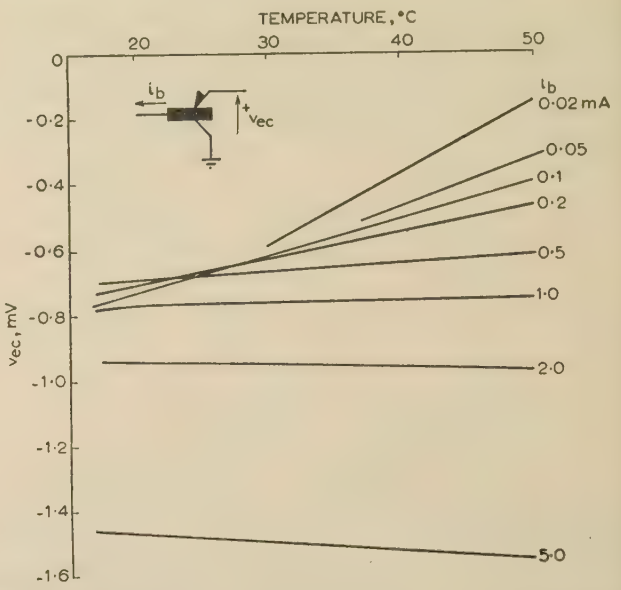

Fig. 13.—Dependence of chopper voltage error on temperature and base current for type OC71 transistor.

the optimum base current for the type was applied. By individual adjustment of the base current the drift can be reduced to a few microvolts.

(4.2) Reduction of Current Error

The reduced current error after reversal of the transistor, i_{esim}, is still excessive for many applications, since the resulting drift is 2 or 3 μA. However, this error can be considerably reduced by modifying the open condition of the chopper. If the base is not taken positive with respect to the other electrodes when the switch is open, but instead is returned through a resistance to earth potential, the potential difference which causes leakage currents to flow is removed and the leakage currents vanish.

The open condition of the switch is now represented by the curve for $i_b = 0$ in Fig. 12(*b*), which passes through the origin. In fact, if no signal current is present there is no current flowing in any electrode since all are at earth potential. There is therefore no error current.

The price paid for eliminating the leakage current is a reduction in the open impedance of the chopper, r_0, which falls to about 5 kilohms at 20° C, but the chopper still exhibits a useful ratio of impedance between being open and closed. The open impedance r_o is, however, a function of temperature. As the temperature rises, so r_o falls, as shown in Fig. 14, and the gain of the d.c. amplifier will be reduced owing to the shunting effect of the chopper across the input terminals. However, provided that the input impedance, R_{in}, of the a.c. amplifier is small compared with r_o, most of the signal current will flow into the amplifier and the loss in gain will be negligible.

The complete chopper circuit is shown in Fig. 15(*a*). When the chopping waveform is positive with respect to earth, the diode D is cut off and the resistors R_2 and R_1 hold the base almost at earth potential. R_1 is made much greater than R_2 so that only a fraction $R_2/(R_1 + R_2)$ of the reverse leakage current of the diode flows into the base of the transistor. This small base current divides between the collector and emitter in the ratio of $i_{csim} : i_{esim}$, typically a ratio of 15 : 1. If $R_1 = 10R_2$ only 1/150th of the diode leakage current appears as an error current at the transistor emitter when the chopper is opened. If D is a silicon junction diode, it will have a maximum leakage

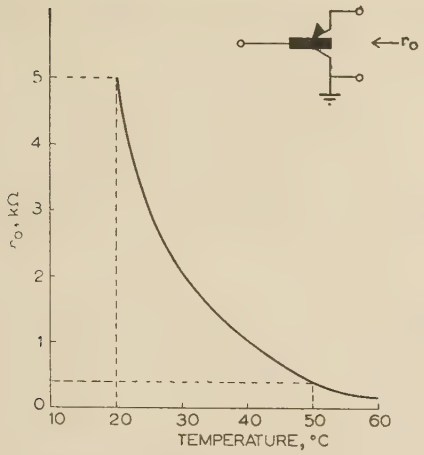

Fig. 14.—Temperature dependence of chopper open impedance r_o for type OC71 transistor.

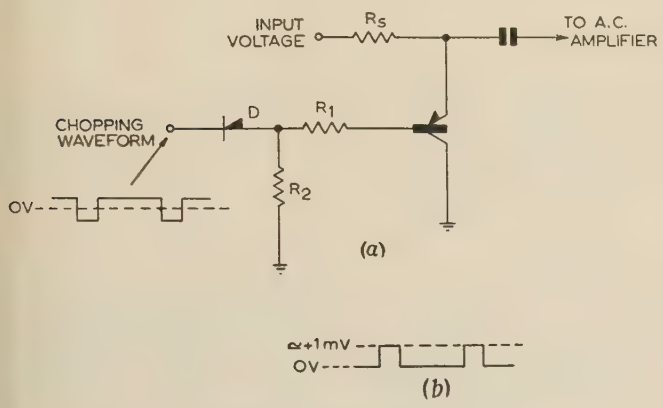

Fig. 15.—Input chopper.
(*a*) Complete circuit.
(*b*) Compensating waveform.

current of about 10^{-7} amp at +50° C, resulting in a drift of less than 10^{-9} amp at the emitter of the transistor chopper.

(4.3) Balancing the Voltage Error

When the chopper of Fig. 15(*a*) is closed, the emitter potential, V_E, falls to −1 mV causing a 1 mV error signal to be fed into the a.c. amplifier. This error can be prevented by returning the collector to a potential of about +1 mV, which is adjusted for zero a.c. output voltage. However, when the chopper is open the collector is positive with respect to the emitter by 1 mV, causing a small error current to flow into R_s. By applying the zero-setting voltage to the collector only during the clamped period, using the inverse phase of the chopping waveform [Fig. 15(*b*)], this error is removed.

The main source of drift is now the actual variation of the error voltage with temperature, ΔV_E. Although ΔV_E is a voltage drift, it can be resolved conveniently into an equivalent current drift as shown by the equivalent circuit of Fig. 16. ΔV_E is effectively in series with both the closed and open impedances of the chopper, r_s and r_o, and causes a drift current of $\Delta V_E/(r_o + r_s)$, which is approximately equal to $\Delta V_E/r_o$ since $r_o \gg r_s$.

If the chopper of Fig. 15(*a*) is set to zero at +20° C by adjusting the amplitude of the collector waveform [Fig. 15(*b*)] to produce zero a.c. output for zero d.c. input, the current drift at +50° C will be $\Delta V_E/r_o$, where r_o is measured at 50° C (Fig. 14). The

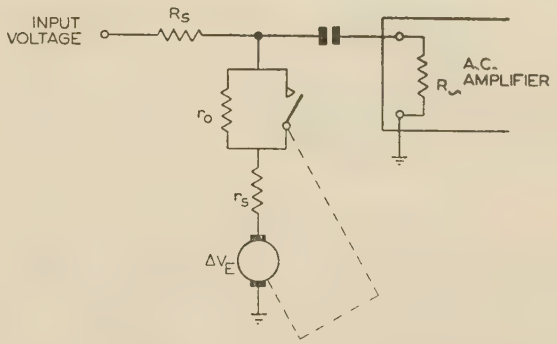

Fig. 16.—Equivalent circuit of compensated input chopper.

minimum value of r_o at 50° C for the type OC71 transistor is 300 ohms, and so if $\Delta V_E = 100\,\mu$V the maximum current drift is

$$\frac{100\,\mu\text{V}}{300\text{ ohms}} \simeq 3 \times 10^{-7}\text{ ampere}$$

This current drift is reduced by setting to zero at +50° C, for then the value of r_o at the lower temperature must be used in computing the drift at that temperature. The three curves in Fig. 17 show the drift when the chopper is set to zero at 20° C,

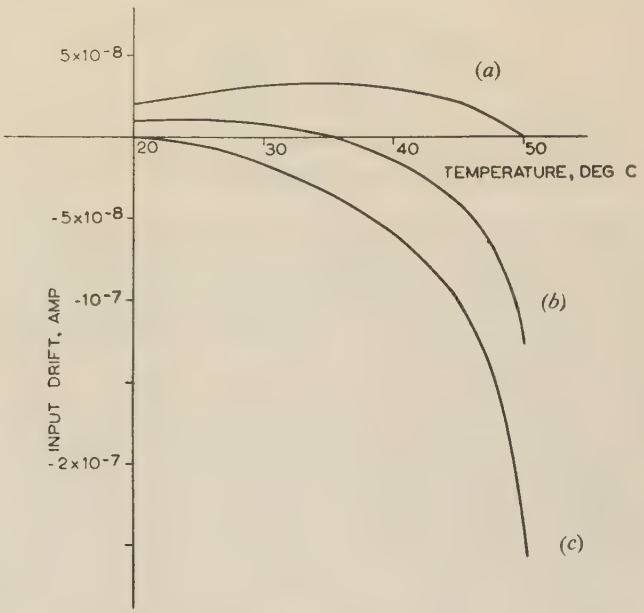

Fig. 17.—Theoretical drift curves for type OC71 transistor.
Chopper set to zero at (*a*) 50°C, (*b*) 35°C, (*c*) 20°C.

35° C and 50° C, using values of r_o taken from Fig. 14 and assuming ΔV_E to be 100 μV and a linear function of temperature.

For a type OC71 transistor a drift of 3×10^{-8} amp is typical when the zero is set at 50° C. This is a factor of ten smaller than the drift obtained when the same transistor type is used in the basic chopper circuit, where the drift is due to i_{esim}. The use of a medium-frequency transistor such as the type OC45 yields a fivefold increase in r_o, giving a corresponding reduction in chopper drift. i_{esim} is smaller by a factor of five, so that the basic chopper drift is also decreased by the same amount. The chopper drift thus remains smaller than the i_{esim} drift by a factor of ten. A high-frequency transistor such as the type SB100 shows a further reduction in i_{co}, giving a higher value of r_o, and since the chopper voltage drift remains the same, the chopper

current drift is further reduced. Since this type of transistor is less asymmetrical than those previously mentioned, no decrease in i_{esim} is evident, and its use in the basic chopper circuit yields no improvement. The proposed chopper circuit therefore enables this type to be used to its best advantage, and shows an improvement of twenty times over the corresponding basic chopper performance.

(4.4) Errors produced by Transients

Owing to carrier storage and the inter-electrode capacitance of the transistor, a differentiated version of the base chopping waveform appears at the output of the transistor chopper. Fig. 18(*b*) shows the effect of applying a square chopping waveform to the basic chopping circuit of Fig. 18(*a*). The amplitude of the

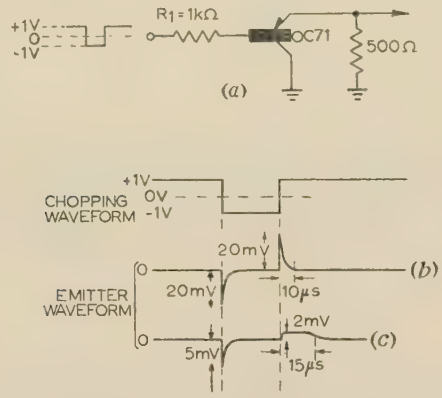

Fig. 18.—Input chopper transients.

chopping waveform is ± 1 volt with respect to earth potential, and R_1 is chosen so that the base current, when the transistor is clamped, is about 1 mA, which is the optimum current for minimum drift for a type OC71. To simulate the input resistance of a transistor amplifier a 500-ohm resistor is connected from emitter to earth.

The transients at the emitter have a peak amplitude of about 20 mV and a width of about 10 microsec. The amplitude is several times greater than the input signal to be measured, resulting in a substantial error, and variation of amplitude with temperature causes a drift. To reduce this drift the duration of the open period must be chosen to make the available signal area large compared with the area of the positive transient, although this reduces the chopping frequency. In addition, the subsequent a.c. amplifier must be able to handle a large overload without blocking.

Fortunately the inclusion of a diode D in the chopping circuit of Fig. 15(*a*), to reduce the current drift, also substantially reduces the transients, as shown by the waveform of Fig. 18(*c*). The amplitude of the negative transient is reduced by a factor of approximately five, owing to the reduced amplitude of the base voltage, while that of the positive transient is reduced by a factor of twelve at the expense of a slight increase in width. The transients are reduced considerably if higher-frequency transistors are used.

In general, for chopping frequencies below about 3 kc/s, the drift caused by transients can be neglected compared with that caused by ΔV_E.

(5) CONCLUSIONS

The drift of operating point in transistor d.c. amplifiers depends on the type of circuit used. The lowest drift figures are obtained when the transistor is used as a chopper. For a low-frequency germanium transistor the voltage and current drifts, between the temperatures of 20° C and 50° C, have maximum values of 100 μV and 3×10^{-8} amp, respectively, without recourse to selection or balancing of transistors. The relative importance of the voltage and current drifts depends on the source impedance. Thus, if the source impedance is high, the current drift will be the limiting factor. These drift figures compare favourably with those of thermionic valves and should enable the transistor to make important contributions in such applications as analogue computers and high-sensitivity null detectors.

Transistors having higher α cut-off frequencies tend to have lower leakage currents owing to the smaller collector area, and hence introduce lower current drifts in d.c. amplifiers. Thus a reduction in current drift by a factor of approximately 10 can be obtained with a transistor having an α cut-off frequency, $f_{c\alpha}$, of 5 Mc/s, and by a factor of 20 with a surface barrier type SB100 transistor ($f_{c\alpha} \simeq 50$ Mc/s).

Even more promising is the prospect of using silicon junction transistors having leakage currents less than 1/1 000th that of the low-frequency germanium types, which may enable direct currents of less than 10^{-11} amp to be measured.

(6) ACKNOWLEDGMENTS

The authors wish to express their gratitude to Mr. E. H. Cooke-Yarborough, Mr. W. R. Jackson and Dr. C. J. N. Candy for many helpful discussions.

Much of the experimental work was carried out by Mr. J. P. Kerry, whose contribution is very much appreciated.

(7) REFERENCES

(1) Blecher, F. H.: 'Transistor Circuits for Analogue and Digital Systems', *Bell System Technical Journal*, 1956, **35**, p. 295.

(2) Bright, R. L., and Kruper, A. P.: 'Transistor Chopper for Stable D.C. Amplifiers', *Electronics*, April, 1955, p. 135.

(3) Hillbourne, R. A.: 'D.C. Amplifiers and Associated Circuits', Borough Polytechnic Lectures on Special Applications of Transistor Circuits 1955–1956.

(4) Burton, P. L.: 'An All Transistor D.C. Chopper Amplifier' (English Electric Report LEL.t.054).

(5) Ebers, J. J., and Moll, J. L.: 'Large Signal Behaviour of Junction Transistors', *Proceedings of the Institute of Radio Engineers*, 1954, **42**, p. 1761.

(8) APPENDIX

The electrode potentials and currents of an idealized junction transistor may be described by the equations[5]

$$i_e + \alpha_i i_c = i_{e0}\left[\exp\left(e\frac{v_e}{kT}\right) - 1\right] \quad . \quad . \quad . \quad (1)$$

$$i_c + \alpha i_e = i_{c0}\left[\exp\left(e\frac{v_c}{kT}\right) - 1\right] \quad . \quad . \quad . \quad (2)$$

where i_e and i_c = Currents flowing *into* the transistor,
v_e and v_c = Potential difference across the junctions, at the emitter and collector, respectively.
i_{e0} and i_{c0} = Reverse leakage currents of each junction considered separately.
α = Forward current gain of the transistor.
α_i = Reverse current gain, measured when emitter and collector leads are interchanged.
k = Boltzmann's constant.
T = Absolute temperature.
e = Charge on an electron.

The leakage currents are related to each other[5] by the ratio α and α_i:

$$i_{e0} = \frac{\alpha_i}{\alpha} i_{c0} \quad . \quad . \quad . \quad . \quad . \quad . \quad . \quad (3)$$

(8.1) Simultaneous Leakage Currents

When the collector and emitter junctions are simultaneously biased in the reverse direction, the resulting leakage currents are designated $i_{e\,sim}$ and $i_{c\,sim}$. The condition for this test is that v_e and v_c are both large and negative, so that eqns. (1) and (2) reduce to

$$i_e + \alpha_i i_c = -i_{e0} \quad . \quad . \quad . \quad . \quad . \quad . \quad . \quad (4)$$

$$i_c + \alpha i_e = -i_{c0} \quad . \quad . \quad . \quad . \quad . \quad . \quad . \quad (5)$$

The currents flowing *out* of the emitter and collector are therefore

$$i_{e\,sim} = -i_e = i_{e0}\frac{1-\alpha}{1-\alpha\alpha_i} \quad . \quad . \quad . \quad . \quad . \quad (6)$$

$$i_{c\,sim} = -i_c = i_{c0}\frac{1-\alpha_i}{1-\alpha\alpha_i} \quad . \quad . \quad . \quad . \quad . \quad (7)$$

In terms of i_{c0}, $i_{e\,sim}$ is given by

$$i_{e\,sim} = i_{c0}\frac{\alpha_i}{\alpha}\,\frac{1-\alpha}{1-\alpha\alpha_i} \quad . \quad . \quad . \quad . \quad . \quad . \quad (6a)$$

Typical values for α and α_i are 0·96 and 0·7, respectively, so that

$$i_{e0} = 0{\cdot}73 i_{c0}$$

$$i_{e\,sim} = 0{\cdot}12 i_{e0} = 0{\cdot}087 i_{c0}$$

$$i_{c\,sim} = 0{\cdot}915 i_{c0}$$

These figures may be compared with values actually measured for the transistor plotted in Fig. 8.

The value of i_{c0} is approximately doubled for a rise in temperature of 7°C, and since α and α_i are almost unaffected by temperature, the other leakage currents obey the same law as i_{c0}. This is illustrated by the parallel curves in Fig. 8.

(8.2) Open-Circuit Chopper Impedance r_o

The collector-emitter potential is obtained from eqns. (1) and (2) by adding v_e and v_c in the correct sense. Thus

$$v_{ec} = v_e - v_c$$

$$= \frac{kT}{e}\log_\varepsilon\left(\frac{i_e + \alpha_i i_c + i_{e0}}{i_c + \alpha i_e + i_{c0}}\,\frac{i_{c0}}{i_{e0}}\right) \quad . \quad . \quad . \quad (8)$$

i_b is given by the sum of i_e and i_c.

Hence

$$v_{ec} = \frac{kT}{e}\log_\varepsilon\left[\frac{i_e(1-\alpha_i) + \alpha_i i_b + i_{e0}}{i_e(\alpha-1) + i_b + i_{c0}}\,\frac{i_{c0}}{i_{e0}}\right] \quad . \quad . \quad (9)$$

The impedance between the emitter and collector for a fixed base current is obtained by differentiating eqn. (9):

$$Z_{ec} = \frac{kT}{e}\left[\frac{1-\alpha_i}{i_e(1-\alpha_i) + \alpha_i i_b + i_{e0}} + \frac{1-\alpha}{i_e(\alpha-1) + i_b + i_{c0}}\right] \quad (10)$$

The open-circuit impedance of the chopper is obtained by inserting the appropriate condition $i_b = 0$. Also, since low signal currents are contemplated, we may write $i_e = 0$. Hence

$$r_o = \frac{kT}{e}\left(\frac{1-\alpha_i}{i_{e0}} + \frac{1-\alpha}{i_{c0}}\right) \quad . \quad . \quad . \quad . \quad (11)$$

$$= \frac{kT}{e i_{c0}}\left(1 + \frac{\alpha}{\alpha_i} - 2\alpha\right) \quad . \quad . \quad . \quad . \quad (11a)$$

r_o is thus shown to be inversely proportional to i_{c0}, and a rise in temperature of 7° C results in a halving of r_o, as shown by Fig. 14.

With the values of α and α_i assumed above, and $i_{c0} = 2\,\mu$A; then, since $kT/e = 25$ mV at room temperature, eqn. (11*a*) predicts that $r_o = 5$ kilohms at room temperature.

[The discussion on the above paper will be found on page 266.]

621.375.4.024

The Institution of Electrical Engineers
Paper No. 2442 M
Nov. 1957

A TRANSISTOR HIGH-GAIN CHOPPER-TYPE D.C. AMPLIFIER

By G. B. B. CHAPLIN, M.Sc., Ph.D., Graduate, and A. R. OWENS, M.Sc., Graduate.

(*The paper was first received 29th May, and in revised form 10th September, 1957. It was published in November, 1957, and was read before a joint meeting of the* MEASUREMENT AND CONTROL SECTION *and the* RADIO AND TELECOMMUNICATION SECTION *3rd December, 1957, the* SOUTH-EAST SCOTLAND SUB-CENTRE *20th January, the* SOUTH-WEST SCOTLAND SUB-CENTRE *21st January, the* NORTH-EASTERN RADIO AND MEASUREMENT GROUP *17th March, and the* TEES-SIDE SUB-CENTRE *2nd April, 1958.*)

SUMMARY

In transistor d.c. amplifiers the sensitivity is mainly limited by drift of operating point caused by changes in ambient temperature. A modulated amplifier is necessary to obtain a high sensitivity without recourse to methods of drift compensation requiring the adjustment of several balancing controls. The paper describes a modulated system consisting of a transistor input chopper, a high-gain transistor a.c. amplifier, and a transistor output chopper. Gains are expressed throughout as transfer impedances (output-voltage/input-current), a convention which is well suited to transistor amplifiers. The a.c. amplifier uses four transistors and has a gain of 20 volts/μA over a band covering 60c/s–20kc/s. It contains one capacitor only, giving a single low-frequency time-constant, which simplifies stability problems when feedback is applied. A chopping frequency of 1·6kc/s is used, and the complete system gives an open-loop gain of 50 volts/μA with a bandwidth extending from direct current to 25 c/s. The peak output is ± 10 volts, and the current drift referred to the input is 4×10^{-9} amp in the range 20°C–50°C. The voltage drift at the input is less than 100 μV. Despite the low input impedance the virtual-earth principle is still valid, and the amplifier should be useful in analogue-computer applications. The complete amplifier is suitable for amplification of signals from a wide range of source impedances—ionization chambers and thermocouples being typical extremes.

(1) INTRODUCTION

The ultimate sensitivity of a d.c. amplifier or measuring system is limited by noise occurring in the amplifier, since input signals of amplitude smaller than that of the noise cannot be distinguished.

Noise may be manifested as random fluctuations in the operating point of the amplifier (thermal noise) or in a gradual drift of the operating point. In the case of transistors the latter effect usually predominates and is almost entirely due to change in temperature. Unless the ambient temperature is controlled within narrow limits it is necessary to resort to a modulated system[1] if small d.c. signals are to be amplified without recourse to the complicated adjustments required by temperature-compensated methods. A modulated system normally comprises a comparatively drift-free input modulator for converting the direct signal to an alternating one, followed by an a.c. amplifier and a demodulator. When the modulator and demodulator act as switches which periodically interrupt the input and output signals they are usually known as the input and output choppers, respectively.

Fig. 1 shows such a system. The a.c. amplifier has its input and output terminals periodically clamped to earth simultaneously by the input and output choppers S_1 and S_2. When the choppers are opened the d.c. input signal, coming from a source impedance R_s, is enabled to impress its voltage upon the input terminal of the a.c. amplifier, causing a proportional change in the potential of the right-hand plate of C_3 away from its rest position, which has been previously defined at earth potential by the closure of S_2 during the preceding clamped period. The resulting output waveform is integrated by R_i and C_2 to produce a smoothed direct output voltage. Overall d.c. negative feedback may be provided by the feedback resistor R_f.

Dr. Chaplin and Mr. Owens are at the U.K.A.E.A. Atomic Energy Research Establishment.

(2) SPECIFICATION OF THE D.C. AMPLIFIER

The design of the d.c. amplifier is largely governed by transistor properties. Because of the relatively low input impedance of a transistor it is convenient to express the gain of a transistor amplifier in terms of the output voltage produced by a given input current (i.e. as a transfer impedance). If d.c. feedback is applied, as indicated by R_f in Fig. 1, the gain demanded by the feedback resistor is simply its value, R_f, since, ideally, the whole of the input current i_s flows through R_f and results in an output voltage of $i_s R_f$. For many applications the gain of the amplifier with feedback must be constant to within 1%, which implies that only 1% of i_s must flow into the a.c. amplifier. The gain of the amplifier must therefore be 100 times that defined by R_f, requiring an amplifier transfer impedance of $100R_f$ or greater.

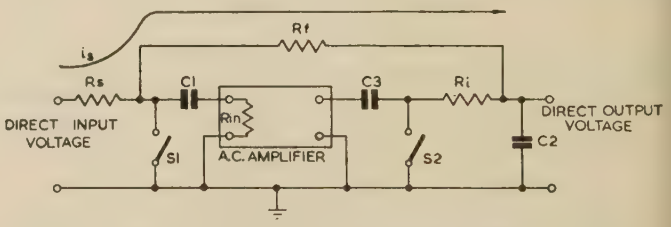

Fig. 1.—Schematic of chopper amplifier.

A very high amplifier gain usually results in an unduly low overall bandwidth for the d.c. amplifier in order to avoid instability, as outlined in Section 7.3.

To maintain a reasonable bandwidth the gain has therefore been limited to 50 volts/μA, corresponding to a transfer impedance of 50 megohms, and the maximum allowable value of R_f for the gain to be constant to 1% is thus 500 kilohms.

The voltage rating of the transistors used limits the output voltage to about 20 volts, allowing a swing of ± 10 volts about a mean level.

(3) INPUT CHOPPER

The circuit of the input chopper is shown in Fig. 2(*a*), its properties being described in detail in Reference 1. As shown by the simplified equivalent circuit of Fig. 2(*b*), the chopper is not a perfect switch since it has a voltage drift ΔV, a resistance r_s when closed and a resistance $r_o + r_s \simeq r_o$ when opened.

(3.1) Operation

When the switch is open practically all the input current, i_s, flows into the amplifier input resistance, R_{in}, through the capacitor C_1, which therefore accumulates a charge. When the switch is closed the input current is shunted to earth through r_s, and C_1 is discharged through R_{in} and r_s [Fig. 2(*c*)]. Since the mean current in C_1 is zero, the areas above and below the

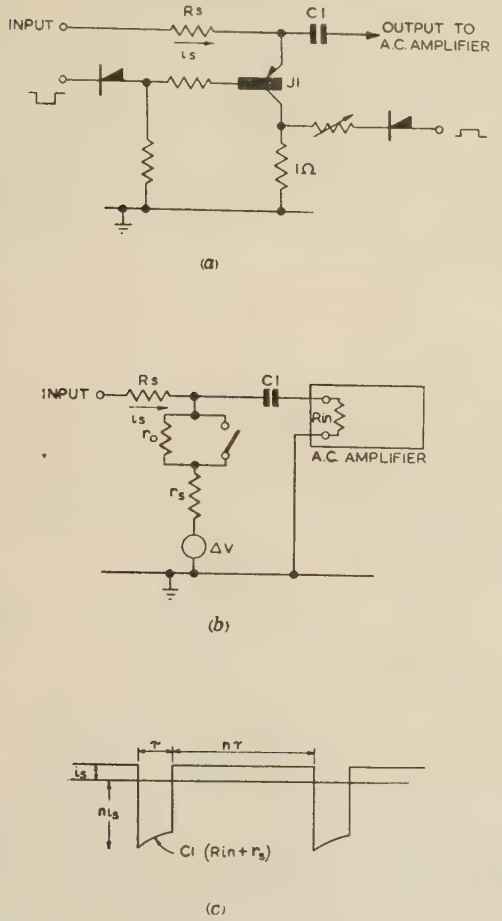

Fig. 2.—Input chopper.
(*a*) Circuit.
(*b*) Equivalent circuit.
(*c*) Current flowing in C_1.

axis in Fig. 2(*c*) must balance. If C_1 is chosen to make the time-constant $C_1(R_{in} + r_s)$ much greater than τ, the clamped period, the discharge current is then equal to ni_s, where n is the mark/space ratio of the clamping waveform. The current flowing into the amplifier therefore consists of pulses of height $(n + 1)i_s$, and the input chopper thus gives a useful current gain.

(3.2) Temperature Effects

The effects of r_o and r_s are to attenuate the input signal by amounts which depend on the ambient temperature, but these effects can be made negligible by choosing a suitable value of amplifier input impedance R_{in}.

When the switch is open all the input current i_s should flow into the amplifier. To prevent a significant fraction being by-passed through r_o it is therefore desirable for r_o to be large compared with R_{in}. On the other hand, when the switch is closed the whole of the input current should flow through its closed impedance, r_s, which should therefore be small compared with R_{in}.

Fig. 3 shows, for a batch of six type SB100 transistors, the outside limits of r_o (in kilohms) and r_s (in ohms) plotted against temperature, r_s being measured at a base current of 100 μA, which is chosen to give minimum voltage drift.[1]

At the maximum ambient temperature (50° C) for which the amplifier is designed, the minimum r_o which may be expected is 5 kilohms. The closed resistance r_s, which is less strongly

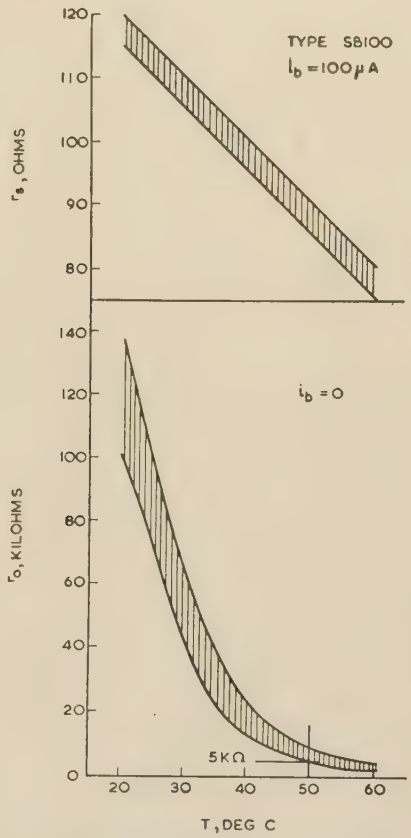

Fig. 3.—r_s and r_o of Fig. 2(*b*) as functions of temperature, showing the spread for type SB100 transistors.

dependent on temperature than r_o, has a mean of 100 ohms and varies by only 40% in the range 20° C–50° C. Thus, if R_{in} is chosen to be about 500 ohms, in the range 20° C–50° C the temperature variations of the chopper impedances will cause a change of attenuation at the input of only a few per cent.

(4) A.C. AMPLIFIER

The gain of the a.c. amplifier must be of the same order of magnitude as the required open-loop d.c. gain of the system. Two important requirements for the a.c. amplifier are that the number of transistors and a.c. couplings should be kept to a minimum, in order to reduce phase shifts in the amplifier and minimize the danger of instability when the d.c. feedback loop is closed, and that there should be a phase reversal between input and output. It is also desirable to keep the number of other components to a minimum for simplicity and reliability.

(4.1) Basic Amplifier

The above conditions are satisfied by the 3-stage common-emitter amplifier shown in Fig. 4. The transistors are directly connected to each other and the operating points are stabilized by the feedback resistors R_1 and R_2. If all transistors are identical and have equal collector loads, their emitter-to-base potentials will be equal and J_2 and J_3 will have zero collector-to-base voltages. The collector potential of J_4, however, will be below that of the base of J_2, owing to the voltage dropped across R_1 by the base current I_{b2} of J_2 and the voltage drop in R_2. The operating point of the collector of J_4 is then adjusted by supplying a current I_{R3} through R_3. The overall gain of the amplifier is small at low frequencies owing to the feedback,

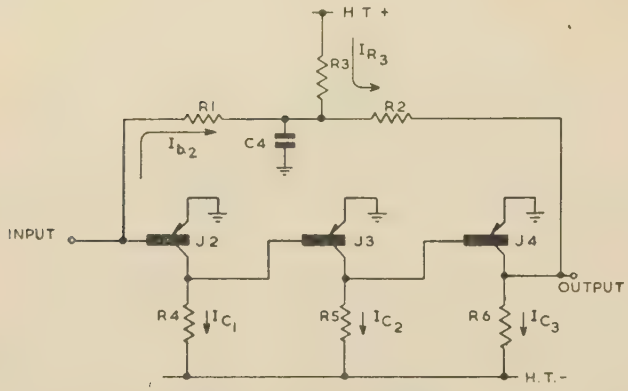

Fig. 4.—Basic a.c. amplifier.

which is made inoperative at higher frequencies by a shunting condenser, C_4, the only reactive component in the circuit.

Operating the first two transistors with zero collector-to-base voltage is attractive since it simplifies the circuit, but unfortunately, when low-frequency germanium transistors are used, some reduction in gain results and the gain also becomes temperature-dependent to a serious extent. Fig. 6 of Reference 1 shows that, although the current gain is maintained at very low collector-to-base voltages, the collector impedance is lowered and becomes very temperature-dependent. The result is that the amplifier gain is reduced owing to the interstage coupling loss caused by the lower collector impedance, and this coupling loss varies with temperature. These effects are not apparent to the same extent with germanium transistors having a smaller collector area, such as many high-frequency types, as the collector impedances at zero collector-to-base voltage are then generally greater by an order of magnitude or more.

If low-frequency transistors are used it is preferable to have a direct coupling voltage between stages of at least 100 mV, as

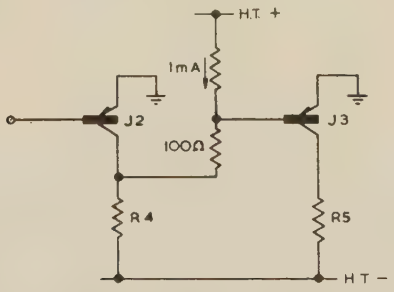

Fig. 5.—Interstage coupling.

shown in Fig. 5, which ensures that the collector-to-base voltages of the first two transistors are both of the order of 100 mV, and the transistors are then operating at their normal values of collector impedance.

(4.2) Addition of Negative Feedback

It is desirable to apply negative feedback to the a.c. amplifier to maintain the gain reasonably close to the value fixed by the d.c. amplifier specification, a condition which is necessary in order to ensure that large increases of loop gain cannot occur which might render the projected overall d.c. feedback loop (R_f of Fig. 1) unstable. There are several possible forms of negative feedback, and the final choice is governed by the need for low input and output impedances.

The simplest method of applying negative feedback is to insert a small resistor in series with the condenser, C_4 (Fig. 4), but stability considerations limit the amount of feedback to a factor of approximately 10 over the three cascaded stages.[2] Owing to the large spread in α' in batches of typical transistors, a variation in amplifier gain by a factor of 10 may be expected and the feedback factor quoted above is clearly insufficient.

The negative feedback is therefore applied through two separate loops in such a way that the whole amplifier is covered by feedback but with negligible interaction between the loops. The complete circuit is shown in Fig. 6. The two feedback loops

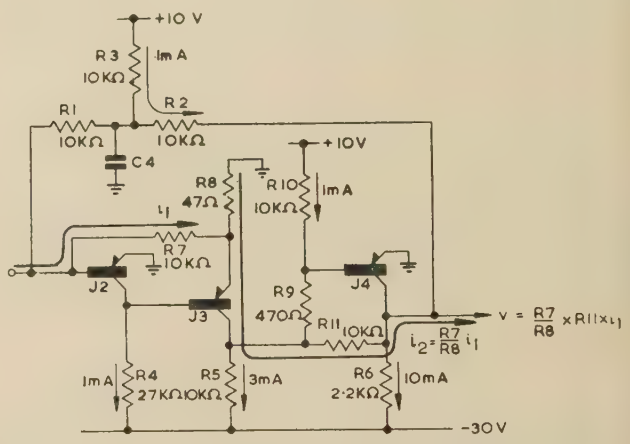

Fig. 6.—Three-stage feedback a.c. amplifier.
Gain = 2 volts/μA.

are from the emitter of J_3 to the base of J_2 (R_7 and R_8) and from the collector of J_4 to the collector of J_3 (R_{11}). Owing to the voltage dropped across R_8 by the 2 mA emitter current of J_3, the base of the latter is approximately 0·1 volt negative to the base of J_2, allowing a direct connection from the collector of J_2 to the base of J_3. To provide an adequate collector-to-base voltage in J_3 a 0·5 volt d.c. coupling (R_9 and R_{10}) is interposed between J_3 and J_4. The direct currents flowing in the amplifier are well defined by the collector loads and are indicated by the thin arrows.

Assuming the applied feedback to be sufficient, the loop R_7, R_8 gives a defined current gain of R_7/R_8 over the first two stages, and produces a low input impedance at the base of J_2. A high output impedance is produced at the collector of J_3, which works into a virtual earth produced by the feedback action of R_{11} upon the last stage. There is, therefore, an efficient transfer of current between the two stages. The transfer impedance of the last stage is defined by R_{11}, and, assuming the current gain of J_3 to be unity, the transfer impedance of the complete amplifier is therefore approximately $R_{11} \times R_7/R_8$. With the circuit values shown, this represents a gain of 2 volts/μA. By disconnecting R_7 and R_{11} the gain is increased to approximately $(\alpha')^3 \times R_6 = (30)^3 \times 2{\cdot}2 \times 10^3 = 60$ volts/μA, indicating a minimum feedback factor of 30, which ensures that the gain with feedback is sufficiently well defined.

With this feedback system there is much less danger of instability than there would be with a single overall feedback loop, but there is less gain for a given feedback factor. The two halves of the loop, R_7 and R_{11}, are separated by the collector-to-emitter path of J_3, which prevents any significant direct feedback from the output to input. The only parameter which is not covered by feedback is the current gain of J_3, which can be regarded as unity to a first approximation. Tolerances in biasing components are wide, owing to the self-adjusting effect of the d.c. stabilizing loop.

(4.3) High-Gain Amplifier

Although the gain of the amplifier of Fig. 6 is quite adequate for many d.c. amplifiers, it is a large factor short of the optimum gain initially specified. However, the gain can be increased by a factor of 10, without affecting the basic structure of the amplifier, by interposing an emitter-follower between transistors J_3 and J_4 of Fig. 6, as shown in Fig. 7. The increased current gain thus

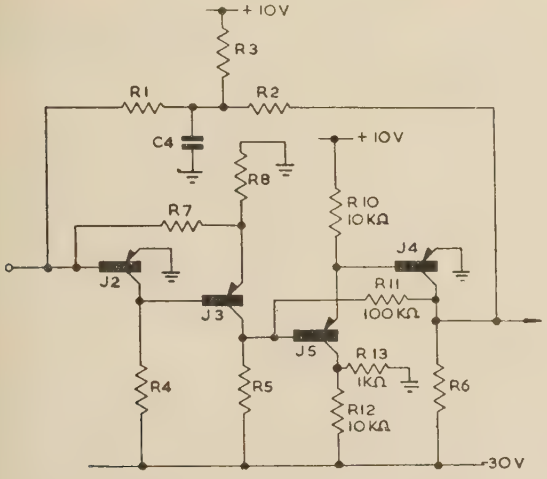

Fig. 7.—Four-stage a.c. amplifier.
Gain = 20 volts/μA.

obtained allows R_{11} to be increased considerably, with a corresponding increase in gain. The resistors R_{12} and R_{13} in Fig. 7 reduce the collector-to-base voltage of J_5 to about -1 volt and also prevent the emitter current from rising excessively if J_3 fails.

An alternative arrangement would be to have the emitter-follower subsequent to J_4 (Fig. 6) instead of preceding it, but this would require both transistors to have allowable collector swings of 20 volts, whereas the arrangement in Fig. 7 imposes a maximum collector voltage of only 1 volt on all but the final transistor, thus allowing them to be replaced by high-frequency types if required.

(4.4) Frequency Response

Two frequency-response curves are shown in Fig. 8: curve (*a*) is for the amplifier shown in Fig. 6 and curve (*b*) is for that

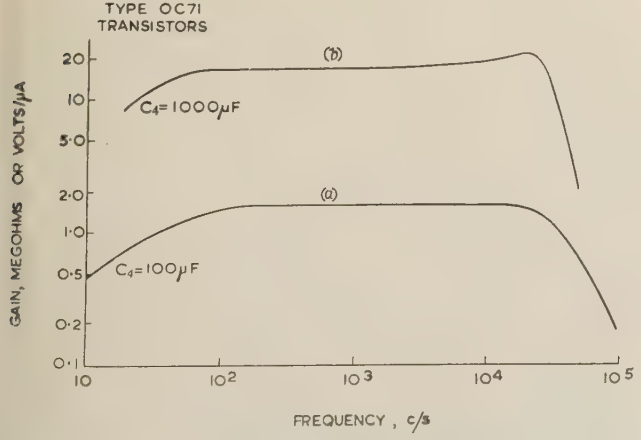

Fig. 8.—Amplifier gain as a function of frequency.
(*a*) Fig. 6. (*b*) Fig. 7.

shown in Fig. 7. The falling-off in gain at low frequencies is due in both cases to the increase in impedance of C_4, the capacitor shunting the d.c. stabilizing feedback loop.

Curve (*a*) shows a smooth reduction in gain at high frequencies owing to the reduction of α' at these frequencies. Curve (*b*), however, shows a slight rise in gain before finally falling, which is due to the addition of a fourth transistor to the circuit, adding an extra source of phase shift and also increasing the gain.

(4.5) Output Stage

Peak outputs of more than 100 mA at ± 10 volts may be required from the amplifier, so that a large standing current would be necessary in the output stage of Fig. 7, giving rise to a high mean power dissipation.

The quiescent power dissipation may be eliminated by increasing R_8 and adding a complementary emitter-follower, as shown in Fig. 9(*a*). A negative signal on the combined bases cuts off

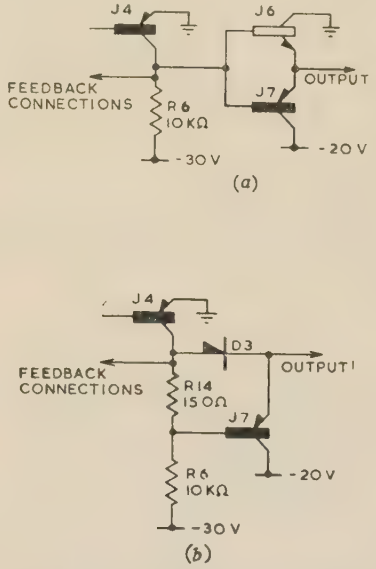

Fig. 9.—Amplifier output stages.
(*a*) Complementary emitter-follower.
(*b*) Diode and emitter-follower.

J_6 and causes J_7 to conduct, and a positive signal has the reverse effect. The *n–p–n* transistor required for J_6 is not yet a standard type in Great Britain, but if it is not required to provide current gain it may be replaced by a diode D_3, as shown in Fig. 9(*b*). For positive output signals J_4 conducts and drives the output through the diode D_3, and for negative signals J_7 conducts. Resistor R_{14} provides a potential difference of about $+0{\cdot}3$ volt to prevent both D_3 and J_7 from being back-biased together. If necessary it can be replaced by a diode similar to D_3, but it can usually be omitted altogether. This stage is not included in the a.c. amplifier feedback loops, in order to avoid the effects of the additional phase shift at high frequencies.

(5) OUTPUT CHOPPER

(5.1) Operation

In the output-chopper circuit shown in Fig. 10(*a*) the a.c. signal is supplied from the amplifier output impedance R_o to the chopper transistor J_8 through a capacitor C_3. The demodulated output signal appearing across the chopper is then integrated by R_{15} and C_2 to provide a smoothed d.c. output. The voltage waveform appearing at the a.c. amplifier output

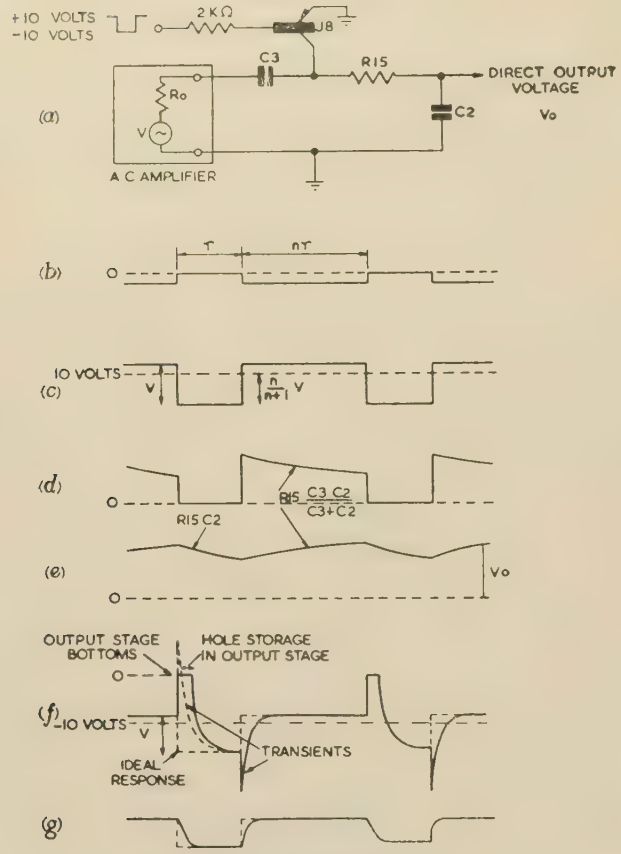

Fig. 10.—Output chopper.
(*a*) Circuit.
(*b*) Waveform at input chopper.
(*c*) A.C. amplifier output for no-load (V).
(*d*) Output-chopper collector.
(*e*) Integrator output.
(*f*) Effect of transient on (*c*).
(*g*) Effect of amplifier response on (*c*).

terminal on no-load is shown in Fig. 10(*c*), and corresponds to the input signal shown in Fig. 10(*b*). Fig. 10(*d*) shows the accompanying voltage waveform at the chopper J_8, in which the right-hand plate of C_3 is set to earth potential when J_8 is clamped. At the instant when J_8 opens, a voltage step occurs in the amplifier output, which is transmitted by C_3 to the integrator R_{15} and C_2 and results in the output waveform shown in Fig. 10(*e*).

The output capacitor C_2 discharges through R_{15} when the chopper is clamped, and the lost charge must be replaced during the unclamped period by the discharge of C_3 if equilibrium is to be maintained. The resulting charge lost by C_3 is then replaced when the chopper is next clamped, and to do this a large current must flow from the a.c. amplifier. The magnitude of this current may be estimated as follows:

It is assumed that the time-constant $R_{15}C_2$ is very large in comparison with the clamped interval τ, so that if a steady output voltage V_o appears on C_2, the discharge current during the clamped period is V_o/R_{15} and the charge lost is $\tau V_o/R_{15}$. This charge is replaced by an equal quantity supplied by C_3, which the latter acquires by being charged through R_o during the clamped period. The initial current flowing through R_o to charge C_3 is obtained by equating the charge lost by C_2 to the charge gained by C_3, and is given by the expression

$$I_o = \frac{\tau V_o/R_{15}}{R_o C_3(1 - \varepsilon^{-\tau/R_o C_3})}$$

With typical values of $\tau = 100$ microsec, $R_oC_3 = 50$ microsec, $R_{15} = 1$ kilohm and a maximum $V_o = 10$ volts, the maximum I_o is 23 mA. This is the current which the amplifier must be capable of supplying. The peak current which must be sustained by the chopper is $I_o - V_o/R_{15} = 23 - 10 = 13$ mA. These requirements alone may be readily met, but conditions are considerably modified by the presence of transients in the signal.

(5.2) Transient Effects

The presence at the amplifier output of transients originating from the input chopper and of signals delayed by the rise-time of the a.c. amplifier causes an increase in the peak currents in the output-chopper circuit.

The chopper transients consist of a sharp positive spike occurring at the beginning of the clamped period and a negative spike at the end, whilst the rise-time of the amplifier in effect delays the point at which the output pulse reaches a steady level. These conditions are illustrated separately in Figs. 10(*f*) and 10(*g*). In the first case the transient is superimposed upon an idealized output signal but is being limited in amplitude by the output stage, and in the second case the delay due to the amplifier rise-time only is shown.

The effects in both cases are similar, and when superimposed, as in practice, the result is a delay of about 30 microsec before a steady reference level is set up during the clamped period.

Taking the extreme case as illustrated, when the d.c. amplifier output is +10 volts, the closing of the chopper causes the right-hand plate of C_3 to be clamped to earth, but for a short while its left-hand plate is held 10 volts above the amplifier mean level owing to the delay. Since the output impedance R_o is 100 ohms, a discharge current of 100 mA peak flows from C_3. When the amplifier output is eventually allowed to fall to its mean level at the end of the delay period, the charge lost by C_3 must be replaced by a large charging current in the opposite direction. C_3 must be completely recharged by the end of the clamped period, otherwise the output signal may be set to an incorrect reference level (proportional to the error in the charge on C_3) and the d.c. output will therefore be offset from zero.

The large peak currents and possible errors arising from the effects described above may be eliminated by arranging for the leading edge of the output-chopper clamping waveform to be delayed sufficiently to overcome the effective delay of the signal. In this case the operation is similar to that described in the previous Section.

(5.3) Connection of the Output Chopper

The output-chopper transistor, shown in Fig. 10(*a*), is connected as an earthed-emitter switch, instead of earthed-collector as in the input chopper, to prevent the output voltage swing from being limited by the output chopper. During the unclamped period the base of the output chopper must be held more positive than the maximum positive swing of the collector, in order to ensure that the chopper will maintain a high impedance. In the present case, with an output swing of ±10 volts, the base must be held higher than +10 volts. If the amplifier happens to be supplying the maximum negative voltage, the base is then 20 volts positive to the collector and 10 volts positive to the emitter. Since the collector voltage rating is usually higher than that of the emitter, this connection allows a greater maximum output voltage to be handled than would be the case if the transistor were reversed. Although this chopper arrangement results in greater output-chopper drift, the latter is insignificant when it is referred to the input, since it is then divided by the amplifier gain.

The choice of component values in the circuit of Fig. 10(*a*) is discussed in Section 12.

(5.4) Alternative Output-Chopper System

An alternative arrangement which avoids the repeated charging and discharging of condenser C_3 (Fig. 10), but which is limited mainly to open-loop applications, is obtained by inserting the output chopper in the stabilizing feedback loop of the a.c. amplifier, as shown in Fig. 11(*a*). R_{16} and J_8 replace the feedback

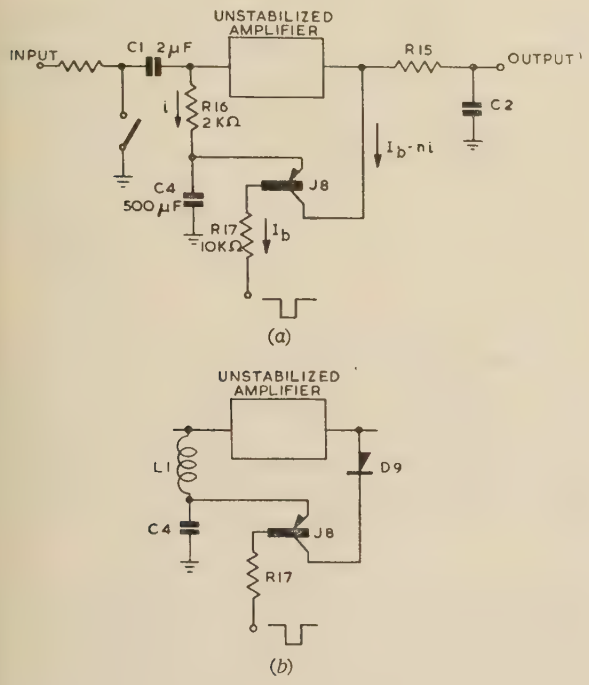

Fig. 11.—Alternative output-chopper system.
(*a*) Basic system.
(*b*) Reduced drift.

resistors R_1 and R_2 shown in Fig. 7, and the a.c. amplifier is modified to have a mean output level at earth potential by inserting a 10-volt Zener diode in series with the J_5 emitter (Fig. 7) and returning the J_4 emitter to +10 volts. During the clamped period J_8 [Fig. 11(*a*)] connects the output of the a.c. amplifier to the lower end of R_{16}, and the amplifier adjusts itself so that the current i extracted by R_{16} is just sufficient to maintain the output near earth potential. When J_8 becomes unclamped the stabilizing loop is opened and R_{16} draws the stabilizing current from the large condenser C_4. The time-constant C_4R_{16} must therefore be long compared with the unclamped period multiplied by the amplifier gain.

The potential to which the a.c. amplifier output is clamped is the sum of the emitter-to-base voltage of the first transistor in the a.c. amplifier, the voltage iR_{16} dropped across R_{16} by the stabilizing current, and the emitter-to-collector voltage of J_8. Now if the base of the first amplifier is at −150 mV and the stabilizing current, i, is 50 μA, the emitter of J_8 will be at approximately −250 mV. The current which this emitter must extract from C_4 during the clamped period is ni, where n is the mark/space ratio of the clamping waveform, and, if a current I_b is extracted from the J_8 base, the output of the amplifier must supply a difference current of $I_b - ni = 0{\cdot}75$ mA if $I_b \simeq 1$ mA and $n = 5$. Under these conditions the collector of J_8 is positive to its emitter by about 50 mV and the output voltage level of the amplifier is $-150\,\text{mV} - iR_{16} + 50\,\text{mV} = -200\,\text{mV}$. This error voltage decreases to approximately zero when the temperature increases from 20° C to 50° C and, when divided by the d.c. amplifier gain of 50 volts/μA, represents an input current drift of 4×10^{-9} amp, which is similar in magnitude to that originating in the input chopper and so must be substantially reduced.

To reduce the variation of the voltage across R_{16} due to the change of i_{co} in the first stage of the amplifier, it is desirable to reduce R_{10}, which would require a corresponding increase in C_4 to maintain the time-constant $R_{16}C_4$. However, by replacing R_{16} by an inductance having an impedance of several thousand ohms at the chopping frequency and a d.c. resistance of 20 ohms or less, as shown in Fig. 11(*b*), this objection may be removed. The error from this source is then made negligible, but there remains the base-to-emitter voltage of the first stage of the amplifier (−150 mV) and the collector-to-emitter voltage of J_8 (+50 mV). The resulting error of −100 mV at the output of the amplifier can be largely removed by adding a diode D_9 [Fig. 11(*b*)] in series with the chopper. The current $I_b - ni$ flowing through D_9 produces a voltage drop across it which subtracts from the error. Furthermore, the drift of diode voltage with temperature opposes that of the rest of the chopping loop, resulting in a final drift which is small compared with that originating in the input chopper.

However, the inductance, L_1, increases the danger of low-frequency oscillation when overall d.c. feedback is applied, and so the circuit of Fig. 11(*b*) is limited mainly to open-loop applications.

(6) CHOPPING-WAVEFORM GENERATOR

The chopping waveform is generated by the blocking oscillator shown in Fig. 12(*a*). The duration of the conducting state is

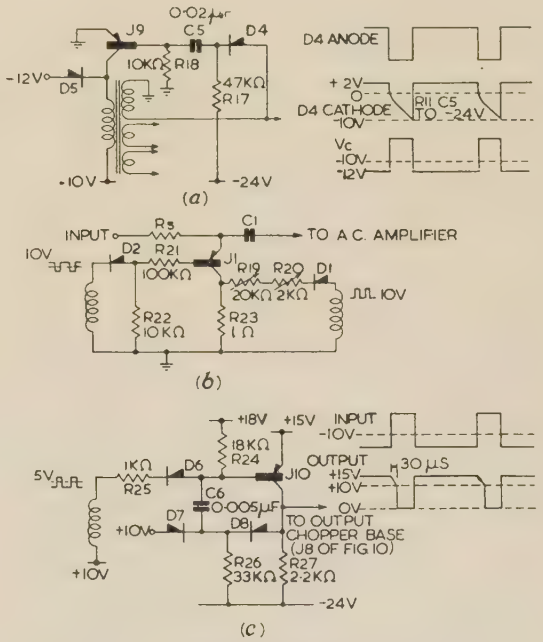

Fig. 12.—Chopping-waveform generator.
(*a*) Circuit.
(*b*) Connections to input chopper.
(*c*) Connection to output chopper via delay circuit.

defined by the run-down of the D_4 cathode with the time-constant C_5R_{17}. Instead of defining the duration of the non-conducting state in a similar manner, a catching diode D_5 defines the mark/space ratio by the potential to which it is returned. The areas of the collector voltage waveform above and below −10 volts must be equal, since there can be no direct voltage across the transformer; the duration of the non-conducting state is thus

10/(12 − 10) times that of the conducting state. The resulting collector waveform has a flat base line and top and can be applied to the choppers in the correct phase and amplitude by other windings on the transformer.

The arrangement of the input chopper is shown in Fig. 12(*b*). A 5-volt clamping waveform is applied to the base circuit and a 10-volt waveform of inverse phase is applied to the collector circuit for setting the zero.[1] Variable resistors R_{19} and R_{20} are the coarse and fine zero controls, respectively. The waveform amplitudes are made sufficiently large for the change in forward conducting potentials of D_1 and D_2 with temperature to produce negligible drift.

The negative-going edge of the waveform applied to the output chopper must be delayed slightly to allow for the signal delay in the amplifier (Section 5.2). The chopping waveform is therefore applied to the output chopper via the delay circuit of Fig. 12(*c*). During the first part of the clamped period the collector executes a Miller run-down from +15 volts to +10 volts and then falls rapidly, with the result that the falling edge of the collector waveform is delayed by 30 microsec.

(7) INSTABILITY

Three separate types of negative feedback have been used in the complete d.c. amplifier, namely d.c. stabilization of the operating point of the a.c. amplifier, local a.c. feedback on the a.c. amplifier, and d.c. feedback over the complete d.c. amplifier. Instability will occur if at any frequency where the loop gain exceeds unity the total feedback becomes positive through unwanted phase shifts.

(7.1) D.C. Stabilizing Loop of the A.C. Amplifier

The d.c. stabilizing loop consists of R_1, R_2 and C_4 [see Fig. 13(*a*)]. If C_4 is too small there will be a frequency near the upper

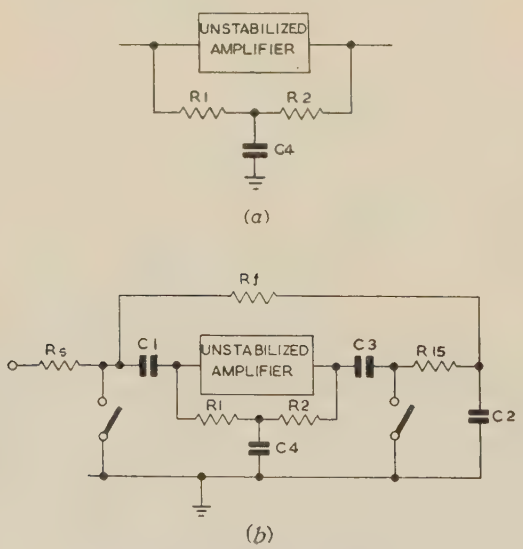

Fig. 13.—Feedback loops.
(*a*) D.C. stabilization of a.c. amplifier.
(*b*) Addition of overall d.c. feedback.

end of the pass-band at which the phase lags in the transistors of the a.c. amplifier, together with the lag due to C_4, are sufficient to cause phase reversal around the feedback loop. However, such a low value of C_4 would also cause the gain at the chopping frequency to be unduly small, and is therefore not likely to occur in practice.

(7.2) Local Feedback Loops

Because each local feedback loop in the a.c. amplifier embrace only two transistors there is no danger of instability at hig frequencies, and, owing to the absence of interstage couplin condensers, there is also no possibility of instability at lo frequencies.

(7.3) Overall D.C. Loop

The addition of the overall d.c. loop, comprising the integrato (R_{15}, C_2) and the resistor R_f, is shown in Fig. 13(*b*). This loo is similar to the stabilizing loop R_2, C_4 and R_1, and can alway be made stable by making $R_{15}C_2$ sufficiently large. Unfor tunately, increasing $R_{15}C_2$ reduces the bandwidth of the d.c amplifier, and so the final choice must be a compromise. Anothe factor affecting the choice of $R_{15}C_2$, which was mentioned i Section 5.4, is that it must be large enough to prevent excessiv ripple appearing on C_2, and in general if this requirement is me the amplifier is stable for values of R_f as low as 20 kilohms.

(8) PERFORMANCE OF THE D.C. AMPLIFIER

The performance figures which follow were obtained from ar amplifier consisting of the input chopper shown in Fig. 12(*b*) with $R_s = 1$ megohm, the high-gain a.c. amplifier shown i Fig. 7, the output chopper and integrator shown in Fig. 10, and the chopping waveform generator shown in Figs. 12(*a*) and 12(*c*). The transistors were chosen at random and wide-tolerance components were used.

(8.1) Temperature Effects

For the purpose of testing, temperature effects originating in components other than transistors were prevented by keeping them at 20° C and subjecting only the transistors to a rise in temperature.

(8.1.1) Drift.

The temperature drift was ascertained by adjusting the 'zero setting' control for zero d.c. output at 20° C, and then measuring the current required at the input to restore the d.c. output voltage to zero at intermediate temperatures up to +50° C. Curve (*a*) of Fig. 14 shows that the drift is 3×10^{-8} amp in the

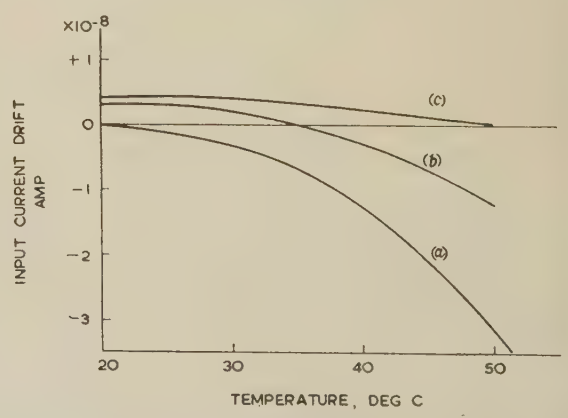

Fig. 14.—Amplifier current drift as a function of temperature, referred to the input.
Zero adjustment being made at (*a*) 20° C, (*b*) 35° C, (*c*) 50° C.

range 20° C–50° C, which can be regarded as the temperature range for most thermionic equipment, while in the range 20° C–35° C, which is a reasonable temperature range for all-transistor equipment, the drift is only 6×10^{-9} amp. Making the zero adjustment at the higher temperature in each case reduces the drifts for the temperature ranges 20° C–50° C and 20° C–35° C

$3 \cdot 6 \times 10^{-9}$ amp and $2 \cdot 8 \times 10^{-9}$ amp, respectively, as shown by curves (*c*) and (*b*). It is, of course, not necessary to control the temperature accurately when making the zero adjustment at the higher temperature.

The curves show that for a given temperature difference the drift decreases as the temperature decreases, and for this reason the drift for temperatures below 20° C has not been plotted.

(8.1.2) **Gain.**

The gain without feedback of the complete d.c. amplifier is shown in Fig. 15. The gain at 20° C corresponds quite closely

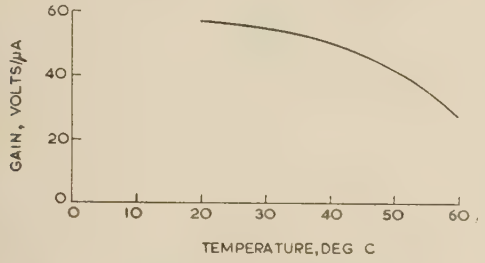

Fig. 15.—Variation of gain with temperature.

to that of the a.c. amplifier (Fig. 7) multiplied by the mark/space ratio and allowing for the attenuation in the output chopper. The variation with temperature is due almost entirely to variation of input-chopper attenuation.

(8.2) Bandwidth

The bandwidth without feedback is determined by the output integrator for reasons of either output ripple or feedback system stability, as explained in Section 7.3. If stability is the main consideration, the bandwidth is limited to about 25 c/s. It is possible, however, to increase the bandwidth by the use of compensating networks in the a.c. amplifier which increase stability, as described, for example, in Reference 4. The aim of these methods is to shape the frequency-response curve so that the rate of fall-off of response at the high-frequency end is reduced over a critical region, with a consequent reduction in phase shift.

A considerable improvement in bandwidth is possible by these methods, but components must be carefully selected and may have to be trimmed with individual amplifiers. For this reason such methods have not been included in this investigation.

Another well-known method of increasing the bandwidth is to use the low-drift properties of the chopper amplifier to control the drift of a directly-coupled d.c. amplifier, as shown in Fig. 16.

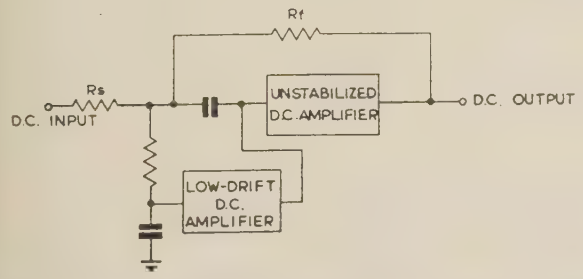

Fig. 16.—Use of low-drift low-bandwidth d.c. amplifier to stabilize a high-bandwidth d.c. amplifier.

This upper amplifier could be similar, for example, to the a.c. amplifier shown in Fig. 7, with the d.c. stabilizing loop removed. Such an amplifier has a bandwidth of several kilocycles per second, which could be fully utilized if the stability problem outlined in Section 7.3 were absent. However, the limitations imposed by stability considerations on the lower amplifier still apply to the upper amplifier, although the absence of an output integrator (which gave dominant lag stabilization in exchange for bandwidth[3]) now makes possible the use of other compensating networks to ensure stability. Thus the increase in bandwidth with this system is not likely to be as great as the increase obtained in the case of thermionic-valve systems using mechanical choppers, where the bandwidth of the chopper amplifier itself is limited more by output ripple, resulting from the low chopping frequency, than by instability.

(8.3) Effects of Supply-Voltage Variations

Variations in supply potentials may give rise to drift by causing changes in the chopping waveform or by changing the characteristics of the amplifier.

(8.3.1) **Amplifier Characteristics.**

Changes in amplifier characteristics are mainly evidenced by their effect upon the spurious transients (Section 5.2) which are handled.

Changes of shape of transients result in a small change in the integrated contribution due to transients at the output chopper, which is equivalent to a current drift at the input. This is a second-order effect only, and changes in individual supply potentials of as much as 20% give rise to equivalent drifts of only 5×10^{-10} amp at 25° C.

(8.3.2) **Chopper-Waveform Variations.**

The effects of supply variations upon the chopping waveform are rather more serious. Separate variations of supply potentials cause amplitude changes and also mark/space ratio variations, which upset the zero setting of the input chopper and also vary the input-chopper base current, thus giving rise to comparatively large voltage errors at the input. Referred to the input, changes of individual supply potentials to the waveform generator of 10% are equivalent to 3×10^{-9} amp at 25° C.

It thus appears necessary to provide a stabilized chopping waveform to obtain the best results. Assuming the effect of supply-voltage variation to be linear, 1% stabilization of supply should limit the drift to a tenth of the above figure, namely 3×10^{-10} amp.

(8.4) Reduction of Drift by means of Temperature Control

The data presented in Section 8.1.1 and Fig. 14 indicate that a considerable reduction in drift may be obtained by holding the operating temperature constant.

The improvement thus obtained is eventually limited by supply regulation, as shown in Section 8.3.2. There is, in fact, little to be gained by reducing temperature variations to less than one or two degrees centigrade at 25° C when a drift figure of 3×10^{-10} amp is attainable.

(9) CONCLUSIONS

A transistor chopper amplifier has been described which, in many respects, compares favourably with high-gain thermionic-valve d.c. amplifiers. Referred to the input, the current drift is 4×10^{-9} amp and the voltage drift is less than 100 μV in the temperature range 20° C–50° C. This performance has been achieved without the necessity for the selection of transistors or adjustment of component values, and shows a distinct improvement over that of previous designs of transistor chopper amplifier. The voltage drift is less than that of a valve d.c. amplifier and compares favourably with vibrating-reed chopper amplifiers.

Whereas thermionic-valve drift is mainly random in character, the drift of the transistor amplifier is dependent largely upon ambient temperature, and an improvement in performance may

be obtained by a simple control of ambient temperature, the drift eventually being limited by power-supply regulation to about 3×10^{-10} amp.

The amplifier should be suitable for many analogue-computer applications if its narrow bandwidth is not a limiting factor, and also as a high-sensitivity null detector or instrument amplifier for both voltage and current inputs. Its application in these fields should result in a valuable increase in reliability and a substantial reduction in heat dissipation and power drain, together with the advantages of small size and freedom from microphony.

(10) ACKNOWLEDGMENTS

Thanks are due to Messrs. E. H. Cooke-Yarborough and W. R. Jackson and Dr. C. J. N. Candy for many helpful discussions during the course of this work.

The authors would also like to record their appreciation of Mr. J. P. Kerry's contribution in carrying out much of the experimental work.

(11) REFERENCES

(1) Chaplin, G. B. B., and Owens, A. R.: 'Some Transistor Input Stages for High-gain D.C. Amplifiers' (see page 249).

(2) Almond, J., and Boothroyd, A. R.: 'Broadband Transistor Feedback Amplifiers', *ibid.*, Paper No. 1929 R, January, 1956 (**103** B, p. 93).

(3) Thomason, J. G.: 'Linear Feedback Analysis' (Pergamon Press Ltd., London, 1955).

(4) Blecher, F. H.: 'Transistor Circuits for Analog and Digital Systems', *Bell System Technical Journal*, 1956, **35**, p. 295.

(12) APPENDICES

(12.1) Integrator Component Values

The magnitude of R_0 [Fig. 10(*a*)], which should be as small as possible, is a property of the a.c. amplifier and is therefore fixed within a limited range, being of the order of 100 ohms.

The choice of R_{15} is governed by two opposing considerations. The output impedance of the d.c. amplifier is proportional to R_{15}, which should therefore be small in order to give a low output impedance. However, a small value of R_{15} gives rise to a large discharge current from C_2 during the clamped period. This current has to be replaced by a much larger pulse of current flowing from the amplifier, as explained in Section 5.1, and it is thus desirable to make R_{15} large in order to limit the value of this recharging current. A reasonable compromise is to make R_{15} equal to 1 kilohm.

In the choice of chopping waveform, high mark/space ratio is desirable in order to realize gain in the input chopper (Section 3.1), and a high chopping frequency is required to achieve a reasonable overall bandwidth. However, the mark/space ratio cannot be increased indefinitely by decreasing the clamped period, since the latter has a minimum value which is fixed by th need to include a delay time of 30 microsec within the perio to overcome the effects described in Section 5.2, and by the nee to recharge C_3 in the remainder of the clamped period. On th other hand, increasing the mark/space ratio by increasing th unclamped period results in a decrease in the chopping frequenc and the bandwidth is therefore reduced.

The minimum permissible value of the unclamped period determined by the error introduced into the d.c. output by transient which occurs at the start of the unclamped perio [Fig. 10(*f*)]. This transient is integrated by R_{15} and C_2 durin the unclamped period and contributes to the output. Assumin the transient to be triangular, with typical dimensions o 20 microsec width and 0·5-volt amplitude, then its integrate contribution is reduced to 0·1% of full-scale output (10 volts in 500 microsec, which is therefore the lower limit of the unclampe period.

The choice of C_3 is governed by the need to compromis between having a time-constant C_3R_0 which is small, allowin the clamped period to be made small, and a time-constan $R_{15}C_3C_2/(C_3 + C_2)$ ($\simeq R_{15}C_3$ if $C_2 \gg C_3$) which is large com pared with the unclamped period. Unless this latter conditio is satisfied a considerable loss in gain can occur. Choosin $C_3 = 0{\cdot}5\,\mu$F results in a time-constant $R_0C_3 = 50$ microsec and a time-constant $R_{15}C_3 = 500$ microsec, which is a reasonabl compromise.

If the clamped period is made 100 microsec, C_3 is allowe 70 microsec in which to be recharged (allowing for the dela in the output chopper), and with an unclamped period o 500 microsec this results in a mark/space ratio of 5 : 1 and a pulse repetition frequency of 1·6 kc/s.

The integrator time-constant $R_{15}C_2$ is given a lower limit by the amount of ripple which may be tolerated in the final output The ripple is caused by the discharge of C_2 through R_{15} during the clamped period [Fig. 10(*e*)]. When the clamped period is 100 microsec the output ripple is 1% if $R_{15}C_2$ is made equal to 10 millisec. This corresponds to an overall bandwidth of 17 c/s since the output integrator is in series with the output of the amplifier. A bandwidth of 85 c/s is obtained with $R_{15}C_2 =$ 2 millisec, when the ripple is 5%.

(12.2) Transistor and Diode Types

Apart from the input chopper, where a surface-barrier tran sistor is used, the circuits described all use low-frequency transistors of the OC71 type, except for the circuits shown in Figs. 9, 10 and 12, where transistors of the OC72 type are necessary because of the higher voltage and current levels. A low-leakage silicon diode is necessary in the base circuit of the input chopper, but elsewhere germanium point-contact diode of the CV448 type are adequate, except for D_3, Fig. 9, and D_5 Fig. 12, where germanium junction diodes with a low forward voltage drop are used.

DISCUSSION ON THE ABOVE FOUR PAPERS

Before a joint meeting of the Measurement and Control Section *and the* Radio and Telecommunication Section *3rd December, and th* Mersey and North Wales Centre *at* Liverpool* *18th November*, 1957.

Mr. I. Wilson: I shall confine my remarks to the papers on d.c. amplifiers. In the type of analogue computer which uses a large number of high-gain d.c. amplifiers and which usually works on a single-shot or real-time basis rather than in the repetitive mode, amplifier gain and drift should be commensurate with computing accuracies of the order of 0·01% in individual linear operations, if the overall accuracy of a large system is not to become too poor.

In view of Dr. Chaplin's claim that the chopper d.c. amplifie might be useful in analogue computers, it is interesting to con sider how satisfactory it would be for electronic analogue computer applications in which valve d.c. amplifiers have bee in widespread use. If one is prepared to use capacitances o up to 10 μF—and it is not unlikely that smaller lower-working voltage high-grade capacitors will become available in th

* Mr. Ettinger's paper only was read at Liverpool.

ature—and to use resistances of between 10^4 and 10^7 ohms, en input drift figures of 10^{-9} amp and 10^{-4} volt seem to be ceptable, particularly since the authors are optimistic about ducing the current drift by at least one order of magnitude. owever, the gain and bandwidth are not suitable for highly ccurate analogue computers. In the more sophisticated achines feedback factors of 80–100 dB are commonly available to frequencies of several hundred cycles per second. To chieve a comparable performance, the transistor d.c. amplifier ould have to provide a gain of 10^4 megohms at such frequencies. o the authors foresee any difficulties in designing an amplifier ith this specification and having a transfer function which ould permit the application of up to 120 dB feedback? Owing the low input impedance of the transistor amplifier, the feedack factor varies inversely with the impedance of the feedback omponent. Whilst this might be an embarrassment the low put impedance can have advantages. Compared with the igh input impedance of the valve d.c. amplifier the effect of apacitance at the input terminal is likely to be a less critical esign factor as far as loop stability in the presence of feedback concerned. This should result in greater flexibility in routing put leads to a central patchboard system.

Fig. 16 in Paper No. 2442 M shows a reasonable way of creasing bandwidth, with the chopper amplifier placed, with s output-smoothing filter, in a side chain of relatively low gain.

In connection with Fig. 13 in Paper No. 2382 M, would the uthors please explain why the bottoming voltage increases with ase current? It is usual for the transistor to bottom more ully as i_b is increased, but in this case some other effect obviously redominates. I am sorry that the authors could not dwell ore on the use of transistors as d.c. switches, since they can e made to bottom satisfactorily even in the presence of quite igh emitter currents. The weakest components in analogue omputers are the non-linear units, such as multipliers and unction generators. It seems reasonable to suppose that ransistors might profitably be used as switches in non-linear nalogue devices using quasi-digital techniques. In this conection, the values of i_{e0} which are encountered with germanium ransistors are rather high, and the grown-junction silicon ransistors which I have tried have been unsuitable as d.c. witches because of their high effective collector and emitter esistances. Can the authors say whether alloy-type silicon ransistors are likely to become available in due course?

Mr. F. Oakes: I also should like to confine my remarks to he papers on d.c. amplifiers.

The authors compared the performances of the balanced mplifier and the chopper-type amplifier, and have pronounced n favour of the latter. I quite agree with their preference but or different reasons.

Dr. Chaplin mentions that the main drawbacks of the direct-oupled amplifier are its stringent matching requirement and umbersome setting-up procedure. Colleagues of mine have ucceeded in rendering the setting-up procedure quite easy. So ar as matching is concerned, only 10% matching is required or α' to achieve stabilities of the order of about 10^{-8} amp, or 0μV for a low-impedance source. However, there are other idden snags.

It is very difficult to maintain the balance of such an amplifier fter it has been set up initially, because the standing current is f the order of 10^{-4} amp but has to be maintained to at least 0^{-8} amp. In a balanced amplifier, any ambient temperature anges should affect both halves in the same way. This means hat normally the transistors must be inserted into a metal block. his, however, provides a large thermal capacitance, resulting a very large thermal time-constant. If the amplifier is hermally unbalanced it will take a long time to settle down again. Asymmetric non-linearities are compensated by linear components, so that at best something like 3-point tracking in the matching of the two halves is achieved over the working temperature range.

The balanced amplifier is more difficult to stabilize so far as gain is concerned. A single-ended a.c. amplifier is quite an easy problem by comparison. Battery voltage fluctuations play an important part and affect the amplifier because of unavoidable deviations from perfect balance. Finally, there is inverse-frequency noise, which affects the balanced amplifier more than it does the chopper.

These reasons indicate that real advantages are offered by the chopper amplifier where bandwidth and basic simplicity are not of importance. On the other hand, for a bandwidth from zero to, say, 100 kc/s the balanced amplifier is still an attractive proposition.

Mr. L. C. Burnett: It could be inferred from Paper No. 2440 M that pairs of rectangular pulses must be used to ensure reliable operation of a Dekatron. This is not so: this type of drive was added to those recommended by the manufacturer at the request of the U.K.A.E.A. The manufacturer's circuit tests and life tests show that this drive system has no advantages over the integrated pulse drive, and is usually more costly to apply.

Dr. E. H. Frost-Smith: In Section 2.2 of Paper No. 2353 M, the author says:

> Transients in the control circuit may, however, be ignored during the conducting or forward half-cycle, where increase of core flux is mainly controlled by the supply voltage applied through the relatively low rectifier forward and load resistances.

The second half of this passage may very well be true, but I do not think it is right to say that one can ignore transients, because one is primarily interested, in this device, in the power gain of the amplifier.

Mr. Ettinger considers the control current during the reverse half-cycle, the reset period, and ignores that which is flowing during the positive half-cycle. Prior to saturation of the core, both the control circuit and the load circuit are coupled, the rectifier is conducting and a current is induced in the control circuit. The magnitude of this current depends on the control-circuit resistance. During saturation the control current is governed by Ohm's law ($= V_c/R_c$), and during the reset period the control current is that required to reset the flux.

Three essential times therefore have to be considered, and the mean control current must be obtained by integrating the control current over all these three periods and dividing by the total time (i.e. one complete period). The mean control current, as the author says, is given by the control voltage divided by the control-circuit resistance, and I do not see how this can be reconciled with the fact that he has considered only one-half of the total period of flow of current.

Also in Section 2.2, the rectifier becoming non-conducting is assumed to be equivalent to the superposition of a negative quantity at the instant of switching. This, of course, is an established method of dealing with transients in linear systems. The present system is non-linear, however, and I feel that the author should justify the validity of this step.

Mr. F. Holmes: My remarks apply to Paper No. 2440 M.

First, many of us are concerned with problems involving reverse counting, and I wonder whether Dr. Chaplin has any remarks to make on this application of the transistorized counter that he has shown us to-night.

My second point concerns the use of a transistorized Dekatron for parallel printing-out techniques. I wonder whether, on the basis of the circuit demonstrated, it would be possible to put a supervisory signal into the transformer itself, by having an additional winding and arranging the waveform so that the

output waveform from the preceding Dekatron cathode no longer causes the follow-on Dekatron to step forward, but merely to leave the control in the hands of the supervisory signal. Applied in parallel, say to four Dekatron stages, there would be a train of 10 impulses going in and stepping all the tubes round in unison. This technique enables one to use a simple parallel read-out register, either indicating or printing.

Finally, what does Dr. Chaplin consider to be the maximum rate of operation of a solenoid register or control-solenoid by a transistor circuit such as he has used in the mechanical register?

Dr. J. E. Flood: The work on transistor drive circuits for Dekatrons is significant because it enables these components to be used not only in simple scalers but also in complicated transistor logical circuits for control purposes and in digital computers. This is because the output from a Dekatron can operate a transistor logical circuit whose output is sufficient to trigger another Dekatron-driving circuit.

My colleagues have designed a telephone-exchange register on this principle,*† using Dekatrons driven by transistor blocking-oscillators similar to those described by Dr. Chaplin and Mr. Williamson. The counters have to be reset by circuit action instead of manually. This is done by a transistor blocking-oscillator, which can reset 10 tubes at once. The h.t. supply for the Dekatrons is provided by a transistor d.c. convertor, which also can serve 10 tubes. In this way, the whole circuit can operate from the low-voltage supplies provided for the transistors. This is particularly convenient for battery-operated equipment.

We have used transistor blocking-oscillators to drive Dekatrons at their maximum recommended speeds and have obtained greater reliability than we ever obtained from the integrated-pulse drive using thermionic valves. For operating transistor circuits the Dekatrons require only small cathode-load resistances; this also makes for reliability at high counting speeds. Like the authors, we have found it convenient to operate on the negative-going edge of the Dekatron output pulse. However, this may be less advantageous when *n-p-n* transistors are available.

It is unfortunate that the inefficient magnetic circuit and long operating time of the message register have prevented the authors from operating it by using an extra winding as part of a transistor blocking-oscillator. We have found this technique very satisfactory for operating telephone relays from short pulses.

Mr. J. S. Walker: Has Dr. Chaplin considered using transistor circuit-integrators in the output stage of chopper amplifiers, in view of the difficulties he mentions with the integrator time-constants?

As a comparison of some parameters of silicon and germanium transistors, with particular reference to the papers under discussion, I give some figures relating to a grown-junction silicon transistor, namely the 2S005 used in the common-emitter mode, dealing in general with a temperature range of 25° C–150° C.

The three important parameters mentioned by Dr. Chaplin are r_s, the closed-switch impedance, r_0, the open-switch impedance, and the change in closed-switch residual voltage with temperature, ΔV. For the 2S005, r_s increases with temperature, typically from 100 to 150 ohms over the range 25° C–150° C; r_0 decreases with temperature from about 10^8 ohms at 25° C to 5×10^4 ohms at 150° C. Dr. Chaplin gives a drift, ΔV, of 50μV from 20° C to 50° C, giving a coefficient of 1·5μV per deg C. For the 2S005 a figure of 10 times this might be expected.

To summarize: although the voltage drift ΔV is larger, the very large increase in r_0 is such as to more than counterbalance this, and I estimate that, using the above transistor, drift figures over the range 25° C–150° C will be of the same order as fo Dr. Chaplin's germanium amplifier, i.e. 4×10^{-9} amp in th range 20° C–50° C. If, however, one operates over a temperatur range of 25° C–100° C, the corresponding drift figure is tw orders better, i.e. 4×10^{-11} amp.

Mr. D. C. Pressey: Could Dr. Chaplin give some figures fo linearity?

Mr. R. M. Langdale: In Paper No. 2440 M Dr. Chaplin onl mentions Dekatrons with a maximum speed of 4 kc/s. He is n doubt aware of the 20 kc/s single-pulse Dekatron, which require only a single 25 microsec pulse. The use of this tube woul simplify transformer design and also reduce the number o components—in particular the number of diodes used. I woul be interested to hear from Dr. Chaplin if he has done any wor with these tubes.

Dr. C. J. N. Candy: In Paper No. 2442 M a very attractiv a.c. amplifier is described; the use of a single decoupling capacito is a real advance over the more conventional circuits. However inconveniently large capacitances are demanded in circuits tha have high gains at low frequencies.

A previous speaker suggests the use of a Miller circuit t replace this decoupling capacitor. Unfortunately this is not very satisfactory solution to the problem because the impedanc of the Miller circuit becomes resistive at high frequencies. Thi effective series resistance in the Miller capacitance introduces unwanted feedback which may cause instability.

An indirectly heated thermistor has been used successfully t replace the decoupling capacitor. The system makes use of the thermal lag between the heater and the bead to separate a.c. signals from changes in d.c. levels. An amplifier gain o 10 volts/μA at 1 c/s has been obtained in this way. This amplifie may be used with a mechanical chopper operating at low frequencies (50 c/s). However, the transistor chopper described in the paper operates at a high frequency and avoids the use of very large capacitors. It also results in a reduction in circuit noise, since transistor noise is approximately inversely proportional t the chopping frequency.

Mr. I. C. Hutcheon (*communicated*): The use of feedback integration has been suggested, and I think this method may have considerable advantages.

Figs. A(i) and A(ii) show a simple *RC* integrator and a feedback (bootstrap) integrator respectively, the a.c. amplifier and output chopper being represented by a battery V, resistor r, and switch. [V may have either polarity. Although the feedback integrator is one-sided it could be made symmetrical by use of a complementary emitter-follower, as in Fig. 9(*a*) o Paper No. 2442 M.] The two circuits have the following characteristics, r being assumed very much less than R, Z_0 low Z_i high, $A = 1 - \delta$, δ of the order of 0·01.

	Simple integrator	Feedback integrator
Fractional response rate $\frac{1}{v_{max}}\frac{dv}{dt}$	$\frac{1}{RCv_{max}}\left(\frac{n}{n+1}V - v\right)$	$\frac{1}{RCv_{max}}\left(\frac{n}{n+1}V - v\delta\right)$
Fractional ripple voltage across C	$\frac{\tau}{RC}\frac{n}{n+1}\frac{V}{v_{max}}$	$\frac{\tau}{RC}\frac{n}{n+1}\frac{V}{v_{max}}$
Input V required to maintain v steady	$\frac{n+1}{n}v$	$\delta\frac{n+1}{n}v$

Response of the simple integrator falls off as v approache $nV/(n+1)$, and the limiting drive, V_{max}, must appreciabl exceed the required greatest output, v_{max}.

In the feedback circuit, v_{max} is not limited by the amplifie and may be extended from ±10 to, say, ±30 volts (about mean 30 volts in this case) with an OC77 transistor.

If *RC* is reduced by the same factor (i.e. 3), the fractiona response rate and fractional ripple for a given drive ar

* 'Handbook of Scientific Instruments and Apparatus' (Physical Society, London, 1957), p. 83.

† Warman, J. B., and Bibb, D. M.: 'Transistor Circuits for Use with Gas-filled Multicathode Counter Valves', *Electronic Engineering*, March, 1958, 30, p. 136.

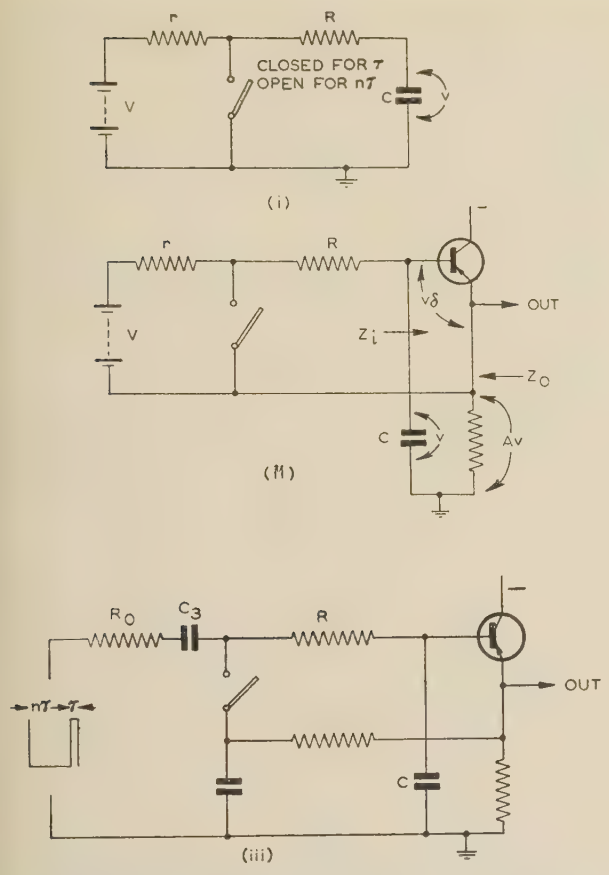

Fig. A.—Alternative output integrator circuits.

unchanged. The drive, V, required to maintain the larger output at a steady value and the fractional ripple content of this steady output are, however, lower by a factor of, say, 0·03. I think this could be a considerable advantage in systems with overall d.c. feedback. Finally, the drive V_{max} may be reduced if desired with the feedback circuit, thus easing the amplifier and output-chopper requirements.

The circuit shown in Fig. A(*ii*) provides a low-impedance output, though containing an additional ripple voltage due to the ripple current in C flowing through Z_0. This part of the ripple cannot be reduced by increasing C, but is relatively small if Z_0 (of the order 20 ohms) is less than X_c. A common earth can be obtained by the circuit shown in Fig. A(iii). Since either the charging current [Fig. A(*ii*)] or the clamp current [Fig. A(*iii*)] flows through the transistor, a symmetrical arrangement is necessary if the full response rate is to be achieved in both directions for all values of the output. Feedback of high frequencies developed across Z_0 can be prevented by, for example, clamping to a capacitor which follows the emitter potential, as shown in Fig. A(iii).

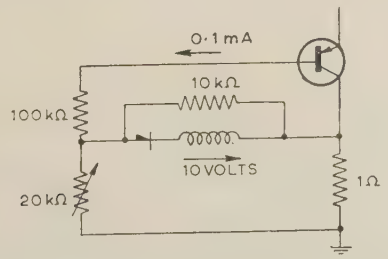

Fig. B.—Alternative circuit for balancing voltage error in the input chopper.

Would the authors say why they make R_0C_3 so small, when a moderate increase in C_3 would reduce the current demanded from the amplifier without affecting gain? Is it to minimize this second time-constant in the d.c. loop?

The circuit shown in Fig. B for balancing the voltage error in the input chopper, would seem a useful simplification, since it uses one less diode and one less transformer winding.

Dr. J. N. Fletcher (*at Liverpool*): Although Mr. Ettinger attempts a useful task by investigating the resetting process, his work is not convincing.

I seriously doubt the validity of the analysis from which eqn. 7(*a*) is derived as a foundation for the paper. For core materials which exhibit rectangular characteristics, I am quite certain that this equation is incorrect, and that it should not be of exponential form with the implication of inductive behaviour.

When dealing with rectangular characteristics, the concept of inductance is so misleading that it should be abandoned. To illustrate this point, Fig. C shows a simple circuit and the

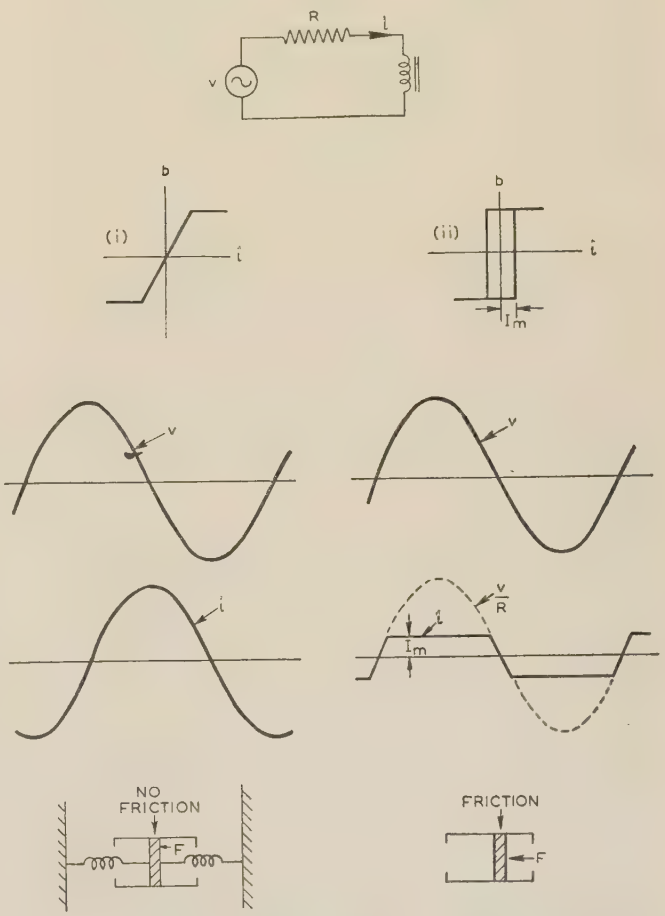

Fig. C.—Voltage/current relationships for different magnetizing characteristics.

voltage/current relationships for two types of core under non-saturating conditions, with mechanical analogies for the part played by each core in the circuit. In case (i) we recognize inductive behaviour, including the ability to store and return energy; in the absence of circuit resistance the current would lag the voltage by 90°. In case (ii), however, the current is in

phase with the voltage, and the behaviour is entirely that of a non-linear resistance. The concept of inductance can hardly be justified simply because it accords with the physical appearance of a component.

The author confuses his analysis by using current changes to represent changes in flux, instead of adhering to the more satisfactory voltage-change approach. Indeed, with a rectangular characteristic, the entire flux change takes place at constant current.

Since reasonable agreement is obtained between experimental and theoretical results, I can only conclude that the method of verification is open to question. It is unfortunate that comparisons are based on control current, or current-gain, which depends upon control current. With rectangular characteristics, variations in control current simply reflect variations in eddy currents arising from different rates of change of flux. A knowledge of flux behaviour would determine whether the author's basic equation was correct; to measure this in terms of eddy currents, which depend upon so many other factors, is asking a great deal.

We must not be misled into believing that we can make a good prediction of magnetizing currents on any simple basis, particularly that of the static or hysteresis characteristic put forward by the author. Owing to eddy-currents, the dynamic characteristic can exhibit magnetizing currents several times larger than are given by the static characteristic, even at power frequencies, and there are an infinite number of dynamic characteristics, depending on the exact cycle of magnetization.

Mr. F. H. Belsey (*at Liverpool*): The author describes half-wave magnetic amplifiers and states that they have half to one cycle response. In my experience, the circuit shown in Fig. has a quick (half-cycle) response to a signal resulting in a increase of output, but has a slower response to a signal resultin in a decrease of output. Would the author comment on th relative efficiency of the half-wave and full-wave types? Th circuit shown in Fig. 1 appears to be relatively inefficient, par ticularly with resistive loads: can it therefore only be used fo small output powers?

One of the advantages of the full-wave type is that relatively small harmonic voltages are induced in the control circuit. Th harmonic voltages induced in the control windings of the half wave type can be a nuisance when flowing in the controllin signal source.

Conductance-controlled magnetic amplifiers are important A carbon pile has been used to control such an amplifier (Britis Patent Application No. 13507 : 1956), and promises to hav many useful applications. In my experience, 'top slope' of th B/H characteristic as shown in Fig. 3(*b*) has an unexpectedly large effect on the maximum output obtainable from such an amplifie and is traceable to the fact that the lag of load current (assuming resistance load) caused by the series inductance due to the top slope results in an area of negative voltage-change appearing across the core windings. This has to be balanced by a corresponding positive area which subtracts from the maximum possible voltage change which can appear on the load. The type of magnetic amplifier here referred to has reset rectifiers in the control circuits, which are not shown in any of the author's circuits.

THE AUTHORS' REPLIES TO THE ABOVE DISCUSSION

Dr. G. B. B. Chaplin and **Mr. R. Williamson** (*in reply*): We agree with Mr. Burnett that his inference that pairs of rectangular pulses must be used to ensure reliable operation of a Dekatron is not true. The statement is of course only true if the words 'at their maximum recommended speed' are added. We have made many tests at the maximum recommended speed, and in almost every instance Dekatrons which had failed to operate in equipment using the integrated pulse drive advocated by Mr. Burnett operated correctly in the transistor-driven equipment.

We agree with Mr. Flood's interesting comments on transistors and Dekatrons, and note that he confirms the reliability of rectangular-pulse operation. The 20 kc/s single-pulse Dekatron mentioned by Mr. Langdale is a very attractive proposition, leading as it does to a reduction in components and faster operation, but as yet we have no figures on the lifetime of this Dekatron.

In reply to Mr. Holmes, we have not considered the problem of reverse counting with Dekatrons, but have had experience of parallel read-out from six decades of the transistor-driven scaler.

Mr. G. M. Ettinger (*in reply*): In reply to Dr. Frost-Smith, it may be stated that the voltage induced in the control circuit during the forward half-cycle, while flux is rising towards saturation, represents a transfer of power from the load circuit to the control circuit. This may lead to reduced efficiency and may affect the 'firing angle' somewhat, unless load circuit resistance is large. The effectiveness of flux reset from saturation, on the other hand, depends on the control-circuit time-constant during the reverse half-cycle and, as Dr. Frost-Smith points out, on control voltage divided by control-circuit resistance. Allowance may also be made for eddy-current effects (Reference 12 of the paper). Pipes's method, which allows for arbitrary core-material properties, is discussed on page 36 of Reference 7 of the paper.

The comparison of the self-excitation rectifier to a switch is, of course, permissible only if reverse conductance is either very small or is allowed for, as shown in Section 8.1 of the paper.

In reply to Dr. Fletcher, it is pointed out that eqn. (11*b*) and the design data derived therefrom are, in effect, based on the core characteristics shown in Fig. 6(*c*) of Reference 15 of the paper. Analysis may be in terms of either current or voltage, provided that allowance is made for conductance across, or finite resistance in series with, the control winding. Assumption of voltage control alone presupposes a control signal source of negligible resistance. Analysis in terms of voltage is not necessarily more satisfactory.

The magnetic properties employed in the analysis of any form of a.c.-operated magnetic device must, of course, be the dynamic properties. The reactances shown in column 6 of Table 1 were obtained from 50 c/s measurements of magnetizing current as a function of alternating voltage.

Referring to Mr. Belsey's remarks, I would confirm that transient response to positive and to negative increments of control signals may be different. This problem has been studied by Gill.* It should be noted that transient response to step changes of control signals depends, to some extent, on the portion of the cycle of excitation voltage during which such step changes are applied.

Half-wave circuits may be employed up to fairly high power levels. As shown in Table 2 of the paper, the power dissipated in the bias resistances may be significant.

Dr. G. B. B. Chaplin and **Mr. A. R. Owens** (*in reply*): Mr. Wilson gives a specification for amplifiers for analogue computers which demands a gain-bandwidth product 10^3 times greater than that of the present amplifier. Some of the limitations of the present system are due to the use of low-frequency transistors

* Gill, F. D.: R.A.E. Technical Note EL 107, 1955.

the amplifier. Had higher-frequency transistors been readily available during the course of this work the increase of bandwidth in the a.c. amplifier thus made possible would have considerably reduced the h.f. stability problem and allowed smaller values of output integrator to be employed with a consequent increase in bandwidth. However, the ultimate limit of the bandwidth is set indirectly by the transients occurring in the input chopper, which determine the maximum chopping frequency. It seems unlikely, therefore, that the required increase in gain-bandwidth could be obtained by such detail improvements, and a more promising approach would be, as Mr. Wilson points out, to employ a low-gain chopper amplifier to stabilize the main a.c. amplifier.

The bottoming voltage curves of Fig. 13, Paper No. 2382 M, although at first sight rather unusual, do in fact correspond closely with those predicted from theory. Commencing with eqn. (8) of Paper No. 2382 M, the input chopper conditions are inserted by making $i_e = 0$ and $i_c = i_b$, which yields the result

$$v_{ec} = \frac{kT}{e} \log_\varepsilon \left(1 - \frac{1-\alpha}{i_{c0}/i_b + 1}\right)$$

This expression approximates to

$$v_{ec} = \frac{-kT}{e} \frac{1-\alpha}{i_{c0}/i_b + 1} \quad \text{for} \quad \frac{1-\alpha}{i_{c0}/i_b + 1} \ll 1$$

There are two temperature-dependent terms, namely kT/e and i_{c0}. When i_b is small, being within an order of Δi_{c0}, the variation of kT/e may be neglected, and v_{ec} tends rapidly towards zero as i_{c0} increases with temperature.

This is illustrated by the curves for $i_b = 0{\cdot}02$–$0{\cdot}50$ mA.

At high values of i_b, such that i_{c0}/i_b is always much less than unity, the expression approximates to $v_{ec} = -kT(1-\alpha)/e$, which is directly dependent on T. In this case there is a linear increase in $|v_{ec}|$ of $k(1-\alpha)/e$ volts per deg C, which is quite independent of i_b. This condition is illustrated by the $i_b = 2$ mA and $i_b = 5$ mA curves, which are roughly parallel.

The difference between the latter two curves, which from the above should be coincident, is explained by the presence of a small ohmic resistance of about 0·15 ohm in the collector lead, due either to the resistivity of the collector material or to the lead itself. The base current flowing in the collector path produces a voltage drop across this resistance which appears across the transistor as a bottoming error.

From the above it can be shown that a certain intermediate value of i_b may be chosen to give the least variation in v_{ec} over a given temperature range when the variation of kT/e approximately balances the variation of $1 + i_{c0}/i_b$. Since i_{c0} is smaller by about a decade in a high-frequency transistor, it can be seen that the optimum value of i_b should also be a decade less for the SB100.

The same calculations are equally valid for germanium and silicon transistors, the appropriate figures for the rate of variation of i_{c0} being used in each case. The difficulty which has been encountered with silicon grown-junction transistors is due to the comparatively large collector series resistance—a base current which yields optimum voltage drift also gives a very large standing error. However, silicon alloy transistors have series collector resistances comparable with germanium alloy units, and owing to the improvement in leakage current in these units, they promise to give very good chopper characteristics. A possible limitation may be their poor high-frequency characteristics when compared with the SB100. These characteristics determine the level of chopper transients, and thus the maximum chopping frequency.

Mr. Oakes's remarks concerning his experience of direct-coupled amplifiers are valuable as they illustrate very clearly some of the difficulties encountered with this type of circuit. It may be that the final answer lies in using a chopper amplifier as a stabilizing loop for the balanced amplifier, when both low drift and large bandwidth may be obtained. As Mr. Oakes has mentioned, inverse-frequency noise in the direct-coupled amplifier may be troublesome, whereas the chopper-type amplifier noise occurs in a band 1·6 kc/s ± 25 c/s, which, being outside the inverse-frequency region, contains mainly shot noise of a lower level.

Mr. Walker's figures for a grown-junction silicon transistor are very interesting and show up well the advantages to be obtained from the low-leakage properties of silicon. In certain applications, however, the large voltage drift and the large standing error might prove embarrassing.

It might prove difficult to make full use of the improved current drift figures which can be obtained, owing to the noise level of the a.c. amplifier, this being roughly of the same order as the current drift of the silicon chopper. It seems unlikely that any great improvement will be forthcoming in this direction, and the ultimate limit will therefore be decided not by the chopper transistor but by the first stage of the a.c. amplifier.

No detailed figures can be quoted in reply to Mr. Pressey's inquiry regarding linearity. It has been assumed that the amplifier will always operate under feedback conditions, and that a high degree of linearity is therefore not required. However, the only non-linearities present are at the extremes of the input/output characteristic where the output stage of the amplifier becomes saturated. At all other points, including the origin, the characteristic seems quite linear.

Dr. Candy's use of a thermistor to replace the large capacitor in the stabilizing feedback path of the a.c. amplifier is rather ingenious and has some real advantages when very-low-frequency amplifiers are required, such as when 50 c/s choppers are employed.

Messrs. Hutcheon and Walker both extol the virtues of the feedback-type integrator for the output chopper. This possibility was considered during the course of design of the amplifier, but was rejected because of the large drift which can arise in this stage.

A drift of 50 μA in i_{c0} flowing in the 1 kilohm resistance of the integrator, combined with 100 mV emitter-base voltage drift, is equivalent to a voltage drift of 150 mV at the output. When referred to the input terminal this becomes a current drift of

$$(150 \times 10^{-3})/(50 \times 10^{6}) = 3 \times 10^{-9} \text{ amp},$$

which is comparable with the drift of the input chopper.

No improvement in bandwidth can be obtained by this method: a feedback integrator using R and C may be regarded as a simple integrator of time-constant RC/δ cascaded with an amplifier of gain $1/\delta$, and the ripple output from such a circuit is equal to that from a simple integrator of time-constant RC. Reduction of the feedback-integrator capacitor to C' $(=\delta C)$ to obtain a bandwidth equal to that of the simple integrator results in a proportional increase in output ripple; a state of affairs which is entirely equivalent to attaching an amplifier of gain $1/\delta$ to the simple integrator first used. Thus, for a given bandwidth, the fractional ripple output is constant, whatever the integrating circuit.

The advantages of using a physically smaller capacitor and obtaining a greater output voltage swing for a given bandwidth must therefore be weighed against the drift problem which arises. Consideration must also be given to the falling-off of integrator transistor current gain at high frequencies, which may increase

the likelihood of instability under conditions of external feedback, as the external feedback loop will then contain a physical time-constant of only δRC (where $\delta \simeq 0{\cdot}01$) compared with an integrator of value RC in the simple case.

The circuit proposed by Mr. Hutcheon for balancing the input chopper represents a useful simplification whose only disadvantage might be the effect of inter-winding capacitances in th transformer.

We agree with Mr. Hutcheon that a slight increase in C_3 migh help to reduce the peak current in the output of the amplifier Doubling C_3 should give a 30% reduction in gain and a 75% reduction in peak current.

DISCUSSION ON 'THE REMOTE AND AUTOMATIC CONTROL OF SEMI-ATTENDED BROADCASTING TRANSMITTERS'* AND 'THE DESIGN OF HIGH- AND LOW-POWER MEDIUM-FREQUENCY BROADCASTING TRANSMITTERS FOR AUTOMATIC AND SEMI-ATTENDED OPERATION'†

Mr. K. L. Rao (*India: communicated*): The B.B.C. engineers and associated bodies must be congratulated for bringing about the change-over in order to conserve technical man-power. I agree with the authors of the first paper that the older men do not object to a job without prospects. My experience has shown that the younger men lack the tenacity so essential for the success of an arduous task. The success of the scheme put into operation is in no small measure, I suppose, due to the senior staff or staff who have shown themselves highly reliable in the service.

In Section 2.7 of the second paper the slight fall in power on modulation has been attributed to h.t. regulation. I have observed a similar effect in most of the transmitters, but the h.t. regulation alone does not seem to account for it. There appears to be an inherent limitation imposed owing to non-linearity of modulation. The BR189 valves seem to give better results.

I do not think that the transmitting equipment need be designed for the full a.f. range of 30–10 000 c/s. With adjacent-channel separation of only 10 kc/s and limitation in bandwidth of even the highest-quality receivers put into commission at the radio-relay receiving stations, there does not appear to be much point in designing for an a.f. range greater than 6 000 c/s. This would also considerably ease design and monitoring problems.

Messrs. R. T. B. Wynn and **F. A. Peachey** (*in reply*): The policy of offering the watchdog posts to elderly staff of proven reliability gives them continued employment for a few years more. It is not because younger men have generally been found unreliable in this work, but it is considered that such men should not be allowed, early in their career, to vegetate in a job which, by its nature, provides insufficient incentive to gain wider experience.

Messrs. W. J. Morcom and **D. F. Bowers** (*in reply*): The fall in carrier power with modulation is due to h.t. regulation. The difference between the figures for the BR161 and BR189 valves is due in the main to errors of measurement, the power being measured by the rise in temperature of water through a resistive load.

Whilst appreciating Mr. Rao's point on limiting the a.f. range of the transmitter, it is considered good practice to design for the wider ranges. Although the channel spacing is 10 kc/s, it is not necessarily a fact that all transmitters are so restricted. Furthermore, music lines are often available, and as a result the full range of the transmission can be utilized.

* Wynn, R. T. B., and Peachey, F. A.: Paper No. 2329 R, April, 1957 (see **104 B**), p. 529.

† Morcom, W. J., and Bowers, D. F.: Paper No. 2362 R, April, 1957 (see **104 B**, p. 540).

621.385.1 : 621.387

The Institution of Electrical Engineers
Paper No. 2560
May 1958

THERMIONIC AND COLD-CATHODE VALVES

A Review of Progress.

By W. H. ALDOUS, B.Sc., Associate Member.

(1) INTRODUCTION

The thermionic valve has been the subject of continuous and rapid development from Fleming's invention of the diode in 1904 to the present day. It is convenient to start the present review in the immediate pre-war years, when two papers, one on receiving valves[1] and one on transmitting valves,[2] were presented before The Institution to give a general account of the position in their respective fields at the time. Since then, various limited aspects have been covered, in both papers and Chairmen's addresses to the Radio Section, and a broad historical survey was made at the celebration[3] of the fiftieth anniversary of Fleming's diode patent in 1954.

The immediate pre-war years also saw the start of the B.B.C. high-definition television service at 45 Mc/s. This gave an impetus to the development of valves for use on higher frequencies which was continued and accelerated for Services applications during the war. The post-war period, although initially expected to be one of consolidation, has, in fact, seen considerable development in a number of directions.

The original development of the thermionic valve was for communication by telephony and telegraphy, but at the start of the present review period this use had been far outstripped by that for broadcast reception, while a considerable market had built up for valves in industrial control and scientific equipment. The war period saw a reversion to the communication field, now including radar, of a magnitude which required considerable increases in the production facilities of valve manufacturers. In the post-war period some of this communication use has been retained, but expansion of television coverage, coupled with increasing use for industrial and scientific purposes, in computers, control systems, etc., now requires an output of valves even greater than the peak of war-time production.

This review is confined, on the high-vacuum side, to the more classical types of valve, and on the gas-filled side embraces both hot- and cold-cathode types. In the latter class a selection has been made to confine the text to those types which perform functions which could be achieved—possibly with some complexity—with vacuum valves. This selection excludes such devices as t.r. cells (as used in radar duplexers) and Geiger–Müller counters.

Mr. Aldous is at the Research Laboratories of the General Electric Co., Ltd.

(2) RECEIVING VALVES

(2.1) Valve Size

Probably the greatest difference between earlier receiving valves and those of the present day is the very large reduction in size that has been achieved. Typical r.f. tetrodes (or pentodes) in production at various periods are shown in Fig. 1, and data regarding some of their dimensions and characteristics are given in Table 1.

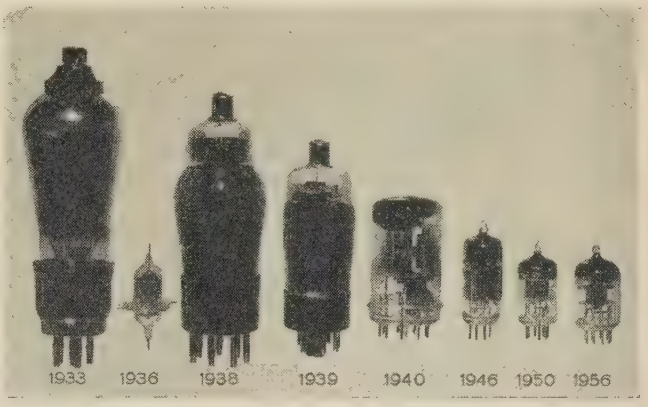

Fig. 1.—Progressive reductions in the size of r.f. pentodes.

The valves of 1936, with a mutual conductance of 3–4 mA/volt, gave a very good performance in radio receiving sets and other relatively low-frequency applications, but were strained to the limit when adopted for the wide-band r.f. and i.f. amplifiers used in television receivers, while their low ratio of mutual conductance to capacitance meant that the amplification per stage was low. The first attempt to improve the position lay in the use of closer inter-electrode clearances with finer grid wires. The electrode system was shortened by using a wide flat cathode, and was mounted on a shortened pinch. In this manner the mutual

Table 1

R.F. PENTODE DATA

Year	Approximate cathode power	Cathode-to-grid spacing	Grid-wire diameter	Mutual conductance	Input capacitance	Output capacitance
	watts	mm	mm	mA/V	pF	pF
1933	4	0·33	0·11	4·0	17	10
1936*	1	0·09	0·03	1·4	3	3
1938	6	0·18	0·075	7·5	14	10
1939	4	0·17	0·07	8·0	11	5
1939	3	0·14	0·05	7·5	11	8
1940	2	0·11	0·05	7·5	11	5·5
1946	2	0·1	0·05	7·5	7·5	3
1950	1	0·08	0·03	5·0	4	3
1956	2	0·03	0·008	16·5	8	3

* Acorn.

conductance was increased to 7·5 mA/volt at an anode current of 10 mA, and such valves gave much improved performance. The decrease of clearance, however, caused increase of capacitance, which was detrimental to wide-band amplification. The direction in which valve development should go to overcome this defect had already been shown by B. J. Thompson in his Acorn valves, in which linear reduction of all valve dimensions was used to give reduced capacitance with the same mutual conductance.[4] However, manufacturing techniques were not then at the stage where Acorn valves could be made economically, and they were never used in very large numbers.

The move to smaller valves had to be made in a number of stages. The first step was to halve the heating power and therefore approximately the area of the cathode, and to decrease clearances, etc. Such valves, mounted on short pinches, were used extensively, not only in pre-war radio and television receivers, but in i.f. amplifiers required for radar equipment. A major development at this stage was the all-glass valve,[5] in which a flat pressed-glass base was used instead of a pinch. Stiff wires through this base supported the electrode system and formed the pins for insertion into the socket, thus avoiding the use of a Bakelite base. All electrode connections were brought to the base of the valve. This form of construction gave an immediate decrease in lead length, and improved stability of amplification at the higher frequencies.

A much smaller form, the pressed-glass 7-pin button base,[6] was introduced in America for battery valves in 1939, and was soon adopted for indirectly-heated valves as well. Used with a bulb 19 mm in diameter and 49 mm long, the construction enabled major reductions to be made in the size of radio and radar equipments. It also had great manufacturing advantages, and the design was therefore followed in this country, but full mass-production was not complete at the end of the war. In its original 7-pin form, and the slightly larger 9-pin (or Noval) form which allows for more-complicated electrode forms, the button base is used for the majority of receiving-valve developments at the present time. Such valves are called 'miniature' valves. It will be seen from Table 1 that the typical r.f. pentode of the present time has inter-electrode clearances as small as those used in the Acorn valves. Such is the improvement in manufacturing technique that valves with performance as good as the Acorn can now be made by mass-production methods.

The reduction in bulb size has, of course, increased the bulb temperature, but by using bulbs 70 mm long, miniature valves can be made having a total dissipation (cathode + screen + anode) of 20 watts. Some output valves and rectifiers must still be mounted in larger bulbs. In these, the older pinch form of construction limits the amount of heat which can be dissipated, and some valves have therefore been produced using a form of button mount, which keeps the glass further from the hot electrodes. This mount is then attached to a normal Bakelite base.

During the war, much work was carried out to reduce valves to the smallest possible size for use in electronic fuses for projectiles.[7] Bulb diameters as small as 7·5 mm were used, with forms of button base or with inverted seals (as used in pre-war television diodes). In the post-war era, these have been developed as distinct ranges of 'subminiature' valves (usually with 10 mm bulbs). Because of the space limitations it is difficult to obtain the same characteristics with these as with miniature valves, and at the moment it seems unlikely that subminiature valves will be adopted for radio and television receivers. For Services use, where space is often more limited, they may well be preferred.

One of the features of subminiature valves is that they do not plug into sockets, but are supplied with 'flying' leads for soldering into circuits. This is a useful feature where equipment is subjected to vibration, but makes replacement of the valves more difficult. A change to flying leads on the valve ranges used in domestic equipment has been considered, but seems unlikely at the present time.

(2.2) Internal Construction

The standard form of construction of receiving valves has been, and is, to mount the electrodes between a pair of mica bridges, the upper one being located in the valve envelope to give added support to the structure. The steady decrease in electrode size and clearances since 1936 has required that the accuracy of construction of the electrodes and of the mica bridges should be increased proportionately, and mica bridges are now in regular use with numbers of small holes stamped in them to a spacing accuracy of 0·01 mm.

To obtain valves with the highest possible mutual conductance, e.g. the last type quoted in Table 1, it is necessary to use very fine wires to wind the grid. These wires, although of molybdenum or tungsten, are not sufficiently strong to maintain the shape of a conventional type of grid. Special grids are therefore made in which the side supports are larger than normal and are held rigidly apart at each end by metal strips to form a frame (Fig. 2)

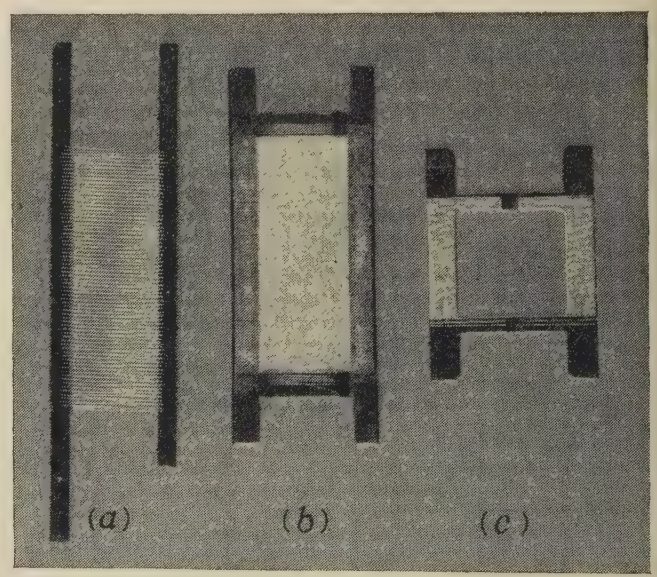

Fig. 2.—Grids for receiving valves.
(*a*) Conventional miniature type.
(*b*) Framed grid for double-sided cathode.
(*c*) Framed grid for planar cathode.

on which the grid wire is wound under tension and brazed or glazed to the side rods to maintain the tension. Such framed grids, in conjunction with accurately made box cathodes, are then mounted between precision-punched mica spacers as in the conventional valves.

The greatest change in internal construction has taken place in the special-quality valves developed since the war for use under conditions of shock or vibration. Valves of normal construction give very long lives in broadcast and television receivers in the home, but in industrial and military equipment they sometimes fail for mechanical reasons in a relatively short time. The miniature valves are a great improvement on the early large types in this respect, since the mechanical forces for a given acceleration are less with lower mass and smaller size.

The development basis[8] of these special-quality valves was the

etermination of the cause and rate of failure of standard niniature types under various mechanical stresses. Following his, successive steps were taken to strengthen the weak parts hat had been found, not only in the electrode system and its upports, but also in the glass envelope. The result of this work as been that miniature valves are now available which will have n acceptable life under conditions of vibration and shock.

(2.3) Valve Types

The types of valve used in modern television and radio receivers re, apart from their size, largely the same as in pre-war sets. There has been a tendency to combine valves in the same nvelope, e.g. triode-pentodes and triple-diode-pentodes, but this more a matter of economic convenience than new valve design. The adoption of the electromagnetic deflection cathode-ray tube or television led to special valve development.[9] To withstand he high peak voltages developed during the fly-back period, ight modifications of normal-output pentodes sufficed at first. The trend to wider scanning angles, which has continued during he post-war period, has required pentodes for the line-generating ircuits which can handle higher power, higher peak-voltage, nd, in particular, high screen dissipation. Other developments ave been special rectifiers, both for the production of the e.h.t. upply from the flyback voltage and for boosting the h.t. supply n transformerless receivers.

The use of secondary-emission multiplication to enhance the nutual conductance appeared in a practical form in valves prior o the war. The concurrent improvement in normal pentodes, nabling them to give comparable amplification, rendered these irst secondary-emission valves obsolete, since extra circuit omplication was involved in their operation. Little use was herefore made of them during the war, but interest has been enewed since then, and miniature valves with secondary-emission multiplication are now available with a mutual conductance f 19 mA/volt at an anode current of 15 mA.[10] Their success as been due to the development, for the secondary-emission lectrode or dynode, of a surface which is not affected by electron ombardment or by the deposition of evaporated material from he thermionic cathode. The alternative approach of controlling he electron paths so that the dynode is shielded from evaporated naterials has also been successful, but valves using this form f construction must inevitably have long electron paths, and heir high-frequency performance is not so good as those of the irst type.

The deflection of a well-focused flat electron beam from ne anode to another to obtain high mutual conductance as always appeared to be an attractive alternative to space-harge control by means of grids. Many attempts have been nade to design such beam-deflection valves, sometimes incorporating secondary-emission multiplication, but, so far, nothing as been marketed with a performance equal to that obtainable ith grid-controlled valves. New valve types, using control of lectron streams by a multiplicity of grids, or using a combination f grid and deflection control, have been suggested for such pecial purposes as detection in f.m. receivers. Such valves are often no technical improvement over a number of simpler valves, ut offer advantage in the reduction of space.

(2.4) U.H.F. Receiving Valves

Before 1939 the only receiving valves designed specifically for se at higher frequencies were the Acorn types, of which the riode would operate up to about 600 Mc/s. In consequence, hen the exploitation of ultra-high frequencies was required for nilitary purposes, intense development of improved triodes was required, and great advances were made.[11, 12] The u.h.f. valves developed differed from former constructions in having disc seals and planar electrodes. The use of disc seals instead of pins for electrode connections gave a very great decrease in the inductance of the leads and therefore of the coupling and feedback between input and output circuits. At the same time, the construction lent itself admirably to use of the valves in the concentric-line circuits which are necessary at high frequencies. The use of planar electrodes, with the grid in the form of a series of parallel wires or a mesh stretched across a metal frame, enabled closer clearances to be obtained between electrodes than with the conventional receiving valve. Such disc-seal valves, in suitable circuits, operated as amplifiers and oscillators up to frequencies in excess of 3 000 Mc/s.

Since the war, progress has been made in two directions. The first is the straightforward one of designing suitable precision envelopes so that even closer clearances can be used between the planar cathode and grid (Fig. 3). This has been achieved, and

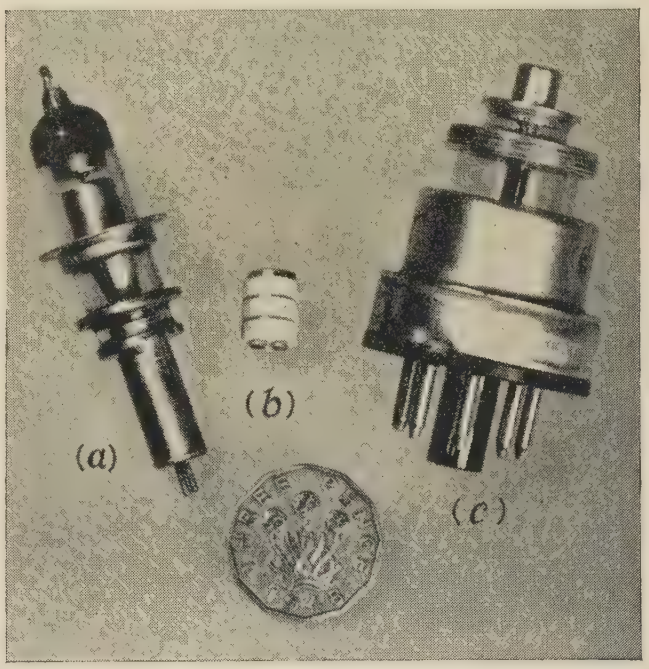

Fig. 3.—Modern u.h.f. triodes.
(*a*) and (*c*) Metal and glass construction.
(*b*) Ceramic and metal construction.

valves are being produced to-day with grid wires only 7 μ in diameter spaced only 25 μ from the cathode surface. These valves are well adapted for use up to about 6 Gc/s. An alternative to the planar system has been used in America in the so-called 'pencil tubes', which use cylindrical electrodes mounted on disc seals.[13]

The second direction is in the use of planar electrode systems, with their very close grid-cathode clearance and fine grid wires, on button bases in miniature valves, using mica bridges to support the electrodes. Valves of this type will not work at such high frequencies as the disc-seal valves, but are cheaper and, because of the high ratio of mutual conductance to anode current, are well adapted for use as i.f. and r.f. amplifiers up to a few hundred megacycles per second, their low noise factor being an additional advantage in input stages.

More recently there has been a tendency to adopt ceramics instead of glass for u.h.f. valve envelopes, and this has spread to the receiving types. This form of construction lends itself to great reductions in the size of the valve envelope, and triodes little larger than a pea have been produced in America (Fig. 3).

(2.5) Valves for Special Purposes

The use of valves for instrument purposes was described in a 1939 paper;[14] the improvements in normal valve types since made have in many cases enabled better performance to be obtained with these than with the former special valves, but new and improved special valves have appeared and new uses have been found for them. Electrometer triodes and tetrodes have been made which occupy a fraction of the volume of their predecessors. Ionization gauges of improved construction can measure vacuum down to 10^{-10} mm Hg. Diodes have been developed for use as standard noise sources, and in the coaxial form they can be used up to 1 Gc/s. The field of use of valves as voltage and current stabilizers has been greatly extended by the development of special types with high current ratings.

The high-speed switching and counting required in communication circuits and in electronic computers has given rise to special vacuum devices using strip beams, which may be deflected electrostatically or magnetically to one or more of a series of anodes. Combined with fluorescent indication of the beam, these devices may be used as high-speed visual counters.

Considerable advances have been made in the techniques necessary for obtaining long life in the repeater valves used in telephone circuits, and the types which are now installed in the transatlantic-telephone-cable repeaters have lives of 100 000 hours.[15]

(2.6) Materials

Decrease in the size of valves for the same dissipation has led to steady increase in the temperature of operation, and in many cases it has been necessary to modify or purify materials in order to obtain the necessary reliability. The use of molybdenum-tungsten alloy for the heaters of indirectly-heated valves, which was just starting in 1937, has, over the years, not been found to be entirely satisfactory, and the present tendency is to use pure tungsten. The voltage stress which the thin layer of insulating coating on this tungsten must withstand has been increased by the post-war introduction of ranges of valves with the heaters designed to run in series directly from the mains. The coating has therefore to be of alumina, and special precautions must be taken regarding its purity.

Receiving valves invariably use oxide-coated cathodes as emitters, and the up-to-date position on these and other cathodes has recently been given.[16] A difficulty with the oxide-coated cathode which has been encountered during modern long-life applications of receiving valves is the development during life of a resistive interface between the cathode metal and the oxide coating; this gives rise to unwanted negative feedback at audio frequencies, and the solution to the problem appears to lie in the avoidance of silicon impurity in the core metal.

Battery valve filaments in 1937 were of nickel and the normal rating was 100 mA, but the need for filaments which can be run directly from dry batteries has led successively to 50, 25 and 15 mA ratings. Adequate strength for the lower ratings can be obtained only be using tungsten as the core material, the wire diameter for the 15 mA filament being only $7{\cdot}8\,\mu$.

Apart from their size, there has been little change in conventional grids since 1937. Molybdenum or tungsten must still be used for the winding wire when maximum strength is needed; otherwise nickel alloys are employed. Copper side-rods with end radiators are still employed where a large amount of heat must be dissipated, and the use of framed grids in high-performance valves has already been mentioned.

Alternative materials to nickel and carbonized nickel, for use as anodes, have been developed because of the scarcity and expense of nickel. Iron, nickel-plated iron, and aluminium-clad iron, which develops a surface with high thermal emissivity when heated in vacuum, have all been used.

Barium continues to be the best form of getter material. Many methods have been evolved, including chemical decomposition, for obtaining it in a pure form in the valve. The present method is very similar to that used in 1937, namely a piece of barium-cored iron wire eddy-current heated to vaporize the barium.

(2.7) Electronic Theory

The basis of the design of space-charge-control valves was summarized[17] in 1946. This basis has since been altered only in minor details, such as in refinement of the formulae and curves for amplification factor for the cases of open grid pitch and finite grid wires. The effects on the characteristics of tetrodes of electron deflections and of space-charge between the screen and anode have been determined in more detail. In general, the greatest advances have been made in the fields of noise[18] and transit-time effects.[19] A sound theoretical basis exists for the explanation, at both low and high frequencies, of the noise introduced into sensitive amplifier circuits by the fluctuations of the electron current in valves. The effects of the time taken for electrons to travel through a valve in determining the impedances between electrodes is known qualitatively, but, for appreciable changes from the low-frequency values, quantitative predictions cannot generally be made.

(2.8) Manufacturing Technique

The manufacture of the standard modern type of miniature valve has been described recently,[9] and although the basic principles have not changed over the review period, the adoption of the glass-based miniature-valve technique has enabled great advances to be made in the speed of production and in the output for a given manufacturing area. Mechanization has been introduced to a large extent in the handling of valves during their sealing-in, pumping and ageing. Assembly of the components is still normally carried out by hand with the aid of jigs, but even this phase is capable of mechanization, and recently machines have been introduced into American factories which produce the assembled electrodes between the mica end-plates, ready for welding to the base connections, at the rate of about 2000 per hour. The greater standardization that has been achieved between valve manufacturers, as the result of miniature-valve production, makes the use of such mechanical assembly more economically feasible.

In addition to the standard type of construction, other methods of envelope making have been introduced which avoid the glass-melting operation involved in joining the glass bulb to the base or pinch. The earliest of these was the metal envelope, which was introduced in America in about 1935, and was subsequently used to some extent in this country. The technique was not found to be favourable to flexibility of manufacture, and was largely obsolete by the end of the war. With pressed-glass bases, where the edge of the bulb follows the contour of the base, it is possible to join the two components by using a lower-melting-point glass as a solder.[20] An alternative to this is the *poli-optique* method[21] introduced in France in 1947, in which the envelope and the base are separately ground with optically fitting surfaces, which, when joined together, give a vacuum-tight envelope on baking.

An alternative to the usual method of exhaust of the valve through a narrow pumping stem is to pump the valve under a bell-jar, and to attach the bulb to the base in the vacuum as the finishing operation. Although attractive in principle, this technique has not been adopted on a large scale.

Life-testing[22] continues to be a necessary adjunct to valve manufacture, in order to ensure that the qualities designed and processed into the valve are maintained over many thousands of hours of use. Life-testing technique has progressed with valve design, in order that the maximum information may be obtained. This is particularly so in the case of special-quality valves, where service specifications call for manufacturing release on the basis of life test of a statistically adequate number of samples.

(3) TRANSMITTING VALVES

(3.1) Glass- and Silica-Envelope Types

The older types of glass-envelope transmitting valve with anode dissipations up to some hundreds of watts, such as were used in the earliest broadcasting stations, had, from the design points of view, become obsolescent before 1938. The necessity for a large envelope area, to keep the temperature low, made this type of valve compare unfavourably with the alternatives.

The development of silica-envelope valves continued during the war and afterwards. Some early radar sets used these valves, but, as operational frequencies increased, the long lead lengths used made them less suitable than their metal-glass counterparts. Since the war, silica-envelope valves have been used extensively in industrial r.f. heating equipments for powers up to a few kilowatts. When small numbers are wanted, this type of valve is economical to construct, and, in use, the cooling problem is somewhat simpler than with external-anode valves.

The chief field for development has been with valves using hard (boro-silicate) glass envelopes, and considerable advances in design have been made. At the beginning of the review period, triodes were available with the anode lead, or both the anode and grid leads, coming through the top of the bulb, and such valves would operate up to about 300 Mc/s with output powers of some tens of watts. Great efforts—mostly in America —were made in the late 1930's to obtain higher power at higher frequencies from glass-envelope valves, and designs appeared of the so-called 'door-knob' class, with the grid and anode supported on straight rods sealed right through both sides of the envelope. This artifice enabled useful outputs to be obtained above 600 Mc/s, but these valves were soon superseded by metal-glass designs having superior performance.

A step forward was made at slightly lower frequencies, about 600 Mc/s, by the introduction of two tetrodes in a common envelope, with a pressed-glass base so that short internal and external leads could be used. By joining the cathodes and screens of the two tetrodes internally, bringing the two grid leads through the pressed-glass base and the two anode leads through the top of the envelope, a good circuit arrangement could be obtained. This form of construction has been further developed since the war by the introduction of double tetrodes with a single cathode and an electrode system on each side of it, the screen being electrically common by taking it right round the cathode [Fig. 4(*a*)]. By this means output powers of 40 watts up to 200 Mc/s and 10 watts up to 400 Mc/s are obtained. These double tetrodes normally use oxide-coated indirectly-heated cathodes, and a maximum h.t. voltage of about 600 volts. The philosophy of using two electrode systems in one bulb has also been applied to earthed-grid triodes. In this case, either by low-impedance cross-connection between the grids of two separate systems, or by a common grid surrounding two cathodes, glass-envelope valves capable of giving about 20 watts output at 600 Mc/s have been made.

Development of single tetrodes in hard-glass envelopes has also taken place, and valves of this form are made with dissipation up to 1 kW. These valves use thoriated-tungsten filaments,

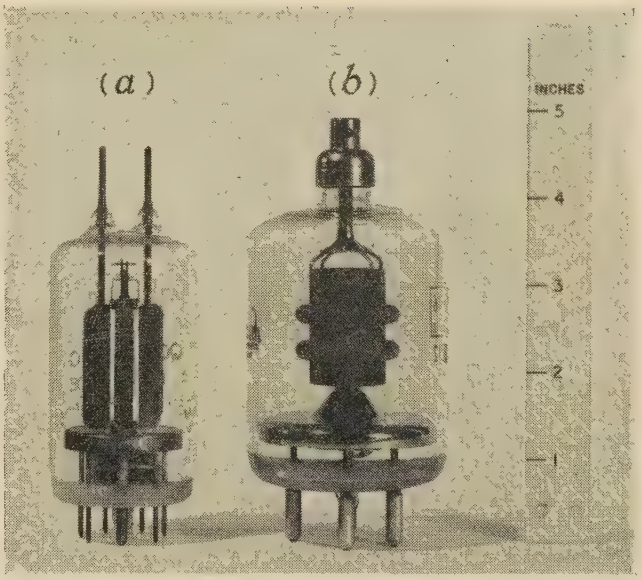

Fig. 4.—Small transmitting valves with hard-glass envelopes.
(*a*) 40-watt double tetrode.
(*b*) 125-watt single tetrode.

and, in consequence, the anode voltage that can be applied may be 3–5 kV. The grid wires are aligned with those of the screen to minimize screen current, and high gain and efficiency are obtained up to about 100 Mc/s for the larger types, and up to about 200 Mc/s for the smaller types with dissipation up to 100 watts [Fig. 4(*b*)].

At one time the anodes of these smaller glass valves were of carbon, and this was followed by the use of tantalum for both anodes and grids. At present the most favoured material is molybdenum, which, for the anode, is coated with a layer of zirconium to provide gettering action during operation when the electrodes are hot.

Particular forms of tetrode were developed during the war for use as pulse modulators. The requirement for these valves was the ability to hold off a high applied anode voltage without internal flashover when no anode current was passing and to pass a high current with low voltage drop when suitable short pulses were applied to the control grid. The largest glass-envelope tetrodes of this form, using oxide-coated cathodes, will pass a peak pulse current of 18 amp with a hold-off voltage of 20 kV. With a silica envelope (and also with metal-glass construction) and using thoriated-tungsten filaments, peak pulse currents of 50 amp with hold-off voltages up to 60 kV have been obtained.

(3.2) Cooled-Anode Valves

Little change took place in the design of large valves during the war, since effort was concentrated on the u.h.f. and microwave fields. Medium-power cooled-anode valves similar to those originally designed for mobile television transmitters were used in 200 Mc/s radar transmitters, and in order to give the high power required for pulse operation, thoriated-tungsten filaments were introduced into these valves. In spite of the use of direct anode voltages up to 25 kV, these dull-emitter filaments gave very good lives.

One of the post-war changes in cooled-anode valves has been the general extension of the use of thoriated-tungsten filaments,[23] which has been made possible by the achievement of better vacuum conditions. The use of pumping schedules even more rigorous than those to which the earlier pure-tungsten-filament

valves were subject was not uniformly satisfactory. A better solution was the adoption of zirconium as a getter, and with its use valves up to the largest size, with anode dissipations up to 100 kW, are now made with lives as good as or better than their bright-emitter counterparts. The change of emitter material reduces the filament power consumption by about 60%.

The usual cathode construction for cooled-anode valves takes the form of a squirrel cage of straight wires. Two attempts to shorten this structure have been successful, the first using a cage of crimped filaments and the second a mesh cage with a centre return. Indirectly-heated cathodes of thoriated tungsten have been used, but the additional heating power required makes them compare unfavourably with directly-heated filaments.

The use of dull-emitter filaments is not without its drawbacks, for the primary electron emission from the control grid of the valve at its working temperature can be much increased by the evaporation on to it, during life, of thorium from the filament. For this reason grid wires in modern valves are coated with platinum or other material which inhibits primary emission from deposited films of thorium.

On the construction side, great reductions in size have been made, leading to lower electrode inductances and operation at higher frequencies. This has involved increasing the power loading of the anodes, and to avoid large local differences of temperature, the wall thickness of copper anodes, especially in the valve types for use in industrial equipment, has therefore been increased, in some cases to 0·25 in or more. A major factor in reducing valve size has been the evolution of new forms of construction at the grid-cathode end (Fig. 5). In one a large pressed-glass base is used with outward pointing metal thimbles sealed to it; these thimbles support short stout rods which, in turn, carry the filament and grid structures. In another, which is more suitable for higher frequencies, a metal 'header' is used; this is a dished metal component to which the grid is attached, giving very low inductance, and which also carries the filament supports via glassed metal thimbles. A third form uses a series of concentric seals to support the various electrodes. In all these constructions considerable use is often made of a nickel-iron-cobalt alloy and its matching glass, by means of which thick-edge glass-to-metal seals can be made. These seals are much stronger than the former feather-edge seals using copper or copper-plated nickel-iron, although they give rise to an increase in r.f. loss.

A great deal of attention has been given to methods of anode cooling. Water is still used to a large extent in broadcasting stations, where deposition of materials on the anode surface can be avoided by the use of pure de-aerated water. Air cooling, however, is sometimes preferred, and for industrial equipment is often considered essential by the equipment designer. Changes have been made to the design of cooling fins to give better heat exchange, but this process is limited by the tendency for the cooler to become choked on the input side by foreign bodies in the air stream if the passages between fins becomes too small. Reduction of the power required for air cooling has been obtained in some cases by feeding the air in at several places along the length or circumference of the cooler. One approach to the problem of anode cooling has been by the use of latent heat of vaporization,[24] and a self-contained cooling system with small volume can be contrived in this manner.

The scale of use of continuously pumped valves has contracted since the pre-war years. In general, the added complication of the pumping equipment makes the use of these valves uneconomic compared with the sealed-off variety, which have a long life of thousands, or—in some cases—tens of thousands, of hours. In addition, the better vacuum in the sealed-off valves gives greater freedom from internal flashover.

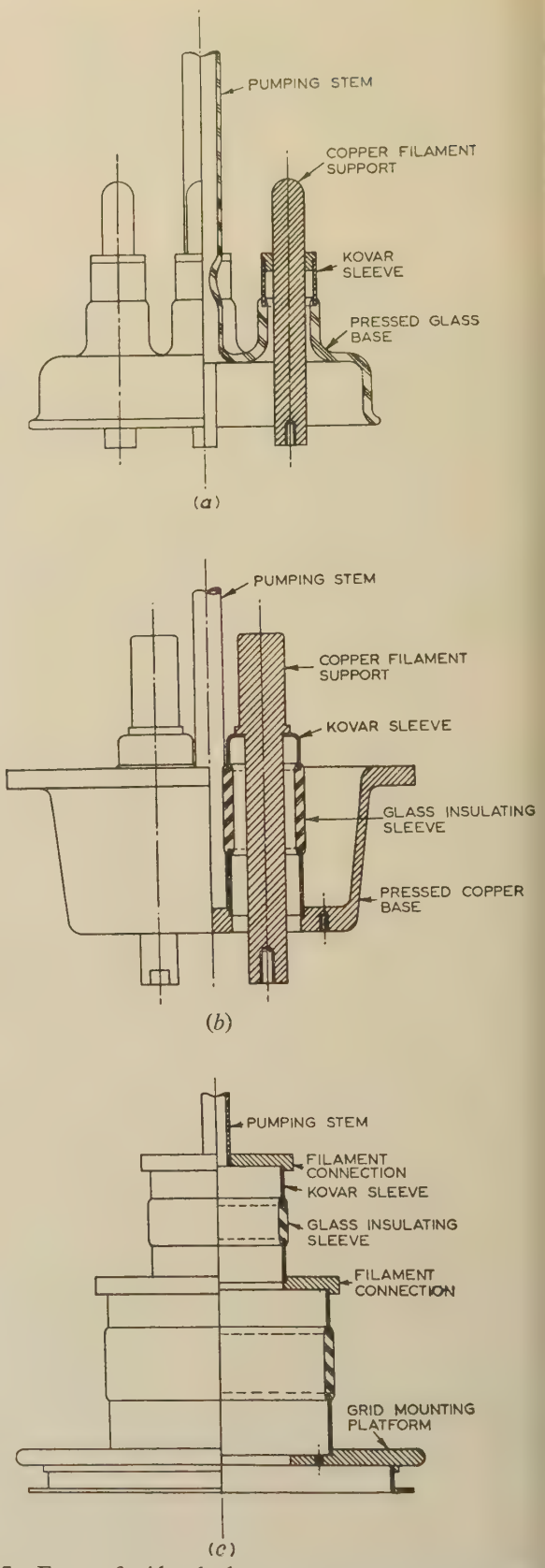

Fig. 5.—Forms of grid-cathode support structure in high-power valves.

(*a*) Pressed glass base.
(*b*) Metal header.
(*c*) Coaxial support.

(3.3) V.H.F. and U.H.F. Types

The development of u.h.f. transmitting triodes for radar purposes was fully dealt with at the Radiolocation Convention[11] in 1947. In that development, very major advances were made in the application of metal-to-glass seals to valve envelopes, both in mechanization of the processes of manufacture to reduce the skill formerly necessary, and in increasing the dimensional accuracy. The internal metal parts of the disc seals employed could then be used as precision platforms on which to mount planar or cylindrical cathodes and grids, with inter-electrode spacings of a small fraction of a millimetre. At the same time these disc seals gave the lowest possible inductance between the external circuit and the active parts of the electrodes.

This general form of construction has been continued in c.w. valves developed since the war for communication and television. Advances in techniques have made possible the use of smaller grid-cathode clearances, and therefore higher frequency of operation for a given power level. Indirectly-heated-cathode valves are now available with an anode dissipation of 2 kW which have a useful efficiency at 1 Gc/s. While lower-power valves use normal oxide-coated cathodes, in these higher-power types the cathode coating is sometimes loaded with nickel powder, which allows operation at a higher anode voltage.

For higher frequency of operation at a given power level it is necessary to make the envelope smaller. This has been aided by the development of shorter forms of seal than the older feather-edge glass-copper type. These seals are also mechanically more robust.

The most recent constructional trend is towards the use of ceramics instead of glass for the insulating parts of the envelope,[25] which gives added strength and allows a higher baking temperature to be used during processing of the valves, with consequent improvement in the degree of vacuum obtained.

An interesting development[26] during the war was a high-power c.w. tetrode giving an output of 50 kW at 600 Mc/s, with an efficiency of 60%. In this valve, known as a 'resnatron', the input and output circuits were in the form of coaxial cavities or resonators which were incorporated in the vacuum envelope. The cathode was a series of tungsten strips, the emission from each of which was individually focused between grid and screen bars lying parallel to the filament. The high emission required in these valves led to short filament life. Similar designs of cathode-grid systems, but more conservatively rated, have been used in post-war valves. In triodes, the form of construction has enabled the grid current to be so much reduced that, in a valve of 150 kW dissipation, the drive required is only 1 kW compared with 10 kW for the more normal construction. In tetrodes,[27] with thoriated-tungsten strip filaments on the outside of a concentric system, valves are made with dissipation up to 35 kW, which operate with good efficiency up to 1 Gc/s (Fig. 6).

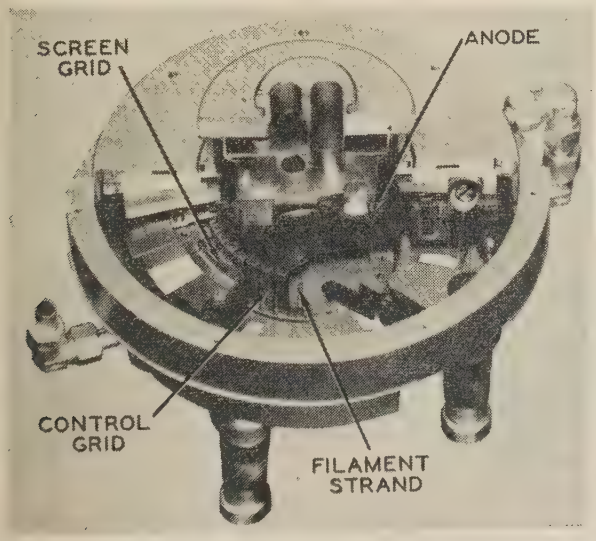

Fig. 6.—High-power u.h.f. tetrode with multi-element construction.

(4) HOT-CATHODE GASFILLED VALVES

(4.1) Diodes

The role of the gasfilled diode has been, and continues to be, power rectification, where the mean current rating is too high for vacuum diodes to be of economical size. Before the war mercury vapour was the filling used, and types were available with mean current ratings up to several amperes and peak inverse voltages up to 20 kV. Little further development took place on these during the war, and the same types are largely available to-day.

During the last few years major progress has been made in the introduction of xenon-filled hot-cathode diodes. Rare gases—usually argon or helium—had previously been used in small thyratrons, and during the war, small argon-filled rectifiers were developed for military use. These showed little advantage over vacuum rectifiers, and since their production was more difficult, they did not become popular. Xenon is chosen as the filling in the modern rectifiers in preference to the other rare gases, because it has a low ionization potential, and consequently the anode-to-cathode p.d. is low. The problem with rare-gas fillings in valves is to increase the life, which is limited by the clean-up of gas. This problem is not present when mercury vapour is used, since the excess liquid mercury acts as a reservoir. A high initial xenon filling pressure will give longer life, but, to use this, special electrode design is necessary, in order to avoid long-path breakdown under the action of the peak inverse voltage. Successful xenon-filled diodes are now available with a mean current rating up to 4·0 amp and peak inverse voltages exceeding 10 kV (Fig. 7).

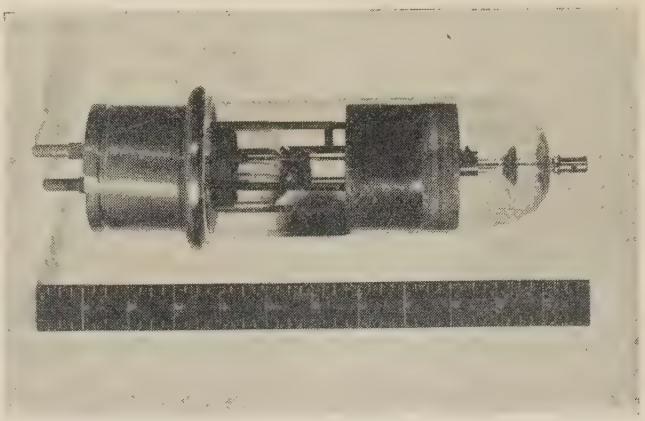

Fig. 7.—Xenon-filled diode.

(4.2) Thyratrons

In the pre-war years, mercury-vapour thyratrons were in general use in welding and other industrial equipment, while small thyratrons with argon and helium fillings were used as time-base valves in television receivers. With the advent of radar a new problem arose, namely the repetitive switching of large amounts of energy from an electrical network into a high-

frequency oscillator in pulses lasting a few microseconds. The requirements of high hold-off voltage and large current-carrying capacity were admirably met by suitably designed mercury-vapour thyratrons: valves to hold off 15 kV and pass 200 amp were produced.[28]

Mercury-vapour thyratrons are limited to a pulse repetition frequency of about 500 c/s by the rate of deionization of the vapour. The rate of rise of current through the valve, and therefore the squareness of the pulse produced, is limited by the ionization time. The ideal gas to use from these aspects is hydrogen, and hydrogen thyratrons were developed for radar purposes at the end of the war. These early valves suffered from short life, owing to the clean-up of the hydrogen in the gas discharge. This limitation has now been removed by development in the last few years of a method of hydrogen replenishment depending on the reversible absorption of hydrogen in metal hydrides, such as that of titanium. The pressure of hydrogen in equilibrium with such hydrides is a function of their temperature, so that, by mounting some hydride in contact with a heater, a constant pressure of hydrogen can be maintained in the bulb. The use of these replenishers has increased the life of hydrogen thyratrons (Fig. 8) many times, the end of life now being due to loss of cathode emission.

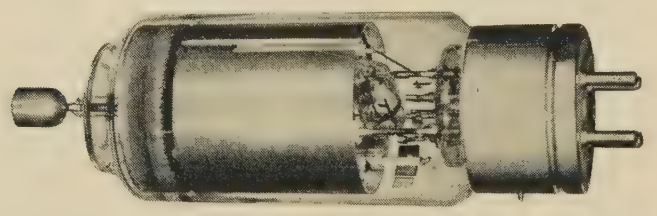

Fig. 8.—Hydrogen-filled thyratron.

(5) COLD-CATHODE VALVES

(5.1) Diodes

At the start of the period covered by the review the use of the cold-cathode gasfilled diode as a stabilizer to provide a relatively constant output voltage from a variable voltage supply was well established. The early diodes, which were small neon lamps developed for lighting purposes, had been superseded by types specifically developed for stabilization. The discharge had been enclosed, to avoid any disturbing effects of the glass envelope, and the cathode surface was suitably activated to give uniformity to the discharge. Diodes were available with running voltages between 70 and 150 volts, and many of these types are still available. The use of a number of diodes in series in the same envelope, with the anode of one diode forming the cathode of the next, had been developed much earlier in Germany, and such valves, known as Stabilovolts, were very useful in circuits where a number of separate output voltages, each stabilized, were required.

Developments have taken place during and since the war in two directions.[29, 30] The first, as in receiving valves, is the trend towards smaller devices for the same performance. Older types have been redesigned to enable them to use the miniature valve envelope, and in some cases, with reduction in maximum current rating, the subminiature envelope. The second, and probably more important, trend is the design of diodes with extremely constant voltage drop and freedom from discharge fluctuations which would give rise to noise. This result is obtained by careful attention to the cleanliness of the cathode and of the gas filling, and by limitation of the magnitude and range of the current rating. For example, with a molybdenum cathode in a suitable gas mixture, giving a mean running voltage of abou 85 volts, the variation in this voltage is less than 0·5% durin life and less than 0·1% over short periods, when the current maintained between 1·5 and 3·5 mA. This compares with 2–3% obtained with pre-war diodes.

Cold-cathode diodes are also used as switching elements, sinc conduction through the device can be started by an auxiliar voltage pulse applied in the circuit. These diodes are usuall small and wire ended, so that they can be soldered directly int circuits. Typical diodes have a maximum operating current o 1 mA and break down at 60–80 volts. Their use is not wide spread, however, since the triggered cold-cathode valve can per form the same function with greater versatility.

The possibilities of stabilization by cold-cathode devices hav been extended to higher voltages by the post-war introduction o corona stabilizers.[31] These work in the low-current-densit region of the gas discharge and are available for operatio at 300–1 500 volts and from 20 μA to 0·5 mA. A differentia resistance of about 50 kilohms is obtained over this current rang when hydrogen is used as the gas filling.

(5.2) Trigger Devices

Three-electrode cold-cathode valves, in which a voltage on a auxiliary electrode is used to trigger the discharge in the mai gap, were introduced in 1938 as devices which could be used i place of mechanical relays in telephone switching circuits. I this application they have the obvious advantage over vacuum valves that no heater power is required. A major advance in thi field has occurred since the war with the development of nev valve types and new circuits.[32] In the valve the change has bee in the cathode, where methods for activation of the surface b the alkali or alkaline-earth metals have been developed whic give reliable operation at low voltage and which also allow th valves to be gas-filled and pumped with automatic machinery These valves have the very long life necessary for their use i telephony.

The size of valves developed for use as relays varies accordin to their current-carrying capacity. The newer miniature type are used in the current range 1–5 mA, but earlier larger valve could be used up to 50 mA. In tubes developed primarily to giv high-intensity light flashes, pulse currents of tens or ever hundreds of amperes may be carried by the discharge. In thes devices there is usually some small delay in breakdown followin the application of the trigger pulse, depending on the externa circuit conditions. The delay can be reduced and the triggerin potential stabilized by using a further electrode or electrodes, t which a priming discharge is maintained.

In general, control of the anode current by the trigger electrod is not possible with cold-cathode valves, and they are used a 2-position switches. A recent development, however, indicate that continuous change-over of discharge between two positiv electrodes in a gas is possible,[32] and although this is frequenc dependent in the audio range, the device may prove to be usefu in telephony.

A much larger form of triggered cold-cathode valve—th so-called Trigatron—was developed during the war, for use a a high-power pulse modulator.[34] The valves had to withstan potentials of many kilovolts between anode and cathode an pass currents of many tens of amperes for microsecond pulse The devices were unique in that the gas pressure used was abov atmospheric, and thus the bulb had to be suitably reinforced t withstand internal pressure.

(5.3) Counter Tubes

Multiple trigger tubes[35] have been developed in the last fe years, using a common anode and a number of cathodes, i

hich the discharge between the anode and one cathode may be ade to transfer to an adjacent cathode by an input pulse applied a number of guide electrodes situated between the cathodes. e transfer of the glow from one cathode to another is visible, d the device, when made with ten electrodes, therefore forms very useful decade pulse counter. Counting speeds of 20 kc/s e possible.

(6) CONCLUSION

The valves in radio receivers and broadcasting stations have en part of our daily life for well over a generation. Com- titors to valves, in the form of semi-conductor diodes and nsistors, have appeared in the last few years, and some of the nctions previously performed by valves are likely to be carried t in the future by the new devices, which share with the cold- thode gasfilled valve the advantage that no cathode heating wer is required. However, this change is likely to extend over significant period of time, and there will still be large fields of e for the devices reviewed here, more especially where operation high power, high voltage, high frequency or high temperature concerned. The use of improved materials and improved chniques of manufacture should enable the present rate of ogress to be continued during the next decade.

(7) ACKNOWLEDGMENT

The photographs of valves have been included with the rmission of the following firms: the M.O. Valve Co. Ltd., ullard, Ltd., the International General Electric Co., and the adio Corporation of America.

(8) BIBLIOGRAPHY

(1) Benjamin, M., Cosgrove, C. W., and Warren, G. W.: 'Modern Receiving Valves: Design and Manufacture', *Journal I.E.E.*, 1937, **80**, p. 401.

(2) Bell, J., Davies, J. W., and Gossling, B. S.: 'High-Power Valves: Construction, Testing and Operation', *ibid.*, 1938, **83**, p. 176.

(3) 'Thermionic Valves, 1904–1954' (The Institution of Electrical Engineers, 1955).

(4) Thompson, B. J., and Rose, G. M.: 'Vacuum Tubes of Small Dimensions for use at Extremely High Frequencies', *Proceedings of the Institute of Radio Engineers*, 1933, **21**, p. 1707.

(5) 'A New Principle of Construction for Radio Valves', *Philips Technical Review*, 1939, **4**, p. 162.

(6) Smith, N. R., and Schooley, A. H.: 'Development and Production of the New Miniature Battery Tubes', *RCA Review*, 1940, **4**, p. 469.

(7) Acheson, M. A.: 'Proximity Fuse Tubes', *Electronics*, 1946, **19**, p. 228.

(8) Rowe, E. G., Welch, P., and Wright, W. W.: 'Thermionic Valves of Improved Quality for Government and Industrial Purposes', *Proceedings I.E.E.*, Paper No. 1740 R, December, 1954 (**102** B, p. 343).

(9) Stephenson, J. D., Powell, F. H., Price, T. W., and Walker, F. M.: 'Cathode-Ray Tubes and Valves for Television Receivers', *ibid.*, Paper No. 1334 R, April, 1952 (**99**, Part IIIA, p. 479).

(10) Atherton, A. H.: 'The Secondary-Emission Valve and Its Application', *Journal of the Television Society*, 1956, **8**, p. 23.

(11) Bell, J., Gavin, M. R., James, E. G., and Warren, G. W.: 'Triodes for Very Short Waves—Oscillators', *Journal I.E.E.*, 1946, **93**, Part IIIA, p. 833.

(12) Foster, J.: 'Grounded Grid Amplifier Valves for Very Short Waves', *ibid.*, p. 868.

(13) Rose, G. M., Power, D. W., and Harris, W. A.: 'Pencil-type U.H.F. Triodes', *RCA Review*, 1949, **10**, p. 321.

(14) James, E. G., Polgreen, G. R., and Warren, G. W.: 'Instruments Incorporating Thermionic Valves, and Their Characteristics', *Journal I.E.E.*, 1939, **85**, p. 242.

(15) McNally, J. O., Metson, G. H., Veazie, E. A., and Holmes, M. F.: 'Electron Tubes for the Transatlantic Cable System', *Proceedings I.E.E.*, Paper No. 2279 R, January, 1957 (**104** B, Supplement No. 4, p. 60).

(16) Wright, D. A.: 'A Survey of Present Knowledge of Thermionic Emitters', *Proceedings I.E.E.*, Paper No. 1404 R, November, 1952 (**100**, Part III, p. 125).

(17) Liebmann, G.: 'The Calculation of Amplifier Valve Characteristics', *Journal I.E.E.*, 1946, **93**, Part III, p. 138.

(18) Van der Ziel, A.: 'Noise' (Chapman and Hall, 1955).

(19) Beck, A. H. W.: 'Thermionic Valves' (Cambridge University Press, 1953).

(20) Alma, G., and Frakke, F.: 'A New Series of Small Radio Valves', *Philips Technical Review*, 1946, **10**, p. 289.

(21) Danzin, A., and Despois, E.: 'Le poli-optique, élément de la construction des tubes à vide', *Annales de Radio-électricité*, 1948, **3**, p. 281.

(22) Brewer, R.: 'Radio Valve Life Testing', *Proceedings I.E.E.*, Paper No. 1021 R, July, 1950 (**98**, Part III, p. 269).

(23) Ayer, R. B.: 'Use of Thoriated-Tungsten Filaments in High-Power Transmitting Tubes', *Proceedings of the Institute of Radio Engineers*, 1952, **40**, p. 591.

(24) Ashdown, G.: 'The Vapotron', *Electronic Engineering*, 1953, **25**, p. 378.

(25) Jenkins, D. E. P.: 'Ceramic to Metal Sealing', *ibid.*, 1955, **27**, p. 290.

(26) Salisbury, W. W.: 'The Resnatron', *Electronics*, 1946, **19**, p. 92.

(27) Bennett, W. P.: 'A Beam Power Tube for Ultra-High-Frequency Service', *RCA Review*, 1955, **16**, p. 321.

(28) Knight, H. de B., and Herbert, L.: 'Development of Mercury-Vapour Thyratrons for Radar Modulator Service', *Journal I.E.E.*, 1946, **93**, Part IIIA, p. 949.

(29) Benson, F. A.: 'Voltage Stabilisers', *Electronic Engineering*, 1950.

(30) Benson, F. A., and Bental, L. J.: 'Glow-Discharge Tubes', *Wireless Engineer*, 1956, **33**, p. 33.

(31) Shelton, E. E., and Wade, F.: 'Corona Discharge Tubes for Voltage Stabilisation', *Electronic Engineering*, 1953, **25**, p. 18.

(32) Peddle, E. A. R.: 'Electronic Switching', *Wireless World*, October, 1952, **58**, p. 2.

(33) Beck, A. H., Jackson, T. M., and Lytollis, J.: 'A Novel Gas-Gap Speech Switching Valve', *Electronic Engineering*, 1955, **27**, p. 7.

(34) Craggs, J. D., Haine, M. E., and Meek, J. M.: 'Development of Triggered Spark-Gaps for High-Power Modulators', *Journal I.E.E.*, 1946, **93**, Part IIIA, p. 963.

(35) Hough, G. H.: 'Development of Multi-Anode Decade Gas Tube Counters', *Proceedings I.E.E.*, Monograph No. 30 R, March, 1952 (**99**, Part IV, p. 177).

621.395.43:621.396.813

The Institution of Electrical Engineer
Paper No. 2565 I
May 195

DISTORTION IN FREQUENCY-DIVISION-MULTIPLEX F.M. SYSTEMS DUE TO AN INTERFERING CARRIER

By R. G. MEDHURST, B.Sc., Mrs. E. M. HICKS, B.Sc., and W. GROSSETT, Associate Member.

(*The paper was first received 7th September, 1957, and in revised form 2nd January, 1958.*)

SUMMARY

A theoretical investigation has been made of the distortion produced in f.m. frequency-division-multiplex trunk radio systems by the simultaneous reception of a wanted and an unwanted carrier, not necessarily identical in frequency. This form of disturbance can occur both between different systems and within a single system.

It is found that, unless there is substantial failure of the receiver limiter action, the distortion generated in a particular channel is accurately proportional to the relative level of the interfering carrier. Thus, it is possible to plot curves of distortion in the worst channel against frequency separation of wanted and unwanted carriers, from which, for a given separation, a permissible level of interfering carrier can be deduced. Curves are presented for 240- and 600-channel systems when the interfering carrier is either modulated or unmodulated. Numerical results are shown for various carrier-frequency separations that can arise under the C.C.I.R. frequency plan for systems of six r.f. channels each carrying 600 speech channels.

The distortion due to this mechanism can be divided into intelligible and unintelligible crosstalk. Reasons are given for the expectation that the former will not normally be important.

Some measurements of distortion due to an unmodulated interfering carrier, using components of a 600-channel system, show good agreement with the theory when the frequency separation is not too large. For separations of the order of 9 Mc/s, or greater, distortion levels substantially above the theoretical were noticed. The discrepancy is considered to be due to departure in the demodulator from the ideal behaviour assumed (i.e. frequency insensitivity of the limiter and adequate broadness of band of filters, etc., and of the discriminator).

LIST OF PRINCIPAL SYMBOLS

ω_c = Wanted carrier frequency, rad/sec.
ω_D = Difference between unwanted and wanted carrier frequencies, rad/sec.
μ_t = Phase modulation of wanted carrier, rad.
ν_t = Phase modulation of unwanted carrier, rad.
r = Relative amplitude of unwanted carrier (voltage ratio).
A = Amplitude of composite wave, relative volts.
μ_d = Phase error of composite wave, radians.
$\hat{\omega}_m$ = Maximum frequency of wanted modulation, rad/sec.
$\check{\omega}_m$ = Minimum frequency of wanted modulation, rad/sec.
ω_m = Representative base-band frequency, rad/sec.
ω_Δ = Total r.m.s. deviation due to wanted modulation, rad/sec.
Δ_L = Compression factor of limiter (voltage ratio).
V_0 = Response of discriminator at carrier frequency, volts.
V_Δ = Response of discriminator at $\omega_c + \omega_\Delta$, volts.
$\frac{1}{\hat{\omega}_m}F(\omega_m)$ = Sum, at frequency ω_m, of the continuous parts of the power spectra of $\cos \mu_t$ and $\sin \mu_t$.
B_0, B_1 = Coefficients of zero-order and first-order terms respectively, in expansion of discriminator amplitude characteristic.

Written contributions on papers published without being read at meetings are invited for consideration with a view to publication.
The paper is a communication from the Staff of the Research Laboratories of The General Electric Company, Limited, Wembley, England.
Mr. Grossett is at the G.E.C. Telephone Works, Coventry.

(1) INTRODUCTION

Extensive use is now being made of v.h.f., u.h.f. and s.h.f radio links for the transmission of multi-channel telephony signals. These links may be over line-of-sight paths or over greater distances utilizing tropospheric scatter.

The paper is concerned with frequency-modulated microwave links carrying multi-channel telephony signals in frequency-division multiplex. Such systems are vulnerable to disturbance due to a variety of causes, one important class of which takes the form of non-linearity, with respect to frequency, of the radio transmission path. Such non-linearities can appear in terminal and repeater circuits (amplifiers, filters, modulators and demodulators), in aerial feeders (owing to aerial mismatch and to feeder defects) and in the path between the aerials (owing to multiple transmission). The resulting disturbances give rise to distortion of the multiplex signal, which appears in each audio channel either as unintelligible noise (made up of energy taken from many other channels and combined in a non-linear way) or as intelligible crosstalk, comprising a reproduction of the content of another channel. Since, over a long radio link, the same type of distortion source can appear many times, the disturbance due to the individual sources must be kept very small.

The sources of disturbance listed above have all been investigated theoretically and experimentally, with varying degrees of success, by a number of authors. A further distortion mechanism, which has been extensively treated for single-channel f.m. transmission but does not appear to have been previously discussed for the multi-channel case,* is provided by the detection, along with the wanted modulated carrier, of another carrier which may be modulated or unmodulated. In single-channel broadcasting systems the interfering carrier will normally originate from another station; in multi-channel telephony systems it may originate either from another system (a 'crossing route') or inside the same system. The latter contingency can arise since it will often be desired to transmit simultaneously a number of r.f. carriers, each modulated with a large number of speech channels. Possible combinations of wanted and unwanted carrier within a receiver pass-band which could give rise to excessive distortion are listed in Table 1 (Section 4).

It will be valuable to have some indication of the level of interfering carrier which can be tolerated under all conditions likely to arise, both for tracing sources of observed distortion and for deciding what precautions are necessary in practice. In the paper, theoretical curves are presented showing the variation with carrier-frequency separation of the unintelligible crosstalk generated by modulated and unmodulated interfering carriers for 240- and 600-channel systems. The curves are constructed assuming multi-channel levels which have for some years been widely used as system design bases.[1,2] These levels were related

* It has been learned since acceptance of the paper that work on this subject has been carried out in the Radio Branch of the Post Office Engineering Department.

the r.m.s. power not exceeded for more than 1% of the busy hour, an allowance being made for average levels of pilots, test tones, telegraphy channels, signalling tones, etc., in addition to the speech channels. Since the work presented here was completed, there have become available C.C.I.R. recommended levels[3] substantially lower than those previously assumed. They are based on an average over the busy hour, rather than on the 1% figure; it is not clear what allowance has been made for signal components other than speech. The difference between the old and the new levels is about 3 dB for 240 channels and 2 dB for 600 channels. It is considered that adoption of the new levels for the white-noise test signal would reduce the distortion level for large carrier separations (exceeding a few megacycles per second), while for smaller separations there may be some increase in distortion.

The level of intelligible crosstalk is also evaluated. It is concluded that, in practice, the latter form of distortion should not be important.

The assumptions are made that the interfering carrier frequency lies within the pass-band of the receiving equipment and in the substantially linear portion of the discriminator characteristic, and that the limiter merely reduces the level of amplitude modulation presented to it (irrespective of the frequency range of the a.m. components) without introducing additional distortion.

It is found that, unless substantial amplitude modulation is passing through the limiter, the distortion should be proportional to the interfering carrier level up to the condition of equality of wanted and interfering carriers. Thus, from the curves provided, tolerable levels of interfering carrier can be deduced if a permitted distortion level is specified. As an example, allowable levels of interfering carrier are tabulated for various carrier frequency separations that can arise under the C.C.I.R. frequency plan for systems of six r.f. channels each carrying 600 speech channels.[4]

To bring the problem within the scope of analysis, the conventional assumption is made that the frequency-division-multiplex (f.d.m.) signal can be adequately represented by a band of random noise of suitable level, covering the spectrum range appropriate for the number of channels to be transmitted. An f.m. system without pre-emphasis is considered, so that the phase modulation, μ_t, is represented by a band of noise whose spectral power density is inversely proportional to the square of the base-band frequency.

Measurements of the disturbing effect on a 600-channel system produced by an unmodulated carrier have verified the expected linear relation between distortion level and added carrier level, and show adequate agreement with the predicted variation with added carrier frequency, for separations less than about 6–9 Mc/s (depending on the channel frequency). For larger separations, measured distortion levels are very substantially higher than those predicted. This discrepancy is presumed to be due to departures, in the demodulator, from the ideal behaviour assumed. It is hoped that further work will clarify this effect.

(2) DISTORTION DUE TO ADDED CARRIER OF SMALL AMPLITUDE

On the assumption that the added carrier frequency falls within the receiver pass-band and on the linear portion of the discriminator characteristic, expressions are now derived for unintelligible and intelligible crosstalk generated by either a modulated or an unmodulated added carrier when the relative level of the added carrier is much less than unity. The distortion must be evaluated in two parts—one which accompanies the wanted phase modulation through the receiver, and hence cannot be reduced by limiter action, and the other which arrives at the demodulator as amplitude modulation. The eventual contribution of the latter depends on the characteristics of the limiter and discriminator.

(2.1) Added Carrier Unmodulated

The sum of the wanted (modulated) and unwanted carriers can be written as

$$\cos(\omega_c t + \mu_t) + r\cos(\omega_c + \omega_D)t \quad . \quad . \quad . \quad . \quad (1)$$

$$= A\cos(\omega_c t + \mu_t + \mu_d)$$

where $$A = \sqrt{[1 + r^2 + 2r\cos(\omega_D t - \mu_t)]} \quad . \quad . \quad (2)$$

and $$\mu_d = \arctan\left[\frac{r\sin(\omega_D t - \mu_t)}{1 + r\cos(\omega_D t - \mu_t)}\right] \quad . \quad . \quad (3)$$

When $r \ll 1$, these expressions become, approximately,

$$A = 1 + r\cos(\omega_D t - \mu t) \quad . \quad . \quad . \quad (4)$$

and $$\mu_d = r\sin(\omega_D t - \mu_t) \quad . \quad . \quad . \quad . \quad . \quad (5)$$

Thus, the composite wave can be regarded as having the same carrier frequency as the wanted wave, an amplitude modulation given by expression (4) and a phase modulation consisting of the wanted modulation plus a phase error given by expression (5).

(2.1.1) Unintelligible Crosstalk: Receiver with Perfect Limiter.

If the receiver demodulator consists of a perfect limiter followed by an exactly linear discriminator, the output will be proportional to

$$\frac{d}{dt}[\mu_t + r\sin(\omega_D t - \mu_t)] \text{ from eqn. (5)},$$

$$= \frac{d}{dt}[\mu_t + r\sin\omega_D t\cos\mu_t - r\cos\omega_D t\sin\mu_t] \quad . \quad (6)$$

The first term in the bracket represents the undistorted signal; the distortion is contained in the remaining terms.

It is shown in Section 7.1 that the ratio between the non-linear distortion and the wanted signal in the same narrow band centred on ω_m can be written in the form

$$\frac{\text{Distortion}}{\text{Signal}} = \frac{r^2\omega_m^2(\hat{\omega}_m - \check{\omega}_m)}{4\hat{\omega}_m\omega_\Delta^2}[\mathrm{F}(\omega_D + \omega_m) + \mathrm{F}(|\omega_D - \omega_m|)] \text{ (power ratio)}$$

$$. \quad . \quad . \quad . \quad (7)$$

The analytical form of $\mathrm{F}(\omega_m)$ is given in Section 7.1 and its numerical evaluation is discussed in Section 7.2.

(2.1.2) Unintelligible Crosstalk: Receiver with Imperfect Limiter.

Distortion deriving from the amplitude modulation of the composite wave [given by expression (4)] will depend on the performances of the limiter and the discriminator. Suppose that the limiter reduces the level of the amplitude modulation without introducing additional distortion, and consider the balanced type of discriminator whose two sides have—ideally—exactly linear amplitude/frequency characteristics. Let these characteristics be

$$B_{0l} + \frac{B_{1l}}{\omega_c}(\omega - \omega_c)$$

and $$B_{0h} - \frac{B_{1h}}{\omega_c}(\omega - \omega_c)$$

where ω is a general frequency. Then, to first order in r, the discriminator output, obtained by subtracting the outputs of the two sides, will be (see Section 7.3)

$$\left(\frac{B_{1l}}{\omega_c}+\frac{B_{1h}}{\omega_c}\right)\left\{\frac{d}{dt}[\mu_t + r(1-\Delta_L)\sin(\omega_D t-\mu_t)]\right.$$
$$\left. + r\Delta_L\left[\frac{B_{0l}-B_{0h}}{\frac{B_{1l}}{\omega_c}+\frac{B_{1h}}{\omega_c}}+\omega_D\right]\cos(\omega_D t-\mu_t)\right\} \quad (8)$$

This may be evaluated in terms of the function $F(\omega_m)$ by expanding the sine and cosine terms and carrying out the necessary rearrangements. It is found that the ratio between the distortion and the wanted signal in the same narrow band centred on frequency ω_m is given by

$$\frac{\text{Distortion}}{\text{Signal}} = \frac{r^2\omega_m^2(\hat{\omega}_m-\check{\omega}_m)}{4\hat{\omega}_m\omega_\Delta^2}$$
$$\left\{\left[1+\frac{\Delta_L}{\omega_m}\left(\frac{B_{0l}-B_{0h}}{\frac{B_{1l}}{\omega_c}+\frac{B_{1h}}{\omega_c}}+\omega_D-\omega_m\right)\right]^2 F(|\omega_D-\omega_m|)\right.$$
$$\left. + \left[1-\frac{\Delta_L}{\omega_m}\left(\frac{B_{0l}-B_{0h}}{\frac{B_{1l}}{\omega_c}+\frac{B_{1h}}{\omega_c}}+\omega_D+\omega_m\right)\right]^2 F(\omega_D+\omega_m)\right\}$$
(power ratio)

A slightly more general form of this expression, applicable to any discriminator having a linear amplitude/frequency characteristic, is

$$\frac{\text{Distortion}}{\text{Signal}} = \frac{r^2\omega_m^2(\hat{\omega}_m-\check{\omega}_m)}{4\hat{\omega}_m\omega_\Delta^2}$$
$$\left\{\left[1+\frac{\Delta_L}{\omega_m}\left(\frac{\omega_\Delta V_0}{V_\Delta-V_0}+\omega_D-\omega_m\right)\right]^2 F(|\omega_D-\omega_m|)\right.$$
$$\left. + \left[1-\frac{\Delta_L}{\omega_m}\left(\frac{\omega_\Delta V_0}{V_\Delta-V_0}+\omega_D+\omega_m\right)\right]^2 F(\omega_D+\omega_m)\right\} \quad (9a)$$
(power ratio)

In the balanced discriminator $V_0 \ll V_\Delta$, so that, in general, except when ω_D is close to ω_m, expression (9*a*) becomes, to a close approximation,

$$\frac{r^2\omega_m^2(\hat{\omega}_m-\check{\omega}_m)}{4\hat{\omega}_m\omega_\Delta^2}\left\{\left[1+\frac{\Delta_L}{\omega_m}(\omega_D-\omega_m)\right]^2 F(|\omega_D-\omega_m|)\right.$$
$$\left. + \left[1-\frac{\Delta_L}{\omega_m}(\omega_D+\omega_m)\right]^2 F(\omega_D+\omega_m)\right\} \text{ (power ratio)} \quad (9b)$$

It is apparent that, for carrier frequency separations less than a particular base-band frequency, the distortion observed at that frequency will actually be increased as the limiter action is improved. For larger carrier-frequency separations the reverse effect is to be expected (since, in general, the first term in the curly brackets will dominate). Distortion in the lower base-band channels will generally be more susceptible to the effects of incomplete limiting than that in the upper channels. Thus it is seen from expression (9*b*) that when, for example, the carrier separation is 2·5 Mc/s (the highest base-band frequency in the 600-channel case), the limiter compression factor must be substantially better than −30 dB in order that distortion in the bottom channel shall not be appreciably affected by the amplitude modulation appearing at the discriminator input.

(2.1.3) **Intelligible Crosstalk.**

If the separation of carriers does not exceed twice the maximum modulating frequency, there may be generated a form of crosstalk by virtue of which one channel appears intelligibly in another. Thus, expansion of eqn. (5) yields a term of the form $-r\sin\mu_t\cos\omega_D t$, and if the term coherent with μ_t is extracted from $\sin\mu_t$, the relevant component of the phase modulation is found to be

$$-r\exp\left(-\frac{1}{2}\frac{\omega_\Delta^2}{\hat{\omega}_m\check{\omega}_m}\right)\mu_t\cos\omega_D t$$

A speech channel centred on ω_q will thus be audible in a channel centred on ω_m if

$$\omega_m = \omega_D + \omega_q \text{ or } |\omega_D-\omega_q| \quad . \quad . \quad . \quad (10)$$

In such a case, the power level of the unwanted channel relative to the wanted one will be

$$r^2\frac{1}{4}\exp\left(-\frac{\omega_\Delta^2}{\hat{\omega}_m\check{\omega}_m}\right)\frac{\omega_m^2}{\omega_q^2} \quad . \quad . \quad . \quad . \quad (11)$$

An additional term of similar form can appear when the limiting is incomplete.

When the number of channels is large, this form of intelligible crosstalk can reach quite high levels, and for 600 channels the second factor of expression (11), i.e.

$$\tfrac{1}{4}\exp\left(-\frac{\omega_\Delta^2}{\hat{\omega}_m\check{\omega}_m}\right)$$

contributes −40 dB to the total. The third term, ω_m^2/ω_q^2, will be greatest when ω_m and ω_q are the maximum and minimum base-band frequencies, respectively, ω_D being then required to be 2·48 or 2·60 Mc/s; its contribution will then be +32·5 dB. Thus, the relative level of the intelligible crosstalk is obtained by adding (−40 + 32·5), i.e. −7·5 dB, to the relative level of the unwanted carrier.

It is to be expected that this form of crosstalk will be troublesome only on very rare occasions. As the two carriers drift, ω_D should pass fairly rapidly through the condition given by eqn. (10): the effect will be to alter the frequency distribution of the speech in such a way as to diminish intelligibility. Furthermore, there will normally be accompanying unintelligible crosstalk which, when a large proportion of channels are occupied, will appear at a higher level than the potentially intelligible crosstalk. Thus, in the case just considered, the unintelligible crosstalk will exceed the intelligible crosstalk by about 13 dB [see Fig. 2(*a*)].

(2.2) Added Carrier Modulated

The modulation of the unwanted carrier may be taken as occupying the same range of base-band frequencies and producing the same r.m.s. deviation as that of the wanted carrier, although the two modulations will be incoherent.

The sum of the wanted and unwanted carriers is

$$\cos(\omega_c t+\mu_t) + r\cos[(\omega_c+\omega_D)t+\nu_t] = A\cos(\omega_c t+\mu_t+\mu_d) \quad . \quad (12)$$

where $$A^2 = 1 + r^2 + 2r\cos(\omega_D t+\nu_t-\mu_t) \quad . \quad . \quad (13)$$

and $$\mu_d = \arctan\left[\frac{r\sin(\omega_D t+\nu_t-\mu_t)}{1+r\cos(\omega_D t+\nu_t-\mu_t)}\right] \quad . \quad (14)$$

When $r \ll 1$ the approximations corresponding to expressions (4) and (5) are

$$A = 1 + r\cos(\omega_D t+\nu_t-\mu_t) \quad . \quad . \quad . \quad (15)$$

and $$\mu_d = r\sin(\omega_D t+\nu_t-\mu_t) \quad . \quad . \quad . \quad (16)$$

ince ν_t and μ_t are incoherent, $\nu_t - \mu_t$ may be regarded as a oise band occupying the same frequency range as either ν_t or μ_t, but having an r.m.s. amplitude increased by $\sqrt{2}$. Thus the on-linear distortion (appearing as unintelligible crosstalk) can e computed from expressions (7) and (23) if in the latter we eplace ω_Δ by $\sqrt{2}\omega_\Delta$.

When the unwanted carrier is modulated, intelligible crosstalk onsisting of transfer from one channel of the wanted base-band o another, as considered in Section 2.1.3, will be considerably iminished. It can readily be shown that the level of this form f crosstalk is now given by an expression of a form similar to xpression (11) but with the exponent doubled. There can also e transfer from a channel of the unwanted base-band to one in ne wanted base-band; this again will normally be at a negligibly ow level.

(3) VARIATION OF DISTORTION WHEN THE ADDED CARRIER AMPLITUDE IS NOT SMALL

When r cannot be taken as small compared with unity, we ust revert to the exact expressions (2) and (3). For any value f r less than 1 it will remain true that the composite wave can e regarded as having the carrier frequency of the wanted wave nd an amplitude modulation and added phase modulation iven by eqns. (2) and (3). It will be shown in this Section that or systems carrying up to 600 channels the distortion voltage ill be closely proportional to r up to $r = 1$, provided that the nwanted carrier frequency appears within the receiver i.f. ass-band and on the linear portion of the discriminator charac- eristic, and that a perfect limiter is used. When $r > 1$ it can e readily shown that the composite wave must be regarded as aving the carrier frequency of the unwanted wave and that the anted modulation is largely suppressed. At $r = 1$ there is a athematical discontinuity which has its physical counterpart n the circumstance that this condition results in 100% amplitude odulation, making perfect limiting impossible.[5] These con- iderations apply to both modulated and unmodulated added arriers, but, for simplicity, only the unmodulated case will be onsidered here.

With the assumption of a perfect limiter, the phase modulation istortion is given by eqn. (3), which can be written out as a ourier expansion of the form

$$\mu_d = r\sin(\omega_D t - \mu_t) - \frac{r^2}{2}\sin 2(\omega_D t - \mu_t) + \frac{r^3}{3}\sin 3(\omega_D t - \mu_t) + \ldots \quad . \quad (17)$$

he contribution from the first term has already been considered n Section 2.1.1. We now obtain an approximate expression or the contribution of the remaining terms.

It has first to be noticed that distortion arising from successive erms of eqn. (17) is substantially incoherent with that arising rom previous terms, and hence the contributions must be added ower-wise. This can be seen if we attempt to extract, for xample, the part of $\sin(n\mu_t)$ which is coherent with in $[(n-1)\mu_t]$: we find that

$$\sin(n\mu_t) = \sin[(n-1)\mu_t] \times (\text{constant term from } \cos\mu_t) + \text{terms incoherent with } \sin[(n-1)\mu_t]$$

t can be shown (Section 7.1) that the constant term from $\cos\mu_t$ s $\exp(-\omega_\Delta^2/\hat{\omega}_m\check{\omega}_m)$, which is about 0·000 4 for the 600-channel ase, and decreases as the number of channels decreases.

he contributions of terms of eqn. (17) after the first can now e estimated as follows. When the r.m.s. amplitude of $n\mu_t$ is ufficiently large, the power spectra of $\cos n\mu t$ and $\sin n\mu_t$ will both approach a Gaussian form, with maxima at zero frequency. For systems carrying up to 600 channels the Gaussian distribution will be a good approximation for $n \geqslant 2$ (but not for $n = 1$). Making use of this, we find that the contribution to the distortion/signal ratio at base-band frequency, ω_m, due to the terms of eqn. (17) after the first is approximately

$$\frac{\omega_m^2(\hat{\omega}_m - \check{\omega}_m)}{4\omega_\Delta^2}\sum_{n=2}^{\infty}\frac{r^{2n}}{n^2}[A_n(n\omega_D + \omega_m) + A_n(|n\omega_D - \omega_m|)] \quad \text{(power ratio)} \quad (18)$$

where $$A_n(\omega) = \sqrt{\frac{2}{\pi}}\frac{1}{n\omega_\Delta}\exp\left(-\frac{\omega^2}{2n^2\omega_\Delta^2}\right)$$

When the terms in the square brackets are added, eqn. (18) can be written in the form

$$\frac{\omega_m^2(\hat{\omega}_m - \check{\omega}_m)}{\sqrt{(2\pi)}\omega_\Delta^3}\sum_{n=2}^{\infty}\frac{r^{2n}}{n^3}\exp\left(-\frac{\omega_D^2 + \omega_m^2/n^2}{2\omega_\Delta^2}\right)\cosh\frac{\omega_D\omega_m}{n\omega_\Delta^2} \quad (19)$$

This must be compared numerically with the distortion contribution of the first term of eqn. (17), given by expression (7), whose numerical evaluation is considered in the next Section. It is found that, for systems carrying up to 600 channels, distortion levels computed from expression (19) are always substantially less than those computed from expression (7). Thus with the receiver conditions assumed, the distortion level will vary linearly with the added carrier level up to the condition of equal added carrier.

Imperfect limiting will destroy the linearity between the distortion and the added carrier level as the latter becomes large. This will be true even if the limiter compresses the amplitude modulation of the composite wave without introducing additional distortion. There are two reasons for this: one is that the output from a discriminator and detector supplied with a signal carrying simultaneous amplitude and frequency modulation is not a simple linear sum of the two modulations (except as an approximation when the modulation levels are small); the other is that the expansion of the amplitude modulation [given by expression (2)] in harmonics of $\omega_D - \mu_t$, analogous to the expansion of the phase modulation shown as expression (17), has a fundamental coefficient which becomes non-linear in r when r is not very small. In fact, the first few terms are

$$\frac{2}{\pi}(1+r)\mathrm{E}\left(\frac{2\sqrt{r}}{1+r}\right) + \frac{4}{3\pi}\frac{1}{r}[(1+r^2)\mathrm{E}(r) - (1-r^2)\mathrm{K}(r)]\cos(\omega_D t - \mu_t) - \frac{4}{15\pi}\frac{1}{r^2}[2(1-r^2+r^4)\mathrm{E}(r) - (1-r^2)(2-r^2)\mathrm{K}(r)]\cos 2(\omega_D t - \mu_t) \quad . \quad . \quad . \quad . \quad (20)$$

where E and K are complete elliptic integrals.

(4) NUMERICAL RESULTS FOR 240- AND 600-CHANNEL SYSTEMS

The following parameters were assumed:

Number of channels	Limits of base-band	Multi-channel power level*	R.M.S. deviation per channel	Total r.m.s. deviation
	Mc/s	dBm0	kc/s	Mc/s
240	0·06–1·052	12·2	200	0·812
600	0·06–2·540	14·8	200	1·100

* Relative to one milliwatt at a point of zero relative level.

The total r.m.s. deviation is conventionally taken as the deviation due to speech channels, test tones, etc., which is exceeded

Table 1

MINIMUM FREQUENCY SEPARATIONS AND ALLOWABLE LEVELS OF INTERFERING CARRIERS WHICH CAN APPEAR UNDER THE C.C.I.R. FREQUENCY PLAN FOR SYSTEMS OF SIX R.F. CHANNELS EACH CARRYING 600 SPEECH CHANNELS (DISTORTION/SIGNAL IN TOP SPEECH CHANNEL TAKEN AS −65 dB†)

Item No.	Mechanism of interfering-carrier generation	Condition of interfering carrier	Minimum frequency separation	Allowable level of interfering carrier relative to wanted carrier [from Figs. 2(*a*) and 2(*b*)]
			Mc/s	dB
1	Transmit channel on the same frequency as a receive channel or crosstalk at intermediate frequency	Modulated	0	−66
2	Harmonics of shift frequency close to a receiver local-oscillator frequency	Modulated‡	7	
3	Harmonics of shift frequency close to transmit or receive channels ..	Unmodulated	4·5	−61
4	Harmonics of shift frequency close to image channel of a receiver ..	Unmodulated	10·5	−17
5	Transmit channel close to the image channel of a receiver	Modulated	(14)	−5§
6	Image signal from a transmitter close to a receive channel	Modulated	>100	
7	Receiver local oscillator frequency close to another receive channel ..	Unmodulated	12	−5§
8	Receiver local oscillator frequency close to a transmit channel	Unmodulated	(2)	−69
9	Transmit channel close to a receiver local-oscillator frequency	Modulated*	(2)	−68
10	Transmitter local-oscillator frequency close to a receive channel	Unmodulated	>100	
11	Transmitter local-oscillator frequency close to another transmit channel	Unmodulated	12	−5§
12	Products arising from intermodulation between transmit channels close to a receive channel	Modulated*	10	−33

Figures in parentheses refer to cases where cross-polarization will reduce the interference.
* The frequency deviation of the modulation on the resultant interfering carrier may be a multiple of that on the wanted carrier, in which case the permitted level shown would be modified.
† This corresponds to an absolute distortion level of −78 dBmo in a flat unweighted 4 kc/s channel.
‡ The modulation will here be coherent with that of the wanted carrier (see Section 4).
§ For these separations, measurements so far made suggest more stringent requirements on the interfering level than appear in the Table (see Section 5). This is considered to be due to departures in the demodulator from the assumed ideal behaviour.

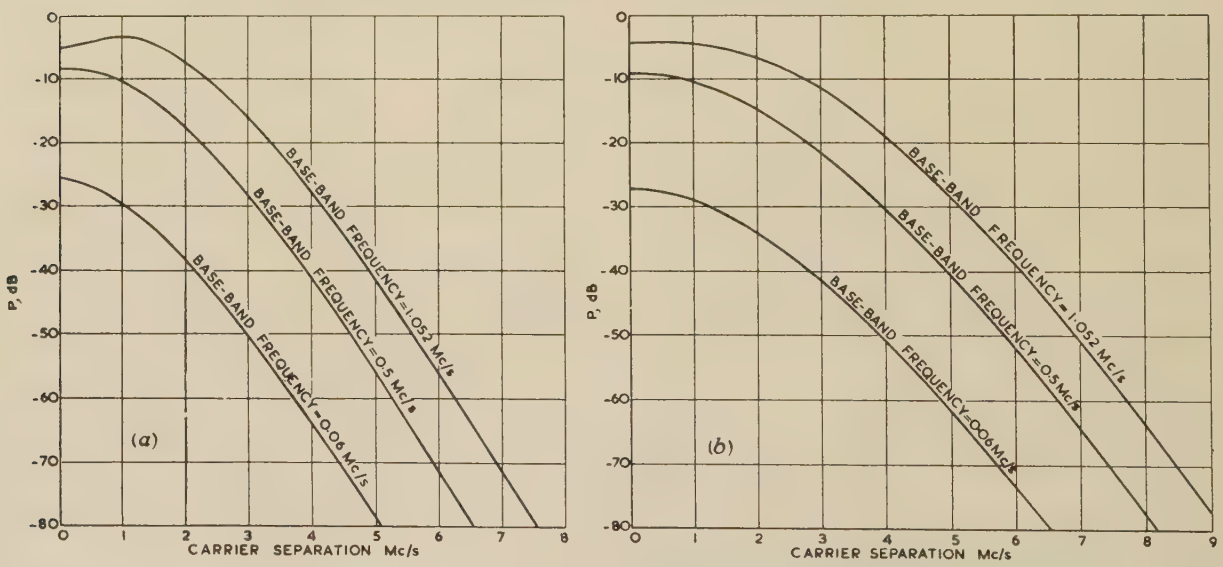

Fig. 1.—Distortion due to an interfering carrier in 240-channel systems with perfect limiting.
The distortion/signal ratio is $(P + 20 \log_{10} r)$ dB.
(*a*) Unmodulated carrier.
(*b*) Modulated carrier.

for not more than 1% of the busy hour. This system parameter can only be estimated, since it depends on such uncertain factors as the statistical properties of large numbers of simultaneous conversations.*

Figs. 1 and 2 show the variation of distortion with carrier separation for three base-band frequencies with both modulated and unmodulated interfering carriers for 240- and 600-channel systems. It is assumed that the limiting is sufficient to ensure that the distortion is adequately represented by expression (7). Under these circumstances the distortion will be linearly proportional to the added carrier level, up to equal added carrier. In all cases the distortion shown consists of unintelligible crosstalk. As shown in Section 2.1.3, intelligible crosstalk can also appear, but this should not normally be troublesome.

The application of the present results to the C.C.I.R. frequency plan[4] for systems comprising six r.f. channels each carrying 600 speech channels is indicated in Table 1, which shows the minimum frequency separations for interference which could

* The most recent C.C.I.R. recommendation[3] suggests that the white-noise-band test signal should produce substantially lower deviations, corresponding to an average value of speech power over the busy hour, rather than to a 1% value. Specifically, the r.m.s. deviations for 240 and 600 channels would be 0·551 and 0·871 Mc/s respectively (corresponding to 8·8 and 12·8 dBm0 multi-channel levels). Unfortunately, this recommendation became available only after the completion of the present work. The use of the new deviations would not be expected greatly to change the interfering effect of an r.f. carrier at small carrier separations (up to 1 Mc/s, say), but for large separations (exceeding a few megacycles per second), there should be an improvement. A more precise statement of the situation would require further detailed calculation, particularly in the 600-channel case, where the system is being pushed further into the low-deviation region.[6] The distortion levels given in the paper are still of interest, since they give an indication of what is to be expected under 'worst' conditions.

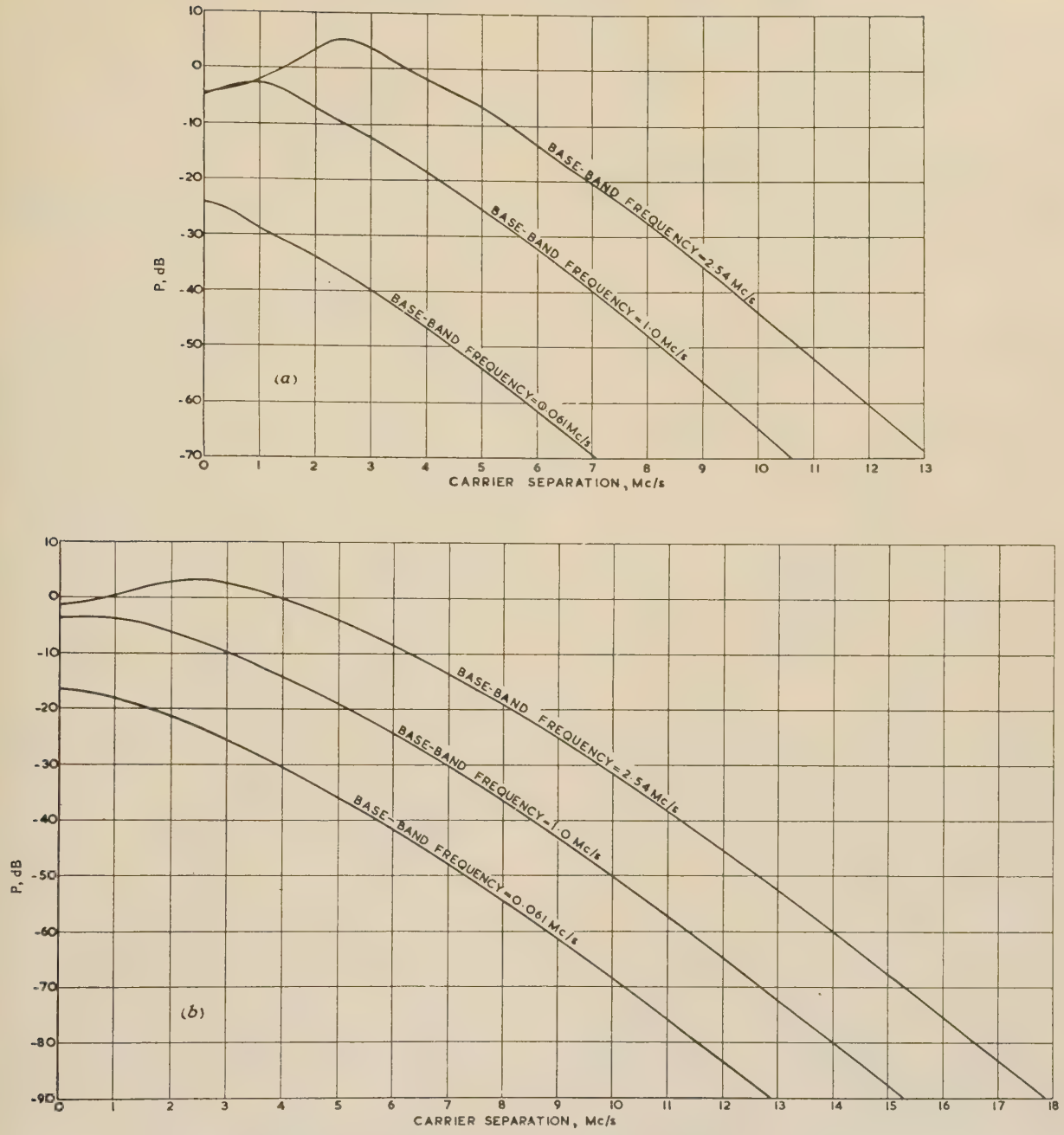

Fig. 2.—Distortion due to an interfering carrier in 600-channel systems with perfect limiting.
The distortion/signal ratio is $(P + 20 \log_{10} r)$ dB.
(*a*) Unmodulated carrier.
(*b*) Modulated carrier.

arise in various ways, together with the levels of interfering carrier which could be tolerated. These levels have been read off from Figs. 2(*a*) and 2(*b*), on the assumption that, if one type of interference predominates, a distortion/signal level of −65 dB in the top speech channel could be tolerated at each repeater. Of course, if more than one interference mechanism contributes significantly, the allowable level of each interfering carrier must be correspondingly reduced. No permitted levels are shown for items 6 and 10, since the frequencies of the interfering carriers will fall outside both the i.f. pass-band and the linear portion of the discriminator characteristic. The high tolerable interference levels shown for items 5, 7 and 11 could not be accepted in practice, owing to the stringent limiter requirements which would be imposed. The interference listed as item 2 will appear as a carrier modulated with a coherent signal (unlike the other modulated cases shown in the Table, where the modulation is incoherent with that of the wanted carrier). It can be seen from expressions (13) and (14) that, in such a case, no crosstalk will be generated if the modulations have no relative delay. The situation will, in fact, be closely similar to that of echo distortion. In practice, the two modulated carriers will undergo different delays when traversing the i.f. stage, so that some distortion will appear. The resultant distortion level, however, will normally be very small in comparison with that due to similar interfering carriers unmodulated or modulated with incoherent signals.

In Table 1 only the main route has been considered. A

crossing route would introduce further possible mechanisms for introducing interfering carriers. Since interference from this cause would be likely to occur less often in a system than interference generated solely in the main route, the allowable distortion/signal ratio could be taken at a higher level.

(5) RESULTS OF MEASUREMENT

A block diagram of the test equipment is shown in Fig. 3. The frequency of the wanted carrier was 70 Mc/s, the C.C.I.R.

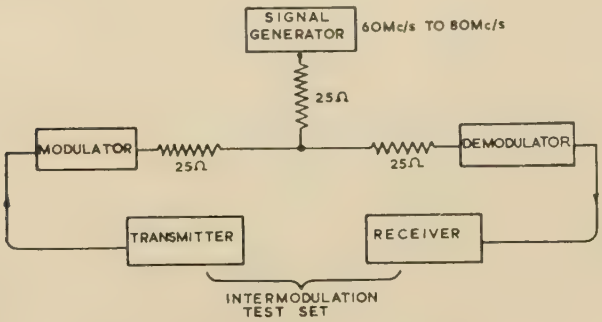

Fig. 3.—Block diagram of test equipment.

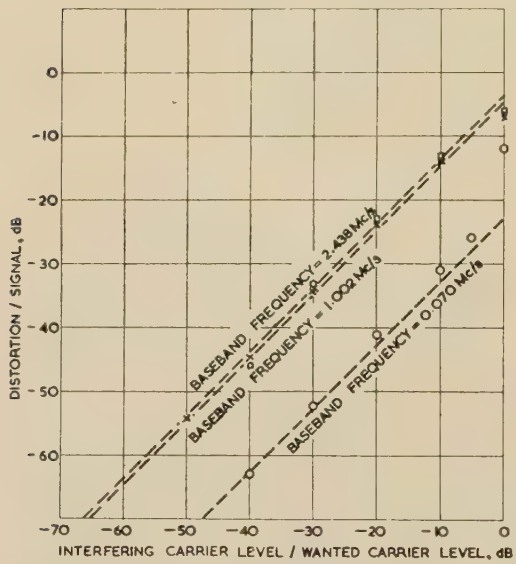

Fig. 4.—Measured variation of distortion level with interfering carrier level for a 600-channel system.

Zero-carrier frequency separation; interfering carrier unmodulated.

recommended intermediate frequency; the modulating signal was a flat noise band simulating a 600-channel f.d.m. transmission, and the interfering carrier (unmodulated) originated from a signal generator whose output frequency was varied between 58 and 82 Mc/s. Two sets of measurements were made, one with varying interfering carrier level and fixed frequency separation, and the other with varying frequency separation at fixed level.

In Fig. 4 the expected linearity of distortion with added carrier level is seen to hold up to levels of −5 dB or higher. When the added carrier level approaches that of the wanted carrier there is some departure from linearity, particularly at the bottom end of the base-band, presumably due to partial failure of the limiters.

In Fig. 5, distortion is plotted against carrier-frequency separation. The added carrier level is at each point arranged to be on the linear portion of curves such as those in Fig. 4. Satisfactory agreement with the theoretical figures is obtained

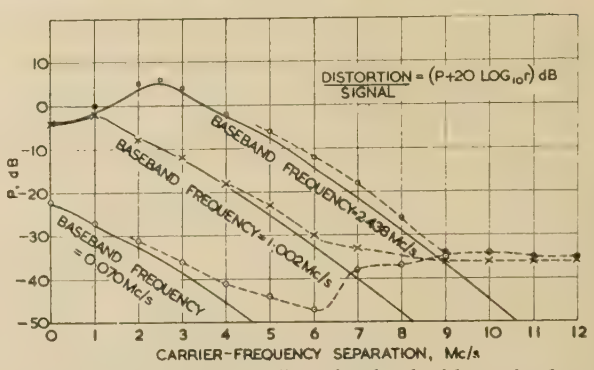

Fig. 5.—Measured variation of distortion level with carrier-frequency separation for a 600-channel system.

Unmodulated interfering carrier level substantially less than wanted carrier level.

when the frequency separation is not too large. For separations over about 9 Mc/s, distortion components (well above basic noise) are observed which are far in excess of those predictable from the mechanism considered in the paper. These measurements are considered to indicate that there is departure of the demodulator behaviour from the idealizations assumed. Frequency sensitivity of the limiter, for example, could substantially increase the intermodulation distortion level. It is hoped that further work will reveal the detailed mechanism of the effect observed.

(6) REFERENCES

(1) Smith, J. R. W., and Slow, J. L.: 'Energy Distribution in a Wave Frequency Modulated by a Multichannel Telephone Signal', *A.T.E. Journal*, 1956, **12**, p. 182.

(2) Bray, W. J.: 'Basic Factors in the Design of Frequency- and Phase-Modulation Radio-Relay Systems for Multi-Channel Telephony', Post Office Engineering Department, Radio Report No. 2100, 1952.

(3) C.C.I.R.: Documents of the VIIIth Plenary Assembly, Warsaw, 1956, volume 1 (International Telecommunications Union, Geneva, 1957), p. 204, Recommendation No. 197.

(4) *Ibid.*, p. 201, Recommendation No. 194.

(5) Lewin, L., Medhurst, R. G., and Small, G. F.: Discussion on 'An Extended Analysis of Echo Distortion in the F.M. Transmission of Frequency Division Multiplex', *Proceedings I.E.E.*, 1956, **103** B, p. 447.

(6) Medhurst, R. G.: 'R.F. Bandwidth of Frequency-Division-Multiplex Systems using Frequency Modulation', *Proceedings of the Institute of Radio Engineers*, 1956, **44**, p. 189.

(7) Lawson, J. L., and Uhlenbeck, G. E.: 'Threshold Signals' (McGraw-Hill, 1950), p. 41.

(8) Rice, S. O.: 'Mathematical Analysis of Random Noise', *Bell System Technical Journal*, 1944, **23**, p. 282, and 1945, **24**, p. 46.

(9) Bennett, W. R., Curtis, H. E., and Rice, S. O.: 'Interchannel Interference in F.M. and P.M. Systems', *ibid.*, 1955, **34**, p. 601, Appendix 1.

(10) Titchmarsh, E. C.: 'Introduction to the Theory of Fourier Integrals' (Oxford University Press, 1937), p. 60.

(7) APPENDICES

(7.1) Derivation of Expression (7) and of the Analytical Form of $F(\omega_m)$

We must extract from expression (6) the distortion power at ω_m. Suppose that

$$\cos \mu_t = \sum_{\omega_q} C(\omega_q) \cos (\omega_q t + \phi_q)$$

and $$\sin \mu_t = \sum_{\omega_q} S(\omega_q) \cos (\omega_q t + \psi_q)$$

Then, since

$$\sin \omega_D t \cos \mu_t - \cos \omega_D t \sin \mu_t = \Sigma \tfrac{1}{2} C(\omega_q) \{\sin [(\omega_D - \omega_q)t - \phi_q] + \sin [(\omega_D + \omega_q)t + \phi_q\} + \Sigma \tfrac{1}{2} S(\omega_q) \{\sin [(\omega_D - \omega_q)t - \psi_q] + \sin [(\omega_D + \omega_q)t + \psi_q]\} \quad . \quad . \quad . \quad . \quad . \quad . \quad . \quad . \quad (21)$$

Thus, making suitable choice of ω_q, the power in a distortion tone of frequency ω_m becomes

$$\{\tfrac{1}{4}[C(\omega_D + \omega_m)]^2 + \tfrac{1}{4}[S(\omega_D + \omega_m)]^2 + \tfrac{1}{4}[C(|\omega_D - \omega_m|)]^2 + \tfrac{1}{4}[S(|\omega_D - \omega_m|)]^2\} \quad (22)$$

Since distortion tones of the same frequency arising from cos μ_t and sin μ_t will be mutually incoherent and hence must be added on a power basis.

Expression (22) may be written in the form

$$\frac{1}{4\hat{\omega}_m}[F(\omega_D + \omega_m) + F(|\omega_D - \omega_m|)]$$

where $\frac{1}{\hat{\omega}_m} F(\omega_m)$ represents the sum of the continuous portions of the power spectra of cos μ_t and sin μ_t at angular frequency ω_m. It is shown in this Section that the total combined power spectra of cos μ_t and sin μ_t is

$$\frac{1}{\tau}\varepsilon^{-\psi_0}\delta(f) + \frac{2}{\pi}\frac{\varepsilon^{-\psi_0}}{\hat{\omega}_m}\int_0^\infty [\varepsilon^{\psi_u(y)} - 1] \cos \left(\frac{\omega_m}{\hat{\omega}_m} y\right) dy - \left[\frac{\omega_\Delta^2}{\omega_m^2(\hat{\omega}_m - \check{\omega}_m)}\varepsilon^{-\psi_0} \text{ (when } \check{\omega}_m \leqslant \omega_m \leqslant \hat{\omega}_m) \text{ or 0 (when } \omega_m < \check{\omega}_m \text{ or } > \hat{\omega}_m)\right] \quad (23)$$

where

$$\psi_u(y) = \frac{\omega_\Delta^2}{\hat{\omega}_m - \check{\omega}_m}\left\{\frac{1}{\check{\omega}_m}\cos\left(\frac{\check{\omega}_m}{\hat{\omega}_m} y\right) - \frac{1}{\hat{\omega}_m}\cos y + \frac{y}{\hat{\omega}_m}\left[\text{Si}\left(\frac{\check{\omega}_m}{\hat{\omega}_m} y\right) - \text{Si}(y)\right]\right\}$$

$$\psi_0 = \frac{\omega_\Delta^2}{\check{\omega}_m \hat{\omega}_m}$$

$$\text{Si}(x) = \int_0^x \frac{\sin z}{z} dz$$

and $\delta(f)$ is the Dirac delta function.[7]

The first term is a d.c. one which, when μ_t is a phase modulation, is proportional to the power in the carrier. The third term is that portion of sin μ_t which is coherent with μ_t: after this is subtracted, the residue consists of unintelligible crosstalk. Thus, $\frac{1}{\hat{\omega}_m} F(\omega_m)$ is given by the last two terms of expression (23).

As a first step towards deriving expression (23), we remember that μ_t is a phase modulation corresponding to a frequency modulation consisting of a band of white noise. Thus, μ_t can be written in the form

$$\mu_t = \sum_{\omega_m = \check{\omega}_m}^{\hat{\omega}_m} \frac{a}{\omega_m} \sin (\omega_m t + \phi_m)$$

where ω_m is supposed to increase in unit steps and ϕ_m is a random phase angle. The spectral density of μ_t is evidently

$$G(\omega_m) = \frac{\omega_\Delta^2}{(\hat{\omega}_m - \check{\omega}_m)\omega_m^2} \text{ power/(radian/sec)} \quad . \quad (24)$$

in the range $\check{\omega}_m - \hat{\omega}_m$, and zero outside it.

The auto-correlation function, $\psi_u(\tau)$, of μ_t is obtained from the relation (e.g. Reference 8)

$$\psi_u(\tau) = \int_0^\infty G(\omega_m) \cos (\omega_m \tau) d\omega_m \quad . \quad . \quad . \quad (25)$$

With some rearrangement we find

$$\psi_u(\tau) = \frac{\omega_\Delta^2}{\hat{\omega}_m - \check{\omega}_m}\left\{\frac{1}{\check{\omega}_m}\cos (\check{\omega}_m \tau) - \frac{1}{\hat{\omega}_m}\cos (\hat{\omega}_m \tau) + \tau [\text{Si} (\check{\omega}_m \tau) - \text{Si} (\hat{\omega}_m \tau)]\right. \quad (26)$$

where Si is the sine integral. At $\tau = 0$,

$$\psi_0 = \frac{\omega_\Delta^2}{\hat{\omega}_m \check{\omega}_m} \quad . \quad . \quad . \quad . \quad . \quad (27)$$

In order to find the sum of the power spectra of cos μ_t and sin μ_t, we write down expressions for the auto-correlation functions of cos μ_t and sin μ_t and apply the transformation inverse to eqn. (25), i.e.

$$G(\omega_m) = \frac{2}{\pi}\int_0^\infty \psi_u(\tau) \cos (\omega_m \tau) d\tau \quad . \quad . \quad . \quad (28)$$

The auto-correlation functions follow from the probability distribution of μ_t which, since μ_t is a normal random process, may be stated in the form (see Reference 8, expression 3.2–4) that μ_t will lie between x and $x + dx$ and $\mu_{t+\tau}$ between x_τ and $x_\tau + dx_\tau$ for a fraction of the time t given by

$$\frac{1}{2\pi\psi_0\sqrt{(1 - R^2)}} \exp\left[-\frac{x^2 + x_\tau^2 - 2Rxx_\tau)}{2\psi_0(1 - R^2)}\right] dx dx_\tau \quad (29)$$

where $R = \psi_u(\tau)/\psi_0$, and $\psi_u(\tau)$ and ψ_0 are given by eqns. (26) and (27). Then, by definition, the auto-correlation function of cos μ_t, for example, is given by

$$\overline{\cos \mu_t \cos \mu_{t+\tau}} = \frac{1}{2\pi\psi_0\sqrt{(1 - R^2)}} \int_{-\infty}^{\infty}\int_{-\infty}^{\infty} \cos x \cos x_\tau \exp\left[-\frac{x^2 + x_\tau^2 - 2Rxx_\tau}{2\psi_0(1 - R^2)}\right] dx dx_\tau$$

This integrates to give

$$\overline{\cos \mu_t \cos \mu_{t+\tau}} = \varepsilon^{-\psi_0} \cosh [\psi_u(\tau)]$$

Then, from expression (28), we find the power spectrum of cos μ_t in the form

$$G(\omega_m) = \frac{1}{\pi}\varepsilon^{-\psi_0}\delta(f) + \frac{2}{\pi}\varepsilon^{-\psi_0}\int_0^\infty \{\cosh [\psi_u(\tau)] - 1\} \cos (\omega_m \tau) d\tau \quad \text{(power/radian/sec)} \quad (30)$$

The 1 in the integral must be inserted to obtain convergence: to compensate, it is necessary to add the term containing the Dirac delta function, which gives the constant part of cos μ_t.

In a similar way, the power spectrum of sin μ_t is found to be

$$\frac{2}{\pi}\varepsilon^{-\psi_0}\int_0^\infty \sinh [\psi_u(\tau)] \cos (\omega_m \tau) d\tau$$

This includes a term coherent with $\psi_u(\tau)$, which contains any intelligible crosstalk. We remove this by subtracting from the expression sinh $[\psi_u(\tau)]$, under the integral sign, a term of the form[9]

$$\psi_u(\tau) \operatorname*{Lt}_{x\to 0} \frac{d}{dx} \sinh(x)$$

i.e. $\psi_u(\tau)$. Thus the required portion of the power spectrum of sin μ_t becomes

$$\frac{2}{\pi}\varepsilon^{-\psi_0}\int_0^\infty \left\{\sinh\left[\psi_u(\tau)\right] - \psi_u(\tau)\right\}\cos(\omega_m\tau)d\tau \quad . \quad (31)$$

Adding expressions (30) and (31), applying the transformation given as expression (28) to the latter part of (31), and writing $y = \hat{\omega}_m\tau$, we arrive finally at expression (23).

(7.2) Technique of Numerical Evaluation of $F(\omega_m)$

From expression (23), $F(\omega_m)$ is given by

$$\frac{2}{\pi}\int_0^\infty (\varepsilon^{\psi_u-\psi_0} - \varepsilon^{-\psi_0})\cos(\beta y)dy - \left[\frac{\omega_\Delta^2\hat{\omega}_m}{\omega_m^2(\hat{\omega}_m - \check{\omega}_m)}\varepsilon^{-\psi_0}\right.$$
$$\left.\text{(when } \check{\omega}_m \leqslant \omega_m \leqslant \hat{\omega}_m\text{) or 0 (when } \omega_m < \check{\omega}_m \text{ or } > \hat{\omega}_m)\right]$$

where $\beta = \omega_m/\hat{\omega}_m$, and ψ_u and ψ_0 are defined in Section 7.1. The second term is immediately computable, but the integral is unexpectedly difficult to deal with numerically.

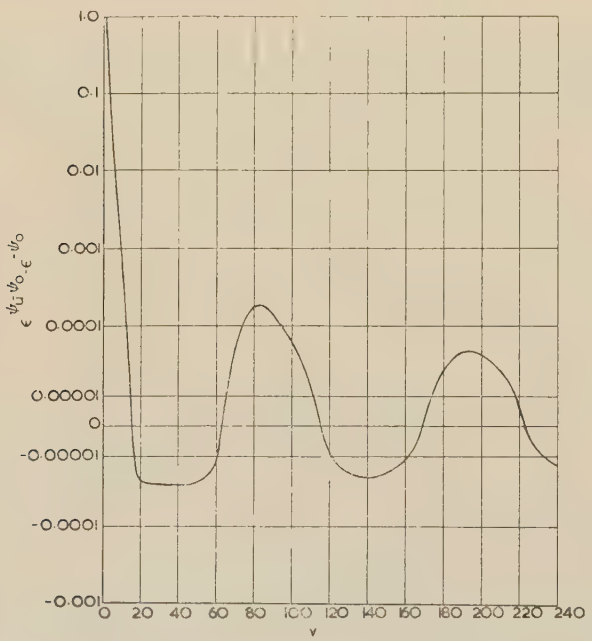

Fig. 6.—Variation of $\varepsilon^{\psi_u-\psi_0} - \varepsilon^{-\psi_0}$ with y, with parameters corresponding to a 240-channel system.

The expression $(\varepsilon^{\psi_u-\psi_0} - \varepsilon^{-\psi_0})$ is shown in Fig. 6 plotted against y, for 240 channels. The function exhibits abrupt changes of slope at somewhat irregular intervals, this behaviour resulting from the interaction of terms of widely differing periodicities.

When the numerical evaluation is completed it will be found that the integral decreases rapidly with increasing β. The largest value of β that must be considered will be determined by the distortion levels in which we are interested. For 240- and 600-channel systems values of β up to 6 and 4 respectively will be of interest, and for these, the integral will be found to be of order 10^{-7}. At $\beta = 0$ the integral in both cases is of order unity.

For small values of β the integral can be computed straightforwardly by use of one of the numerical integration formulae, such as Simpson's rule. For the larger values such a computation would be quite prohibitive unless one of the faster digital computers were available. Thus for $\beta = 6$, in the 240-channel case, over the range shown in Fig. 6 there would be about 460 half-cycles of the term cos (βy). In view of the very small expected value of the integral for this β value, it is to be expected that there will be not only substantial cancellation between portions of the integral taken over successive half-cycles of cos (βy), but also considerable further cancellation between the resultant contributions of the various pairs of half-cycles. Consequently, the contribution of each half-cycle must be evaluated with high accuracy, so that a considerable number of points per half-cycle must be taken. If, for example, 10 were found to be adequate, something of the order of 5000 values of $(\varepsilon^{\psi_u-\psi_0} - \varepsilon^{-\psi_0})$ would appear to be a likely requirement for this one β value: the complicated nature of the function ψ_u seems to rule out such a project.

Under such circumstances one would normally seek an asymptotic expansion in powers of $1/\beta$, valid for large values of β. Such an expansion for cosine transforms of this kind can often be derived by repeated integration by parts. This procedure breaks down in the present case, since the function $\varepsilon^{\psi_u-\psi_0}$ has the peculiarity that all its odd derivatives with respect to y vanish at $y = 0$. An expansion in inverse powers of β derived by an alternative procedure was found to converge too slowly to be of practical value. It is, in fact, somewhat unlikely that this integral can be represented by a small number of terms of an expansion except possibly when $\omega_\Delta/\hat{\omega}_m$ is fairly large, since as $\omega_\Delta/\hat{\omega}_m$ decreases the integral must—being related to the r.f. spectrum of a wave frequency-modulated by white noise of limited bandwidth—show abrupt variations as β changes.[6]

The present treatment is based on Poisson's formula,[10] which may be written in the form

$$\sum_{n=1}^{\infty}\int_0^\infty f(y)\cos(n\beta y)dy = \frac{\pi}{\beta}\left[\tfrac{1}{2}f(0) + \sum_{n=1}^{\infty} f\left(\frac{2\pi n}{\beta}\right)\right] - \tfrac{1}{2}\int_0^\infty f(y)dy$$
$$\ldots \quad (32)$$

where f(y) is a decreasing function of y such that all the integrals converge.

The left-hand side of eqn. (32) is not simply the integral required, but the sum of an infinite number of such integrals. However, since it is to be anticipated from the physics of the problem that in the present case $\int_0^\infty f(y)\cos(\beta y)dy$ decreases rapidly with β, it is evident that, when β is not too small, the first term of the left-hand side will largely dominate. If necessary, we can correct for the contributions of later terms in an obvious way.

Thus, the problem is reduced to the evaluation of the right-hand side of eqn. (32). There is still an integral to be dealt with, but we shall show that excessively high accuracy is not required in its evaluation, and also that, above a certain value of y, numerical quadrature can be replaced by an approximate process.

First, we consider the error involved in evaluating $\int_0^\infty f(y)dy$ by Simpson's rule using ordinates spaced at interval α, i.e. we shall find a measure of δ when eqn. (32) is written in the form

$$\delta(A) = \sum_{n=1}^{\infty} \int_0^{\infty} f(y) \cos(n\beta y) dy$$

$$= \frac{\pi}{\beta}\left[\tfrac{1}{2}f(0) + \sum_{n=1}^{\infty} f\left(\frac{2\pi n}{\beta}\right)\right] - \frac{1}{2}\left\{\frac{\alpha}{3}[f(0) + 4f(\alpha) + 2f(2\alpha) + 4f(3\alpha) + \ldots]\right\} + \delta$$

where $A = 2\pi/\beta$.

Since α is necessarily small, we see from eqn. (32) that a good approximation to $S(\alpha)$ is given by

$$S(\alpha) \simeq \frac{\alpha}{2}\left[\tfrac{1}{2}f(0) + \sum_{n=1}^{\infty} f(\alpha n)\right] - \frac{1}{2}\int_0^{\infty} f(y) dy$$

and similarly

$$S(2\alpha) \simeq \alpha\left[\tfrac{1}{2}f(0) + \sum_{n=1}^{\infty} f(2\alpha n)\right] - \frac{1}{2}\int_0^{\infty} f(y) dy$$

Hence,

$$S(\alpha) - S(2\alpha) \simeq \frac{\alpha}{2}[f(0) + 4f(\alpha) + 2f(2\alpha) + 4f(3\alpha) + \ldots] - \frac{3}{2}\int_0^{\infty} f(y) dy$$

and so

$$\delta(A) = \frac{A}{2}\left[\tfrac{1}{2}f(0) + \sum_{n=1}^{\infty} f(An)\right] - \frac{1}{2}\left\{\frac{\alpha}{3}[f(0) + 4f(\alpha) + 2f(2\alpha) + \ldots]\right\} + \tfrac{1}{3}[S(2\alpha) - 4S(\alpha)]$$

Thus, α must be chosen so that $\frac{1}{3}[S(2\alpha) - 4S(\alpha)]$ is substantially smaller than the required integral for the largest value of β considered. For the 240- and 600-channel cases, α was taken as 0·2 and 0·3 respectively.

For computational purposes, advantage can be taken of the circumstance that groups of terms of the summation in the right-hand side of eqn. (32) can be taken with portions of the integral to form substantially cancelling pairs. Such a rearrangement ensures that the integral is not evaluated up to an unnecessarily high upper limit. Eqn. (32) now takes the form

$$\sum_{n=1}^{\infty} \int_0^{\infty} f(y) \cos(n\beta y) dy = \frac{1}{2}\left[\sum_{n=0}^{\infty}\left(\frac{\pi}{\beta}\left\{f\left(\frac{2\pi}{\beta}n\right) + f\left[\frac{2\pi}{\beta}(n+1)\right]\right\} - \int_{(2\pi/\beta)n}^{(2\pi/\beta)(n+1)} f(y) dy\right)\right] \quad . \quad . \quad . \quad . \quad (33)$$

It will be noticed that in each term of the summation on the right-hand side of eqn. (33) the value of the integral over a certain range is subtracted from an approximation to it.

Successive terms of the right-hand side of eqn. (33) are now evaluated by applying Simpson's rule to the portions of the integral, using intervals of 0·2 and 0·3 for the 240- and 600-channel cases respectively. It is still found, however, that further measures are required to keep the computation within reasonable bounds. For the larger values of n the following approximation is applied. The integral is represented by the 3-point Simpson formula, so that the nth term of the summation becomes

$$\frac{2}{3}\frac{\pi}{\beta}\left\{f\left(\frac{2\pi n}{\beta}\right) - 2f\left[\frac{2\pi}{\beta}\left(n+\frac{1}{2}\right)\right] + f\left[\frac{2\pi}{\beta}(n+1)\right]\right\} \quad (34)$$

Now Taylor's expansion is applied to give the values of f at the ends of the interval in terms of values of f and its derivatives, up to second order, at the centre. Expression (34) now becomes

$$\frac{2}{3}\frac{\pi}{\beta}\left\{\left(\frac{\pi}{\beta}\right)^2 f''\left[\frac{2\pi}{\beta}\left(n+\frac{1}{2}\right)\right]\right\} \quad . \quad . \quad . \quad (35)$$

where $$f''(y) = \varepsilon^{\psi_u - \psi_0}\left[\frac{d^2\psi_u}{dy^2} + \left(\frac{d\psi_u}{dy}\right)^2\right]$$

$$\frac{d^2\psi_u}{dy^2} = \frac{\omega_\Delta^2}{\omega_m(\hat{\omega}_m - \check{\omega}_m)}\frac{1}{y}\left[\sin\left(\frac{\check{\omega}_m}{\hat{\omega}_m}y\right) - \sin y\right]$$

$$\frac{d\psi_u}{dy} = \frac{\omega_\Delta^2}{\omega_m(\hat{\omega}_m - \check{\omega}_m)}\left[\mathrm{Si}\left(\frac{\check{\omega}_m}{\hat{\omega}_m}y\right) - \mathrm{Si}(y)\right]$$

and ψ_u and ψ_0 are as defined in Section 2.1.1. The advantage of this is that, since the cancellation has already been carried out, as it were, in the algebra, the quantities making up expression (35) need not be evaluated to high accuracy. In practice, graphs were constructed of

$$\varepsilon^{\psi_u - \psi_0} \text{ and } \mathrm{Si}\left(\frac{\check{\omega}_m}{\hat{\omega}_m}y\right) - \mathrm{Si}(y)$$

and the required values read off. The term

$$\sin\left(\frac{\check{\omega}_m}{\hat{\omega}_m}y\right) - \sin y$$

oscillates too rapidly and irregularly to be treated in this way and requires direct computation. The point at which the terms of the right-hand side of eqn. (33) can be adequately represented by expression (35) has to be determined by trial.

A point of analytical interest is that the term $\varepsilon^{-\psi_0}$ in the original integrand disappears from each term of the right-hand side of eqn. (33), and hence can be omitted at the beginning of the computation. This may seem somewhat unexpected, since this term was introduced initially to secure convergence. The integral

$$\frac{2}{\pi}\int_0^{\infty} \varepsilon^{\psi_u - \psi_0} \cos(\beta y) dy$$

which is what we appear to be evaluating if we omit the $\varepsilon^{-\psi_0}$ term, is certainly divergent. However, the process of rearrangement of the right-hand side of eqn. (32), which led to the converging sequence forming the right-hand side of eqn. (33), will not be valid unless the series and the integral making up the former expression are themselves convergent, and this will be the case only if the term $\varepsilon^{-\psi_0}$ is initially present. Thus, this term may be considered as implicitly present, although self-cancelling, in eqn. (33).

It is of considerable interest to notice that the problem considered in the paper is closely related to the problem of evaluating the r.f. spectrum of a carrier frequency-modulated by a band of 'white' noise. If we consider the physical significance of replacing ω_D, in the left-hand side of eqn. (21), by ω_c, it at once becomes apparent that the power per radian per second in the spectrum of the noise-modulated carrier, at frequency separation ω_m from the carrier frequency, is given by

$$\frac{1}{\pi}\frac{\varepsilon^{-\psi_0}}{\hat{\omega}_m}\int_0^{\infty}[\varepsilon^{\psi_u(y)} - 1]\cos\left(\frac{\omega_m}{\hat{\omega}_m}y\right)dy$$

The r.f. spectrum of a carrier frequency-modulated by 'white' noise simulating an f.d.m. signal has been previously evaluated by a completely different approximate method.[1] In this reference there is no indication of the order of accuracy of the computed spectra. Using exact values of spectral distributions which have

to be computed incidentally to the present work, a comparison has been made with the curves in Reference 1 for 240- and 600-channel systems. It is found that the approximate spectral densities do not differ anywhere from the present values by more than 1 dB, which is a very gratifying measure of agreement.

(7.3) Output from a Linear Discriminator when the Incoming Wave is Simultaneously Amplitude- and Frequency-Modulated

The incoming wave can be written in the form

$$(1 + M_t)\cos(\omega_c t + \phi_t) \quad . \quad . \quad . \quad . \quad (36)$$

If this wave passes through a discriminator whose amplitude characteristic has the form

$$B_0 + \frac{B_1}{\omega_c}(\omega - \omega_c) \quad . \quad . \quad . \quad . \quad . \quad (37)$$

it is easy to see, by considering the result of operating separately on each sideband of expressions (36) with (37), that the output will be

$$(B_0 - B_1)(1 + M_t)\cos(\omega_c t + \phi_t) + \frac{B_1}{\omega_c}\frac{d}{dt}\left[(1 + M_t)\cos\left(\omega_c t + \phi_t - \frac{\pi}{2}\right)\right]$$
$$= (B_0 - B_1)(1 + M_t)\cos(\omega_c t + \phi_t) + \frac{B_1}{\omega_c}\frac{d}{dt}[(1 + M_t)\sin(\omega_c t + \phi_t)]$$

After differentiating and collecting terms, the amplitude modulation of the output is

$$\left[(1 + M_t)^2\left(B_0 + \frac{B_1}{\omega_c}\phi_t'\right)^2 + \left(\frac{B_1}{\omega_c}\right)^2 (M_t')^2\right]^{1/2} \quad . \quad (38)$$

Now, taking a limiter compression factor Δ_L, it follows from eqns. (4) and (5) that

$$M_t = \Delta_L r\cos(\omega_D t - \mu_t)$$

and

$$\phi_t = \mu_t + r\sin(\omega_D t - \mu_t)$$

Substituting in expression (38) and extracting terms up to first order in r, the discriminator output becomes

$$B_0 + \frac{B_1}{\omega_c}\mu_t' + B_0\Delta_L r\cos(\omega_D t - \mu_t) + \frac{B_1}{\omega_c}r\omega_D\cos(\omega_D t - \mu_t) - \frac{B_1}{\omega_c}r(1 - \Delta_L)\mu_t'\cos(\omega_D t - \mu_t) \quad . \quad (39)$$

In order to avoid the complication of extracting distortion tones from terms of the type $\mu_t'\cos\mu_t$ and $\mu_t'\sin\mu_t$, we rewrite expression (39) in the form

$$B_0 + \frac{B_1}{\omega_c}\mu_t' + B_0\Delta_L r\cos(\omega_D t - \mu_t) + \frac{B_1}{\omega_c}r(1 - \Delta_L)\frac{d}{dt}\sin(\omega_D t - \mu_t) + \frac{B_1}{\omega_c}r\Delta_L\omega_D\cos(\omega_D t - \mu_t) \quad . \quad . \quad . \quad . \quad (40)$$

Expression (8), which represents the output of a 2-sided discriminator, is now obtained by substituting in expression (40) $B_0 = B_{0l}$ and $B_1 = B_{1l}$ for one side, and $B_0 = B_{0h}$ and $B_1 = -B_{1h}$ for the other side, and subtracting the resulting expressions.

.1.396.822:621.317.34

The Institution of Electrical Engineers
Paper No. 2619 R
May 1958

ATMOSPHERIC RADIO NOISE AT FREQUENCIES BETWEEN 10 KC/S AND 30 KC/S

By J. HARWOOD, M.A., Ph.D.

(*The paper was first received* 28*th September*, 1957, *and in revised form* 21*st February*, 1958.)

SUMMARY

Measurements of the characteristics of very-low-frequency atmospheric noise in Southern England have been made with automatic equipment during the last few years. The results are described in terms of statistical parameters of the envelope at the output of a narrow-bandwidth receiver (300 c/s between 3 dB points).

The average voltage of the envelope, recorded via an integrating circuit with equal charge and discharge time-constants of 8 sec, showed short-term fluctuations of about 5% and clear diurnal and seasonal variations.

The r.m.s. voltage, deduced by integration of measured amplitude probability distributions, varied between 4 and 8 times the average voltage; the values were very dependent on the incidence of large infrequent pulses.

The noise was always much more impulsive than fluctuation noise. The structure of the envelope was described by two forms of distribution, one being the amplitude distribution of the peaks of pulses, and the other the conventional amplitude probability distribution of voltage. The former was represented by a simple power-law function of voltage involving two parameters, the average voltage and the power-law index. The latter was represented by another simple function involving two similar parameters. The character of the noise was always approximately the same in spite of substantial changes of average voltage from time to time.

Variations of the intensity and structure with frequency and bandwidth were examined.

(1) INTRODUCTION

As part of a programme for determining the interference caused to radio systems by atmospheric noise, measurements of the characteristics of the noise were obtained during 1953–1955 at the Radio Research Station. The measurements were made at very low frequencies (10–30 kc/s); at these frequencies, noise levels were relatively high and interference from stations could easily be avoided. A discussion of technique and a description of the type of result obtained have previously been given.[1] In the present paper, the results of the investigation are summarized, with particular reference to the observations at 10 kc/s (receiver bandwidth 300 c/s) during four months of 1955. An attempt has been made to describe concisely the character of the noise and the significant variations with time. The dependence of noise structure on frequency was studied from simultaneous recordings at two frequencies over long periods, and the dependence on receiver bandwidth by a few short-term experiments.

The low-frequency atmospheric noise was always impulsive in nature, and is contrasted in subsequent Sections with random noise having a Gaussian amplitude distribution (e.g. thermal noise); the latter type of noise will be referred to as 'fluctuation noise'.

(2) MEASURED CHARACTERISTICS

The measurements related to the envelope of the noise after it had been received on a vertical aerial and passed through a narrow-bandwidth receiver. At the output of the receiver, the envelope consisted mainly of a random series of pulses of similar shape but of widely varying peak amplitudes. Long-term recordings of statistical parameters of the envelope were obtained with automatic equipment, and from these the variations of noise intensity and amplitude distribution were studied.

An indication of the magnitude and long-term variations of noise intensity would be given by recording any of several parameters, such as the r.m.s. voltage, the average voltage, the quasi-peak voltage, and so on. The average voltage was chosen as being an easily defined parameter which involved a simple technique of measurement, and which, as will be shown, was closely related to parameters used in expressing the amplitude distributions. The average voltage was recorded continuously via an integrating circuit having equal charge and discharge time-constants of about 8 sec. The r.m.s. voltage was not measured directly, but was deduced by integration of measured amplitude distributions.

The noise structure was defined by two forms of amplitude probability distribution, namely

(*a*) The amplitude distribution of peaks in the envelope, measured in cumulative form as the rate of occurrence n_v of pulses above a series of voltages v (pulse rate).

(*b*) The cumulative amplitude probability distribution of the envelope voltage, or fraction of time $Q(v)$ for which voltages v were exceeded.

Although the two distributions were found to be closely related, the former is concerned essentially with the number and size of pulses in the envelope, whereas the latter refers to the envelope merely as a fluctuating voltage and does not depend for its significance on assumptions about the impulsiveness of the noise. The pulse rate gives a better description of the envelope at the higher voltages, where overlapping of successive pulses can be ignored. The function $Q(v)$, however, can be used as a partial measure of the structure over the whole amplitude range.

To obtain $Q(v)$ over a wide range of amplitude, more than one method has been used. The main results were obtained by recording the average voltage of the parts of the envelope which exceeded each of a series of threshold voltages, and deriving $Q(v)$ by differentiating the curve of average against threshold; this technique will be referred to as method I.[1] At higher voltages, where the average above a threshold was very small, the data were derived from the pulse rate and known pulse shape. More recently, a technique was developed to measure $Q(v)$ directly (method II), by counting 'carrier' cycles which exceeded thresholds at the receiver output; a similar technique at high frequencies has been described recently.[3] Although method II was developed towards the conclusion of the main series of observations, it provided a valuable check of the validity of earlier deductions from measured data, and extended the range of measurements of $Q(v)$ to very low voltages.

(3) AVERAGE VOLTAGE OF THE ENVELOPE

From the pen recordings of average voltage, the mean was estimated over each hour to obtain a series of hourly values. For each month's observations, the median and upper and lower decile hourly values were computed at each hour of the day, and curves of the diurnal variation were constructed; these are shown in Fig. 1. The voltage scale at the receiver output was converted

Written contributions on papers published without being read at meetings are invited for consideration with a view to publication.

The paper is an official communication from the Radio Research Station, Department of Scientific and Industrial Research.

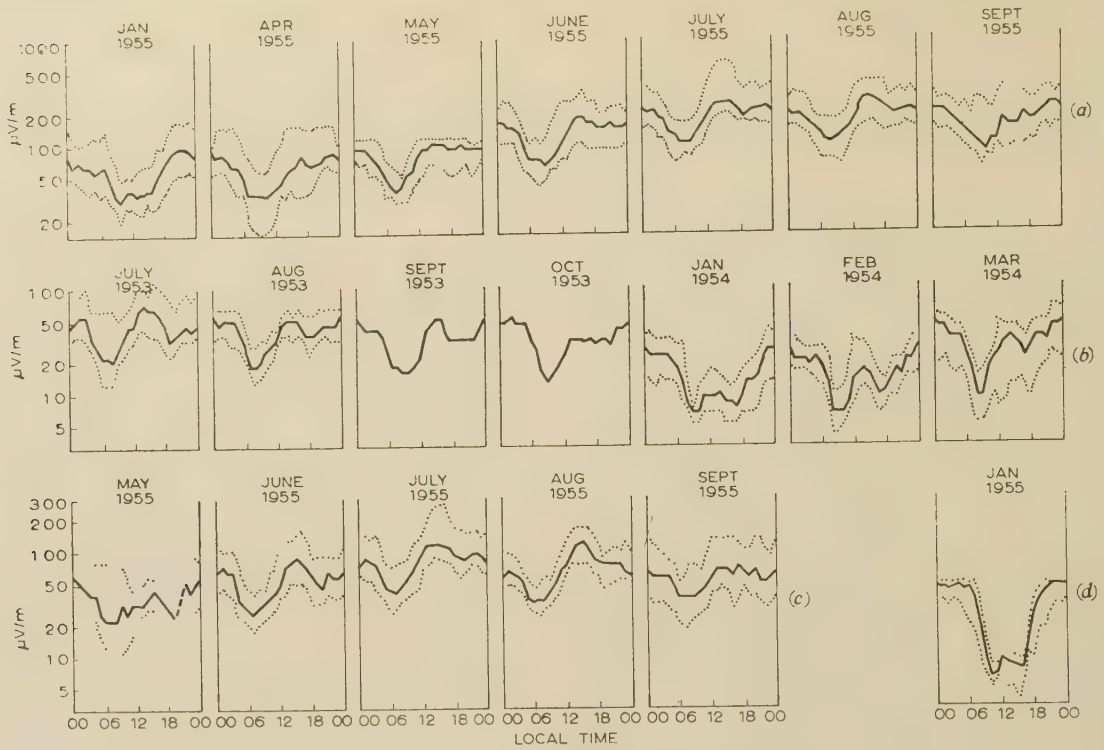

Fig. 1.—Average field strength of noise envelope.

Bandwidth 300 c/s on all frequencies.

—— Median.
···· Upper and lower deciles.

(*a*) 10 kc/s.
(*b*) 23–25 kc/s.
(*c*) 23–25 kc/s.
(*d*) 33 kc/s.

to an equivalent-field-strength scale at the aerial, so as to be independent of aerial and receiver gain. In this way, the amplitude scales in Fig. 1 and in subsequent results are expressed in terms of field strength.

The winter results show a simple diurnal variation in which, at 10 kc/s, the average voltage by day was about a third of that by night. In summer, a high afternoon level produced by relatively local thunderstorm activity was added; this often exceeded the night-time level, and on one occasion reached a field strength of 1 mV/m. At other times of day, levels were higher in summer than in winter. At 24 and 33 kc/s, the average voltages were smaller and showed a more marked diurnal variation. There is other evidence which indicates a maximum noise intensity at about 12 kc/s.

(4) AMPLITUDE DISTRIBUTION OF PEAKS

At most voltage levels, the noise envelope appeared as a series of discrete pulses, and each excursion of the envelope above a threshold was usually associated with only a single maximum above that threshold. Thus, the cumulative amplitude distribution of peaks was given by counting the number of excursions per second above a series of thresholds, and this measured parameter was called the pulse rate. There was a low-voltage region, however, in which the discrete impulsive nature was lost; the combination of the exponential decay of each pulse and the large numbers of the smaller pulses caused significant overlapping. The pulse-rate measurements are therefore applicable only to the higher voltage levels.

(4.1) Results

A graph of pulse rate against threshold voltage, with logarithmic scales on both axes, is shown in Fig. 2. Above the average voltage indicated on the graph the pulses were substantially discrete, and the pulse rate decreased with increasing voltage until the largest pulses occurred so infrequently as to be discounted in the measurements. Below the average voltage, the pulse rate was influenced by interference between an increasing number of pulses as the threshold decreased, so that a maximum was reached, after which the pulse rate decreased as the envelope remained above the threshold for more and more of the time. The maximum pulse rate was found to be correlated with the receiver bandwidth, and did not indicate the maximum rate of arrival of impulses at the aerial.

Routine recordings of pulse rate were restricted to the region above the average voltage in which the rate was between about 100 and 0·5 per second. In this region, graphs plotted with the co-ordinates of Fig. 2 were nearly linear, and hence a simple power-law was an adequate representation of the pulse rate n_v as a function of the threshold voltage v, i.e.

$$n_v = (v/A)^{-p} \quad . \quad . \quad . \quad . \quad . \quad . \quad (1)$$

where A and p are constants at a given time, but could vary from one occasion to another. Several hundred measurements of the distribution were made, and each was represented by parameters p and A.

The parameter p is seen to be the negative slope of the distribution when graphed on the scales of Fig. 2, and A is the voltage

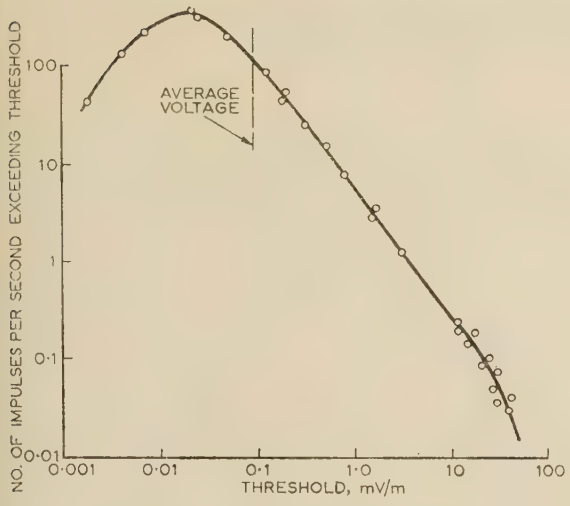

Fig. 2.—Typical distribution of peaks.
0900–1100 hours G.M.T. 30th July, 1956.
300 c/s bandwidth at 10 kc/s.

exceeded by one pulse per second. p thus represents the form of the distribution, in that a small value corresponds to a type of noise containing a wide range of pulse amplitudes, and a large value to a restricted amplitude range such as is found in fluctuation noise; in this connection, it may be noted that the pulse-rate distribution of fluctuation noise has a much greater slope than any of the low-frequency atmospheric-noise distributions.

Values of p are summarized in Table 1, where they are classified into four-hour periods of the day during four months of 1955; median, upper decile and lower decile values are shown. A small regular diurnal change is evident; values are higher than average near sunset and lower in the mornings. There is a variation from month to month but no significant difference between winter and summer conditions. The mean of 400 measurements of p was 1·25, and on 80% of occasions the values lay between 1·0 and 1·5. The variations in the parameter p represented little change in the general appearance of the noise, which was always impulsive in nature, but in particular applications the variations are important. For example, the extremes of the random variation correspond to changes of more than 3 : 1 in the number of pulses exceeding $100\bar{V}$ and a change in the ratio r.m.s./average voltage of 2 : 1.

Whereas p indicates the form of the distribution, the parameter A is in the nature of a scaling factor, and this showed a much more obvious diurnal and seasonal variation. The variation was similar, in fact, to that of the average voltage, to which the parameter A would be proportional if the form of the noise were always the same. The closest proportionality, however, was found between the average voltage and the voltage exceeded by 10 pulses per second, which was nearly always seven times the average voltage (to within 10%). This relationship is shown in Fig. 3 for 113 occasions in June, 1955. Eqn. (1), representing pulse rates between about one and 80 per second, can therefore

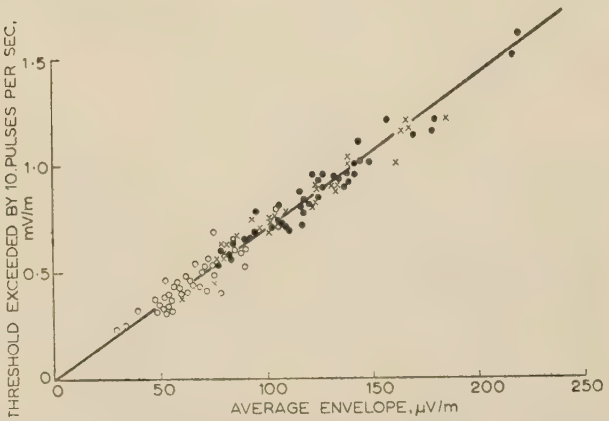

Fig. 3.—Relationship between average and threshold exceeded by 10 pulses per second.
Observations in June, 1955.
○ 0400–1200 hours G.M.T.
× 1200–2000 hours G.M.T.
● 2000–0400 hours G.M.T.

Table 1

PULSE-RATE PARAMETER p DURING 1955

Local time	January			April			June			July		
	Median	U.D. L.D.	No.	Median	U.D. L.D.	No.	Median	U.D. L.D.	No.	Median	U.D. L.D.	No.
hours												
0000–0400	1·08	1·52 0·94	21	1·42	—	6	1·30	1·39 1·11	18	1·21	1·34 1·00	31
0400–0800	1·08	1·18 0·86	17	1·28	—	1	1·25	1·49 1·07	24	1·13	1·30 1·00	31
0800–1200	1·01	1·50 0·88	16	1·40	—	2	1·29	1·48 1·15	17	1·11	1·29 0·95	24
1200–1600	1·29	1·65 1·08	14	1·41	—	5	1·30	1·60 1·10	15	1·13	1·31 0·96	24
1600–2000	1·24	1·34 1·07	15	1·41	—	3	1·41	1·70 1·25	19	1·26	1·50 1·00	27
2000–0000	1·10	1·17 1·10	10	1·30	—	3	1·41	1·58 1·14	25	1·32	1·55 1·16	25
All times	1·14	—	93	1·40	—	20	1·35	—	118	1·20	—	162

U.D. = Upper decile value.
L.D. = Lower decile value.
No. = Number of distributions obtained.

be expressed in terms of the parameter p and the average voltage $\bar{V}$ by

$$n_v = 10\left(\frac{v}{7\bar{V}}\right)^{-p} \quad . \quad . \quad . \quad . \quad . \quad (2)$$

The minimum pulse-rate considered in the above analysis was about 0·5 per second, and there were always less frequent but greater pulses which were studied on a few occasions only. Their distribution was usually similar to that shown in Fig. 2, with a more rapid decrease of pulse rate with increasing voltage than was given by the slope p at lower voltages, but at the highest voltages there was more divergence from one occasion to another. The form of the distribution at the very high voltages, where pulses occurred at rates of only one or two per minute, depended much more on the proximity of thunderstorm activity than did the distribution at lower voltages, but no detailed correlation has yet been sought.

(4.2) Relationship of Pulse Rate to Amplitude Probability Distribution

Measurements of the second type of cumulative distribution, that of the amplitude probability $Q(v)$, will be described in Section 5. The values of $Q(v)$ at the higher voltages were derived from the pulse-rate distribution, and in this Section the relationship between the two distributions is examined. Each counted impulse had a known form determined by the receiver response characteristic, and its width at any fraction of the peak voltage was also known. By integration of the widths of all the counted impulses at a series of voltages, $Q(v)$ could be computed. In the Appendix (Section 13), some equations relating the pulse-rate distribution to $Q(v)$ and to the average voltage of the envelope are derived, when the pulse-rate distribution is given by eqn. (1). Eqn. (8) (in the Appendix) expresses $Q(v)$ as the product of two functions; the first is the power-law function of voltage obeyed by the pulse-rate distribution, and the second is an integral whose value depends on the ratio of v to a high voltage v_0 defining an upper limit to the distribution. For $v \ll v_0$, the integral varies slowly with v, and $Q(v)$ follows the same law as the pulse rate. As v approaches v_0, the integral decreases more rapidly, and a curvature (on log-log scales) is introduced into the amplitude distribution so that its slope becomes increasingly greater than p as the voltage increases. Fig. 4 shows the distribution of amplitude deduced from the pulse-rate curve in Fig. 2, and simultaneous direct measurements of $Q(v)$ by method II are superposed.

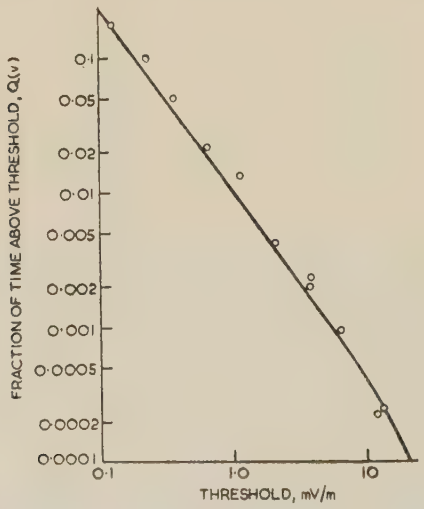

Fig. 4.—Comparison of measured amplitude probability with that derived from pulse rate.
—— Derived from pulse rate.
○ Measured.

(5) AMPLITUDE PROBABILITY DISTRIBUTION OF THE ENVELOPE

A graph of the cumulative amplitude probability distribution is shown in Fig. 5, as a curve of the proportion of time for which the envelope exceeded voltages v against these voltages. The axes are logarithmic, and the voltage scale is expressed in units of the average envelope voltage. It is convenient to examine the form of this distribution in three voltage ranges, a particular method of observation (shown by the coded points) being appropriate to each range.

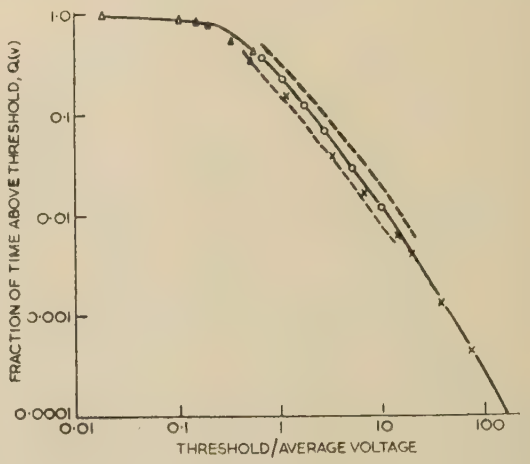

Fig. 5.—Mean cumulative amplitude probability distribution.
△ Low-voltage direct measurements by method II.
○ From average above threshold (method I).
× From pulse rate.

(5.1) Distribution at Low Voltages

At low voltages, the overlapping of successive pulses might be expected to give the envelope a character resembling fluctuation noise. The distribution was therefore replotted on Rayleigh probability paper, on which the Rayleigh distribution appropriate to fluctuation noise would appear as a straight line of unit slope (Fig. 6). It is seen that a similarity to fluctuation

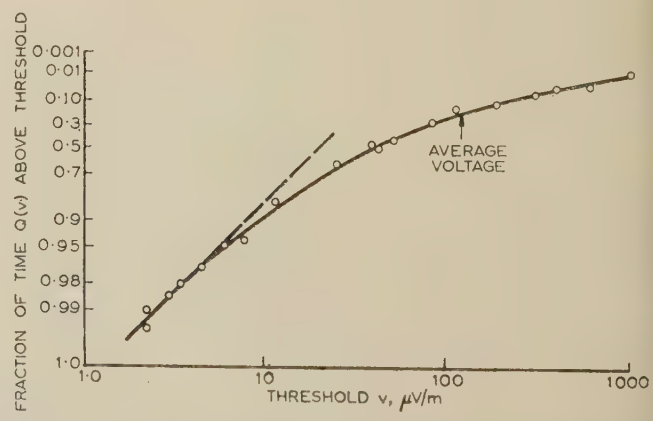

Fig. 6.—Comparison of amplitude probability distributions of low frequency atmospheric noise and fluctuation noise.
10 kc/s, 0900–1100 hours G.M.T. 30th July, 1956.
—— Atmospheric noise.
– – – – Fluctuation noise.
Scales chosen so that fluctuation noise distribution is a straight line of unit slope.

noise is evident only at voltages below 0·1 of the average voltage, and that above this voltage the deviation becomes increasingly marked.

(5.2) Distribution at Intermediate Voltages

The main body of results was obtained by method I at voltages between 0·5 and 20 times the average voltage. About a thousand measurements of the distribution were made during 1954 and 1955, mainly at the frequency of 10 kc/s. Attempts to describe each distribution by two parameters similar to the A and p used in the case of the pulse rate were not satisfactory, although in the course of the analysis it was found that the distribution could sometimes be represented by a straight line when plotted on particular forms of graph paper; two such forms were

(*a*) The log-log presentation used in Fig. 5.
(*b*) A log-normal presentation, in which a normal distribution of the logarithm of the voltage would be a straight line.

Each distribution was finally described by a series of voltage intercepts with particular values of $Q(v)$, and as was done for the pulse rate, each intercept was plotted against the average envelope voltage. Fig. 7 shows one such plot for June, 1955,

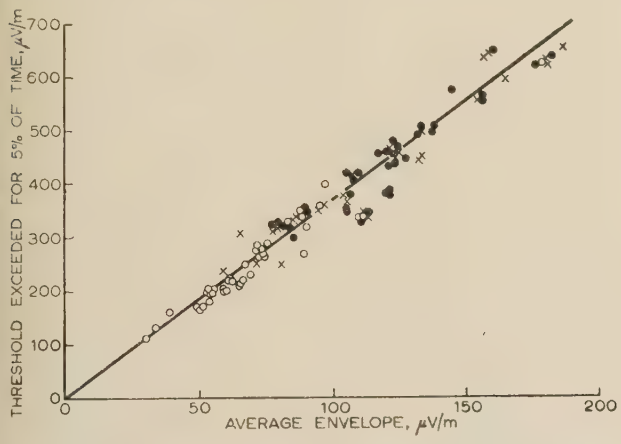

Fig. 7.—Relationship between average voltage and threshold exceeded for 5% of time.
Observations in June, 1955.
○ 0400–1200 hours G.M.T.
× 1200–2000 hours G.M.T.
● 2000–0400 hours G.M.T.

in which the threshold exceeded for 5% of the time [$Q(v) = 0{\cdot}05$] is plotted against the average voltage. Similar plots were made for the 1, 10, 20 and 40% intercepts, and all were classified into time of day and month so that diurnal and seasonal effects would be evident.

As in the similar pulse-rate plots, the threshold voltage corresponding to a given amplitude probability was proportional to the average envelope voltage. Measurement of the factors of proportionality in the plots for various amplitude probabilities allowed the distributions to be presented with their voltage scales in units of the average envelope voltage, and in Fig. 5 the mean of all the distributions is shown in this form. The two dotted curves show the limits between which four-fifths of the distributions lay, including a small diurnal variation in form similar to that found in the distribution of peaks. Although there were slight differences between monthly mean curves, no distinct seasonal effect was evident.

(5.3) Distribution at High Voltages

The distribution above 20 times the average voltage was deduced from the pulse-rate data as described in Section 4.2, and could be represented by a power law up to about 100 times the average voltage. At higher voltages, the amplitude probability decreased more and more rapidly with increasing voltage on the few occasions it was observed.

(5.4) The Complete Amplitude Probability Distribution

The curve in Fig. 5 represents the mean of all the data at 10 kc/s in a bandwidth of 300 c/s. The agreement between the different methods of observation used to obtain the complete curve is shown clearly by the coded points.

In attempts to fit a simple law to the distribution, the curve was redrawn as a graph, again on logarithmic scales, of a new function of the amplitude probability against threshold voltage (Fig. 8); this function was the ratio between the fraction of time

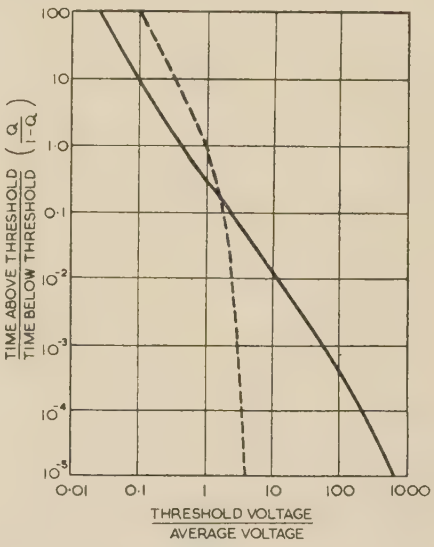

Fig. 8.—Mean cumulative amplitude probability distribution.
—— Atmospheric noise at 10 kc/s.
---- Fluctuation noise.

for which the threshold was exceeded and the fraction of time it was not exceeded, namely $Q(v)/[1 - Q(v)]$. The distribution could then be represented approximately by a straight line in a voltage range from 0·02 to 200 times the average voltage, i.e.

$$Q(v) = [1 + (2v/\bar{V})^r]^{-1} \quad . \quad . \quad . \quad . \quad . \quad (3)$$

where r is the negative slope of the line; for the mean distribution, r was 1·5. At the lowest voltages, the slope approached the value of 2·0 consistent with the tendency towards a Rayleigh distribution.

The distribution of fluctuation noise with the same average voltage is also shown in Fig. 8, to emphasize the impulsive nature of the atmospheric noise and the wide range of voltage covered by the pulses.

A comparison of the distribution expressed by eqn. (3) with recently published American measurements[4] shows substantial agreement in the form of the distribution, and in its location with respect to the average envelope voltage.

(6) R.M.S. VOLTAGE OF THE ENVELOPE

The r.m.s. voltage and noise power are being used in many present-day measurements to express noise intensities, and these, in association with the average voltage, also give an indication of the nature of the noise. The r.m.s. voltage of the noise envelope, which is $\sqrt{2}$ times the r.m.s. noise voltage, was not

measured directly, but was deduced by integration of the amplitude distributions. It can be shown that

$$\overline{V^2} = 2\int_0^\infty vQ(v)dv = 2\int_0^\infty \bar{V}_v dv \quad . \quad . \quad . \quad (4)$$

where $\overline{V^2}$ is the mean square voltage of envelope and $\bar{V}_v$ is the average voltage above threshold v.

Integration of the mean amplitude distribution (Fig. 8) led to an r.m.s. envelope voltage at 10 kc/s of about six times the average voltage, compared with 1·13 for fluctuation noise. Random and diurnal variations of the distribution resulted in minimum and maximum values of 4 and 8, respectively.

The process of integration demonstrated the relative importance of different voltage regions in their contribution to the mean square voltage. For example, by choosing the lower limit of integration at the average voltage instead of at zero, a 1% error only was involved; whereas, if the noise waveform were limited at 100 times the average voltage, the mean square might be less than half its true value. The analysis emphasizes the necessity for preventing receiver saturation on even a small number of pulses if an accurate measure of the r.m.s. voltage is to be made.

The significant effect of the high-voltage regions is brought out by the ratios in Table 2, in which values appropriate to an envelope which has been limited at 50, 100 and 200 times the average voltage are compared with the full values; the figures are of practical interest in that if the gain of a receiving system is set for optimum reception of a weak signal through the noise, limiting at these levels is likely, and the effective r.m.s. noise voltage correspondingly reduced.

Table 2

RATIO BETWEEN R.M.S. AND AVERAGE VOLTAGES

Conditions	R.M.S./Average; waveform limited at			
	$50\bar{V}$	$100\bar{V}$	$200\bar{V}$	∞
Maximum ..	3·7	4·8	6·0	8
Mean	3·2	3·9	4·5	6
Minimum ..	2·7	3·1	3·6	4

(7) DEPENDENCE OF NOISE STRUCTURE ON FREQUENCY

Analysis of about a hundred simultaneous measurements of the distribution at 10 and 23 kc/s, and a few at 10 and 30 kc/s, showed a small but significant dependence of the noise structure on frequency. The parameter p, representing the form of the pulse-rate distribution, was nearly always greater at 23 kc/s than at 10 kc/s; its mean value at 23 kc/s was 1·5, with diurnal and random variations about this value of $\pm 0{\cdot}2$. The cumulative amplitude probability function at 23 kc/s also decreased more rapidly with increasing voltage than did the corresponding function at 10 kc/s. Thus, over the limited frequency range of the observations, there is evidence that the noise becomes less impulsive as the frequency is increased, but it is emphasized that the change in character is only of the same order as the random variation from one occasion to another, and the structure remains very different from that of fluctuation noise. The voltage scale of the distribution at 23 kc/s, relative to the average envelope voltage, remained much the same as at 10 kc/s, but the ratio between the r.m.s. and average voltages was smaller; e.g. the overall mean value of the ratio may be taken as 4·0 (as compared with 6·0 at 10 kc/s).

(8) EFFECTS OF BANDWIDTH VARIATIONS

All the measurements so far described were made in a bandwidth of 300 c/s, and a change of this bandwidth would be expected to modify the form and amplitude of the noise; e.g. the following results concerning an idealized noise envelope are known theoretically:[2]

(*a*) The peak voltage of a pulse at the receiver output due to unit impulse at the input is proportional to the bandwidth.

(*b*) The average voltage of a series of such pulses is independent of bandwidth if they are assumed to be completely separated in time.

(*c*) The average voltage of fluctuation noise is proportional to the square root of the bandwidth.

(*d*) The r.m.s. voltage of discrete pulses or fluctuation noise is proportional to the square root of the bandwidth, and that of the atmospheric noise would also be expected to follow this law.

The results of a series of experiments to determine the effect of a bandwidth variation are described in Reference 1. The average voltage of the envelope was measured as a function of the bandwidth when the latter was varied from 25 c/s to 2 kc/s; some experiments were carried out at 25 kc/s and others at 10 kc/s and the results were similar. For bandwidths up to 200 c/s, the average voltage was proportional to the square root of the bandwidth. As the bandwidth increased above 200 c/s, the noise was observed to become more impulsive and the average voltage varied less rapidly; on two occasions the variations were as the cube root and fourth root of the bandwidth.

The structure of the noise at 10 kc/s was also examined at a few different bandwidths. The pulse-rate distribution was unchanged in form at bandwidths of 190, 310 and 540 c/s, but was displaced along the logarithmic amplitude scale proportionately to the bandwidth; this is consistent with the expected proportionality to bandwidth of the peak voltage of each pulse. The amplitude probability distribution was similarly displaced, but by a much smaller amount consistent with the theoretical analysis in the Appendix. It is shown there that the expected displacement is proportional to the bandwidth to the power $(p-1)/p$, where p is the negative slope of the line representing the pulse-rate distribution, and substitution of the mean value of p, namely 1·25, gives a fifth-root relationship. Comparing this relationship with the cube- or fourth-root law relating changes of average voltage to bandwidth, it appears that, by expressing the amplitude scale of the distribution in units of the average voltage, there will be little change in the position of the distribution curve as the bandwidth is increased above 300 c/s.

At the narrowest bandwidth of 190 c/s, the distribution was slightly steeper than at 310 and 540 c/s, showing a tendency to approach the characteristics of fluctuation noise as the bandwidth was reduced; the noise was still of impulsive character, however, and would probably be similar to fluctuation noise only at bandwidths of a few cycles per second.

Integration of the distributions at the three bandwidths, as described in Section 6, confirmed that the r.m.s. voltage was proportional to the square root of the bandwidth.

(9) TIME DISTRIBUTION OF IMPULSES

The distribution of pulse rate with amplitude refers to the mean numbers of pulses occurring per second with a given peak amplitude, and contains no information on how the occurrences are distributed in time about this mean. Under ordinary conditions, when the storm activity is not local, contributions of pulses must be obtained from many storm centres, and random occurrences would be expected. On the other hand, a lightning flash often consists of a number of strokes, and a grouping of the received pulses might be expected. Three types of experiment were carried out to examine the distribution in time. In the first, a threshold voltage was applied to the receiver output so

it pulses exceeded it on the average about once every 3 sec; f-minute samples were then taken, and the distribution of nts per sample was found to be consistent with random currence. In a second experiment, very much shorter samples millisec) were taken from a fast film record of the noise velope and from photographs of the envelope over short riods following a large pulse. The distributions of counts per mple in these short periods showed a departure from random-ss which could be interpreted as a tendency for groups of a few lses to occur more frequently than by chance. A third type experiment was designed to show any grouping, by presenting e large pulses (rates less than one in 2 sec) as impulsive deflec-ns on a pen recorder. An integrating circuit was used in such way that pulses occurring within a half-second period gave a n deflection proportional to their number, and a gap of longer an this period allowed the pen to fall back to zero. Records this type indicated a dependence of grouping on the presence local activity. For example, at most times the majority of lses exceeding a high threshold were single, but during a rticular local storm, groups of as many as 14 pulses were quently obtained. It is possible, however, that under normal nditions the grouping may be obscured because of large fferences of amplitude between successive pulses of a group.

It may be concluded that the noise envelope contains groups associated pulses, but it seems unlikely that this grouping will ve a major effect on the interference caused by the noise; for is reason, it has not yet been studied in further detail.

(10) CONCLUSIONS

After atmospheric noise has passed through a receiver tuned to frequency between 10 and 30 kc/s, it emerges as an oscillatory aveform whose envelope consists mainly of discrete pulses, nich have a known form determined by the receiver response it vary in peak amplitude over a wide range. At low voltages, ere is interference between the 'bases' of the impulses, and some the properties of a series of discrete pulses are lost; e.g. the erage voltage is dependent on receiver bandwidth.

The noise envelope, measured in Southern England, has been scribed in terms of the measured average voltage, the deduced m.s. voltage, and two forms of amplitude distribution; the ulses may, for most practical purposes, be considered as occur-ng randomly in time, but there is some evidence of grouping, rticularly under local storm conditions. The parameters of e noise intensity and structure were all related to the average oltage of the envelope, which was measured continuously with receiver bandwidth of 300 c/s between 3 dB points of the sponse curve, and these relationships together with variation the average voltage itself are summarized below.

(10.1) Average Voltage of the Envelope

The data on diurnal and seasonal variations of the average oltage are shown in Fig. 1. The lowest values occurred in the ornings and the highest during summer afternoons, when underst orm activity was greater. Noise levels were greater in mmer than in winter. The higher the frequency, above a aximum at about 12 kc/s, the lower was the average voltage at given time of day. Diurnal changes were more pronounced at e higher frequencies.

Variations of average voltage with bandwidth followed a uare-root law below 200 c/s bandwidth, but from 200 c/s to kc/s the variation was less rapid; on two particular occasions, be-root and fourth-root law, respectively, were obtained.

(10.2) R.M.S. Voltage

At 10 kc/s, in a bandwidth of 300 c/s, the ratio between the duced r.m.s. and measured average voltages of the envelope was 6 ± 2. A limiting action at 100 times the average voltage would reduce the ratio to 4 ± 1. At 25 kc/s, a smaller ratio was obtained, namely an overall mean of about 4, with similar variations about this value as at 10 kc/s. The r.m.s. voltage varied as the square root of the bandwidth. The r.m.s. voltage of the envelope is $\sqrt{2}$ times the r.m.s. voltage of the r.f. noise waveform itself.

(10.3) Distribution of Peaks

At 10 kc/s, in a bandwidth of 300 c/s, the number of excursions n_v per second of the envelope above a voltage v was given in terms of the average voltage $\bar{V}$ by eqn. (2) of Section 4.1 for values of n_v between 0·5 and 80. The mean value of the parameter p was 1·25; 80% of values lay between 1·0 and 1·5, lower values than the mean occurred in the morning, and higher ones in the evening.

Changes of receiver bandwidth from 190 c/s to 540 c/s produced proportionate displacements of the amplitude scale of the distribution. The same proportionality, with no change in the form of the distribution, would be expected up to bandwidths of a few kilocycles per second.

At 23 kc/s and 300 c/s bandwidth, eqn. (2) was still approximately valid (more accurately with the term $7\bar{V}$ replaced by $6{\cdot}5\bar{V}$), but the mean value of p was 1·5.

The above results are restricted to amplitudes below $100\bar{V}$. Above this amplitude, the slope p increased with increasing voltage, giving substantial deviations from the power law which holds at lower voltages; pulse rates at voltages above $100\bar{V}$ were less than one in 2 sec.

(10.4) Amplitude Probability Distribution

At 10 kc/s, in a bandwidth of 300 c/s, the cumulative amplitude probability function $Q(v)$ was given by eqn. (3), in which the mean value of the parameter r was 1·5, $Q(v)$ lay between 0·99 and 0·000 5 (v between $0{\cdot}02\bar{V}$ and $100\bar{V}$), and the value of v corresponding to a given $Q(v)$ could be determined to within 20% when the average voltage $\bar{V}$ was known.

Eqn. (3) was expected to hold independently of bandwidth for bandwidths between 300 c/s and 1 kc/s, but as the bandwidth is decreased below 300 c/s, r will increase and the form of the distribution will approach gradually that of fluctuation noise.

Measurements at 23 kc/s (bandwidth 300 c/s) indicated a greater mean value of r in eqn. (3) of about 1·7.

(11) REFERENCES

(1) HORNER, F., and HARWOOD, J.: 'An Investigation of Atmospheric Radio Noise at Very Low Frequencies', *Proceedings I.E.E.*, Paper No. 2147 R, November, 1956 (**103** B, p. 743).

(2) THOMAS, H. A., and BURGESS, R. E.: 'Survey of Existing Information and Data on Radio Noise over the Frequency Range 1–30 Mc/s', Radio Research Special Report No. 15 (H.M.S.O., 1947), Code No. 47–29–15.

(3) YUHARA, H., ISHIDA, T., and HIGASHIMURA, M.: 'Measurement of the Amplitude Probability Distribution of Atmospheric Noise', *Journal of the Radio Research Laboratories*, Tokyo, 1956, **3**, p. 101.

(4) WATT, A. D., and MAXWELL, E. L.: 'Measured Statistical Characteristics of VLF Atmospheric Radio Noise', *Proceedings of the Institute of Radio Engineers*, 1957, **45**, p. 55.

(12) ACKNOWLEDGMENTS

The data described above were obtained as part of the programme of the Radio Research Board. The author wishes to acknowledge the assistance given in the preparation of the paper by Mr. F. Horner, under whose supervision the work was carried

out. The paper is published by permission of the Director of Radio Research of the Department of Scientific and Industrial Research.

(13) APPENDIX

(13.1) Theoretical Relationships between Impulse Peak Distribution and Other Parameters

The noise envelope may be considered as a series of pulses which, above a low-voltage region in which they interfere, take a standard form, determined by the receiver frequency/response characteristic, as though each were produced by a short impulse at the receiver input. As this form is known, a measurement of the distribution of the peak voltages enables a number of parameters of the noise to be deduced by integration, in particular the amplitude probability distribution.

The fraction of time $Q(v)$ for which the envelope exceeds a voltage v is given by

$$Q(v) = \frac{1}{\alpha}\int_{v}^{v_0} n(V)W(X)dV \quad . \quad . \quad . \quad . \quad (5)$$

where $n(V)dV$ = Number of impulses per second whose peaks lie in the voltage range V to $V + dV$.
$W(X)$ = Width of impulse, of peak height V, at threshold v (in units of αt).
$X = v/V$.
α = Bandwidth factor dependent on receiver response curve.
v_0 = Peak amplitude of highest pulse considered.

Assuming a simple power-law expression for the pulse rate, given by eqn. (1), we have

$$n(V) = -\,p/A(V/A)^{p+1} \quad . \quad . \quad . \quad . \quad . \quad (6)$$

Substituting in eqn. (5) and changing the variable from V to X,

$$Q(v) = -\frac{p}{\alpha}\left(\frac{v}{A}\right)^{-p}\int_{1}^{v/v_0} X^{p-1}W(X)dX \quad . \quad . \quad (7)$$

$$= -\frac{p}{\alpha}\left(\frac{v}{A}\right)^{-p} F(v/v_0) \quad . \quad . \quad . \quad . \quad . \quad (8)$$

where $F(v/v_0) = \int_{1}^{v/v_0} X^{p-1}W(X)dX$

Eqn. (8) shows the cumulative amplitude probability to be proportional to the product of two functions, one of which is the same power law of voltage obeyed by the pulse rate, and the other is an integral whose value will depend on the shape of each pulse.

The response to a unit impulse of a receiver containing n similar tuned circuits each having a damping coefficient α is given approximately[2] by

$$v(t) = 2\alpha G_0 \frac{\varepsilon^{-\alpha t}(\alpha t)^{n-1}}{(n-1)!} \quad . \quad . \quad . \quad . \quad (9)$$

where $v(t)$ = Amplitude at time t after input impulse.

G_0 = Central frequency gain of receiver.

Expressing this in terms of X and t, the response of a receiv containing one tuned stage is given by

$$X = \varepsilon^{-\alpha t} \quad . \quad . \quad . \quad . \quad . \quad . \quad (10$$

and, for one containing three tuned circuits,

$$X = \tfrac{1}{4}\varepsilon^2(\alpha t)^2\varepsilon^{-\alpha t} \quad . \quad . \quad . \quad . \quad . \quad (1$$

$W(X)$ and hence the integral in eqn. (7) were calculated, an curves are shown in Fig. 9 for a receiver having three tune

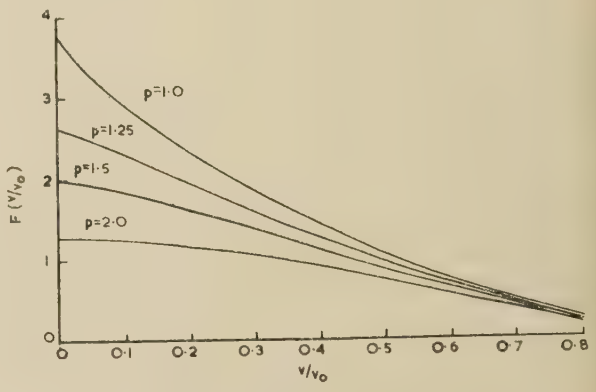

Fig. 9.—Graphs of a function given in eqn. (8).

circuits of the integral as a function of p for various values o v/v_0. The integral was found to vary much more slowly with than did the power-law function in eqn. (7), with the result tha calculated values of $Q(v)$ followed the power law over a wid voltage range, but as v approached v_0, the values decreased mo rapidly with increasing voltage.

(13.2) Effect of Changing the Receiver Bandwidth

An increase of receiver bandwidth has the effect of increasin proportionately the peak amplitude of a pulse, and decreasing i width in such a way that the area under the pulse remai constant. Thus in eqn. (7) a change of bandwidth affects th parameter α (determining the pulse width) and the parameter (voltage scale of the peak distribution).

If the cumulative amplitude probability functions at ban widths f_{b1} and f_{b2} are Q_1 and Q_2, respectively, then it can b shown that

(*a*) At a fixed threshold voltage, $Q_1/Q_2 = (f_{b1}/f_{b2})^{p-1}$.
(*b*) For a fixed value of Q, the ratio of the threshold voltages $(f_{b1}/f_{b2})^{1-1/p}$.

Thus, for the ideal case of a simple power-law distribution the impulse peak voltages, a value of $p = 1$ results in an amp tude distribution independent of bandwidth, and, for $p = 1$ the voltage scale of the distribution is multiplied by the cu root of the ratio of the bandwidths.

1.396.812.4

The Institution of Electrical Engineers
Paper No. 2562 R
May, 1958

PHASE VARIATIONS OF 16 KC/S TRANSMISSIONS FROM RUGBY AS RECEIVED IN NEW ZEALAND

By D. D. CROMBIE, M.Sc., A. H. ALLAN, B.E., Associate Member, and Miss M. NEWMAN, B.Sc.

(*The paper was first received* 10*th August, and in revised form* 30*th December*, 1957.)

SUMMARY

The results of approximately one year's measurement of the diurnal phase variation, in New Zealand, of the highly stable 16 kc/s transmission from GBR are given and discussed. If it can be considered that the signal is received by the short great-circle path, the observed phase variations appear to be in accordance with propagation via the M_{01}-mode which exists between parallel, plane metallic sheets.

(1) INTRODUCTION

An accurate radio frequency of 2·5 Mc/s has been radiated from the Dominion Physical Laboratory at weekly intervals during the past two years. It is intended for the convenience of local users.

At first this frequency was calibrated by reference to the standard frequency of 15 Mc/s radiated from WWVH (Hawaii). It seemed more profitable to check the frequency against a standard frequency transmitted by a laboratory oversea than to check it by time signals received from oversea.

It was found, however, that variations in the frequency of WWVH as received in New Zealand were large[1] and that there was considerable difficulty in relating the frequency of the local standard to the frequency of WWVH to within one part in 10^8.

Early in 1955, the authors became aware[2] that GBR (Rugby) transmissions at 16 kc/s were stabilized to a very high accuracy, and that propagation conditions, across the Atlantic at least, were very stable. In view of this, equipment was set up for the comparison of the frequency of our Laboratory standard with that of GBR. The results have been most satisfactory, and a preliminary report[3] has already been published. The purpose of the present paper is to discuss further observations, extending over one year, of the diurnal phase variations of GBR, and to offer a tentative explanation of the main features which have been observed.

(2) DETERMINATION OF DIURNAL PHASE VARIATION

The signal from GBR is utilized by amplifying and mixing it with a locally generated signal of high stability, offset slightly in frequency from 16 kc/s. The resultant difference frequency (about 10^{-3} c/s) is filtered by a low-pass *RC* filter of long time-constant (about 100 sec) and recorded. The filter determines the overall bandwidth of the receiver and substantially increases the signal/noise ratio of the output, at the same time removing the short-period keying fluctuations on the transmission. A simple 24-hour record in which the beats were made slower than usual is shown in Fig. 1. The amplitude of the oscillations in this record is proportional to the amplitude of the incoming signals, provided that the ratio of 'on' to 'off' periods of the keyed transmission is constant, while the variations in frequency of the oscillations give the variation in frequency difference between GBR and the local reference signal.

The diurnal phase variation is found in the following way.

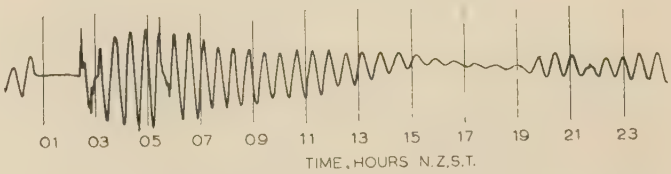

Fig. 1.—Sample 24-hour record.
The beats shown are slower than those usually used.

The average duration of one cycle of the record is found from the total number of cycles occurring in 24 hours. If the difference frequency between GBR and the local reference were constant, then, starting at the first peak (or zero crossing) on the record, the other peaks would occur at successive integral multiples of this mean time. That the peaks do not, in fact, occur at exactly these times, is almost entirely due to changes in the frequency of the signal from GBR. The phase defect of GBR as received, i.e. the difference between its actual phase at any time and the phase it would have had if its frequency had remained constant, is assessed from the time differences. Measured in cycles, it is equal to the difference between the time of the nth peak and n times the mean time per cycle, divided by the mean time per cycle. Fig. 2 shows a number of diurnal phase defect curves obtained in this way.

Some portions of the phase changes plotted in Fig. 2 are, no doubt, due to changes in the reference oscillator. Its frequency increases at a rate of about one part in 10^9 per day, relative to GBR, but there are variations superimposed on this of short duration (hours) which, regrettably, may be as large as 3 parts in 10^9.

If the frequency f varies at a constant rate, $f = f_0 + at$ where f_0 is the initial frequency at $t = 0$. Thus the phase ϕ in cycles at time t is

$$\phi = \int_0^t f\,dt = f_0 t + \tfrac{1}{2}at^2$$

The phase error, ϕ_e, is the difference between the actual phase of the local oscillator and the value it would have had if the phase had been changing uniformly (i.e. if the frequency had remained constant) so as to change by the same total amount in a long period T. In cycles the phase error is

$$\phi_e = f_0 t + \tfrac{1}{2}at^2 - (f_0 T + \tfrac{1}{2}aT^2)t/T$$

$$= \frac{at}{2}(t - T) \quad . \quad . \quad . \quad . \quad . \quad . \quad . \quad . \quad (1)$$

The error is zero at the start and at the end of the period and has a maximum value $aT^2/8$ at the middle. When $T = 24$ hours and $a = 16/86 \times 10^{-9}$ c/s^2 at 16 kc/s the maximum value of $\phi_e = 0{\cdot}17$ cycle. The errors due to short-period variations are not nearly so great since the error is proportional to T^2.

In interpreting the curves of Fig. 2 the possibility of such errors should be kept in mind, but it is thought that their magni-

Written contributions on papers published without being read at meetings are invited for consideration with a view to publication.
The authors are at the Dominion Physical Laboratory, Lower Hutt, New Zealand.

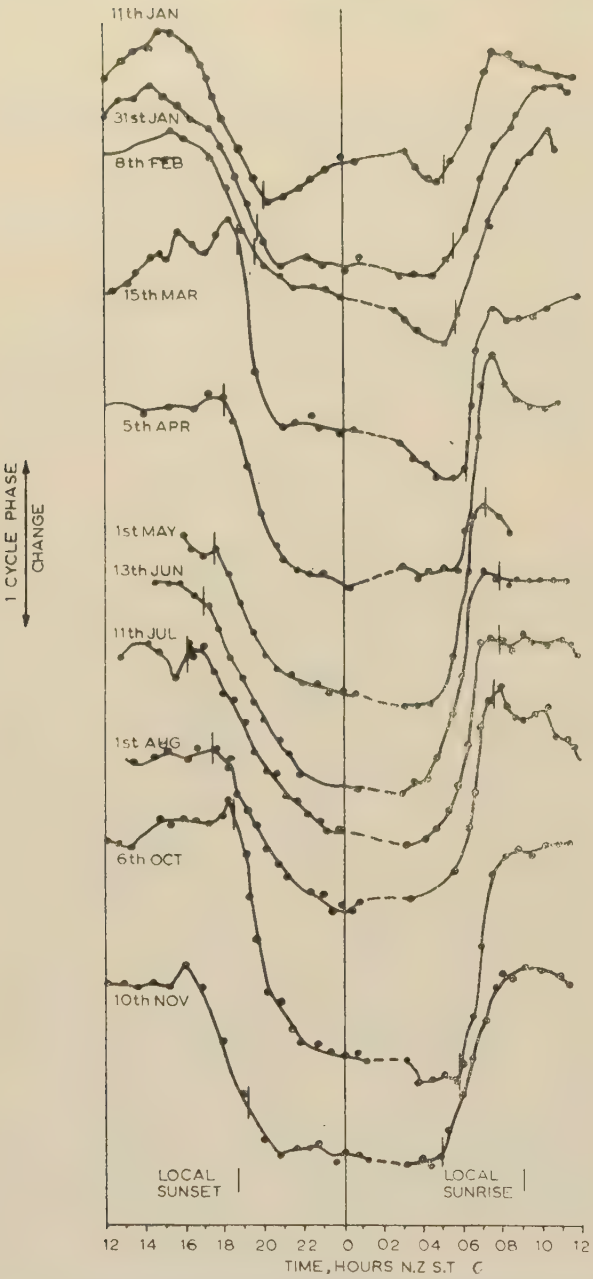

Fig. 2.—Diurnal phase changes in 1956.

Observations are lacking between 0100 and 0300 hours N.Z.S.T. because the station was not transmitting.

tude should be less than 20%. The skewness of some of the curves is possibly due to this cause.

(3) DIURNAL PHASE AND FREQUENCY VARIATIONS

Curves showing the smoothed measured diurnal phase variations at roughly monthly intervals are given in Fig. 2 together with the times of local sunrise and sunset. At sunset the phase lag increases by about one cycle and then remains approximately constant until near sunrise, when the lag decreases to its daytime value. There are also minor phase variations, before and after these major variations, which are probably real. It will be noted that there are seasonal changes in the relationship between the start of the major phase changes and the times of local sunrise and sunset. There are also marked seasonal changes i the slope of the phase at sunrise and sunset. Because of th vagaries of the local reference oscillator it is the regions c maximum slope which are of most significance.

Since frequency is equal to rate of change of phase, it will b seen from Fig. 2 that the maximum frequency change is of th order of 2 parts in 10^{-8} and occurs near local sunset or sunris At other times, particularly near midnight (New Zealand time and, to a lesser extent, midday, the rate of change of phase i much less, indicating frequency variations of the order of one pa in 10^9. These variations are at least an order less than thos obtained over shorter paths at much higher frequencies an demonstrate the utility of a very-low-frequency standard frequency transmission.

(4) EXPLANATION OF DIURNAL AND SEASONAL CHANGES

The features of the phase curves mentioned can be explaine if it is assumed that the signal is received predominantly by th short great-circle path and that propagation takes place b means of the TM_{01} waveguide mode which can exist betwee parallel, plane highly conducting sheets of infinite extent. Fo this type of propagation the phase shift β per unit length o path is given by

$$\beta = \frac{2\pi}{\lambda_0}\sqrt{\left[1 - \left(\frac{\lambda_0}{2h}\right)^2\right]} \quad . \quad . \quad . \quad . \quad (2$$

where λ_0 is the free-space wavelength and h is the distanc between the sheets. Thus if h increases, β increases. The tw conducting sheets are represented by the earth's surface and th D-region of the ionosphere. It is known[4] that at very low fre quencies the effective height of the reflecting region behaves a though it were greater at night than during the day. We wi assume for simplicity that the reflecting properties of th ionosphere are constant, and that the height of reflection depend only on whether the layer is illuminated or not. Thus an seasonal effects or dependence on the angle of elevation of th sun are ignored.

Under these conditions, the total phase change betwee transmitter and receiver will depend on the amount of pat illuminated. If d_D and d_N are the distances in daylight and dar and β_D and β_N are the respective phase changes per unit lengt the total phase lag ϕ_t between transmitter and receiver is

$$\phi_t = d_D\beta_D + d_N\beta_N$$

but $$d_N + d_D = d, \text{ a constant}$$

therefore $$\phi_t = d_D(\beta_D - \beta_N) + \beta_N d \quad . \quad . \quad . \quad (3$$

the last term of which is constant. Thus the diurnal pha change is proportional to the change in length of the path daylight.

In Fig. 3 are shown diurnal phase-change curves for thr days, a few months apart, together with approximate curv showing the diurnal variation of the length of the short grea circle path in daylight for the same month. It will be seen th the shapes of the two curves for each month are quite simila and this tends to confirm the above argument.

The seasonal variations in both the time of maximum ra of change of phase and the magnitude of the rate of chan may also be explained on this basis. Fig. 4 is a map showing t short path between Wellington and Rugby, together with t approximate positions of the sunset and sunrise shadow lin for the 20th of each month at the time when the shadow lin pass through Wellington. In July, for example, sunrise occu

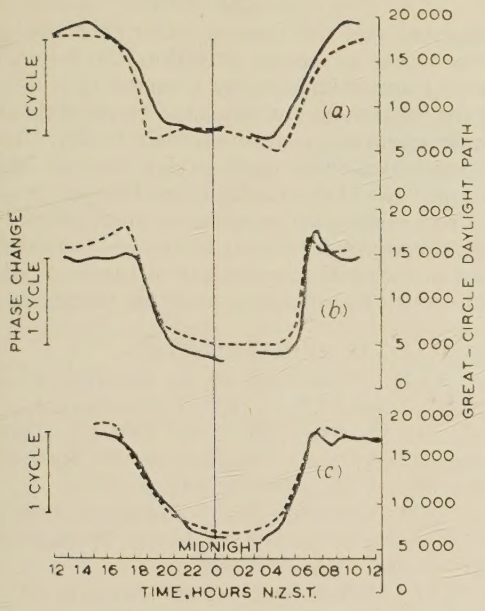

Fig. 3.—Diurnal phase changes compared with variations in the amount of path in daylight.

(*a*) 31st January, 1956.
(*b*) 5th April, 1956.
(*c*) 13th June, 1956.
——— Phase change.
- - - - Amount of sunlit path.

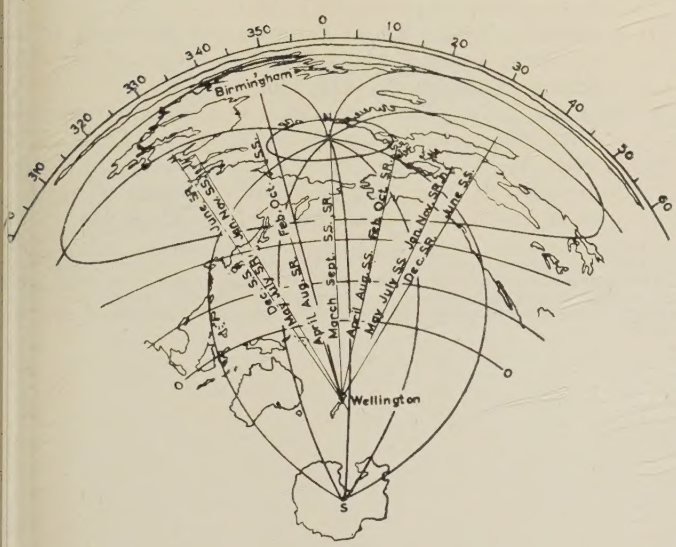

Fig. 4.—Equi-azimuth projection.

The short path between Rugby and Wellington, and the shadow lines at sunrise (S.R.) and sunset (S.S.) through Wellington for each month are shown.

t Wellington after most of the path has become sunlit. ccordingly, the July curve of Fig. 2 shows that the main phase change precedes local sunrise. All the shifts of maximum phase can be explained in this way.

It can also be seen that the change from night to day is most nearly simultaneous over the whole path during April and August. Accordingly, the curves of Fig. 2 show that the morning change of phase is most rapid during April and August. Conversely, the times at which sunset is most nearly simultaneous over the path are the end of February and October; Fig. 2 shows that the evening phase change is most abrupt at these times.

(5) DAY/NIGHT CHANGE OF REFLECTION HEIGHT

From eqns. (2) and (3) it should be possible to estimate the change in height of the reflection region as it changes from night to day conditions. If h_D and h_N are the daytime and night-time heights of reflection,

$$\beta_D - \beta_N = \frac{2\pi\lambda_0}{8} \frac{(h_D^2 - h_N^2)}{h_D^2 h_N^2} \quad . \quad . \quad . \quad (4)$$

Thus, for a given value of $(\beta_D - \beta_N)$, the change in height can be estimated if the initial height is known. The value of $(\beta_D - \beta_N)$ has been estimated from the difference between midday and midnight values shown in Fig. 2, after making an allowance for the difference in oscillator rates of $1 \cdot 2 \pm 0 \cdot 2$ cycles per 10 000 km. If the daytime height of reflection is assumed to be 70 km, the corresponding night-time height is approximately 80 km. This change is smaller than the change of 14–21 km observed by workers from the Cavendish Laboratory,[4] over a distance of about 540 km. However, our value of the night-to-day phase change per unit distance agrees with that obtained from phase curves given by Pierce[5] for measurements of the same type across the Atlantic.

(6) DISCUSSION

In the previous Sections the diurnal phase change has been explained in terms of propagation via the TM_{01}-mode, which can exist between parallel plane conducting sheets representing the earth and ionosphere. The effective height of the ionosphere, and hence the spacing between the sheets, varies from night to day. It is true, however, that other propagation mechanisms which would give an increase in phase-change coefficient of the right magnitude as the path changes from day to night would be equally satisfactory. In this Section some of the considerations involved in choosing a suitable mechanism will be outlined.

Budden[6] has pointed out that, in treating long-distance v.l.f. propagation, it is simpler to consider waveguide modes than successive reflections. Eckersley[7] has indicated that, when the ionosphere can be treated as a sharply defined conducting plane, the attenuation of the zero-order or TEM-wave is, at most, one half that of the higher-order modes. He also states that, when the height of the ionosphere is small compared with the radius of the earth, there is little difference between propagation between plane parallel infinite sheets and between concentric spheres.

Because of the lower rate of attenuation of the TEM-mode between parallel plane conducting sheets, it would be expected that at great distances the signal should be received by this mode. However, in a lossless infinite parallel-plane waveguide the phase-change coefficient of the TEM-mode is independent of the distance between the planes. Thus it is impossible on this model to explain the diurnal phase variations.

The phase changes could be explained, on the basis of the TEM-mode, if it could be assumed that the effective dielectric constant of the space between the ionosphere and earth varied from night to day. It is extremely unlikely that sufficient variation could occur in the troposphere, but it is conceivable that diurnal variations in electron density below the point of reflection might account for the phase variation. The calculation of such effects seems to be very involved and has not yet been undertaken. Alternatively, if it is assumed that propagation is of the TM type, the phase variations can be easily accounted for, provided that the effective ionospheric height does vary from

night to day. It seems that such a height variation could be due either to a change of physical height or to a change of phase shift on reflection. Thus, because of the difficulties associated with the use of the TEM-mode, the TM-modes have been adopted. Since the TM-mode is the least attenuated, attention has been devoted to it.

The difficulties outlined above are, no doubt, due to the supposition (*a*) that the lower surface of the ionosphere is sharply bounded, and (*b*) that the ionosphere behaves as a conductor. Budden[6] has investigated the propagation of v.l.f. waves taking into account some of the characteristics of the ionosphere, but still assuming that its lower surface is sharply defined. He finds that there is a difference in the attenuation rate for modes of order $+n$ and $-n$, but in a particular case at 16 kc/s the attenuation rate of the zero-order mode is about 3% higher than the TM mode of order -1. In another paper[8] he points out that the effect of the earth's curvature will be to increase the zero-order attenuation rate more than that of the higher-order modes. This indicates that, in practice, the least attenuated mode may in fact be the TM_{01}-mode.*

In view of the substantial agreement between our measurements and those of Pierce[5] across the Atlantic, it is considered that, except for regions where the 16 kc/s signal is received equally by both the long and short paths,[9] it should be possible to predict fairly accurately the diurnal phase variation and rate of change of phase for any receiving site, using the metallic sheet model and the TM_{01}-mode.

Because of the nearly antipodal positions of Wellington and Rugby, as shown in Fig. 4, it was uncertain, when this work began, whether the signal would be received from any particular direction for most of the time. From the results presented here, it is probable that the signal is received predominantly by the short great-circle path, since otherwise the diurnal phase variations would not agree with the variation of the amount of this path in daylight. Other supporting evidence for this is provided by the fact that sudden phase anomalies have not been observed when the short path is mainly in darkness, but only during the day. However, it is not impossible that, during the signal minima which occur near sunrise and sunset, some signal is received by the long path. It is hoped to investigate this matter further by means of d.f. measurements.

* Since this paper was written, the authors have seen a paper by Wait and Howe (*Proceedings of the Institute of Radio Engineers*, 1957, **45**, p. 95) which indicates that the attenuation of the zero-order mode is much greater than that of the first-order TM-mode, under typical ionospheric conditions.

(7) CONCLUSIONS

It is suggested that the measured diurnal phase changes a 16 kc/s over a path of nearly 19 000 km can be explained, a least to a first approximation, by a model in which both th earth and the ionosphere are simulated by perfectly conductin sheets, whose separation varies from night to day. The averag change in separation from night to day that the observation suggest, on the basis of this model, is less than has been reporte previously from other experiments using much shorter paths.

Although the use of the simple model has been successful, would seem worth while to investigate a more complex mode taking into account the reflecting properties of the ionosphere.*

(8) REFERENCES

(1) ALLAN, A. H.: 'Variations of the Received Frequency o WWVH', *Journal I.E.E.*, 1955, **1** (New Series), p. 650.

(2) PIERCE, J. A., MITCHELL, H. T., and ESSEN, L.: 'World-Wid Frequency and Time Comparisons by Means of Radi Transmission', *Nature*, 1954, **174**, p. 922.

(3) ALLAN, A. H., CROMBIE, D. D., and PENTON, W. A.: 'Fre quency variations in N.Z. of 16 kc/s Transmissions fro GBR, Rugby', *ibid.*, 1956, **177**, p. 178.

(4) BAIN, W. C., BRACEWELL, R. N., STRAKER, T. W., an WESTCOTT, C. H.: 'The Ionospheric Propagation of Radi Waves of Frequency 16 kc/s over Distances of abou 540 km', *Proceedings I.E.E.*, Monograph 37 R, May, 195 (**99**, Part IV, p. 250).

(5) PIERCE, J. A.: 'The Diurnal Carrier Phase Variation of 16 kc/s Transatlantic Signal', *Proceedings of the Institut of Radio Engineers*, 1955, **43**, p. 584.

(6) BUDDEN, K. G.: 'The Propagation of a Radio Atmospheric *Philosophical Magazine*, 1951, **42**, p. 1.

(7) ECKERSLEY, T. L.: 'Radio Transmission Problems treate by Phase Integral Methods', *Proceedings of the Roy Society of London*, A, 1932, **136**, p. 499.

(8) BUDDEN, K. G.: 'The Propagation of a Radio Atmospheri —II', *Philosophical Magazine*, 1952, **43**, p. 1179.

(9) ROUND, H. J., ECKERSLEY, T. L., TREWELLEN, K., an LUNNON, F. C.: 'Measurements of Signal Strength a Great Distances', *Journal I.E.E.*, 1925, **63**, p. 933.

* Dr. J. R. Wait has recently shown that the reflection coefficient of the ionosphe at these frequencies is approximately -1. The effect of this, for the first-order mod is to make the cut-off wavelength one-quarter of the height of the ionosphere, instea of one-half as implied by the use of the metallic sheet model. The deduced diurn height change then becomes comparable with the earlier measurements over sho paths.

PROCEEDINGS OF THE INSTITUTION OF ELECTRICAL ENGINEERS

Part B. RADIO AND ELECTRONIC ENGINEERING (INCLUDING COMMUNICATION ENGINEERING), MAY 1958

CONTENTS

Bibliographical References.—It is requested that bibliographical reference to an Institution paper should always include the serial number of the paper and the month and year of publication, which will be found at the top right-hand corner of the first page of the paper. This information should precede the reference to the Volume and Part.

Example.—SMITH, J.: 'Reflections from the Ionosphere', *Proceedings I.E.E.*, Paper No. 3001 R, December, 1954 (102 B, p. 1234).

Published by The Institution, Savoy Place, London, W.C.2. *Telephone:* Temple Bar 7676. *Telegrams:* 'Voltampere, Phone, London.'
Printed by Unwin Brothers Limited, Woking and London.